The role of voltage-gated potassium channels in regulating excitability at a central synapse

A thesis submitted for the degree of
Doctor of Philosophy
at the University of Leicester

By

Paul Dodson B.Sc.

Department of Cell Physiology and Pharmacology
University of Leicester

September 2003

ProQuest LLC
789 East Eisenhower Parkway
P.O. Box 1346
Ann Arbor, MI 48106-1346

The role of voltage-gated potassium channels in regulating excitability at a central synapse

Paul D. Dodson

The medial nucleus of the trapezoid body (MNTB) rapidly and precisely relays auditory information used to determine where a sound is originating from. Voltage-gated K^+ channels play an important role in this process by preserving action potential (AP) timing. We investigated the subunit composition of K^+ channels and their role of regulating AP firing in a giant presynaptic terminal (the calyx of Held) and its postsynaptic neurones (MNTB neurones) by combining patch-clamp recordings and immunohistochemistry in brainstem slices from 8-14 day Lister hooded rats and C57/Bl6 mice.

Kv1 currents in MNTB neurones were completely blocked by dendrotoxin-K (DTX-K, which blocks Kv1.1 containing channels) but only half blocked by tityustoxin-Kα (TsTX-Kα, which blocks channels containing Kv1.2 or Kv1.3). Combined with immunohistochemical evidence that only Kv1.1, Kv1.2 and Kv1.6 are present, these data indicate that Kv1.1/1.2 and Kv1.1/1.6 heteromers mediate the Kv1 current. Block of Kv1.1/1.2 heteromers disrupted unitary firing, signifying that it is these channels which preserve AP firing fidelity. In the presynaptic terminal, Kv1 currents were completely blocked by TsTX-Kα but only partially by DTX-K, indicating that Kv1.2 homomers mediate two-thirds of this current, with the remaining third mediated by Kv1.1/1.2 heteromers. Block of Kv1.2 homomers caused aberrant AP firing, suggesting that these channels preserve precise presynaptic AP firing by preventing nerve terminal hyperexcitability.

Presynaptic Kv3 currents were mediated by channels containing Kv3.1, Kv3.3 and Kv3.4 subunits. These channels were resistant to phosphorylation and activated at more negative potentials than their postsynaptic counterparts. These data suggest that specialisations in subunit composition enable Kv3 channels to rapidly repolarise the presynaptic AP, facilitating high frequency firing.

This work not only demonstrates the role of different K^+ channels in preserving reliable high frequency firing at this central synapse, but also highlights how subunit composition can influence the role of K^+ channels in the CNS.

Acknowledgments

First, I must thank God through whom all this was possible. He has blessed me richly and I continue to be amazed by His creation as I study the nervous system. I would also like to thank my wife and best friend Sarah, who has supported, encouraged me and kept a smile on my face throughout my PhD. I also thank my family and friends for their love and support and for helping to maintain my sanity.

I would particularly like to thank my supervisor, Professor Ian Forsythe, for his patience, guidance and encouragement throughout my three years in the lab and for his inspiration to begin a career in research. I have learnt a lot from Ian and his red pen as he has continually pointed me in the right direction and suggested crazy experiments.

I thank Matthew Barker for his hard work on the immunohistochemistry presented in this thesis, for dropping everything to get yet one more 'n' and for often staying late on the confocal microscope. I would like to express my gratitude to all the members of the lab, to Brian Billups for teaching me so much and helping with the dual-patching experiments in chapter 6, to Margaret Barnes-Davies for being prepared to sit and discuss my results on countless occasions and to Adrian Wong, Tom Watano and Martine Hamman for their numerous helpful suggestions. Most of all I thank them for making my time in the lab a wonderful experience and a lot of fun.

I must also acknowledge Noel Davies, for his help with Boltzmann equations; Richard Evans and Blair Grubb, my PhD committee members; and also Rooma Desai and Len Kaczmarek for sharing unpublished data. Finally I thank the Wellcome Trust for funding this research.

Declaration

The material in this thesis is all my own work with the exception of the immunohistochemistry and dual patch experiments. All of the immunohistochemical labelling presented was performed by Matthew Barker, although I assisted with the image collection in each case. In the dual patch experiments Dr Brian Billups assisted by patching the calyx and MNTB neurone whilst I controlled the presynaptic amplifier. Parts of this work have been previously presented in Dodson *et al.,* (2002 and 2003).

Table of Contents

Table of Figures

Page

CHAPTER 1 – Introduction

In this study we have investigated potassium channels in giant presynaptic terminals (the calyx of Held) and their postsynaptic neurones (the medial nucleus of the trapezoid body; MNTB) in the auditory brainstem. The calyx of Held to MNTB synapse forms part of a pathway that rapidly and precisely transmits information used to determine where a sound is coming from. Our laboratory first became interested in the auditory brainstem because of the giant calyceal terminals which are large enough to permit direct electrophysiological recordings (Forsythe, 1994). However, since the physiological role of the auditory brainstem is well established (reviewed in Grothe, 2003), the preparation allows examination of the function of ion channels (Banks and Smith, 1992; Forsythe and Barnes-Davies, 1993a; Brew and Forsythe, 1995) and receptors (Forsythe and Barnes-Davies, 1993b; Barnes-Davies and Forsythe, 1995) in rapidly transmitting auditory information. Previous work in our laboratory had demonstrated that a particular type of potassium channel (Kv1), which activates at low voltages, is important in preserving the fidelity of action potential (AP) firing in MNTB neurones (Brew and Forsythe, 1995). Since then, the availability of selective Kv1 blockers and development of presynaptic recording techniques has opened up the possibility for detailed examination of how pre- and postsynaptic K^+ channels shape AP firing. In this thesis I will describe how I extended the work on low-voltage activated currents in MNTB neurones by using specific toxins to probe the subunit composition of Kv1 channels and their roles in regulating AP firing. Having established these techniques in the postsynaptic neurone, I went on to investigate the nature and role of presynaptic Kv1 channels. To complete my investigation of the presynaptic K^+ channels, I examined how a type of K^+ channel which activates at more positive voltages (Kv3) contributes to rapid AP repolarisation and hence facilitates high frequency firing.

Since pre- and postsynaptic K^+ channels play important roles in ensuring rapid and faithful transmission of auditory information I shall begin by describing some of the salient features of the auditory nuclei involved in sound source localisation and the mechanisms by which they

achieve this. I shall then introduce information about the structure of different types of potassium channels and their roles in regulating neuronal excitability.

1.1 The auditory system

1.1.1 Transduction of sound in the ear

Sound waves enter the auditory canal and cause the tympanic membrane (ear drum) to vibrate; vibrations are amplified by the malleus, incus and stapes bones in the middle ear before entering the cochlea via the round window. The vibrations cause the fluid within the cochlea to oscillate, creating a travelling wave along a stip of tissue in the cochlea called the basilar membrane. Resting upon the basilar membrane lies the organ of corti, which contains the receptor cells (the hair cells). There are two types of hair cell: inner hair cells (IHCs), which serve to detect sound and outer hair cells (OHCs), which regulate the response of the overlying tectorial membrane, acting as the cochlea amplifier (Gale and Ashmore, 1997). Movement of the tectorial membrane distorts the stereocilia of IHCs, resulting in depolarisation and transmitter release onto type I spiral ganglion cells. In turn, these fire action potentials (APs) which travel into the brain along the eighth nerve; hence, the IHCs transduce sound waves into AP firing. Since the stiffness of the basilar membrane increases along the cochlea, the base of the cochlea resonates at high frequencies and the apex at lower frequencies. Sounds of a given frequency will therefore be detected by IHCs at a particular position along the basilar membrane. This differing response to frequency according to position is called tonotopy and occurs in the majority of nuclei in the auditory system (Cohen and Knudsen, 1999). The intensity of sound is coded by the number of APs fired as a result of neurotransmitter release from IHCs.

1.1.2 Auditory nuclei

1.1.2.1 The Cochlear Nucleus (CN)

The cochlear nucleus (CN) is the first central nucleus of the auditory pathway. The spiral ganglion axons, which comprise the eighth nerve, enter the CN before bifurcating; the ascending branch innervates the anterior ventral cochlear nucleus (aVCN) and the descending branch the posterior VCN and the dorsal cochlear nucleus (DCN, Biacabe et al., 2001). Since it is the VCN which relays auditory information to the binaural brainstem, I shall concentrate on this region of the CN.

The VCN contains four major cell types: spherical bushy cells (SBCs), globular bushy cells (GBCs), stellate cells and octopus cells; each has a distinct morphology, firing pattern and projection (Oertel, 1983). The bushy cells derive their name from their sparse 'bushy' dendrites and are involved in relaying information to nuclei of the superior olivary complex (SOC, Brawer et al., 1974; Cant and Morest, 1979a, b; Cant and Casseday, 1986). SBCs receive up to four afferent inputs from the eighth nerve in the form of giant excitatory synapses, called endbulbs of Held (Held, 1893; Lenn and Reese, 1966; Gentschev and Sotelo, 1973; Neises et al., 1982; Ryugo and Sento, 1991; Isaacson and Walmsley, 1995; Ryugo et al., 1996; Ryugo et al., 1997; Nicol and Walmsley, 2002). They project to the ipsilateral medial superior olive (MSO) and lateral superior olive (LSO) and to the contralateral MSO (Cant and Casseday, 1986). GBCs have a slightly more irregular morphology than SBCs, are located slightly more dorsally and receive around 20 to 40 inputs (Nicol and Walmsley, 2002). Convergence of many auditory nerve inputs onto a single GBC cancels jitter in the firing of individual fibres, thus helping to preserve precise timing information (Joris et al., 1994; Oertel, 1997). GBCs are particularly important to this study because they innervate neurones of the medial nucleus of the trapezoid body (MNTB) by way of a giant excitatory synapse known as the calyx of Held (Held, 1893). The large size of this nerve terminal permits direct patch clamp recordings to be made (Forsythe, 1994), facilitating the present study of presynaptic potassium channels (see chapters 5 and 6).

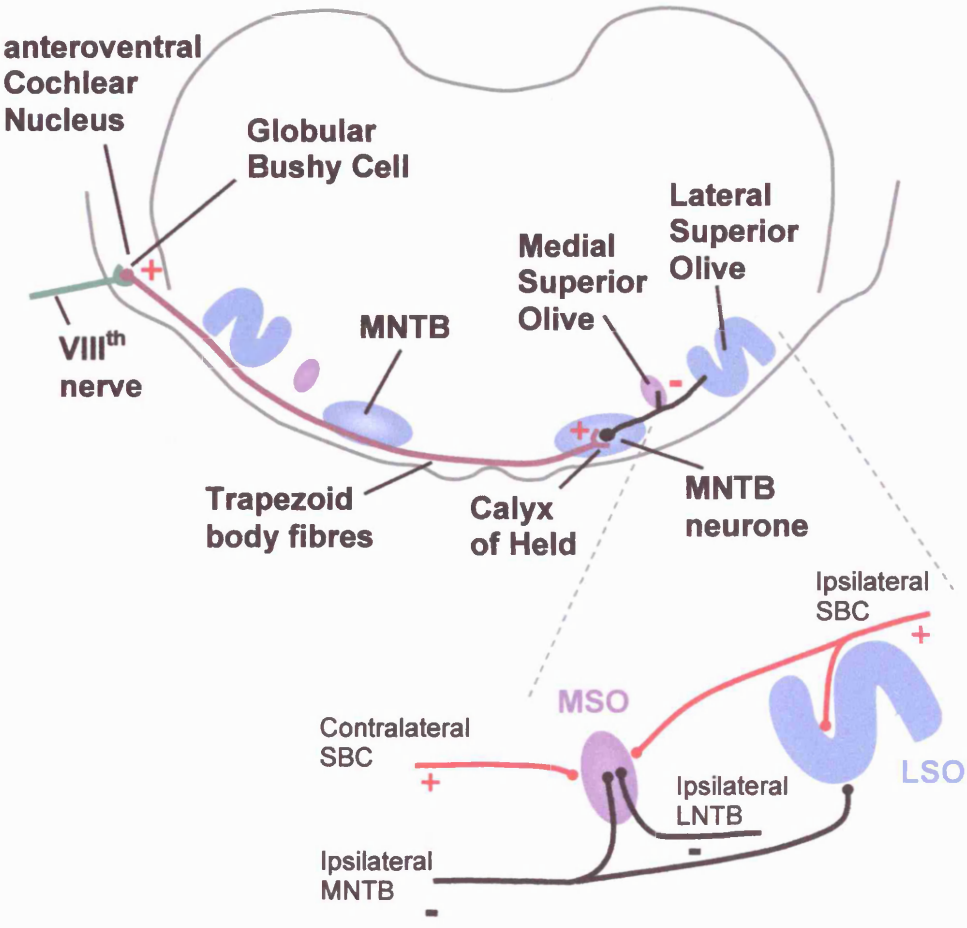

Figure 1.1. Diagram of the superior olivary complex.
Globular bushy cells project to the contralateral medial nucleus of the trapezoid body (MNTB) ending in a giant excitatory synapse, the calyx of Held. MNTB neurones then send inhibitory projections to the ipsilateral medial and lateral superior olives (MSO and LSO). MSO neurones receive bilateral excitatory inputs on their dendrites from spherical bushy cells (SBCs) of the anteroventral cochlear nucleus (aVCN) and somatic inhibitory inputs from the MNTB and lateral nucleus of the trapezoid body (LNTB). The LSO receives ipsilateral excitation from SBCs and contralateral inhibition via the MNTB.

1.1.2.2 The Medial Nucleus of the Trapezoid Body (MNTB)

As described above, each MNTB neurone receives a single excitatory calyceal synapse which surrounds the soma (Kil et al., 1995; Satzler et al., 2002). The MNTB is essentially a relay, involved in converting these excitatory inputs from the contralateral CN to inhibitory projections to the MSO and LSO (Fig, 1.1). In this study we have recorded the basic properties of MNTB neurones (chapter 3) and examined their potassium currents in more

detail (chapter 4). The MNTB contains three cell types: principal (which comprise the majority of cells), elongated and stellate (Morest, 1968; Kuwabara and Zook, 1991). Principal cells can be identified morphologically by their spherical or elliptical soma, which has a diameter of approximately 20μm, and an eccentric nucleus (Banks and Smith, 1992; Forsythe and Barnes-Davies, 1993a; Sommer et al., 1993). In addition, principal cells typically have one or two primary dendrites, which originate from opposite poles of the soma and extend a short distance before repetitively branching. Tonotopy is maintained at the level of the MNTB; the neurones positioned ventromedially respond to high frequencies and those positioned dorsolaterally respond to low frequencies (Guinan et al., 1972). The output of MNTB neurones is an inhibitory glycinergic projection to the adjacent LSO and MSO, with collaterals occasionally projecting to additional nuclei within the SOC (Banks and Smith, 1992; Sommer et al., 1993; Kim and Kandler, 2003).

1.1.2.3 The Lateral Superior Olive (LSO)

Inhibitory glycinergic projections from MNTB neurons terminate on the dendrites of the LSO. This input aids the LSO in responding to interaural level differences (ILDs) coded by the frequency of incoming APs (Park et al., 1997; Sanes and Friauf, 2000; Irvine et al., 2001; Tollin, 2003). In the rat, the LSO forms a distinct 'S' shaped structure and is therefore easily identifiable; it contains seven morphologically distinct cell types, three quarters of which are principal cells (Wu and Kelly, 1991). Principal cells are arranged in laminar sheets that are perpendicular to the transverse axis of the LSO; consequently, in transverse sections principal cells often appear as bipolar with a fusiform soma (Scheibel and Scheibel, 1974; Helfert and Schwartz, 1986, 1987; Wu and Kelly, 1991; Rietzel and Friauf, 1998). Other cell types include multipolar, small multipolar, unipolar, banana-like, bushy and marginal cells (Rietzel and Friauf, 1998). As with other nuclei of the auditory brainstem, the LSO is tonotopically arranged; in general, the LSO is sensitive to high frequency sound (>2Hz) with the lateral limb tuned to frequencies at the lower end and the medial region to higher frequencies (Guinan et al., 1972).

In addition to the inhibitory contralateral inputs from the MNTB already described, the LSO receives an ipsilateral excitatory input from SBCs (Glendenning et al., 1985; Cant and

Casseday, 1986; Smith et al., 1993). The majority of the LSO output to the ipsilateral inferior colliculus (IC) is inhibitory, whereas the output to the contralateral IC is largely excitatory (Clopton and Winfield, 1973; Glendenning et al., 1981; Shneiderman and Henkel, 1987; Wu and Kelly, 1991; Glendenning et al., 1992; Kelly et al., 1998). LSO principal cells can either fire a single AP in response to sustained depolarisation (Sanes, 1990; Kandler and Friauf, 1995) or multiple APs (Adam et al., 1999); differences in firing may be due to the amount of low-voltage activated potassium channels expressed (Barnes-Davies et al., 2003). In contrast to principal cells, olivocochlear cells within the LSO, which are probably banana-like cells in the morphological classification, fire trains of action potentials in response to sustained depolarisation with a variable delay after the first action potential (Adam et al., 1999).

1.1.2.4 The Medial Superior Olive (MSO)

The MSO is another nuclei in the SOC that is important in sound source localisation since it detects small differences in the timing and phase of sound arriving at each ear (interaural timing differences, ITDs; see figure 1.2) Like the LSO, the MSO receives an inhibitory input from the MNTB and is therefore relevant to this study. The MSO consists of three major cell types: principal, bipolar and marginal cells (Smith, 1995). The principal cells predominate and are arranged in a ladder like formation, aligned so that one dendrite projects medially, towards the midline, and the other laterally, towards the ipsilateral aVCN (Warr, 1966). The axons of principal cells arise perpendicularly from the soma and send excitatory projections to the ipsilateral IC (Smith, 1995). As with other nuclei of the SOC, the MSO is tonotopically arranged with cells of a high characteristic frequency (CF) in the ventral region and those with a low CF lying dorsally (Guinan et al., 1972). However, MSO neurones are generally biased towards low frequency sounds (<3 kHz, Smith, 1995).

The MSO receives bilateral excitatory (glutamatergic) inputs from SBCs; fibres from the ipsilateral aVCN synapse on the lateral dendrite and those from the contralateral aVCN synapse on the medial dendrite (Warr, 1966; Cant and Casseday, 1986; Smith et al., 1993). Principal cells also receive inhibitory glycinergic inputs at their soma from the contralateral MNTB and the ipsilateral lateral nucleus of the trapezoid body (LNTB, Banks and Smith, 1992; Kuwabara and Zook, 1992; Grothe and Sanes, 1994; Kapfer et al., 2002; Grothe, 2003).

Like GBCs and MNTB neurones, MSO principal cells only fire a single action potential at the onset of a depolarising current (Svirskis et al., 2002).

1.2 Sound source localisation

The function of nuclei in the SOC is to process binaural information used to determine where a sound is originating from; such sound source localisation is an important feature in predation and defence. The ability of the LSO and MSO to determine a sound's source depends upon differences in the volume or timing of the sound at each ear. This is known as the duplex theory of hearing and was first proposed by Lord Rayleigh (1907). If a sound originates from directly in front of the head (the midsagittal axis), it will arrive at both ears simultaneously and at the same intensity; if the sound originates to one side of the head (i.e. off the midsagittal axis) it will reach that ear before the other and be louder (Fig, 1.2). The increase in volume is a result of sound shadowing; high frequency sounds are deflected by the head, so the sound is quieter in the ear away from the source (Fig, 1.2). Consequently, only the location of high frequency sounds (>1500Hz) can be detected by comparing differences in the volume of a sound. The MSO detects differences in the timing (interaural timing differences, ITDs) and the LSO detects differences in volume (interaural level differences, ILDs) of the sound.

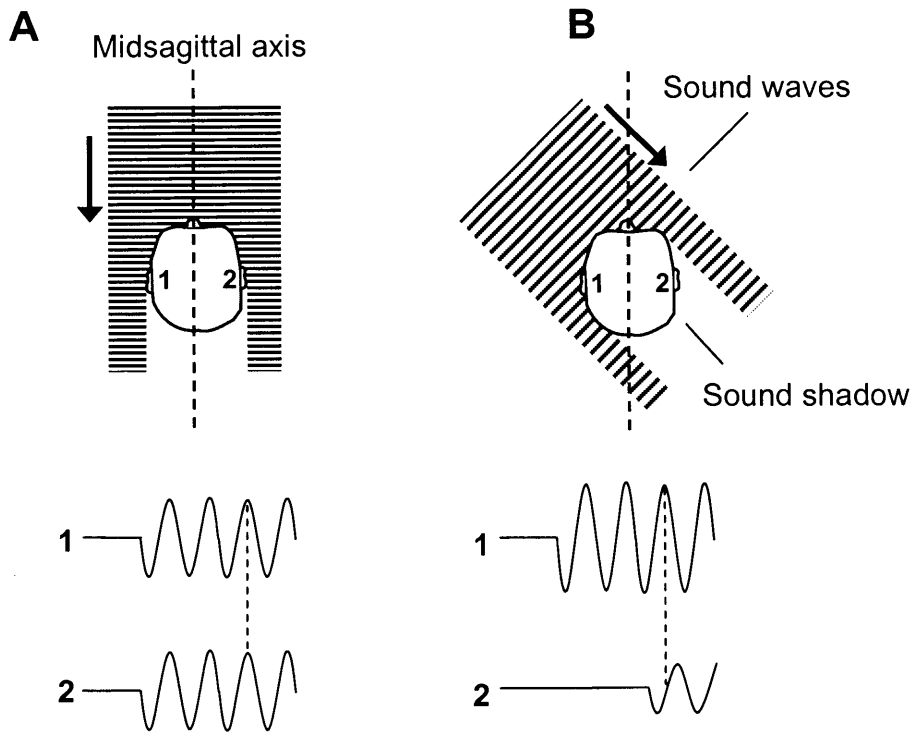

Figure 1.2. Sound localisation and shadowing of the head.
A. When the sound originates from a point on the midsagittal axis it arrives at both ears simultaneously and at the same intensity. The sound-wave lines represent the peaks of the sinusoidal signal which is shown below. At each ear (1 and 2) the sinusoidal wave arrives at the same time and is therefore in phase (dotted line). The volume (amplitude of the wave) is also the same at each ear. **B.** If the source of the sound lies off the midsagittal axis, the sound will arrive at ear 1 first, creating an interaural time difference (ITD, resulting in differences in the start point of the sinusoidal waves). The waves may also be out of phase (see dotted line). High frequency sound will also be deflected, creating a sound shadow and an interaural level difference (ILD, resulting in a decrease in the amplitude of the wave at ear 2).

1.2.1 Processing of ILDs in the lateral superior olive (LSO)

LSO principal neurones are often described as IE cells because they receive a contralateral inhibitory (I) input (from the MNTB) and an ipsilateral excitatory (E) input; hence firing is determined by summation of excitatory and inhibitory postsynaptic potentials (EPSPs and IPSPs, Finlayson and Caspary, 1989; Tollin, 2003). A loud sound in the ipsilateral ear results in a large, short latency, EPSP and a smaller, longer latency, IPSP in LSO neurones (Sanes, 1990; Wu and Kelly, 1992); accordingly, the net postsynaptic potential (PSP) will reach

threshold and an AP will be fired. The latency in the IPSP is important; as the sound in the contralateral (inhibitory) ear gets louder (e.g. if the sound is moved from the side to the front of the head), IPSP latency is reduced and the EPSP and IPSP occur simultaneously, preventing the neurone from reaching threshold (Sanes, 1990; Park et al., 1996; Irvine et al., 2001). Hence, LSO neurones use both timing and volume to determine the location of high frequency sounds (Tollin, 2003).

1.2.2 Processing of ITDs in the medial superior olive (MSO)

Despite the fact that the arrival times of a sound at each ear may only vary by several microseconds, birds and mammals use ITDs to pinpoint the source of a sound. An elegant mechanism for the way this works was proposed over 50 years ago (Jeffress, 1948) based upon SOC neurones that will fire in response to sound at a particular source.

1.2.2.1 Delay lines and coincidence detectors

The Jefress model is built upon a series of coincidence detectors which receive binaural excitatory inputs (EE cells). The input axons have different lengths, which therefore create a delay compensating for a particular ITD; each neurone therefore codes a particular position in space (Joris et al., 1998). All the neurones in the nuclei (the MSO in mammals) receive subthreshold EPSPs from each ear, but because of the different length delays, they will only be coincident in one neurone which will then fire (Fig, 1.3). Whilst this model has been shown to occur in birds (Young and Rubel, 1983, 1986; Carr and Konishi, 1990; Overholt et al., 1992; Joseph and Hyson, 1993), recent evidence has shown that a different mechanism may occur in mammals (Reviewed in Pollak, 2002; Grothe, 2003; McAlpine and Grothe, 2003).

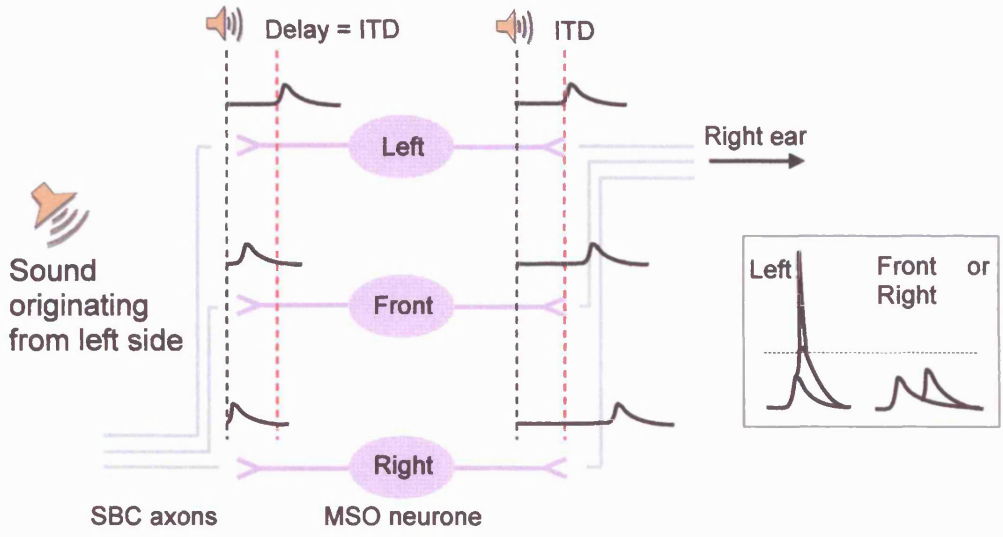

Figure 1.3. The Jeffress model of delay lines and coincidence detectors.
The excitatory inputs from SBCs of the aVCN (grey lines) provide the delay lines and the MSO cells act as coincidence detectors. Each cell (left, front and right) will only fire an action potential when it receives simultaneous inputs (see inset). The 'left' cell fires an action potential when a sound reaches the left ear first, is delayed by the long path of the SBC axons, so the EPSP arrives at the 'left' cell simultaneously with the input from the right ear.

1.2.2.2 ITD discrimination in mammals

Recordings from the IC (McAlpine et al., 2001) and MSO (Brand et al., 2002) of small mammals have shown that many neurones respond maximally to ITDs that would only be experienced if the ears were much further apart (i.e. neurones are tuned to long ITDs, which cannot be detected with a small head). This led to the idea that it is not the response of a single neurone that codes for the position of a sound, but the rate of firing in neurones across the whole MSO (Grothe, 2003). Although the maximum ITD response is often outside the physiological range, the MSO neurone will have a high firing rate for contralateral sounds and a low firing rate for ipsilateral sounds (Fig, 1.4). The brain then uses information from changes in firing rate across the entire MSO (population coding) in each hemisphere to determine the lateral position of a sound (McAlpine and Grothe, 2003). However, further work will be required to tell whether this hypothesised mechanism for locating low frequency sounds proves to be correct.

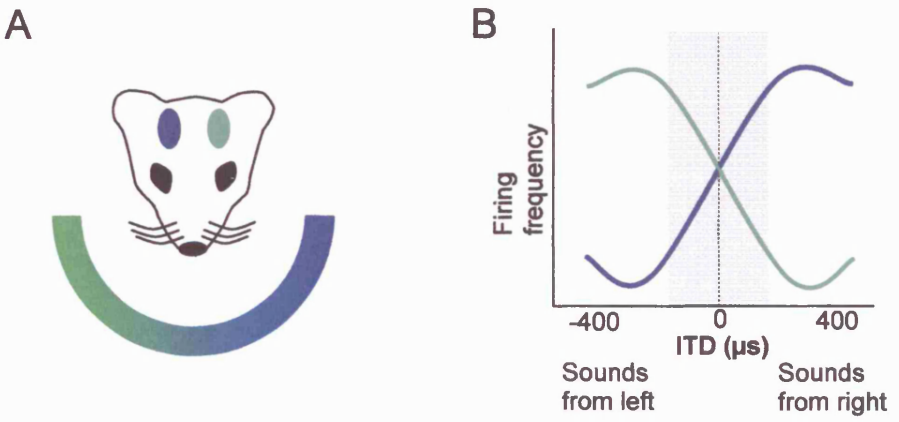

Figure 1.4. Current model of ITD sensitivity in mammals.
A. The relative activity of the entire population of MSO neurones encodes the position of sounds in the contralateral field. The left MSO (blue oval) detects the position of sound originating from the right side of the body. **B.** The tuning curves of each MSO are mirrored. Firing frequency in the left MSO (blue line) is highest for sounds originating from the right. The grey box represents physiological ITDs for the gerbil.

Perhaps the most interesting finding relevant to the role of the MNTB in sound source localisation was that blocking the inhibitory input from the MNTB effectively abolished ITD sensitivity in MSO neurones (Brand et al., 2002). Inhibition normally delays the contralateral postsynaptic potential (PSP, Fig, 1.5A) so firing is greatest when the ipsilateral input is lagging (contralateral sounds); hence the tuning curve is shifted to the right (Grothe, 2003). When inhibition is blocked, both EPSPs arrive simultaneously and coincide at zero ITD (Fig, 1.5B). The vital role of precisely timed inhibition from the MNTB in detecting ITDs (in the MSO) and ILDs (in the LSO) highlight the importance of preserving fidelity of information transfer across the CN to MNTB synapse (the calyx of Held); in this study we have investigated the roles of pre- and postsynaptic voltage-gated potassium channels in preserving such fidelity.

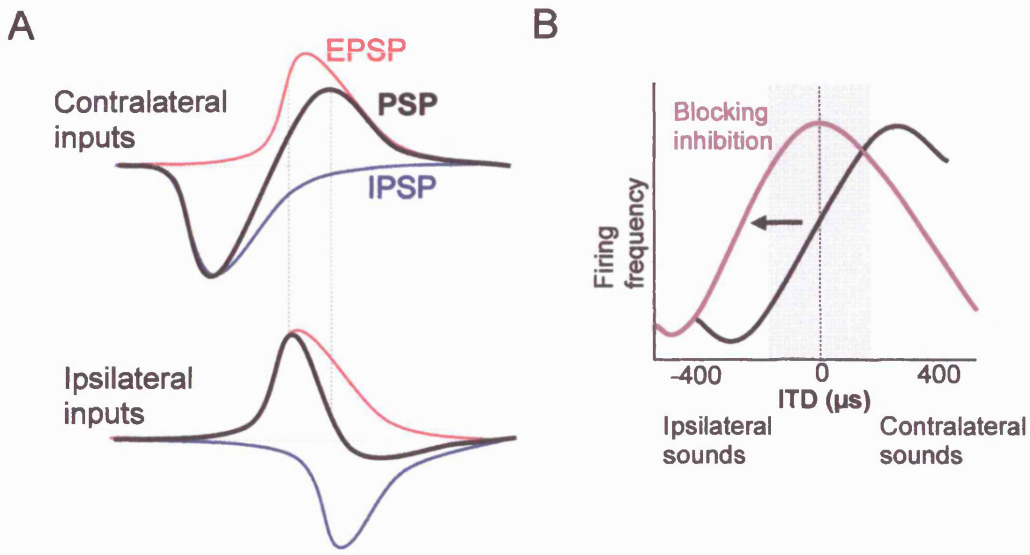

Figure 1.5. Role of inhibition in ITD sensitivity.
A. The postsynaptic potential (PSP) is delayed because the contralateral IPSP (from the MNTB) arrives before the contralateral EPSP. The ipsilateral IPSP (from the LNTB) arrives after the ipsilateral EPSP resulting in a shortened net PSP; consequently summation (and therefore firing rates) will be greatest when the ipsilateral input is lagging (i.e. contralateral sounds), so the tuning curve is shifted to the right. **B.** Blocking inhibition (purple line) means both EPSPs will arrive simultaneously; consequently firing rate will be greatest at zero ITD.

1.3 Potassium channels

1.3.1 Ion channels in excitable membranes

Cells are surrounded by a lipid membrane which acts as a permeability barrier. The lipid bilayer is composed of phospholipids orientated with their hydrophilic 'head' facing the solution and their hydrophobic tail pointing into the membrane. The hydrophobicity of the bilayer core prevents charged molecules from diffusing through the membrane; therefore the cell is able to regulate the passage of ions across the membrane. This regulation is achieved by integral proteins which span the membrane, forming ion channels and carriers. Ion channels are gated pores which, when open allow the passive movement of ions down their electrochemical gradient. This movement of ions is important in many cellular processes including: excitation of nerves and muscles, secretion of hormones and neurotransmitters, and cell proliferation. All ion channels share a number of key features: First, they are membrane spanning proteins which form an aqueous pore at their core. Second, they are highly selective

for one (or sometimes several) ions. Third, they permit rapid, passive movement of ions down their electrochemical gradient, which is otherwise prevented by the hydrophobic lipid membrane. Finally channels are gated, so ionic flow is regulated by opening and closing of the channel. Gating can be influenced by a number of triggers including: voltage, changes in temperature (e.g. the capsaicin receptor), mechanical forces (e.g. epithelial stretch activated channels) and binding of ligands; including intracellular signalling molecules (Hille, 2001). In the absence of the appropriate trigger the probability that a channel will be open is low. However, once triggered (e.g. by ligand binding or a voltage change), the channel undergoes a rapid conformational change which increases the likelihood that it will be open. Carriers differ from ion channels in that they lack an aqueous pore; the carrier undergoes a conformational change to translocate the ion across the membrane. Like ion channels, carriers can transport ions passively down their concentration gradient; however, carriers can also actively pump ions against the gradient.

Ion channels can be broadly divided into two groups according to how their opening is triggered. As their name suggests, ligand-gated ion channels are opened by the binding of a specific ligand to a site on the outside of the channel. The family of ligand-gated channels includes the glutamate receptors (NMDA, AMPA and Kainate), the nicotinic acetylcholine receptor, glycine receptors, $GABA_A$ receptors and P2X receptors. Voltage-gated channels are also aptly named, opening as a result of changes in the cell membrane potential. The voltage-gated channel family is a large family including potassium, sodium, calcium, chloride and non-selective channels. A common feature of voltage-gated channels is their four fold symmetry around the pore which can either be achieved by the union of four subunits (e.g. potassium channels) or four domains of a singe protein (e.g. sodium and calcium channels Aidley and Stanfield, 1996). Voltage-gated channels also possess charged domains, which move through the membrane in response to changes in membrane potential and hence confer voltage sensitivity to these channels.

In this study we investigated the role of voltage-gated potassium channels in regulating excitability in the auditory brainstem. Potassium channels form a large, diverse group of proteins which account for nearly 1% of the human genome (Hille, 2001). The group can be

somewhat coarsely divided into three according to the number of transmembrane domains (TMD) the α-subunits have. The first group which have 2TMDs, are the inward rectifier (Kir) K^+ channels. These channels are essentially just a potassium selective pore; the groups with more TMDs 'bolt on' additional regions (such as a voltage sensor) to this central pore. The second group, known as the twin-pore K^+ channels, have 4TMDs. The third group have 6TMDs and include the voltage-gated (Kv) and the Ca^{2+}-activated K^+ channels. These groupings can be further divided into families (e.g. Kv) and then into sub-families (e.g. Kv1) which contain closely related subunits. There are some channels which do not strictly fit into the three groups since they have an unusual number of TMDs. These include Ca^{2+}-activated K^+ channels which have 7TMDs and TOK twin-pore K^+ channels which have 8TMDs; however, these can be considered as 6TMD and 4TMD respectively since they share many similarities with other channels in those groups.

All potassium channels have a common sequence which confers their selectivity to K^+. This sequence contains the residues -Gly-Tyr-Gly- (or in some cases -Gly-Phe-Gly-) in the pore region (Heginbotham et al., 1992). Deletion of Tyr-Gly results in rather non-selective channels similar to the cyclic nucleotide-gated (CNG) channels (Heginbotham et al., 1994). Although we have concentrated on voltage-gated (Kv) channels in this study, I will briefly describe some of the salient features of the other types of potassium channels to highlight how Kv channels are distinct from these other channels.

1.3.2 Inward rectifiers

The inwardly rectifying potassium channels (Kir) are tetramers composed of four 2TMD subunits. The two membrane-spanning regions are linked by the P domain that forms the selectivity filter and pore. Kir channels are open at membrane potentials near to, or more negative than, the resting potential and allow potassium ions to flow inwards with a near-linear current-voltage relationship (Aidley and Stanfield, 1996). However, the channels do not pass outward current in the same linear fashion, with strong rectifiers almost preventing K^+ efflux at potentials more positive to E_K. This rectification in the current-voltage relationship is not due to conformational changes of the channels, since they lack a

voltage-sensing region (Coetzee et al., 1999); instead inward rectification is achieved due to the ability of Mg^{2+} ions and polyamines to block the channel pore (Jan and Jan, 1997). The inward rectifying channels also include the ATP sensitive K^+ channels (K_{ATP}). Kir6 subunits form the pore of these channels but have to associate with sulphonylurea receptor (SUR) subunits, which is important increasing the ATP sensitivity but also has a role in masking endoplasmic reticulum (ER) retention sequences necessary for surface expression (Zerangue et al., 1999).

1.3.3 Twin-pore channels

The 4TMD potassium channels are known as the twin-pore potassium channels; the name of which is somewhat misleading. Rather than having two pores in the channel, each subunit contains two P-domains and is constructed as a tandem of two 2TMD subunits (Brown, 2000; Goldstein et al., 2001). Functional channels form as dimers so the four P regions come together to form a single pore, retaining four-fold symmetry (Patel and Honore, 2001). The twin-pore channels can be coarsely divided into five functionally and structurally similar groups (Fig, 1.6; and Mathie and Clarke, 2002): The TWIK family (TWIK-1, TWIK-2 and KCNK7), the TREK family (TREK-1, TREK-2 and TRAAK), the TASK family (TASK-1, TASK-3 and TASK-5), the TALK family (TALK-1, TASK-2 and TASK-4) and the THIK family (THIK-1 and THIK-2). To date expression of seven of these genes has been identified in the CNS (Talley et al., 2001). Twin-pore K^+ channels are open at most membrane potentials and do not inactivate which has led to them being termed 'background' or 'leak' channels. Although these channels are virtually insensitive to voltage, different members of the family can be modulated by a variety of stimuli (Lesage and Lazdunski, 2000). TWIK channels, which are weakly inward rectifying, are activated by protein kinase C (PKC) but inhibited by low pH; similarly TASK channels are also regulated by external pH. In contrast, TRAAK and TREK channels are activated by fatty acids and mechanical stimuli. The voltage properties and regulation of these channels means that modulation of twin-pore K^+ channels can have profound effects on neuronal excitability (Millar et al., 2000; Chemin et al., 2003; Meuth et al., 2003).

1.3.4 Six transmembrane domain channels

The 6TMD channels have a similar pore region and four-fold symmetry to the inward rectifiers and the twin-pore K^+ channels, but their extra transmembrane regions allow them to sense voltage. In addition, several members of the 6TMD channels have extended c-termini with sequences that make them sensitive to second messengers. Before I describe Kv channels in detail, I shall briefly describe some of the other 6TMD K^+ channels.

1.3.4.1 KCNQ channels

KCNQ channels (Kv7) are similar in structure to the Kv channels; possessing 6TMDs. However, they lack a tetramerisation domain and hence form functional channels via interactions with accessory subunits or by forming heteromers with other subunits (Ashcroft, 2000). There are five members of the KCNQ family which differ in the length of their C-termini (which can have many modulatory sites, Robbins, 2001). Linkage with cardiac arrhythmias led to the identification of the KCNQ1 gene which encodes the channel underlying a cardiac delayed rectifier current (I_{Ks}); the four other KCNQ genes were later identified based on sequence homology. Mutations in KCNQ1 result in the prolongation of the cardiac AP responsible for long QT syndrome (Wang et al., 1996a; Ashcroft, 2000; Jentsch, 2000; Shieh et al., 2000). In addition to forming homomeric channels, KCNQ2 and KCNQ3 (or KCNQ3 and KCNQ5) can produce heteromeric channels which generate the M-current (Wang et al., 1998a; Jentsch, 2000). Mutations in these KCNQ subunits are associated with benign familial neonatal epilepsy (Ashcroft, 2000; Jentsch, 2000). KCNQ4 is expressed in vestibular and cochlear hair cells and throughout the auditory system including the LSO (Kharkovets et al., 2000). It is thought that KCNQ4 and KCNQ1 channels may play a role in potassium recycling in cochlea OHCs (Vetter et al., 1996; Kubisch et al., 1999; Jentsch, 2000). Consistent with this hypothesis, people with mutations in KCNQ4 channels suffer from dominant deafness (DFNA2) and KCNQ1 mutations can result in Jervell and Lange-Nielsen syndrome, which manifests itself as deafness associated with cardiac arrhythmia (Jentsch, 2000).

1.3.4.2 *Ether-à-go-go* (EAG) K^+ channels

Ether-à-go-go (EAG) channels earned their peculiar name from *Drosophila* with mutations in their EAG gene which resulted in leg-shaking behaviour when anaesthetised with ether (Warmke et al., 1991). Like Kv channels, EAG channels have a 6TMD structure and conserved P-domain, but they also possess a cyclic-nucleotide binding domain on their N-terminus (Bauer and Schwarz, 2001). The EAG (or KCNH) channels are widely expressed in the heart and brain (including the SOC) and can be divided into three sub-families: eag (Kv10), erg (Kv11) and elk (Kv12) (Saganich et al., 2001). Interestingly, members of the EAG family differ markedly in their gating properties. Elk2 and erg channels are closed and deactivated at negative potentials; strong depolarisation only elicits a small transient then sustained current, but upon repolarisation a large transient current occurs (Ashcroft, 2000). These properties can be explained by inverse gating properties; where inactivation occurs faster than activation and recovery from inactivation is faster than deactivation (Bauer and Schwarz, 2001). In contrast, eag and elk1 channels produce typical delayed rectifying currents. The most widely studied member of the EAG channels is erg1 (or HERG) which contributes to repolarisation of the cardiac AP.

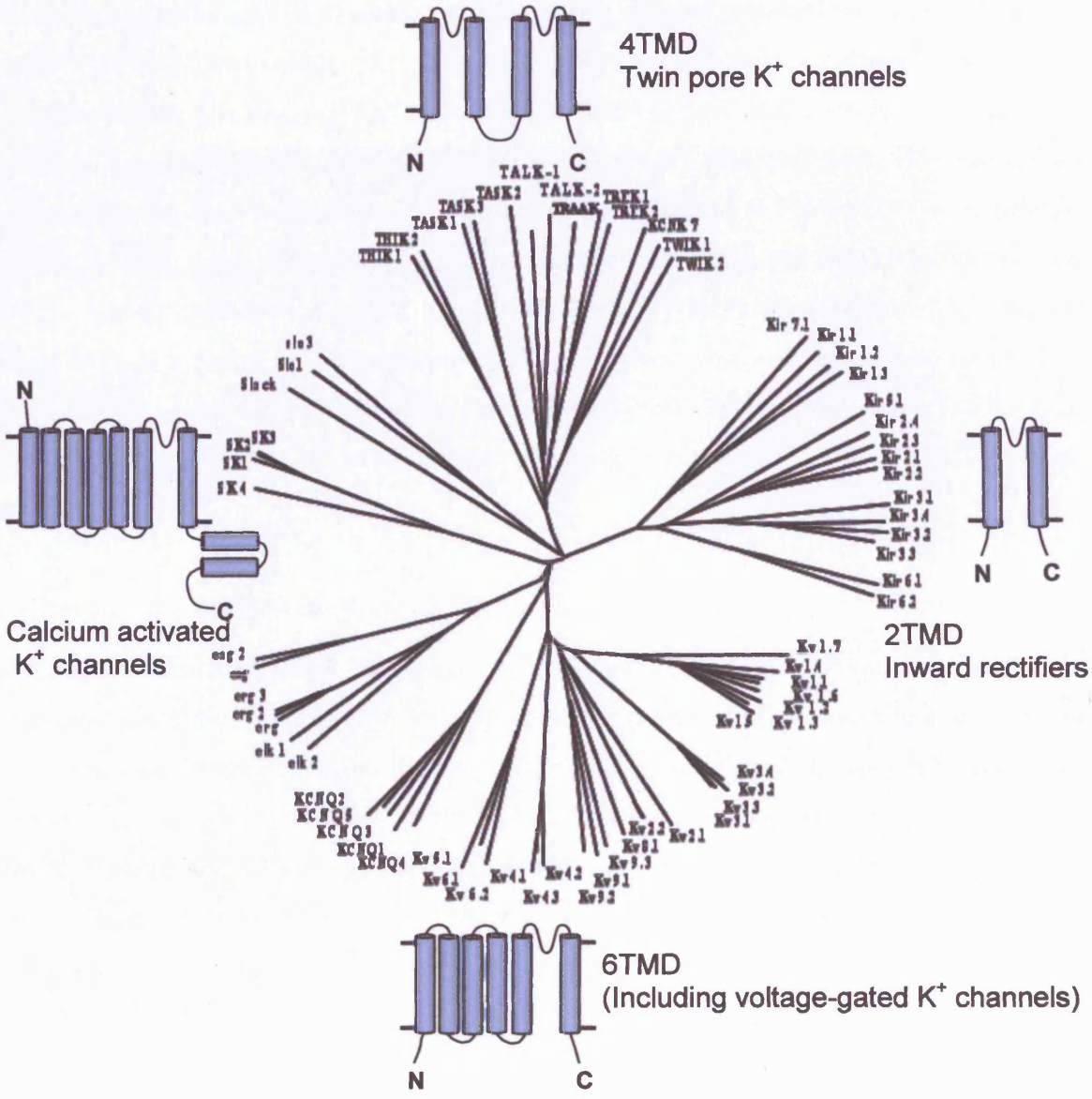

Figure 1.6. K^+ channel diversity.
Dendrogram of cloned mammalian K^+ channels.

1.3.4.3 Calcium activated potassium channels

Calcium activated K^+ channels (K_{Ca}) have a similar structure to other 6TMD channels but have an additional TMD (S0), an intracellular N-terminus and an extracellular N-terminus. The intracellular C-terminus contains a calcium sensing 'bowl'; binding of calcium to this region is thought to shift the voltage dependence of the channel (Vergara et al., 1998). K_{Ca}

channels can be classified according to their single channel conductance (Ashcroft, 2000); small (SK) and intermediate (IK) conductance channels are weakly voltage dependent but sensitive to very low levels of Ca^{2+} (<500nM), whereas large conductance K_{Ca} channels (BK) are more voltage dependent and are activated by higher Ca^{2+} concentrations. BK channels are encoded by the Slo1 gene which has two homologues (Slo2 and Slo3) that also encode K^+ channels. Slo2 (originally called Slack) encodes channels which are cooperatively activated by Na^+ and Cl^- (Joiner et al., 1998; Yuan et al., 2003). These sodium-activated K^+ channels (K_{Na}) have been found in brainstem neurones, cardiac myocytes and motorneurones and may be important in ischaemic protection (Dryer et al., 1989; Martin and Dryer, 1989). Slo3 encodes a pH dependent K^+ channel originally identified in spermatocytes (Schreiber et al., 1998).

1.3.4.4 Cyclic nucleotide-gated channels

Although similar to 6TMD K^+ channels, cyclic nucleotide-gated (CNG) channels lack the K^+ selectivity residues (Gly-Tyr-Gly) in the pore lining region and hence are non-selective ion channels. The C-terminal region harbours a cyclic-nucleotide binding motif which, like K_{Ca} channels, affects the voltage dependence of the channels (Kaupp and Seifert, 2002). The family includes the cGMP-gated channels important in signal transduction in photoreceptor cells and the olfactory bulb and HCN channels which underlie I_H currents. I_H was originally found in the heart (Noma and Irisawa, 1976; originally called the funny current, If, Brown et al., 1979; DiFrancesco, 1993) but has since been identified in neurons throughout the CNS (Pape, 1996; Santoro and Tibbs, 1999). Four HCN subunits have been identified which not only differ in their expression pattern (Santoro and Tibbs, 1999) but homomeric channels also differ in their activation and deactivation kinetics (Robinson and Siegelbaum, 2003; Santoro and Baram, 2003). In addition to forming homomeric channels, HCN subunits are able to form heteromers in expression systems (Ulens and Tytgat, 2001). The expression of multiple HCN subunits in single cells and the similarity between some heteromeric HCN currents and native currents has led to the suggestion that heteromers may be commonly found *in vivo* (Robinson and Siegelbaum, 2003). I_H generally activates at negative potentials, but its activation can be shifted in the positive direction by direct binding of cAMP (DiFrancesco and Tortora, 1991). In spontaneously firing cells I_H contributes to the pacemaker depolarisations

involved in rhythmic activity (McCormick and Pape, 1990; Pape and McCormick, 1990; Bal and McCormick, 1997). In non-pacemaking cells I_H contributes to resting potentials and can regulate the response to depolarisation or hyperpolarisation (Pape, 1996; Luo and Perkel, 1999; Magee, 1999).

1.4 Voltage-gated potassium channels

The voltage-gated or Kv channels form the largest group of the 6TMD K^+ channels; they were also the first K^+ channels to be cloned. Shaker channels (Kv1 homologue) were identified from a *Drosophila* mutation that resulted in a shaking wing (Papazian et al., 1987) and three other Kv homologues were also identified: *Shab* (Kv2), *Shaw* (Kv3) and *Shal* (Kv4, Salkoff et al., 1992). Owing to the number of Kv subunits subsequently cloned, the Kv channel nomenclature has been recently reorganised according to gene families (Fig, 1.6; Catterall et al., 2002). The KCNA gene encodes Kv1.1-Kv1.8; KCNB, Kv2.1-Kv2.2; KCNC, Kv3.1-Kv3.4; KCND, Kv4.1-Kv4.3; KCNF, Kv5.1; KCNG, Kv6.1-Kv6.4; KCNS, Kv9.1-Kv9.3 and KCNV, Kv8.1-Kv8.3. The first four families (Kv1-Kv4) can form functional homomeric or heteromeric channels with members of the same subfamily (i.e. four Kv1 alpha-subunits may form a heteromeric channel Coetzee et al., 1999). The remaining 'electrically silent' families (Kv5, Kv6, Kv8 and Kv9) are unable to form functional homomeric channels but instead coassemble with Kv1-Kv4 subunits resulting in channels with modified properties (Post et al., 1996; Castellano et al., 1997; Salinas et al., 1997; Kramer et al., 1998; Kerschensteiner and Stocker, 1999; Ottschytsch et al., 2002).

1.4.1 Kv channel structure

Figure 1.6 shows the membrane topology of a Kvα subunit. Like other 6TMD channels, Kvα subunits have a charged S4 domain which is important in voltage sensing and a P domain which contains the GYG residues that form the selectivity filter (green line Fig, 1.7); Kvα subunits also form tetramers retaining the K^+ channel four-fold symmetry around the pore. Recently, the crystal structures of several bacterial potassium channels have been solved

(KcsA Doyle et al., 1998; KvAP Jiang et al., 2003b), which have enabled further understanding of the selectivity, permeation, voltage sensing and gating of K^+ channels.

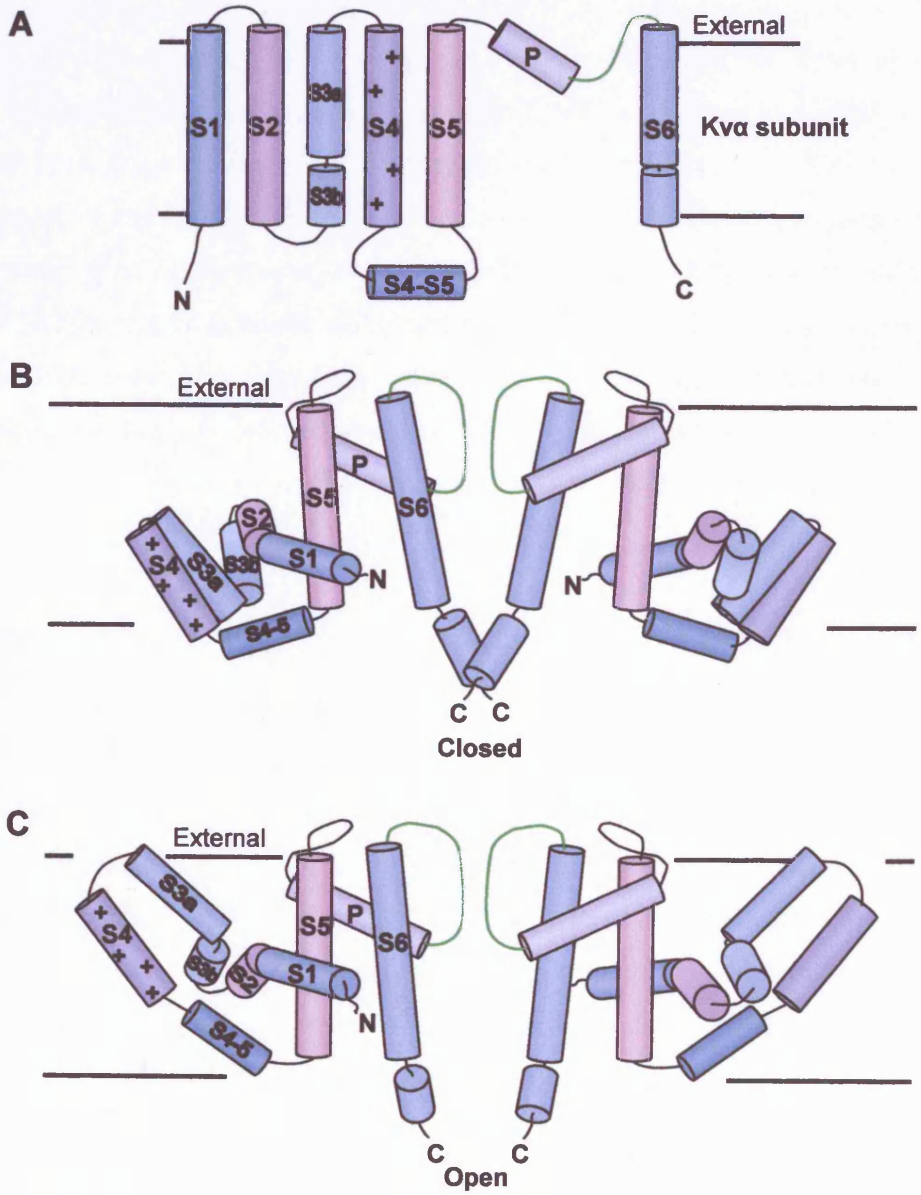

Figure 1.7. Voltage-gated K^+ channel structure.
A. Membrane topology of a Kvα subunit. **B.** Two Kvα subunits arranged in the closed conformation. The selectivity filter is shown in green. **C.** Two Kvα subunits arranged in the open conformation. S4 moves towards the external surface, causing a twisting of S6 which opens the pore. (Diagram after Jiang et al., 2003a).

1.4.1.1 The pore region identified in KcsA

The KcsA channel is encoded by a gene cloned from *S. lividans* on the basis of homology to the GYG motif in the P domain (Shieh et al., 2000). Although the KcsA channel has no voltage sensing regions because it contains only 2TMD (equivalent to S5 and S6) connected by a P domain, it has enabled understanding of the K^+ channel pore. X-ray analysis of the crystal structure has revealed that four subunits come together forming an inverted tepee with the selectivity filter of the pore at its outer end (Doyle et al., 1998). The overall length of the pore is 45Å, varying in diameter along its length. The internal vestibule begins as a narrow tunnel for the initial 18Å, before it widens into a cavity ≈10Å in diameter. The narrow selectivity filter is 12Å long, lined by carbonyl oxygen atoms of the GYG sequence structurally held open to accommodate K^+ ions but not smaller ions (e.g. Na+, Doyle et al., 1998).

1.4.1.2 K^+ permeation

The elucidation of the KcsA structure revealed details that enabled understanding of how K^+ channels allow the rapid permeation of K^+ ions, whilst retaining selectivity. Ions are particularly stable in solution since they are surrounded by water molecules; in order for an ion to pass though a channel, it must be equally stable inside the channel. K^+ channels have four features to maintain this stability (Fig, 1.8). First, the pore contains a central-cavity as described above; this cavity contains a large amount of water which stabilises the K^+ ions (Yellen, 2002). Second, the transmembrane helices which line the pore have a dipole moment, with the negative ends pointing towards the channel centre (Doyle et al., 1998). It is thought that these dipoles stabilise positively charged ions at the entrance to the selectivity filter (Roux and MacKinnon, 1999). Perhaps the most important feature of the pore with regard to selectivity and permeation is the selectivity filter. The selectivity filter contains carbonyl oxygen atoms; each K^+ ion in the filter is surrounded by two-groups of four oxygen atoms which mimic the hydration shell of K^+ ions in solution and thus stabilises the ions (Zhou et al., 2001b). The final aid to permeation is the electrostatic repulsions created

between K^+ ions as they are forced to travel in single file. The selectivity filter creates four stable sites; two K^+ ions at a time move through the filter, separated by water molecules (Morais-Cabral et al., 2001). The electrostatic repulsions between K^+ ions destabilises them in the pore so occupancy of the four sites is short-lived; as a third ion enters, the first is expelled.

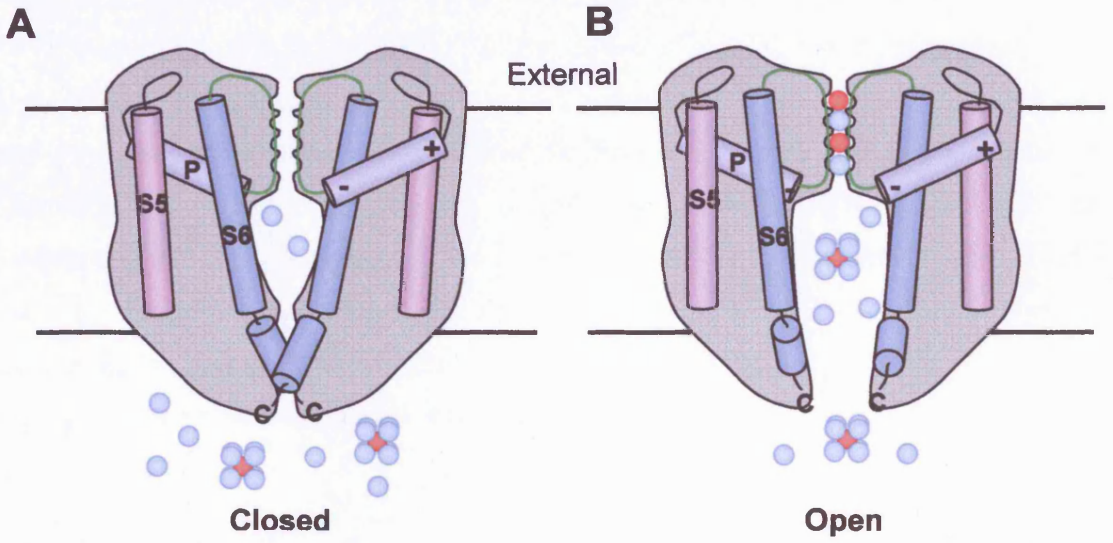

Figure 1.8. K^+ permeation.
A. Pore region of a closed K^+ channel. The central water-filled cavity is enclosed by S6. K^+ ions (red spheres) are surrounded by their waters of hydration (blue spheres) **B.** In the open conformation K^+ ions are attracted to the selectivity filter (green) by the dipole moments of the P-region. The K^+ ions then exchange their waters of hydration for the stable interaction with carbonyl oxygen atoms lining the selectivity filter. Electrostatic repulsions keep K^+ ions apart and cause them to move through the channel.

1.4.1.3 Voltage sensing and activation determined in the KvAP channel

Since the KcsA channel is essentially only an ion pore, investigation of voltage sensing required examination of another channel. The problem is that the X-ray structure of most K^+ channels has been elusive due to the difficulties in crystallisation; probably because of the motility of the voltage sensing region (Jiang et al., 2003b). However, the stability of KvAP channels from the thermophile *Aeropyrum pernix* facilitated their crystallisation (although they also had to employ other tricks to improve the stability, see Jiang et al., 2003b). This enabled the first detailed examination of the structure of the voltage-sensing region of a voltage-gated ion channel. It was previously thought that S4 acted as a corkscrew to open Kv

channels (Aidley and Stanfield, 1996); however, it has now been proposed that the charged S4 region forms part of a 'voltage paddle' attached to the side of the pore region (Jiang et al., 2003a). In its closed conformation the paddle lies close to the intracellular surface; upon depolarisation, the arginine residues cause S4 to move towards the outer surface of the membrane, resulting in conformational changes in S6 which open the channel (Fig, 1.7). Mackinnon and colleagues present a convincing case for such a method of voltage-sensing in KvAP (Jiang et al., 2003b; Jiang et al., 2003a; Ruta et al., 2003), but several lines of evidence suggest that voltage-sensing in eukaryotic Kv channels may be different (Cohen et al., 2003). Perhaps the most important concern is whether the KvAP voltage sensor is conserved across eukaryotic Kv channels; examination of residues in S1-S4 suggests that there maybe considerable differences, particularly in S3b and the S4-S5 linker (Cohen et al., 2003). In addition, mutation studies suggest that S4 may interact with sites on the channel that are not possible in the proposed KvAP structure, suggesting that S1-S4 may have a more vertical arrangement as previously thought (Cohen et al., 2003; Laine et al., 2003).

1.4.2 Kv channel inactivation

In addition to the deactivation of Kv channels (which is brought about by movements in S6 to the closed conformation), Kv channels can also undergo inactivation (Yellen, 2002). This inactivation can either be rapid, N-type or slower C-type inactivation.

1.4.2.1 N-type inactivation

The rapid inactivation observed in some Kv channels is also called 'ball and chain gating' because the distal region of the N-terminus (originally thought to be a ball, chained by the rest of the N-terminal region) snakes into the cavity region to block the channel (Fig, 1.9; Zhou et al., 2001a). N-type inactivation can either be caused by the N-terminus of certain Kvα (Hoshi et al., 1990) or Kvβ subunits associated with the channel (Rettig et al., 1994). Once the S6 regions have opened the channel, the N-terminal 'ball' can gain access to the cavity. N-type inactivation is rapid, generally channels have completely inactivated within 20ms (Coetzee et al., 1999). Since each Kv channels consists of four subunits associated with up to four Kvβ subunits (Xu et al., 1998), there are potentially eight 'inactivating ball and chains'. Even

though each functions independently and only one is needed for inactivation to occur, the more inactivating 'balls' present, the faster the inactivation (Xu et al., 1998).

1.4.2.2 C-type inactivation

Slower inactivation of Kv channels occurs as a result of a 'pinching' of the selectivity filter resulting in decreased conductance through the pore (Fig, 1.9; Liu et al., 1996; Yi and Jan, 2000). The partial collapse of the selectivity filter has been observed upon crystallisation of KcsA channels in low [K^+] (Zhou et al., 2001b). In a state of C-terminal inactivation, some K^+ channels can conduct Na^+ (when K^+ is removed), suggesting that only a slight constriction of the selectivity filter occurs (Kiss et al., 1999).

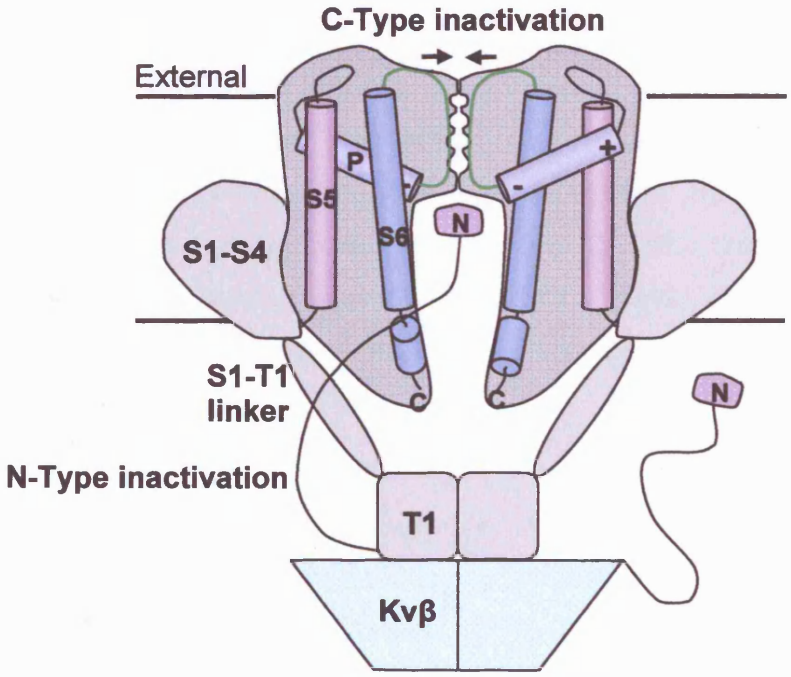

Figure 1.9. Inactivation of voltage gated K^+ channels.
C-type inactivation occurs as a result of a narrowing of the selectivity filter. N-type inactivation occurs where the N-termini of certain Kvα or Kvβ subunits snakes into the central cavity to block the channel (after Yi and Jan, 2000).

1.4.3 Channel formation

Four Kvα subunits associate to form tetrameric channels, either as homomers containing four identical Kvα subunits or heteromers with different Kvα subunits. However, heteromers can only be formed with other members of the same subfamily (with the exception of the 'electrically silent' subunits, Coetzee et al., 1999). This specificity for members of the same subfamily is conferred by the tetramerisation domain (T1, see Fig, 1.9) on the N-terminus (Shen et al., 1993; Babila et al., 1994). Deletion of T1 results in formation of tetramers with other subfamilies but at a lower efficiency (Tu et al., 1996). Kvα subunits associate whilst still in the ER (Rosenberg and East, 1992; Shen et al., 1993; Babila et al., 1994; Deal et al., 1994; Nagaya and Papazian, 1997; Schulteis et al., 1998) and the T1 tetramers form while their nascent Kvα subunit is still attached to the ribosome (Lu et al., 2001). The association of Kvα T1-regions is thought to bring the transmembrane regions into close proximity required for channel tetramerisation (Deutsch, 2002). It has been demonstrated that homomeric Kv1.3 channels first form as dimers and then two dimers associate as a heteromer (Tu and Deutsch, 1999) although whether this is the case for heteromeric channels remains to be determined (see section 7.2.2.2 for further discussion) . Since only a limited number of subunit combinations have been detected in the brain (Koch et al., 1997; Shamotienko et al., 1997; Koschak et al., 1998; Coleman et al., 1999; Wang et al., 1999a), it seems that *in vivo* there may be further mechanisms which regulate heteromer formation.

1.4.3.1 Accessory subunits

In addition to Kvα subunits, some voltage-gated K^+ channels (e.g. Kv1) can contain up to four Kvβ subunits (Xu et al., 1998; Pongs et al., 1999), which bind to the T1 domain (see Fig, 1.9) on the Kvα subunit N-teriminus (Gulbis et al., 1999). These accessory subunits can modify activation and inactivation of the channel (discussed in section 7.3.1.4), increase surface expression or a particular subcellular localisation (see section 7.2.3.2) and may have an oxoreductase function (Accili et al., 1997; Nagaya and Papazian, 1997; Gulbis et al., 1999; Pongs et al., 1999; Bahring et al., 2001; Campomanes et al., 2002; Gu et al., 2003).

1.4.4 Function of Kv channels

K^+ channels play important roles in regulating many aspects of cellular development and excitability including: heart rate, smooth muscle contraction, immune response, neuronal excitability, insulin secretion, cell volume regulation, and epithelial electrolyte transport (Shieh et al., 2000). However, since this study is concerned with neuronal Kv channels, I shall limit discussion to the regulation of neuronal excitability.

1.4.4.1 The role of Kv channels in regulating AP firing

Action potentials are triggered by voltage-gated sodium channels; activation of these channels causes Na^+ influx, resulting in rapid depolarisation of the cell (the up-stroke of the AP). This depolarisation activates high-voltage activated K^+ channels (e.g. Kv3); K^+ efflux through these channels, combined with rapid inactivation of Na^+ channels causes repolarisation of the AP (Hodgkin et al., 1949; Hodgkin and Huxley, 1952; Aidley and Stanfield, 1996). K^+ channels which open at more negative voltages (e.g. Kv1 channels) also play a role in AP firing by opposing small depolarisations and hence preventing activation of Na^+ channels.

1.4.4.2 Low-voltage activated channels

K^+ channels which are open at negative voltages both contribute to the resting potential and regulate AP threshold. In many auditory neurones it is important that each synaptic stimulus only results in a single postsynaptic AP to preserve faithful encoding of AP trains. Consequently low-voltage activated K^+ channels (of the Kv1 family) activate during an AP, causing hyperpolarisation of the membrane potential and preventing generation of subsequent APs (Brew and Forsythe, 1995; Dodson et al., 2002; Brew et al., 2003). In presynaptic terminals, Kv1 channels prevent the generation of aberrant APs during the depolarisation that follows each AP (Dodson et al., 2003). These functions are described in more detail in chapters 4 and 5. Similar low-voltage activated K^+ channels, localised to somatodendritic regions, may play a role in coincidence detection by causing the rapid decay of EPSP (by decreasing the membrane time-constant, see section 2.2.1.2) so only coincident inputs summate to trigger an AP (Rothman and Manis, 2003). Similarly, A-type channels rapidly

inactivate during an EPSP, reducing the threshold for a coincident EPSP to trigger firing (Pongs, 1999).

1.4.4.3 High-voltage activated channels

Kv channels which activate at potentials more positive than around -30mV generally only open during an AP; consequently these channels play important roles in regulating AP duration and frequency. AP repolarisation is mediated in part by inactivation of sodium channels but also by delayed rectifier channels (see section 1.4.4.1). In chapter 6, I discuss how Kv3 channels generate extremely brief APs. In some cases, inactivating K^+ channels contribute to AP repolarisation; inactivation of A-type channels causes a gradual broadening of presynaptic APs during repetitive activity and is involved in activity-dependent facilitation of transmitter release (Jackson et al., 1991; Geiger and Jonas, 2000). Inactivation of A-type K^+ channels can also be important in regulating inter-spike interval and hence oscillatory firing rates; the delay between spikes is caused by hyperpolarisation before the A-current has inactivated (Connor and Stevens, 1971; Pongs, 1999). High-voltage activated channels can also be involved in the generation of after-hyperpolarisations (AHPs) following an AP. AHPs can be important in the rapid recovery of sodium channels from inactivation necessary to support high frequency firing (McIntyre et al., 2002).

1.4.4.4 Kv channels and disease

Mutations in the KCNA1 gene (which encodes Kv1.1) have been implicated in both episodic ataxia type 1 (EA1 Browne et al., 1994) and epilepsy (Smart et al., 1998; Spauschus et al., 1999). Episodic ataxia is a rare neurological disorder which gives rise to short attacks of cerebellar incoordination, triggered by stress or excitement (Ashcroft, 2000; Kullmann, 2002). Over a dozen EA1 mutations have been identified, occurring in conserved regions throughout the channel except the N terminus and selectivity filter (Kullmann, 2002). Examination of these mutations in channels expressed in oocytes has revealed changes in current amplitudes and gating kinetics (Adelman et al., 1995; Zerr et al., 1998; D'Adamo et al., 1999; Spauschus et al., 1999; Zuberi et al., 1999; Eunson et al., 2000; Rea et al., 2002). The observation that EA1 sufferers sometimes experience epilepsy (Zuberi et al., 1999), combined with the

susceptibility of Kv1.1 null mice to seizures (Smart et al., 1998) has led to the suggestion that Kv1.1 mutations may underlie other cases of epilepsy.

1.4.5 Kv channel pharmacology

Voltage-gated potassium channels can be blocked by a variety of pharmacological agents which vary in their potency and selectivity. We have employed several of these agents, including highly specific toxins, to dissect out different components of the current in MNTB neurones and their presynaptic terminals. In this section I shall give a brief overview of some of the compounds which block Kv channels.

Some of the less specific Kv blockers include 4-aminopyridine (4-AP) and tetraethylammonium (TEA). 4-AP will block Kv1-Kv3 channels at concentrations of less than 1mM, although higher concentrations are required to block Kv4 channels. Similarly, at concentrations above 10mM, TEA will block most Kv channels (except Kv4's) and some other types of K^+ channels (Coetzee et al., 1999). However TEA does show some selectivity, only blocking Kv3 channels and Kv1.1 homomers at low concentrations (IC_{50}'s <0.2mM and 0.5mM respectively, Coetzee et al., 1999). Another compound which shows some selectivity is CP339,818. This compound is most selective for Kv1.3 and Kv1.4 (IC_{50}'s of 0.23 and 0.3μM, Nguyen et al., 1996) but at higher concentrations it will also block other Kv channels (IC_{50}>14μM).

Generally, peptidergic toxins from the venom of scorpions, snakes, spiders, sea anemones and sea snails are more specific than other pharmacological agents. An example of such a toxin is dendrotoxin-I (DTX-I) from the venom of the black mamba (Strydom, 1977), which is specific for channels containing Kv1.1, Kv1.2 or Kv1.6 subunits (Stuhmer et al., 1989; Robertson et al., 1996; Harvey, 2001). The potency and selectivity of the pharmacological agents used in this study is listed in table 1. Peptidergic toxins are generally large molecules (several thousand Daltons), which bind to specific residues on Kvα subunits and plug the pore (Tytgat et al., 1995; Lipkind and Fozzard, 1997; Gasparini et al., 1998; Wang et al., 1999b; Ellis et al., 2001). Recently the method by which toxins bind to Kv1 heteromers was

examined by Hopkins (1998). In this study Hopkins coexpressed pairs of Kv1 subunits (Kv1.1/1.2, Kv1.1/1.4 and Kv1.2/1.4) in oocytes and examined block of the current by DTX-I, δ-DTX and tityustoxin-Kα (TsTX-Kα). He compared the proportion of the current blocked at different toxin concentrations with 3 models of toxin block: First, the single subunit model, where only one toxin-sensitive subunit is required for the toxin to block. This model assumes that the IC_{50} decreases linearly as the number of toxin-sensitive subunits is reduced. Second the energy additivity model, which is based on TEA binding to Kv1.1 homomers (Heginbotham and MacKinnon, 1992). In this model all subunits contribute to binding, so the IC_{50} decreases exponentially with the number of toxin-sensitive subunits present. Third, the dominant negative model, where a single toxin-insensitive subunit prevents block. This model was based on binding of charybdotoxin to Kv1.2/1.5 heteromers cloned from smooth muscle, where one insensitive subunit (Kv1.5, which differs in residues near the pore mouth) is enough to prevent charybdotoxin block (Russell et al., 1994). Hopkins found that block of Kv1.1/1.2 heteromers by DTX-I, δ-DTX and TsTX-Kα was well fit by the single subunit model. The single subunit model also best described block of Kv1.1/1.4 heteromers by δ-DTX and Kv1.2/1.4 heteromers by DTX-I but not by TsTX-Kα (Hopkins, 1998). TEA block however, follows the energy additivity model; the IC_{50} is reduced as the number of TEA-sensitive subunits increases (Christie et al., 1990; Hopkins, 1998). We have been able to exploit the single-subunit block by several toxins to determine the subunit composition of Kv1 channels in MNTB neurones and the calyx of Held (see chapters 4 and 5).

	IC_{50} (nM)						
	Kv1.1	**Kv1.2**	**Kv1.3**	**Kv1.4**	**Kv1.5**	**Kv1.6**	**Kv1.7**
Dendrotoxin-I (DTX-I)	3.1 (1)	0.13 (1)	ni	ni	ni	i	nd
Dendrotoxin-K (DTX-K)	0.03 (2)	ni	ni	ni	ni	nd	nd
Tityustoxin-Kα (TsTX-Kα)	ni	0.55 (3)	3.9 (4)	ni	ni	nd	nd
Noxiustoxin (NTX)	ni	2 (5)	1 (5)	ni	ni	nd	18 (6)
CP339,818 (see ref 7)	62000	14000	230	300	19000	20000	nd
Tetraethyammonium (TEA) ref 8	500000	ni	ni	ni	ni	17000000	ni

Table 1. Selectivity of K^+ channel blockers.
Values represent the concentration required to block 50% of the current (IC_{50}, recorded in oocytes unless otherwise stated). i = known to be inhibited, ni = not inhibited by <1μM, nd = not determined. (1. Hopkins et al., 1994) (2. CHO cells, Owen et al., 1997) (3. Hopkins, 1998) (4. Rodrigues et al., 2003) (5. Mammalian cells, Grissmer et al., 1994) (6. Kalman et al., 1998) (7. T cells, Nguyen et al., 1996) (8. Coetzee et al., 1999).

It is important to remember that in the majority of cases, pharmacological agents have only been tested on homomeric channels in expression systems. Since many Kv channels *in vivo* may be heteromers, one must be careful when interpreting block of native currents. Another potential problem with using pharmacological blockers is that they sometimes change the kinetics of a channel. 4-AP has been shown to slow activation and inactivation of Kv1 channels (Castle et al., 1994b; Castle et al., 1994a), consequently if subtractions are used it can appear as if 4-AP has blocked an A-current (see Forsythe and Barnes-Davies, 1993a). Since other blockers may also slow activation (e.g. DTX-I, Robertson et al., 1996) we generally avoid subtracting K^+ currents after pharmacological block. Further discussion on the use of subunit specific toxins is provided in section 7.3.1.7.

1.4.6 Presynaptic Kv channels

Although there is immunohistochemical evidence for localisation of Kv channels in presynaptic terminals (Wang et al., 1993), investigation of the function of these channels has been hampered by the small size of the majority of nerve terminals in the brain. In this study I exploited a giant synapse in the auditory pathway (the calyx of Held) to investigate presynaptic K^+ currents (see chapters 5 and 6). In addition to the calyx there are several other nerve terminals which are large enough to facilitate direct electrophysiological recording.

Examination of the currents at these terminals has provided some clues to the role of presynaptic K^+ channels.

Basket cells in the cerebellum provide the major inhibitory input to Purkinje neurones, forming basket terminals around the soma and pinceau on the axon hillock (Palay and Chan-Palay, 1974). Hence basket cells regulate the firing of Purkinje cells and exert control over the output of the cerebellar cortex. The unique structure of these inhibitory terminals has permitted direct electrophysiological examination of K^+ currents (Southan and Robertson, 1998b, 2000). Such recording demonstrated the presence of both low-voltage activated α-DTX sensitive currents and high-voltage activated TEA-sensitive currents, suggesting the involvement of Kv1 and Kv3 channels respectively. Consistent with these findings, immunoreactivity for Kv1.1, Kv1.2, Kv3.2 and Kv3.4 has been detected in basket cell terminals (Wang et al., 1994; Veh et al., 1995; Rhodes et al., 1997; Southan and Robertson, 2000). Blockade of the low threshold current by α-DTX results in an increase in the frequency and amplitude of spontaneous IPSCs (sIPSCs) in mature Purkinje neurons (Southan and Robertson, 1998a, b; Tan and Llano, 1999; Zhang et al., 1999), suggesting a role for the channels in preventing hyperexcitability (see section 7.4.2.2 for further discussion).

In addition to direct recordings, pharmacological blockade of K^+ channels has shown that Kv1 channels may be important in preventing hyperexcitability in a number of nerve terminals. In the entorhinal cortex, application of α-DTX increased both the frequency and amplitude of sIPSCs (Cunningham and Jones, 2001). Since DTX-K had no effect, it suggests that the channels responsible for preventing terminal hyperexcitability contain Kv1.2 and/or Kv1.6 but not Kv1.1. Kv1.2 containing channels also seem to be important in preventing hyperexcitability in thalamocortical axon terminals. Application of α-DTX increased the frequency of spontaneous EPSCs (sEPSCs) in layer V pyramidal neurons of the prefrontal cortex, mimicking the application of 5-HT (Lambe and Aghajanian, 2001). Once again, application of DTX-K and agitoxin2 (which blocks Kv1.1, Kv 1.3 and Kv 1.6) had no effect on sEPSCs, suggesting that the hyperexcitability was induced by blockade of Kv1.2 homomers. This intriguing result also suggests that Kv1.2 homomers play a role in 5-HT induced glutamate release. In the peripheral nervous system Kv1 channels also seem to be

important in regulating excitability at the neuromuscular junction. As in central axons like trapezoid body fibres and the optic nerve (Baba et al., 1999; Dodson et al., 2003), in peripheral nerves Kv1 channels are located at nodes of Ranvier and at the transition between the myelinated nerve and terminal region (Zhou et al., 1998b). Blocking these Kv1 channels with DTX-I or NTX results in repetitive discharge so that several end plate potentials are fired after a single stimulus (Anderson and Harvey, 1988; Vatanpour and Harvey, 1995); similarly, repetitive discharges were observed upon cooling in Kv1.1 null mice (Zhou et al., 1998b). These data suggest that Kv1 channels are involved in preventing hyperexcitability in both central and peripheral nerve terminals.

In the examples presented thus far, presynaptic Kv1 channels are important in preserving faithful transmission by preventing hyperexcitability; the slowly inactivating currents generated by these channels do not affect the AP waveform or $[Ca^{2+}]_i$ and are usually found alongside high threshold Kv3 currents. In other terminals however, rapidly inactivating currents have been identified which have a very different role in the regulation of transmitter release. In the hippocampus, mossy fibre axons form large boutons (MFBs) which synapse with CA3 pyramidal neurones. Direct recording from MFBs demonstrated the presence of a fast inactivating (A-type) K^+ current which is sensitive to TEA and α-DTX (Geiger and Jonas, 2000). Immunohistochemical labelling of these terminals has revealed that they contain Kv1.1, Kv1.4 and Kvβ1 subunits but not Kv1.2 or Kvβ2, suggesting that Kv1.1/1.4 heteromers (which may also contain Kvβ1 subunits) are responsible for the K^+ currents. These A-type currents contribute to AP repolarisation and hence activity dependent facilitation of transmitter release.

Another terminal that permits direct electrophysiological recording is the neurohypophysis terminal of the pituitary. Like the MFBs, in these neuropeptide releasing terminals cumulative inactivation of an A-type K^+ channel during trains of stimulation results in a 37% increase in AP half width, increasing Ca^{2+} entry and therefore potentiating transmitter release (Jackson et al., 1991). This rapidly inactivating A-current activates around -60mV, is sensitive to millimolar concentrations of 4-AP and is not blocked by TEA (Thorn et al., 1991). The low

activation threshold and aminopyridine sensitivity suggest the involvement of Kv1.4 or members of the Kv4 family in these currents.

1.4.7 K^+ currents in MNTB neurones and their presynaptic terminals

As already described in section 1.1.2.2, MNTB neurones convert an excitatory input to an inhibitory output, preserving the temporal pattern of APs necessary to determine a sounds location. In this study we dissected out components of the outward K^+ current in MNTB neurones and their presynaptic terminals. Here I shall describe previous investigations of these currents.

Intracellular recordings from MNTB neurones showed non-linear current-voltage relationships and single AP firing in response to sustained depolarisation (Wu and Kelly, 1991; Banks and Smith, 1992). Application of 4-AP resulted in the firing of multiple broadened APs, suggesting that potassium currents were responsible for AP repolarisation and preserving unitary firing (Banks and Smith, 1992; Forsythe and Barnes-Davies, 1993a). Further investigation of the K^+ currents by Brew and Forsythe (1995) demonstrated that MNTB neurones possessed two currents which differed in their activation range. The low-voltage activated current was blocked by DTX-I, indicating that Kv1 channels were responsible; whereas the high-voltage activated current was sensitive to 1mM TEA, suggesting that it was mediated by Kv3 channels.

Examination of the K^+ currents at the calyx of Held revealed 4-AP sensitive currents with a non-linear current-voltage relationship like that of MNTB neurones, suggesting that similar channels might be expressed presynaptically (Forsythe, 1994). However, multiple firing was observed in response to sustained depolarisation, suggesting that there may be differences in the low-voltage activated currents.

CHAPTER 2 - Methods

2.1 Thin-slice preparation

2.1.1 Solutions

On the day prior to experimentation, artificial cerebrospinal fluid (aCSF; see appendix 1) was prepared. Stock solutions (x10) of aCSF and low-sodium aCSF which contained all the constituents except the $NaHCO_3$, $MgCl_2$, $CaCl_2$ (and sucrose for low-sodium aCSF) were defrosted and poured into 2l conical flasks. 104ml $NaHCO_3$ (0.5M) was added to both stock solutions and 171g sucrose to the low-sodium aCSF. The solutions were then made up to around 1.9l with distilled water. Solutions were gassed with 95% O_2, 5% CO_2 for at least 20 minutes before addition of $MgCl_2$ and $CaCl_2$ (1M). 8ml $MgCl_2$ and 0.2ml $CaCl_2$ was added to the low-sodium aCSF. 2ml $MgCl_2$ and 4ml $CaCl_2$ was added to the normal aCSF. Solutions were made up to 2l and stored in the fridge overnight. The ice-bucket of an ice-cream maker (Morphy Richards, UK) was stored at -20°C overnight for making aCSF slush the following day.

2.1.2 Dissection

P8 to 14 Lister Hooded rats and C57/Bl6 mice were used in this study. Animals were humanely killed by decapitation in accordance with Home Office regulations. Dissection was performed in low-sodium aCSF gassed with 95% O_2, 5% CO_2. aCSF slush was made using the ice-cream maker and then added to liquid aCSF cooled to below 4°C.

Following decapitation, the skin was cut from the forehead towards the spinal cord using a number 4 scalpel (size 26 blade; Swann Morton, UK). The scull was then pierced at the centre of the cerebral hemispheres using ophthalmic scissors and a rostral incision made towards the olfactory lobes. Further incisions were made just rostral from the central point to each eye socket. A rostral incision was also made from the spinal cord back to the central point before

folding each side of the scull back. The brain was then removed from the head cavity by cutting the nerves and blood vessels on the ventral surface.

Once removed the brain was transferred to fresh aCSF and slush and positioned dorsal surface down. Fine forceps were used to remove the meninges and blood vessels on the ventral surface of the brainstem. The brain was then turned ventral side down and held in place by spearing the cerebral hemispheres with a pair of forceps. An incision 20° from the vertical was made 5mm from the spinal cord using the scalpel (Fig, 2.1C). A vertical incision was made just rostral to the inferior coliculli and the cerebral hemispheres discarded.

2.1.3 Slice preparation

The brainstem was then picked up by impaling the cerebellum using a pair of forceps spaced with a 5mm cube of sylgard. A drop of cyanoacrylate adhesive (permabond, UK) was applied to the stage of the microslicer (DSK Japan, Fig, 2.2A) and blotted dry with filter paper. The brainstem was also blotted dry using fresh filter paper and glued caudal surface down, ventral surface forward to the microslicer stage. aCSF with a little slush was added until the brainstem was submerged and the solution was gassed with 95% O_2, 5% CO_2. A stainless steel blade (Campden instruments, UK) was used to make 5 to 8 150μm coronal sections from the level of the trapezoid body fibres. Slices were cut slowly (speed=1.5 on vibroslicer) until the blade had cleared the MNTB, then the speed was increased (to ≈5). Once cut, each slice was transferred to a slice maintenance chamber (Fig, 2.2B&C) using a blunt, fire polished Pasteur pipette. Slices were incubated in the maintenance chamber filled with normal aCSF at 37°C for 30-60 minutes before the chamber was removed to room temperature.

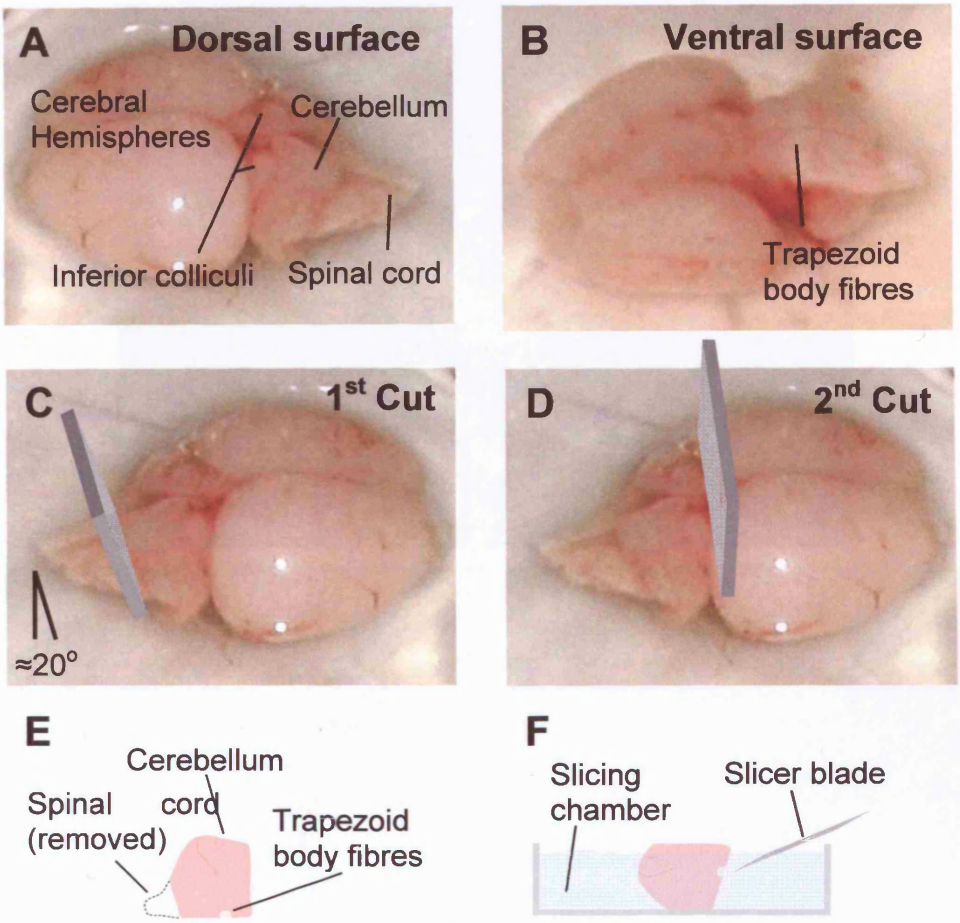

Figure 2.1. Brainstem dissection.
A. Dorsal surface of the brain from a 10 day old rat. **B.** Ventral surface of the brain from a 12 day old rat. The trapezoid body fibres can be seen as a white band across the brainstem. **C.** Position of the first cut to remove the spinal cord. An incision was made just posterior to the cerebellum with a scalpel blade at an approximately 20o angle. **D.** Position of the second cut to remove the cerebral hemispheres. A vertical incision was made just anterior to the inferior colliculi. **E.** Diagram of the brainstem laying ventral surface down as in D. **F.** Diagram of the brainstem mounted on the slicing chamber, caudal surface down.

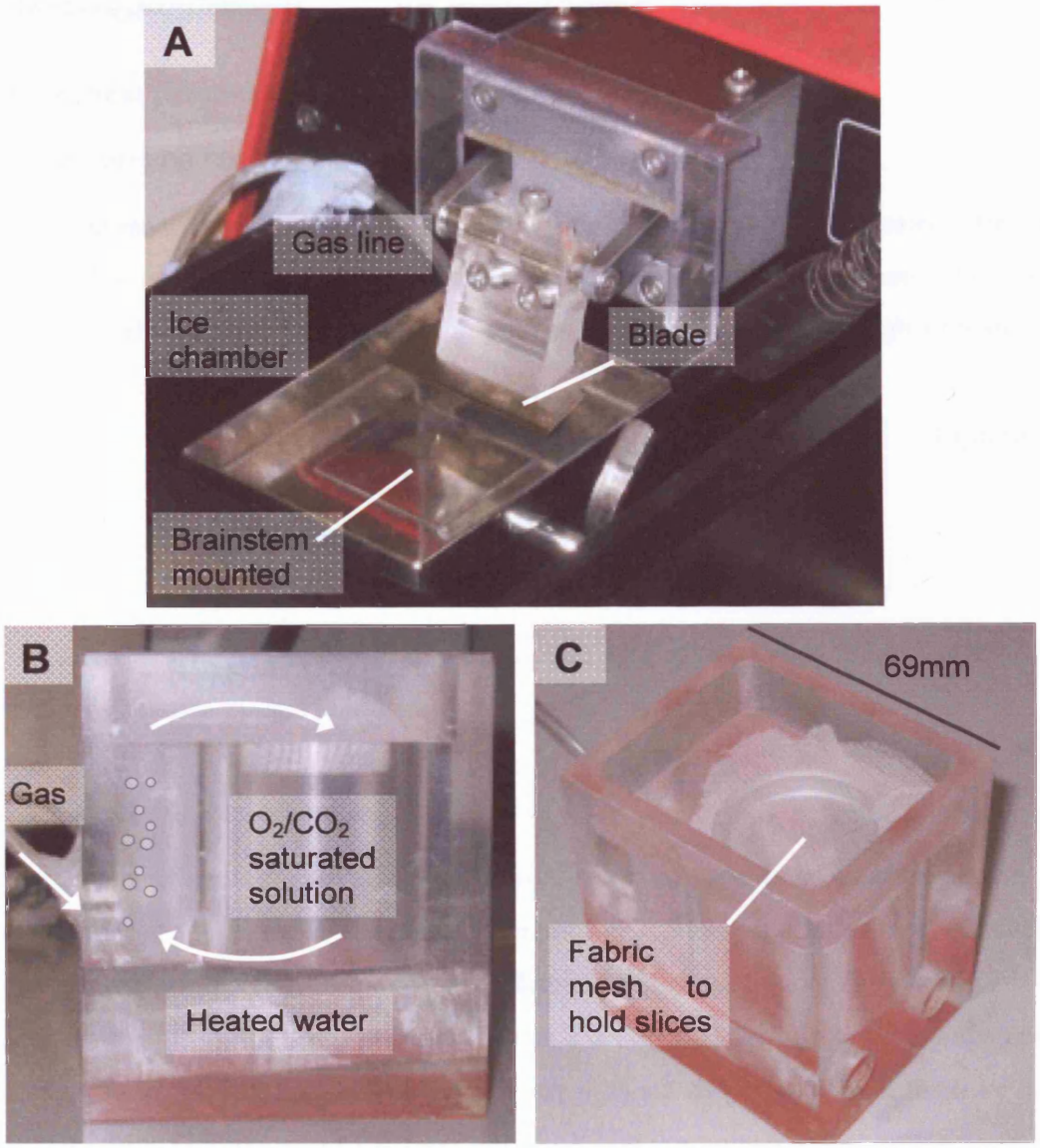

Figure 2.2. Slice preparation equipment.
A. DSK microslicer. The ice chamber was filled with ice before mounting the brainstem to the stage with cyanoacrylate adhesive. The stage was filled with ice-cold aCSF and bubbled with 95% O2, 5% CO2 through the gas line. **B.** Perspex slice maintenance chamber (side view). The chamber was filled with gassed aCSF and heated to 37°C in a water bath. The solution was gassed to maintain oxygenation and mixing of the solution. **C.** Elevated view of the maintenance chamber. Freshly cut slices were transferred to the chamber and placed on the fabric mesh.

2.2 Electrophysiology

2.2.1 Electrical properties of cell membranes

2.2.1.1 Membrane resistance

The cell membrane represents barrier, with ionic flow permitted through channels. Hence the resistance of a membrane is proportional to the number of channels open. Ohm's law (equation 2.1) relates membrane potential (V) to the current (I) flowing through a resistor (R).

$$V = IR \qquad \textbf{Equation 2.1}$$

Where V is voltage in volts, I is current in amperes and R is resistance in ohms.

Hence if there is a large number of channels open at a given voltage (i.e. I is large), the resistance will be low.

2.2.1.2 Membrane capacitance

A capacitance is generated when two parallel conductors are separated by an insulator; since the cell membrane acts as an insulator between the conducting intra- and extracellular solutions it forms a capacitor. Capacitance is determined by the area of the capacitor and the distance between the conductors; since the distance is constant for bilayers, most membranes have a capacitance of $1\mu Fcm^{-2}$. Consequently capacitance can be used as a measure of cell size; the larger the cell the larger the capacitance. When the voltage changes in a given time, charge is stored on the capacitor; accordingly, the current flowing through the membrane (I_m) is a product of ionic (I_i) and capacitive current (equation 2.2).

$$I_m = I_i + C\frac{\delta V}{\delta t} \qquad \textbf{Equation 2.2}$$

Where I_m is current flowing through the membrane, I_i is current flowing through ion channels, C is the capacitance in Farads, V is the voltage and t is time.

A rapid change in voltage (e.g. a voltage step) will therefore result in both ionic and capacitive current; consequently, compensation must be applied when recording ionic currents to cancel the capacitive current. The membrane capacitance is also important because it governs the decay of EPSPs; since the membrane time-constant is a product of membrane capacitance and resistance, an increase in conductance (e.g. due to opening of Kv channels) results in a shorter time-constant and hence faster EPSP decay.

2.2.1.3 Equilibrium potentials

The permeability barrier created by the cell membrane means that electrochemical gradients between the intra- and extracellular solutions can be maintained under the control of ion channels. The potential at which an electrochemical gradient is balanced (called the equilibrium potential, E_{ion}) can be calculated using the Nernst equation (equation 2.3).

$$E_{ion} = \frac{RT}{zF} \ln \frac{[ion]_{out}}{[ion]_{in}} \qquad \textbf{Equation 2.3}$$

Where R is the Gas constant, T is the temperature in Kelvin, z is the valency of the ion, F is the Faraday constant

Our internal solution had a K^+ concentration of 142.5mM and our extracellular solution contained 2.5mM K+, making E_K -95mV.

2.2.2 Voltage clamp

Voltage clamp was developed in the study of the squid giant axon (Cole, 1949; Hodgkin et al., 1949; Marmont, 1949). This technique permits the measurement of currents flowing across the membrane whilst the voltage is controlled by a feedback amplifier. Originally voltage clamp was performed using two microelectrodes (two-electrode voltage clamp) one to measure voltage and the other to pass current (Halliwell et al., 1994). This technique was later adapted to use a single electrode which alternates between measuring voltage and passing current (single-electrode voltage clamp or switch-clamp). An alternative method of voltage clamp was developed in the 1970-80s for both single-channel and whole-cell recording (Neher

and Sakmann, 1976; Hamill et al., 1981) called patch clamp. This technique uses a single electrode to simultaneously record voltage and pass current.

2.2.3 The patch clamp technique

The advantage of the patch clamp technique is that it permits low-noise recordings to be made, owing to the formation of a giga-ohm seal. In addition, small, fast currents can be resolved and cells can be voltage clamped which are inaccessible to other recording techniques (Ogden and Stanfield, 1994). A giga-ohm seal between the pipette and the cell membrane is formed by pressing the pipette against the membrane and applying light suction. Once a giga-ohm seal is established, there are several configurations of the patch clamp technique that can be employed (Fig, 2.3). Most of the experiments in this study were carried out in the whole cell configuration. Whole cell recordings were achieved by applying further suction once in the cell attached mode. The advantage of recording in whole cell mode is that good signal to noise is achieved owing to the large numbers of channels recorded. Whole cell recordings made at the soma also allow measurement of the current originating from other regions of the cell such as the initial segment. However, being able to record from regions distant from the pipette can also be a disadvantage as it can cause space-clamp errors (Ogden and Stanfield, 1994). Optimal voltage clamp assumes that the cell is a perfect sphere; so any processes (e.g an axon) with higher resistance will affect the quality of clamp, potentially causing space-clamp errors. Another potential disadvantage of whole cell recording is the fact that the cellular contents are dialysed out during recording. In order to overcome problems associated with dialysis, the perforated patch method can be used. In this method, antibiotics e.g nystatin or amphotericin B are included in the intracellular solution. These antibiotics form channels in cholesterol containing membranes which are permeable to monovalent cations and chloride but exclude larger divalent ions and molecules such as ATP (Ogden and Stanfield, 1994).

Once in whole cell configuration, an outside-out patch can be excised by pulling back from the cell. The advantage of an outside-out patch over a whole cell recording is that the voltage clamp conditions will be better owing to the reduction in the amount of membrane (and therefore channels) present. In addition, excising a patch allows isolation of channels from a

particular region of the cell e.g. somatic channels. The potential disadvantage of recording from excised patches is that the signal to noise ration is worse since the currents are smaller. However this can often be overcome by reducing the electrical noise 'pick-up' by correctly earthing the equipment or by using larger pipettes to increase the number of channels present in the patch. An alternative form of excised patch is the inside out patch. These are made by pulling back once cell attached. The advantage of inside-out patches is that the internal region of the membrane is exposed so different pharmacological agents can be applied directly to the inside of the channel. The disadvantage to this recording mode is that the internal membrane contents are lost, so cytosolic components such as G-proteins or certain accessory proteins may not be present.

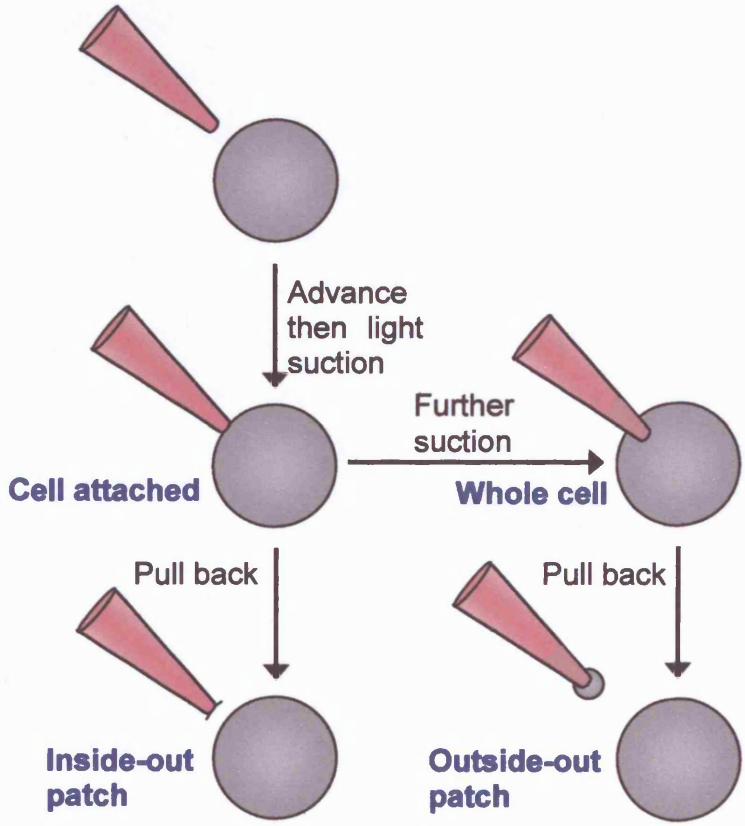

Figure 2.3. Patch clamp configurations.
Once in cell attached mode, whole cell recordings can be made by applying suction to rupture the membrane beneath the pipette. Alternatively, inside-out patches can be excised by pulling the pipette back from the cell. Another from of excised patch is the outside-out patch which is achieved by pulling back off the cell when in the whole cell configuration.

2.2.4 Series resistance

In voltage clamp experiments there is a resistance in series with the membrane known as the series resistance (R_s). In patch clamp recordings a single electrode is used both to measure voltage and pass current. The resistance of this electrode is called the access resistance (R_a) which will contribute to R_s (Halliwell et al., 1994). When a current flows across the membrane, the series resistance causes an error between the true cell potential and the measured potential; this is known as the series resistance error. Series resistance errors can be a particular problem when recording large currents with small pipettes. For example if 2nA of current is flowing and the series resistance is 10MΩ there will be a voltage error of 20mV (10MΩ x 2nA = 20mV from Ohm's law; equation 2.1). Such large errors would be unacceptable so they must be compensated by adding a proportional voltage signal to the command voltage through the R_s correction circuit of the amplifier. However, 100% R_s correction cannot be achieved so there will still be some residual error (Ogden and Stanfield, 1994). If 70% correction was applied in the above example the R_s error would be ≈6mV. Changes in series resistance during recordings can also be a problem. If the series resistance increased from 10 to 20MΩ in the above example and was correctly compensated by 70% there would be a ≈6mV difference. Since this difference could appear as an apparent block of a drug, series resistance was carefully monitored, compensated and noted during our recordings. Typical series resistances were 19.1±2.2MΩ (n=11) for presynaptic and 9.3±0.6MΩ (n=21) for postsynaptic recordings and compensated by 70% with a lag of 10μs. If the series resistance changed by ±2MΩ during the course of an experiment, the data were excluded from further analysis.

2.2.5 Experimental setup

2.2.5.1 Experimental microscope

A Nikon E600FN upright microscope (Nikon, Japan) was used for this study (Fig, 2.4). The microscope was fitted with differential interference contrast (DIC) optics and a 60X (NA 1.00) water immersion objective (Nikon, Japan). A CCD camera (Cohu, CA) was fitted to the microscope and connected to a monitor (Panasonic, Japan). The microscope was mounted on a remotely controlled translation table designed and constructed by the biological workshop

(University of Leicester, UK). The environmental chamber was fixed on a wide-based stage to provide greater stability. This arrangement means that the microscope moves around the preparation. Also mounted on the stage were Burleigh PCS-5000 manipulators (EXFO Burleigh products, NY) which supported the amplifier headstage. A Peltier heat exchange temperature controller (designed and constructed by the biological workshop, University of Leicester, UK) was mounted under the stage to control the temperature of solutions perfused into the environmental chamber. The equipment was supported by a vibration-isolation table and surrounded by a Faraday cage.

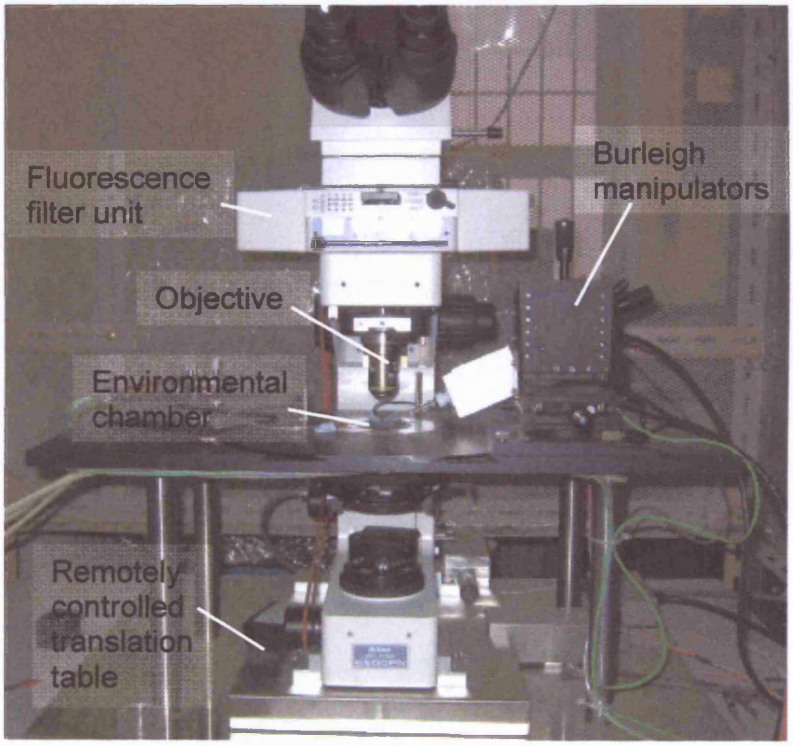

Figure 2.4. Experimental microscope.

2.2.5.2 Differential Interference Contrast (DIC)

Visualisation of neurones on the experimental microscope was achieved using differential interference contrast (DIC) optics (also known as Nomarski). This is a technique used to introduce contrast into non-absorbent objects. Light is first polarised and then passed through a Wollaston prism, which splits the light into two quasi-parallel beams. The light then passes

through the specimen so that some beams will pass through the object and others to the edge of it. Beams that pass through the object will be slightly refracted with respect to those that do not. Both of the beams then pass through another Wollaston prism, which recombines them. Finally the light passes through a polarising filter. Beams that have been refracted by an object will appear a different shade to those that have not due to constructive or destructive interference on recombination of the beams, giving a perception of contrast.

2.2.5.3 Fluorescence microscopy

Fluoresence microscopy was used on the experimental microscope to ensure that recordings were presynaptic and not inadvertently made from postsynaptic cells. Sulphorhodamine 101 (1mg/ml; Molecular probes, OR, USA) was included in the intracellular solution. Flurorescence microscopy was achieved without the use of a Xenon lamp by placing the excitation filter (510-560nm; Nikon, UK) over the conventional light source and having the emission filter (590nm; Nikon, UK) in the filter unit (Fig, 2.4). Filled terminals could then be seen through the eyepieces with the light set to its maximum level.

2.2.5.4 Perfusion and drug application

Slices were transferred as required to the experimental chamber and held down with a platinum harp (Edwards et al., 1989). The environmental chamber was continuously perfused with aCSF by means of a peristaltic pump perfusion system (Gilson minipulse III, France Fig, 2.5). Drugs were bath applied through dedicated perfusion-lines to avoid contamination. Where possible, lines were drug-primed to speed application. This was achieved by perfusing the drug into the bath then sucking back a head (≈0.2ml) of solution into the bubble trap (using the attached 1ml syringe) before cleaning the bath then perfusing in control solution.

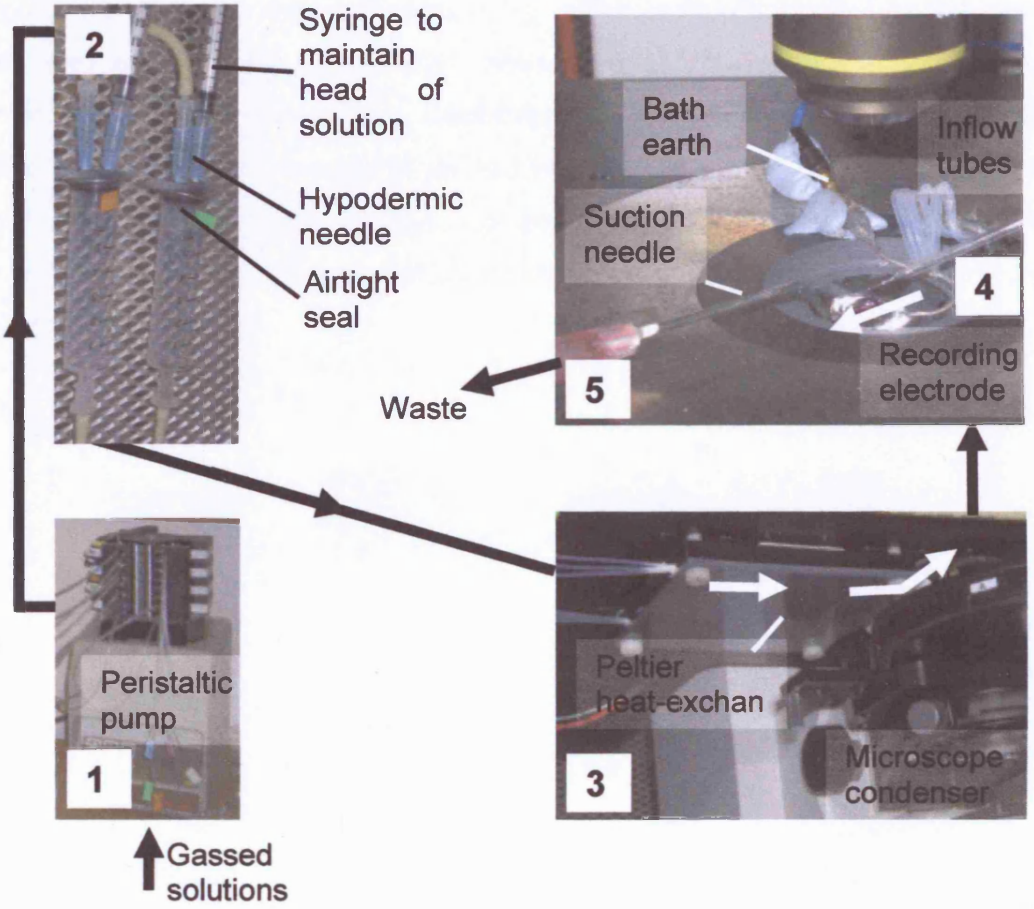

Figure 2.5. Perfusion system.
1. Gassed solutions are pumped through gas-impermeable tubing into bubble traps by means of a peristaltic pump. **2.** The solution drips through the bubble traps and the pressure forces it through the tubes to the Peltier heat-exchanger. **3.** The solution then passes into Teflon tubes in the Peltier heat-exchanger. The tubes are surrounded by heat-sink compound and run through metal tracks which weave their way back and forth through the device. The tracks are in contact with two Peltier devices which exchange heat with the experiment-stage, allowing control of the solution temperature. **4.** The tubes then pass through a hole in the experiment-stage into the recording bath. **5.** The solution is then sucked out of the bath, through an outflow bubble trap by the pump and into a waste container. Images not to same scale.

2.2.6 Patch clamp recording equipment

Recordings in this study were carried out using an Optopatch amplifier (Cairn Research, UK). Data were acquired with a CED1401 interface (Fig, 2.6) using Patch v6.39 software (Cambridge Electronic Design Ltd., Cambridge, UK), filtered at 2 kHz and digitized at 5-15kHz for voltage-clamp recordings and to 35-60 kHz for current-clamp recordings using an 8-pole Bessel filter on the amplifier. A pulse-sum conditioner (Biological workshops, University of Leicester, UK) was used to eliminate noise in the voltage commands from the 1401 interface.

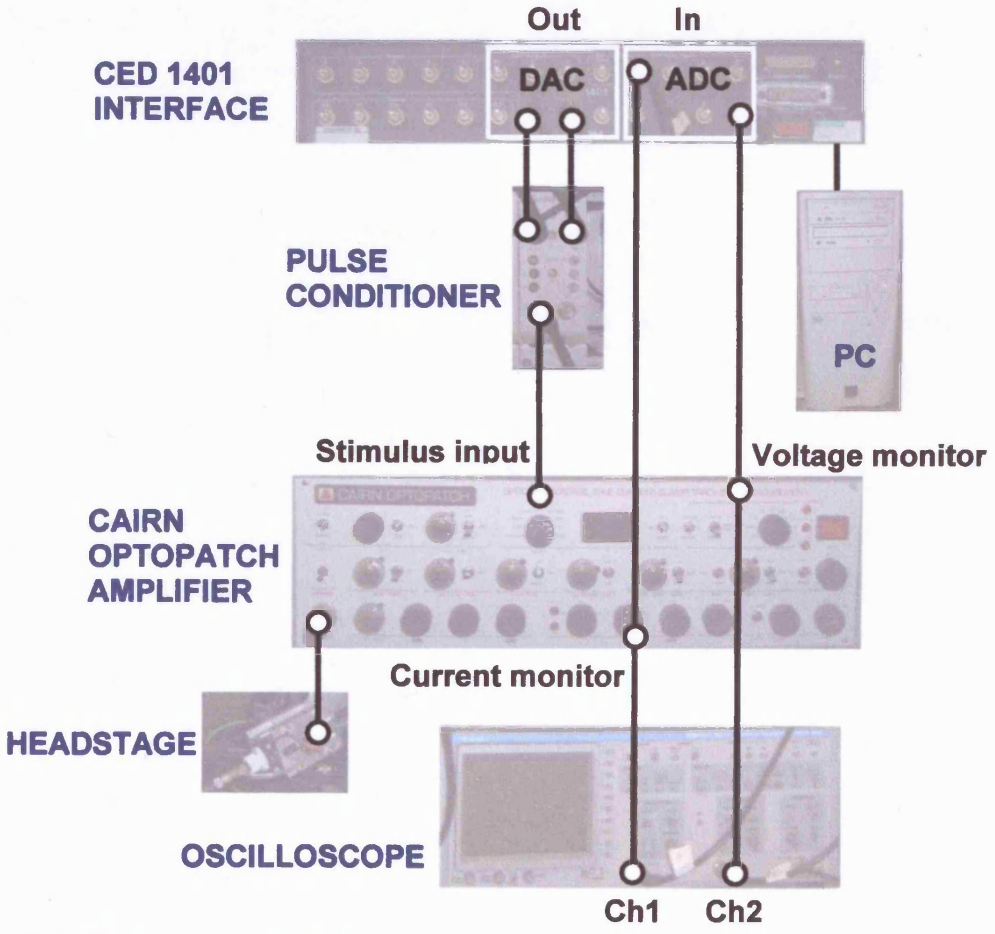

Figure 2.6. Patch clamp recording equipment.

2.2.6.1 Amplifier headstage design

The Optopatch amplifier differs from conventional patch clamp amplifiers in that it has an optical headstage.

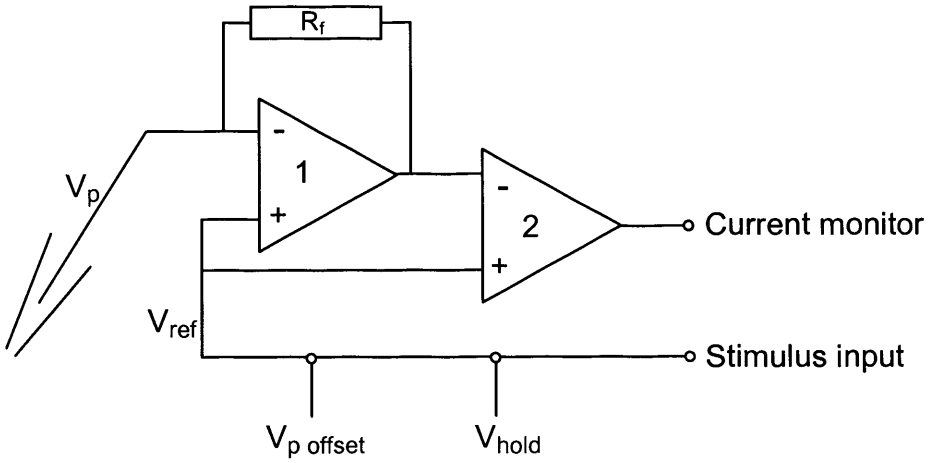

Figure 2.7. Conventional patch clamp headstage.

Conventional headstages consist of two operational amplifiers and act as current to voltage converters (Ogden and Stanfield, 1994). The first operational amplifier ('1' in Fig, 2.7) compares the pipette potential, V_p, with the reference potential, V_{ref} (Fig, 2.7). V_{ref} is determined by the V_{hold} and $V_{p\ offset}$ (set on the amplifier) and the stimulus input (from the V-clamp software). Any difference between V_{ref} and V_p causes an opposing current to be passed through the feedback resistor, R_f. The current passing through the feedback resistor generates a potential difference across it. This difference can be monitored at a differential amplifier ('2' in Fig, 2.7) by subtracting amplifier 1's out put from V_{ref}.

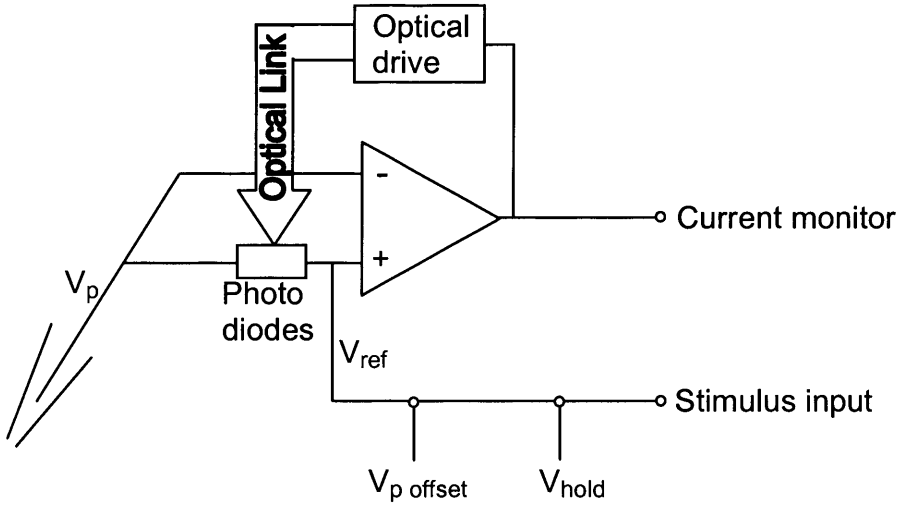

Figure 2.8. Optopatch headstage.

The Optopatch optical headstage (Fig, 2.8) is similar to a conventional resistive headstage except that the feedback resistor is replaced by an optical drive which shines light onto photodiodes to produce a current (Thomas, 2000). The advantage of this is that it eliminates the element of thermal noise generated by the feedback resistor. Any difference between V_{ref} and V_p activates the optical drive to produce a photodiode current which acts to restore the difference. Since V_{ref} does not appear on the amplifier output it does not need to be subtracted.

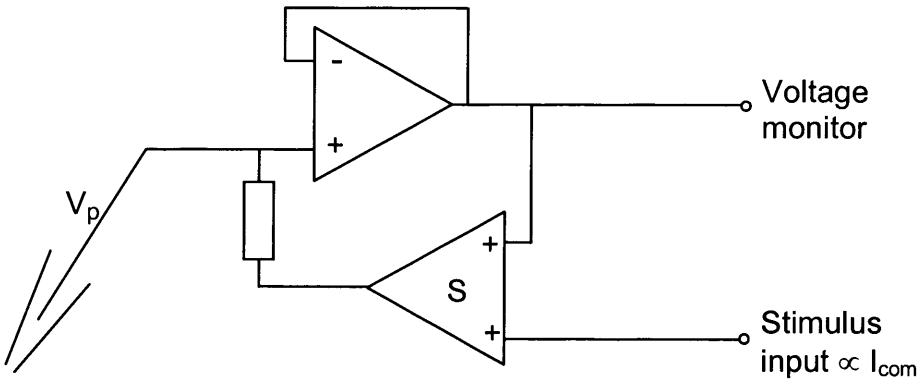

Figure 2.9. Voltage following circuit (current clamp only).

Traditional current clamp amplifiers use a classic voltage following circuit (Fig, 2.9) in which there is essentially infinite resistance between V_p and the voltage monitor (Magistretti et al., 1996). A current command, I_{com}, can be injected into the cell through a summing amplifier (S in Fig, 2.9).

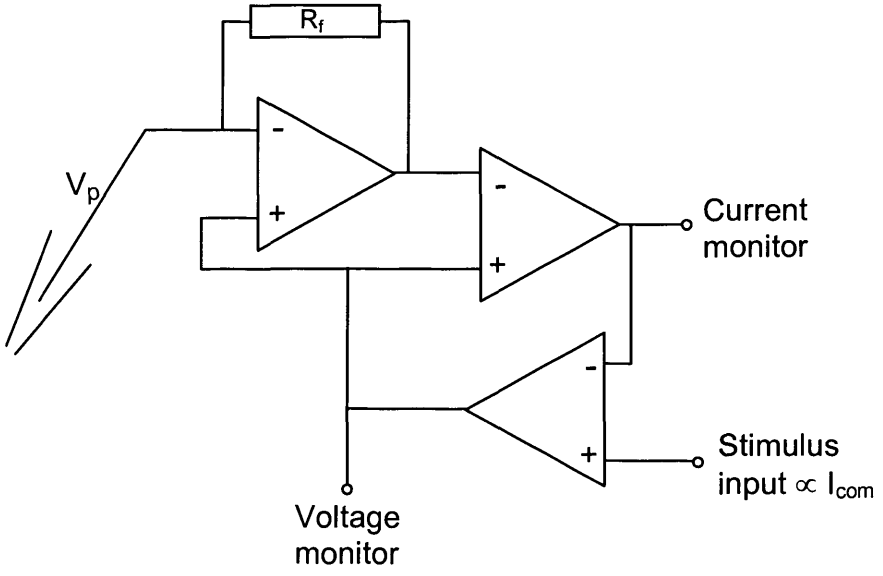

Figure 2.10. Current clamp mode of a conventional patch clamp amplifier.

In conventional patch clamp amplifiers current clamp mode is achieved with an operational amplifier as a feedback between the current monitor and V_p (Fig, 2.10). The difference between the current recorded by the current monitor and a voltage proportional to I_{com} is amplified to generate a voltage which can equalize the pipette and command currents. The desired current is then maintained by varying V_p; the output of the differential amplifier provides the voltage recorded by the voltage monitor. However, the problem with this type of amplifier is that the resistance between V_p and the voltage monitor is not infinite like the voltage follower (Fig, 2.9) so the circuit will draw current from the cell (Magistretti et al., 1996). In the Optopatch headstage the feedback resistor is replaced by an optical drive (Fig, 2.8), so there is essentially infinite resistance. This makes true current clamp easy to achieve with an optical headtage.

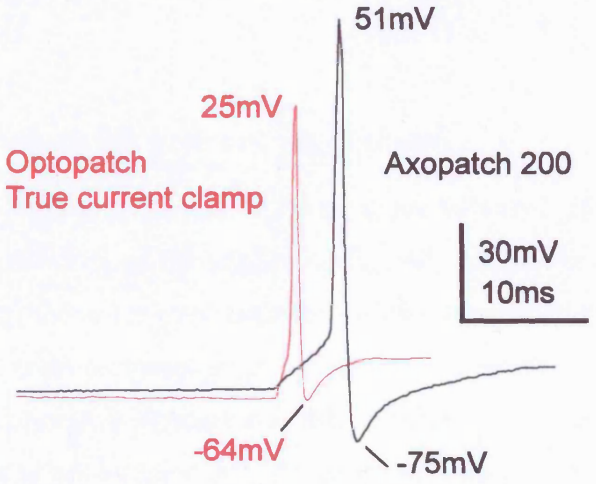

Figure 2.11. Comparison of true current clamp and current clamp mode.
Action potentials were evoked by 200pA sustained current injection in different MNTB neurons. Errors generated by the Axopatch 200 increase the amplitude and the AP of the action potential and increase the time to threshold. The same scale is used for both traces.

Non-infinite resistance in current clamp mode of a conventional patch clamp amplifier can result in errors arising from the amplifier drawing current from the cell (Magistretti et al., 1996; Magistretti et al., 1998). Figure 2.11 shows such errors in the action potentials recorded from two MNTB neurones; one using current clamp mode of a conventional patch clamp amplifier (Axopatch 200) and the other, a true current clamp amplifier (Optopatch). The afterhyperpolarisation (AHP), peak and the time to threshold are all artificially increased in recordings from the Axopatch 200. Later models of the axopatch (200A and B) have an I_{fast} mode of current clamp, which is an improvement from the I_{slow} mode but is still not true current clamp (Magistretti et al., 1996).

2.2.6.2 Electrode preparation

Glass electrodes were pulled from thick-walled borosilicate glass (GC150F 7.5, Harvard Apparatus, UK) using a two-stage puller (PP-83, Narishige, Japan). For presynaptic recording, electrode-tips were fire-polished by advancing the tip towards a glass-coated platinum wire. Current was then applied to heat the wire until the electrode-tip shrank back. Intracellular solution was filtered using a 0.2µm filter (Millipore, UK) and then used to fill the

pipettes. Final pipette resistances were 2.5 to 4 MΩ for postsynaptic and 4 to 10MΩ for presynaptic recordings.

2.2.6.3 Whole cell recordings from brainstem slices

Positive pressure was applied to the rear of the electrode before aligning it over the slice. The pipette was then lowered through the surface of the bath solution using the coarse control of the manipulators. The pipette-tip was visualised on the video monitor and positioned over the cell of interest. The junction control on the amplifier was adjusted to zero any voltage drop across the tip. Further positive pressure was then applied to the rear of the electrode using a 10ml syringe (2ml was applied for MNTB neurones and 0.7ml for calyces). A 10mV voltage-pulse was applied to assess seal formation. The pipette was advanced under fine control until a 'dimple' in the cell membrane could be observed. At this point the positive pressure was released, then light suction applied to achieve a giga-ohm seal. A more severe dimple was necessary when recording from MNTB neurones to ensure that the calyx had been blown aside. During seal formation the V-hold control of the amplifier was set to clamp the cell at -70mV (-75mV for calyces). Once the seal was established, pipette capacitance was cancelled using the fast and slow 'Mag' and 'T' controls on the amplifier. Brief pulses of light suction were then applied to rupture the piece of membrane below the tip and gain whole-cell access. Capacitive transients were then cancelled using the series conditioning and capacitance controls on the amplifier. Series resistance compensation was then set to at least 70%.

2.2.6.4 Stimulation

Trapezoid body axons were stimulated using a bipolar platinum electrode (Fig, 2.12). The stimulating electrode was lowered into the bath and advanced towards the midline using the attached course manipulators (Narishige, Japan) and the electrode 'prongs' were positioned to straddle the slice. The stimulating electrode was connected to a DS2A isolated stimulator (Digitimer, Welwyn Garden City, UK) and axons were stimulated with 0.2ms pulses of 4-10V. The stimulator was connected to a D4030 trigger generator (Digitimer, Welwyn Garden City, UK) which enabled trains of stimuli to be applied at varying rates.

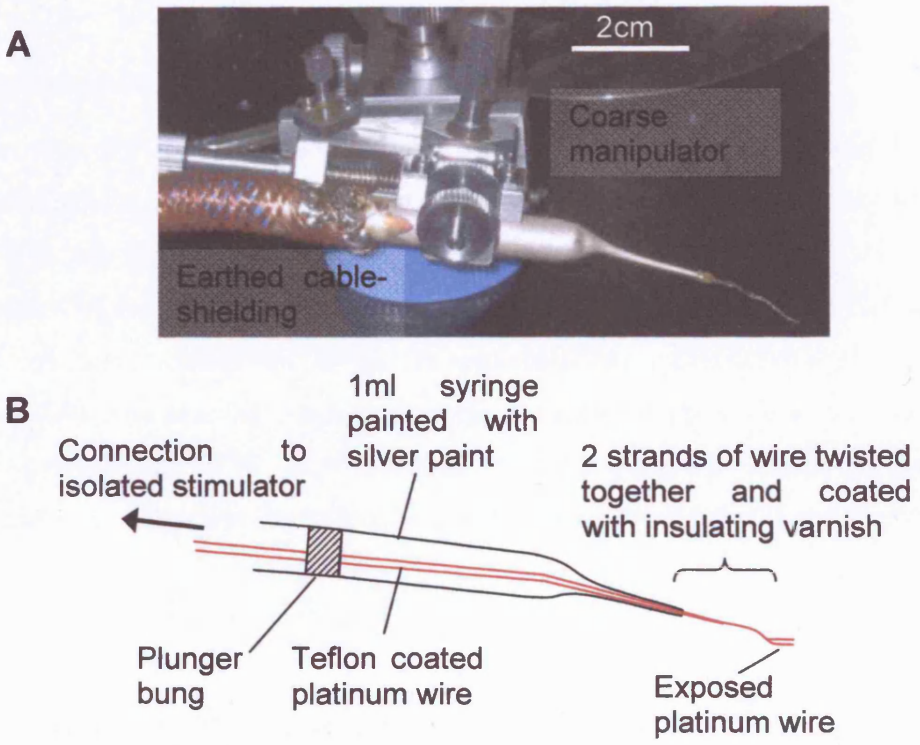

Figure 2.12. Bipolar stimulating electrode.
A. Photograph of the stimulating electrode connected to the coarse manipulators. **B.** Diagrammatic representation of the bipolar electrode. The tip of a 1ml syringe is heated and pulled, then the rear of the syringe is blocked with the plunger bung. Teflon coated platinum wire is fed through the bung and out of the syringe tip. The exposed strands are then twisted together to produce some rigidity before shaping and coating with insulating varnish (Radio Spares, UK). The final 1-2ml of the tip is flamed to remove the Teflon. The syringe is painted with silver paint to which the earthed cable-shielding is soldered.

2.3 Data analysis

Current-voltage (I/V) relationships were produced from the current amplitude was measured 10ms into the test step. Leak currents, estimated from a linear fit between -90mV to -75 mV, were subtracted from the I/V curve using Excel XP (Microsoft, USA). Current records for figures were produced using WinWCP v3.2.9 (written by John Dempster, University of Strathclyde). In a few cases (indicated in the figure legend) current records were leak subtracted off-line using Patch v6.39 software (Cambridge Electronic Design Ltd., Cambridge, UK). Averaged data are expressed as mean ± S.E.M. Data in each figure are from a single cell unless otherwise stated.

2.3.1 Determining half-activation

To determine the half-activation of the presynaptic high-voltage activated current, the normalised whole cell conductance, modified to account for a non-linear single channel current I/V, was fit with a Boltzmann distribution. Since the single channel current is not linear, a plot of the normalized whole cell conductance will not level out as G_{max} is reached but will continue to rise (Clay, 2000). To overcome this, a derivative of the GHK equation (equation 2.4) was used to produce a single channel current with a non-linear I/V. An arbitrary permeability to K^+ (Pk) value was used; since this only alters the gradient of the single channel IV (which is later normalised anyway) the exact value is not important.

$$i = Pk \bullet \frac{F^2 V}{RT} \bullet \left(\frac{[K^+]_{in} - [K^+]_{out} \bullet e^{-(FV/RT)}}{1 - e^{-(FV/RT)}} \right) \qquad \textbf{Equation 2.4}$$

Where Pk is the permeability to potassium, F is the Faraday constant, V is the voltage, R is the gas constant and T is the temperature in Kelvin

The whole cell conductance (G, equation 2.5) was then calculated from the recorded whole cell current (I) and normalised to the single channel conductance (g, equation 2.6) resulting in G/g which takes account of the non linearity.

$$G = \frac{I}{V - E_K} \qquad \textbf{Equation 2.5}$$

Where G is the whole cell conductance, I is the whole cell current and E_k is the potassium equilibrium potential

$$g = \frac{i}{V - E_K} \qquad \textbf{Equation 2.6}$$

Where g is the single channel conductance and i is the single channel current.

G/g was then normalised to $(G/g)_{max}$ and plotted. A Boltzmann distribution (equation 2.7) was then fit to the plot using the least squares method to give the half activation.

$$\frac{G/g}{(G/g)_{max}} = \frac{1}{\left(1+e^{(V_{½}-V)/k}\right)}$$ **Equation 2.7**

Where k is the Boltzmann constant

2.3.2 Determining half-inactivation

To determine the half-inactivation potential of the low-voltage activated current in MNTB neurones we fit the data with a fractional Boltzmann distribution (equation 2.8). Since only a fraction of the low-voltage activated current inactivates, this form of the Boltzmann equation fits the inactivating portion of the data.

$$I - I_{max}\frac{1-fraction}{\left(1+e^{(V_{½}-V)/k}\right)}$$ **Equation 2.8**

2.4 Immunohistochemistry

The subcellular location of a target molecule can be determined with the use of fluorescently-labelled antibodies. Antibodies are produced for use in immunohistochemistry by inoculating animals with the desired antigen which stimulates the animal to raise the appropriate antibodies. Indirect immunohistochemistry involves the use of a primary antibody, specific for the protein of interest, and a fluorescently-conjugated secondary antibody which recognises the primary antibody (Fig, 2.13). Secondary antibodies are produced by immunising a second species (e.g. goat) with antibodies from the primary antibody species (e.g. rabbit). The secondary antibody is fluorescently labelled by covalent attachment to fluorochromes such as Texas red or fluorescein isothiocyanate (FITC). Texas red is exited at 595-605nm and emits at 620nm whereas FITC is maximally excited at 490nm and emits at 520nm. The differing emission spectra of these two fluorescent molecules makes them suitable for use in co-localisation experiments.

Primary antibodies are applied to tissue which has been fixed and permeabilised, allowing the antibodies access to internal sites (Fig, 2.13). Specificity of the primary antibody is particularly important since binding to non-specific sites can raise the 'background fluorescence' or provide false-positive results. The tissue is washed to remove residual primary antibody before introducing the secondary antibody.

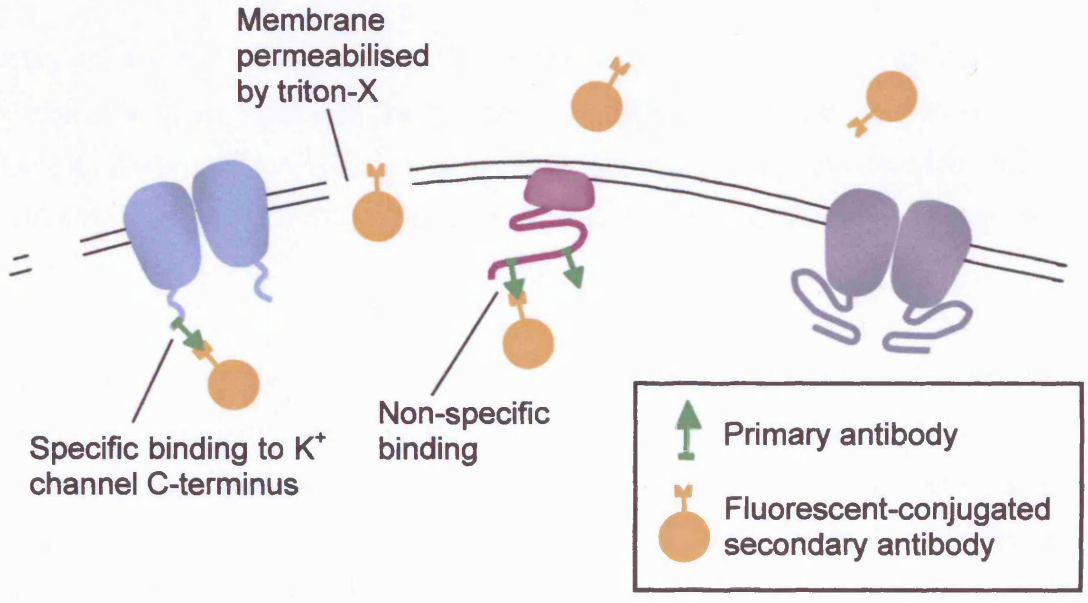

Figure 2.13 Principle of immunohistochemical labelling.
The primary antibody binds to the region of interest. Fluorescently labelled secondary antibody is then applied to enable visualisation of primary antibody binding.

2.4.1 Immunohistochemistry procedure

Brainstems were dissected as previously described. The spinal cord was held with forceps and the brainstem was lowered into a tissue imbedding mould (Polysciences; PA, USA). The mould was then filled with Tissue Tec (Bayer, UK) to just above the brainstem before lowering it into a flask containing hexane and dry ice. Once frozen, the Tissue Tec imbedded brainstems were stored at -20°C.

20µm sections were cut in a rostro-caudal direction on a cryostat (OTF, Bright Scientific Instruments, UK) at -12°C. Sections containing the MNTB were transferred to subbed slides before submerging in 2% paraformaldehyde for 10 minutes at room temperature. Fixed

sections were then washed in phosphate buffered saline (PBS) for 15 minutes on a shaker (STR8, Stuart Scientific, UK) then transferred to fresh PBS for a further 15 minutes. A PBS solution containing 10% blocking serum (derived from species in which the secondary antibody is raised; Dako, UK) and 0.5% Triton-X100 (Sigma, UK) was prepared. Slides were completely covered in this solution and placed in an incubation box (to maintain humidity) for 1 hour at room temperature.

Excess fluid was blotted from around the sections before washing in PBS as before. Sections were ringed with an Immedge pen (Vector Laboratories, UK) and covered with 100μl of primary antibody solution (primary antibody diluted to the appropriate concentration with 10% blocking serum and PBS). The sections were then incubated overnight in an incubation box at 4°C.

Sections were washed for 10 minutes in PBS as before, 6 times. Secondary antibody (directed to the primary antibody host) was spun in a centrifuge at 8000rpm for 5 minutes at 4°C. Sections were then covered with 100μl of secondary antibody solution and placed in an incubation box at room temperature for 2 hours. Sections were washed in PBS twice for 15 minutes as before. Excess fluid was then blotted from the slides and the sections were mounted with Citifluor (Citifluor Ltd, UK).

Slides were then examined on an epifluorescent microscope (Nikon, Japan) fitted with a x10 objective. For more detailed examination an Olympus Fluoview confocal microscope (IX70) with a x60 (NA 1.4) objective was used.

Antibody	Epitope	Homology
Kv1.1	GST fusion protein with sequence HRETE GEEQA LLHV SSPNL ASDSD SRRS SSTIS KSEYM IEED MNNSI AHYRQ ANIRT GNCTT ADQNC VNKSK LTDV, corresponding to residues 416-495 of mouse Kv1.1 C-terminus (Accession P16388).	Rat 78/80 residues identical.
Kv1.2	GST fusion protein with sequence YHRET EGEEQ AQYLQ VTSCP KIPSS DLKK SRSAS TISKS DYMEI QEGVN NSNED FREEN LKTAN CTLAN TNYVN ITKML TDV, corresponding to residues 417-499 of rat Kv1.2 C-terminus (Accession AAA19867).	Mouse identical
Kv1.4	GST fusion protein with sequence PYLPS NLLKK FRSST SSSLG DKSEY LEMEE GVKES LCGKE EKCQG KGDDS ETDKN NCSNA KAVET DV, corresponding to residues 589-655 of rat Kv1.4 C-terminus (Accession P15385).	Mouse identical
Kv1.5	GST fusion protein with sequence HRETD HEEQA ALKEE QGIQR RESGL DTGGQ RKVSC SKASF HKTGG PLEST DSIRR GSCPL EKCHL KAKSN VDLRR SLYAL CLDTS RETDL, corresponding to residues 513-602 of mouse Kv1.5 C-terminus (Accession Q61762).	Rat 86/90 residues identical.
Kv1.6	GST fusion protein with a sequence NYFYH RETEQ EEQGQ YTHVT CGQPT PDLKA TDNGL GKPDF AEASR ERRSS YLPTP HRAYA EKRML TEV, corresponding to residues 463-530 of rat Kv1.6 C-terminus (Accession P17659).	Mouse 67/68 residues identical.
Kv3.1b	peptide CKESP VIAKY MPTEA VRVT, corresponding to residues 567-585 of rat Kv3.1b C-terminus (Accession P25122).	
Kv3.2	peptide DLGGK RLGIE DAAGL GGPDG K(C), corresponding to residues 184-204 of rat Kv3.2 N-terminus (Accession P22462).	
Kv3.3	VTQAS PIPGA PPENI TNVC corresponding to residues of Kv3.3 S1-S2 linker	
Kv3.4	peptide EAGDD ERELA LQRLG PHEG(C), corresponding to residues 177-195 of rat Kv3.4 N-terminus (Accession Q63734).	

Table 2 Antibody epitopes

2.4.2 Confocal microscopy

Confocal microscopy has several advantages over conventional fluorescent microscopy including the ability to collect serial optical sections and the elimination of out of focus glare. In conventional microscopy, fluorescence from areas of the specimen away from the region of interest can interfere with the resolution of the regions that are in focus. This becomes even more problematic when thicker sections are used. Confocal imaging overcomes this problem by blocking out the out-of-focus light by placing a pinhole in front of the detector, so that only the region of the specimen that is in focus is detected

A laser is normally used to provide the excitation light (in order to get very high intensities). A single spot of light is then focussed on the specimen by an objective. Light emitted from the illuminated spot is focused (by the same objective) on a pinhole (the confocal aperture)

before being detected by a photomultiplier tube (PMT). The pinhole ensures that only in-focus light passes through (Fig, 2.14 red line) and therefore it eliminates light from out-of-focus regions (Fig, 2.14 blue line). In order to build an image, the spot of light must be scanned across the specimen, producing an optical section. A three-dimensional image can be produced by compiling several optical sections in what is known as a z-series.

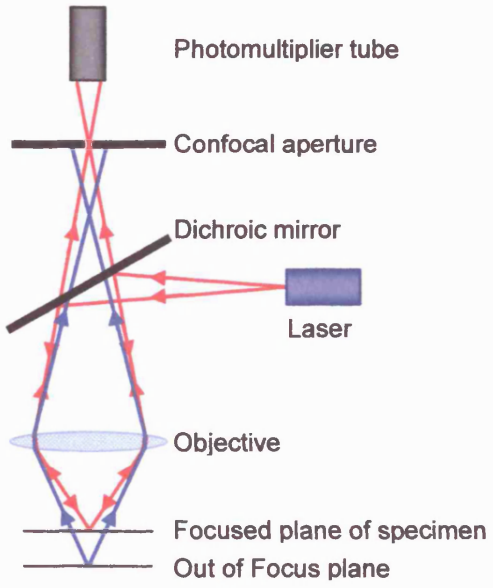

Figure 2.14. Confocal microscopy.
Focused light (red) reaches the photomultiplier tube whereas out of focus light (blue) is blocked by the confocal aperture.

2.5 Genotyping

Genotyping involves the polymerase chain reaction (PCR). In this reaction the double-stranded DNA is introduced with primers (short, synthetic pieces of single-stranded DNA that exactly match the piece of DNA to be amplified), deoxynucleotide triphosphates (dNTPs), buffers and a polymerase. The mixture is heated to separate the template strands of DNA. By cycling the temperature, the polymerase is induced to repeatedly copy the DNA; starting at the primer sequence and building a new complementary strand for each original. At the end of each cycle the DNA count has doubled. So from one DNA molecule, about a billion copies are present after 30 cycles.

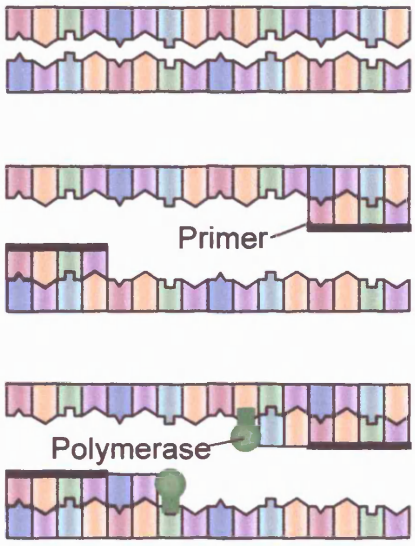

The DNA is heated up to 94°C to unwind the double helix and separate the two DNA strands.

The temperature of the denatured DNA is then reduced to 54°C to allow the primers to specifically bind (anneal) to complementary sites on the single strand DNA.

The temperature is then raised to 74°C so that the DNA polymerase extends the primer (elongates) along the single DNA strand using the original as a template. Elongation is allowed to complete before returning to 4°C to suspend the reaction.

Figure 2.15 Principle the polymerase chain reaction (PCR).

2.5.1 PCR Procedure

Approximately 5mm is cut from the tails of mice older than postnatal day 5. The tails were digested in 0.4ml tail buffer overnight at 55°C. Tail buffer contained (in mM) 10 Tris-HCl pH8, 50 NaCl, 50EDTA, 0.5% SDS and 10µl of a 20mg/ml stock of proteinase-K.

The solutions were vortexed, 0.1ml 5M NaCl was added and then they were vortexed again for 5-10 seconds. 0.5ml of phenol/chloroform was added to each tube. The tubes were rocked 10 times and then spun for 8 minutes in a centrifuge (13000RMP, room temperature). The DNA layer (top) was transferred to clean tubes taking care not to disturb the interface. 1ml 100% ethanol was added to precipitate the DNA and then the tubes were left at -20°C for 3 hours. The tubes were then spun for 15 minutes (13000RMP, at 4°C) before removing the excess ethanol to leave the DNA pellet. The ethanol precipitation and spin was then repeated with 70% ethanol before vacuum drying. 100µl of sterile water was then added before leaving at room temperature overnight.

The DNA was diluted 1:10 with sterile water. PCR solution was added to the PCR beads (Amersham Biosciences, UK). PCR solution contained 19µl sterile water, 40pmoles 3.1X

primer (2μl), 20pmoles 3.1Y primer (1μl), 20pmoles PPRV primer (1μl) and 2μl DNA. After the DNA was added the tubes were placed on ice, then spun for 5-10 seconds (13000RMP, at 4°C), mixed and spun again. 40μl of mineral oil was then added to the surface of the DNA solution. The tubes were then placed in the thermal cycler (Genius, Techne, UK) using the program described in figure 2.15.

Agarose gels were made as follows: 1.5g Agarose was added to 100ml of Tris-acetate-ethylene-diamine-tetra-acetic acid (TAE; Bioline, UK). The solution was microwaved for 3 minutes at medium power, cooled and 5μl (of 10mg/ml stock) of ethidium bromide was added. The solution was then poured into a gel-mould and left to cool. The gel was loaded with 1μl of loading buffer (Promega, UK) to 9μl of the appropriate PCR product in each well. A 100base DNA ladder (Promega, UK) was loaded into the well at either end.

Gels were visualised under UV light (Fig, 2.16). For Kv3.1 knockout mice the bands of interest are at 400 and 200 base pairs; a single band at 400 base pairs indicates a knockout (KO), bands at 400 and 200 base pairs a heterozygote (Hz), and a band at 200 base pairs a wild type (WT).

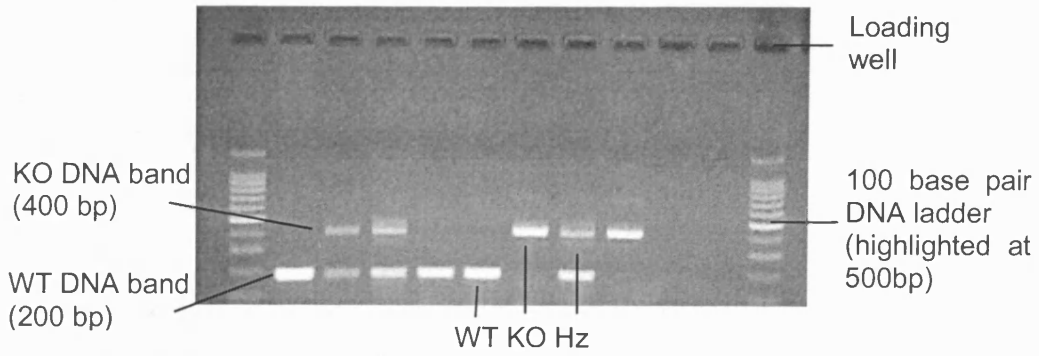

Figure 2.16 Genotyping results.
Example genotype results for a litter of Kv3.1 modified mice.

CHAPTER 3 – Results

Properties of MNTB Neurones

3.1 Introduction

The medial nucleus of the trapezoid body (MNTB) is a relay nucleus in the auditory brainstem which converts an excitatory input to an inhibitory output. MNTB neurones receive their input via giant nerve terminals known as the calyx of Held which surround the soma of each principal cell (Satzler et al., 2002). The nuclei which receive inputs from the MNTB determine the origin of a sound by calculating the timing and volume of the sound at each ear. The MNTB synapse is therefore highly specialised to ensure faithful transmission of the pattern and timing of this information.

The reason our laboratory became interested in this synapse is that the large size of the calyx permits direct patch clamp recordings to be made from the nerve terminal (Forsythe, 1994). It has been shown that more than one type of K^+ channel is present at the calyx and that one of the roles they perform is in reducing the width of the action potential (AP), but little else is known about these channels. We therefore wanted to characterise the K^+ channels present at the calyx and investigate their function. Since presynaptic recordings are technically demanding, we began by investigating the potassium channels present in the MNTB neurones before moving onto study those in the nerve terminal. In this chapter I will briefly describe the response of MNTB neurones under voltage clamp, current clamp and to synaptic stimulation to set the scene for a more detailed examination of the potassium currents in later chapters. The findings of this study are presented in chapters' three to six and described in more detail in chapter seven.

3.2 Inward currents expressed in MNTB neurones

In addition to outward K^+ currents MNTB neurones express several inward currents; in this section I will briefly describe two of these currents in MNTB neurones.

3.2.1 Sodium current

Upon depolarisation under voltage clamp, MNTB neurones elicit a fast inward current followed by a sustained outward current (Fig, 3.1A). The inward current is very rapid (inactivating within 0.5ms at room temperature) and is often in excess of 10nA (Forsythe and Barnes-Davies, 1993a). Application of 1μM tetrodotoxin (TTX), a puffer fish toxin selective for sodium channels, reversibly blocked this inward current, indicating that it is mediated by TTX-sensitive sodium channels. TTX-sensitive inward currents were not observed in outside-out patches excised from MNTB neurones (data not shown), suggesting that sodium channels are not localised to the somatic membrane; it is likely that sodium channels are localised to the site of AP initiation, the initial segment of the axon (Stuart and Sakmann, 1994; Hausser et al., 1995). The large magnitude of these currents, combined with their rapid inactivation, means that the patch clamp amplifier will almost certainly be unable to satisfactorily clamp them in whole cell mode. In order to study the sodium current further one would have to examine it in patches (excised from the initial segment) or alter the sodium concentration to reduce its magnitude. 1μM TTX was routinely included in other voltage clamp experiments to block the sodium current and allow investigation of the outward currents in isolation.

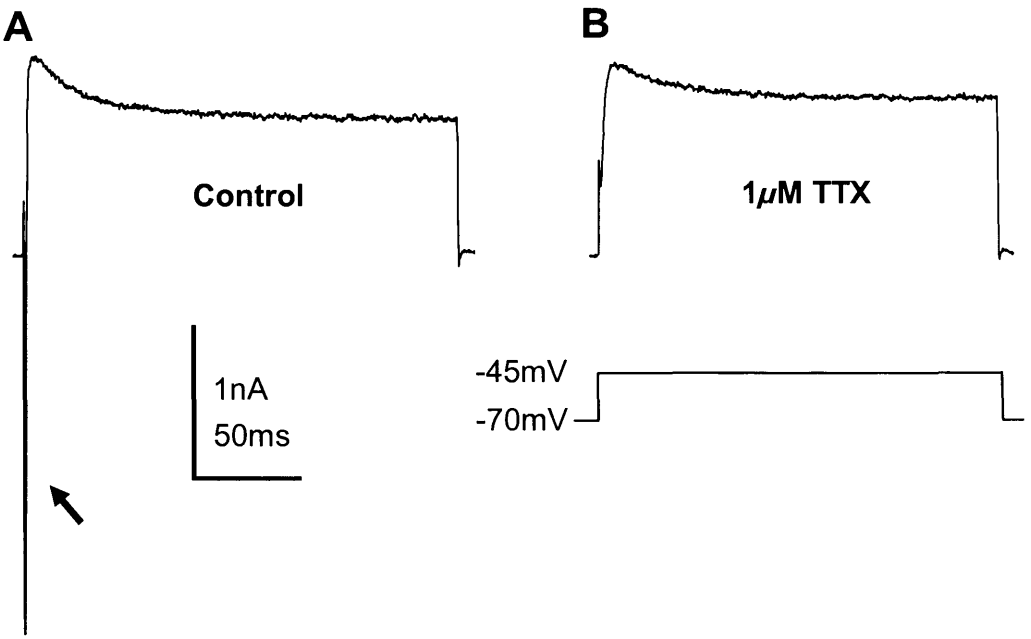

Figure 3.1. MNTB neurones possess a voltage-gated sodium conductance.
A. In control conditions a step to -45mV from a holding potential of -70mV elicits a fast inward current (arrow) followed by a slowly inactivating outward current. **B.** The fast inward current is blocked by bath application of the sodium channel blocker tetrodotoxin (TTX, 1μM).

3.2.2 Hyperpolarisation-activated currents

MNTB neurones exhibit a slowly activating inward current in response to hyperpolarising voltage steps (n=3, Fig, 3.2; Banks and Smith, 1992). This inward current activates around -100mV and is blocked by application of 10μM ZD7288 (Tocris Cookson, Bristol, UK, Fig, 3.2B); this suggests that this current is I_H, which is analogous to I_f in the heart and mediated by HCN channels (see section 1.3.3.4 and Santoro and Tibbs, 1999). In addition to MNTB neurones, I_H is present in many other auditory nuclei including: bushy cells and their calyceal endings (Oertel, 1983; Rusznak et al., 1996; Cuttle et al., 2001), the MSO (Smith, 1995) and octopus cells of the VCN (Bal and Oertel, 2000). In these nuclei it is likely that I_H is mediated by channels containing HCN1 and HCN2 subunits (Santoro et al., 2000).

In MNTB neurones, which also contain low-voltage activated K^+ conductances, it is likely that the resting potential is a balance between I_H depolarisation and Kv1 hyperpolarisation; this means that at rest both types of channel will be open, so the input resistance will be low. In

octopus cells the resulting low input resistance enables them to respond rapidly to large magnitude coincident inputs (Golding et al., 1999; Bal and Oertel, 2000). Since MNTB neurones do not play a role in coincidence detection it is likely that I_H, in concert with Kv1 conductances, acts to reduce the input resistance and so regulate AP threshold and reduce the duration of synaptic potentials (Trussell, 1999).

Activation of I_H at negative potentials means that an inward current will be present during the pre-pulses to -100mV that we used to study the K^+ currents (Fig, 3.2B). The presence of an inward current would affect leak subtraction of the current-voltage (I/V) relationships so we routinely applied ZD7288 in voltage clamp experiments to block I_H.

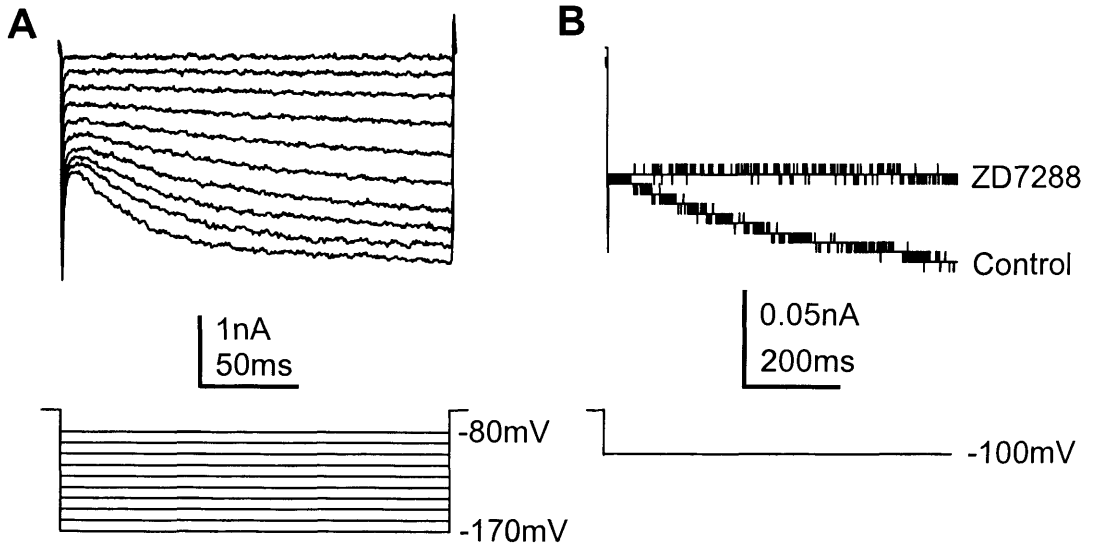

Figure 3.2. MNTB neurons possess a hyperpolarisation-activated cation current, I_H.
A. In control conditions hyperpolarizing steps from -80mV to -170mV (lower panel) from a holding potential of -70mV elicit a slowly activating inward current; this is best observed at more negative potentials (upper panel, lowest traces). **B.** I_H is activated during pre-pulses to -100mV. Application of 10μM ZD7288 blocked I_H.

MNTB neurones also express P/Q type calcium channels at their soma (Barnes-Davies et al., 2001). To minimise contributions from calcium currents (and potentially any calcium activated K^+ currents) in our non-synaptic experiments, we used a low calcium aCSF, containing 0.5mM $CaCl_2$ and 2.5mM $MgCl_2$.

3.3 Outward potassium currents expressed in MNTB neurones

3.3.1 Potassium currents

In addition to inward currents, MNTB neurones have previously been shown to possess outward currents consisting of high and low-voltage activated components (Forsythe and Barnes-Davies, 1993a; Brew and Forsythe, 1995). We applied 200ms depolarising voltage steps from -90 to 0mV to elicit outward currents in voltage clamped MNTB neurones (Fig, 3.3C). The data are presented as overlaid current traces elicited by steps between -70mV (lowest trace, Fig, 3.3A) and 0mV (uppermost trace, Fig, 3.3A) in 10mV intervals. Applying a 750ms pre-pulse to -100mV (Fig, 3.3C) removes the voltage-dependent inactivation, resulting in outward currents which activate rapidly at around -70mV, peak after about 10ms (measured at -30mV) and partially inactivate (Fig, 3.3A). The mean amplitude of currents evoked by a step to 0mV was 4.8±0.4nA (measured 10ms into the step, n=21). Applying a pre-pulse to -30mV inactivates part of the outward current leaving a sustained component which resembles typical delayed rectifiers (Fig, 3.3B).

Currents were plotted as current-voltage (I/V) relationships (Fig, 3.3D). The magnitude of the current was measured 10ms into the current trace and plotted against the voltage of the corresponding test step. The I/V relationship therefore shows how current changes with voltage. The linear 'leak' current was subtracted before plotting the I/V (see section 2.3).

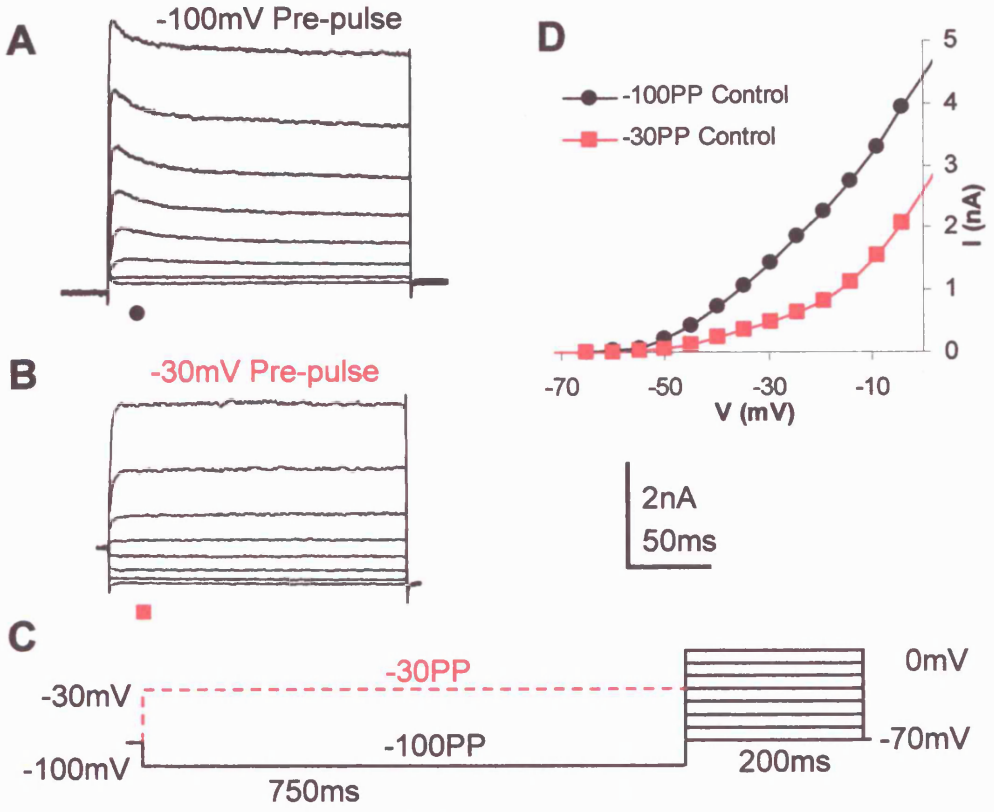

Figure 3.3. Outward currents in MNTB neurones.
A. Typical outward currents activated by test steps between -70mV and 0mV following a pre-pulse to -100mV (-100PP shown in C). Current records were not leak subtracted. **B.** Outward currents activated following a pre-pulse to -30mV (-30PP). **C.** Voltage protocols. Test steps were preceded by a -100mV pre-pulse (-100PP) or a -30mV Pre-pulse (-30PP, red dashed line). **D.** Current-Voltage relationship (I/V) of the currents in A (●) and B (■). Scale bar applies to current records in A and B.

3.3.2 DTX-I sensitive tail currents

The high and low-voltage activated components of the outward current have different deactivation properties; the high-voltage activated current deactivates much faster than the low-voltage activated component (Brew and Forsythe, 1995). We examined the tail currents by applying a brief activating pulse to -40mV followed by test steps to potentials between -120mV and -50mV (Fig, 3.4C). The activating pulse to -40mV will activate mainly the low-voltage activated K^+ channels; as the potential is stepped more negative during the test steps the channels will deactivate, observed as tail currents. In control conditions this approach generated tail currents which deactivated slowly (n=2, within 5ms, Fig, 3.4A1). The

low-voltage activated current is sensitive to the snake-venom toxin dendrotoxin-I (DTX I, Brew and Forsythe, 1995). Application of 100nM DTX-I blocked the slowly deactivating tail currents (Fig, 3.4A2), confirming that they were mediated by the low-voltage activated current. In the presence of DTX-I, a small current can be seen to activate in the test step to -50mV and during the activation pulse to -40mV (Fig, 3.4A2). This is the DTX-I resistant high-voltage activated current, which activates around -50mV in rat MNTB neurones (Brew and Forsythe, 1995).

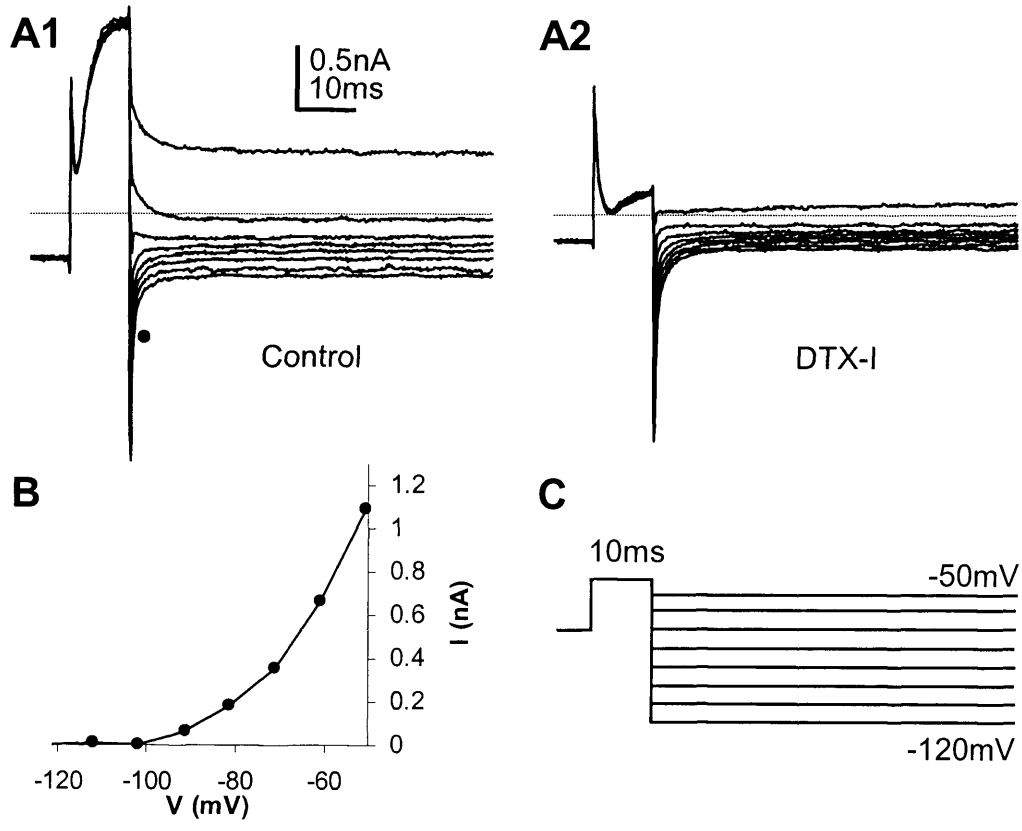

Figure 3.4. Dendrotoxin-I (DTX-I) blocks a slowly deactivating current.
A1. Tail currents recorded using the protocol in C. **A2.** The slowly deactivating tail current is blocked by 100nM DTX-I. **B.** Leak subtracted I/V of the instantaneous tail current in A1. The reversal potential is just negative to -100mV. **C.** Tail current protocol used in A.

3.4 Action potential firing in MNTB neurones

3.4.1 Unitary firing

It is a characteristic feature of MNTB neurones that they fire a single AP in response to sustained depolarisation (Banks and Smith, 1992; Forsythe and Barnes-Davies, 1993a; Brew and Forsythe, 1995). This unitary firing is important in preserving the fidelity of information transmitted from bushy cells of the aVCN to MNTB neurones.

We recorded from MNTB neurones under current clamp and applied 200ms square-pulse depolarising current injections between 50 and 350pA. In control conditions we always observed a single AP in response to sustained current injection (n=6, Fig, 3.5). The current injection threshold for AP generation was quite variable (between 50 and 200pA) and was partly dependent on how 'leaky' the recording was. Sub-threshold current injections resulted in a hump (Fig, 3.5A arrows) where the membrane depolarised and then repolarised. This sub-threshold hump (also referred to as a transient potential), is thought to be caused by the low-voltage activated currents since it is perturbed in Kv1.1 and Kv1.2 knockout mice (Gittelman et al., 2002). After the initial depolarisation, outward rectification of the Kv1 current acts to hyperpolarise the membrane, thus producing the hump. The sub-threshold hump has been described many auditory neurones (Oertel, 1983; Wu and Oertel, 1984; Manis and Marx, 1991; Banks and Smith, 1992; Forsythe and Barnes-Davies, 1993a; Reyes et al., 1994; Smith, 1995; Schwarz and Puil, 1997) and is thought to be important in ensuring a precise latency to the first spike to encode stimulus onset (Adam et al., 1999).

Application of 1μM TTX to block voltage-gated sodium channels abolished AP firing (n=2, Fig, 3.5B), confirming that APs are generated by a sodium conductance in MNTB neurones. In the presence of TTX the sub-threshold hump remains (Fig, 3.5B arrow), but is observed in response to more depolarising current injections. This is probably because in control conditions the sub-threshold hump is generated by Kv1 channels in response to rapid depolarisation by the sodium channels. In the absence of the sodium conductance (in TTX), more current must be injected to activate the Kv1 channels.

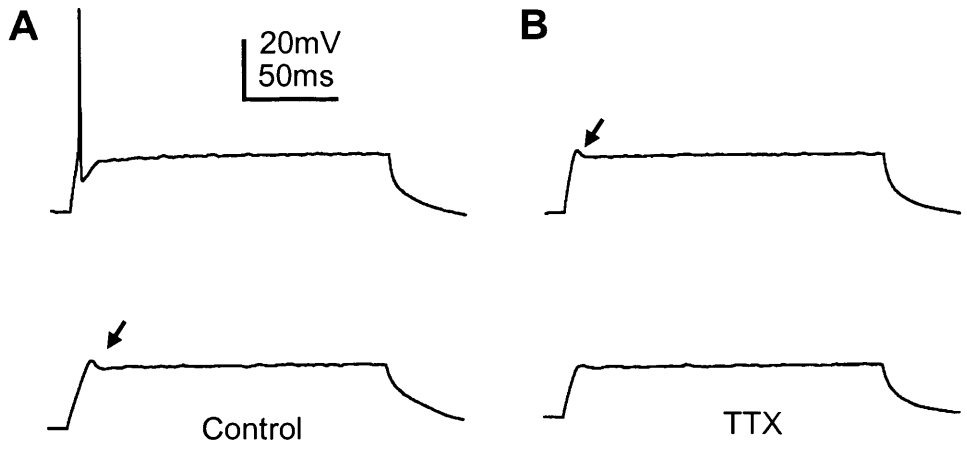

Figure 3.5. A single AP is generated in response to sustained current injection.
A. Typical current clamp recording from an MNTB neurone. In this neurone a sub-threshold hump (arrow) is observed after 100pA current injection and an AP after 150pA. **B.** Recording from the same neurone in the presence of 1μM tetrodotoxin (TTX). No APs were observed in the presence of TTX although the sub-threshold hump remains (arrow).

To investigate the waveform of APs in MNTB neurones, AP parameters were measured under true current clamp (Fig, 3.6). APs had a threshold point of -50±2mV, peaked at 37±2mV had a half-width of 575±28μs and were followed by a shallow afterhyperpolarisation (AHP) with an undershoot of -8.0±0.6mV (n=6).

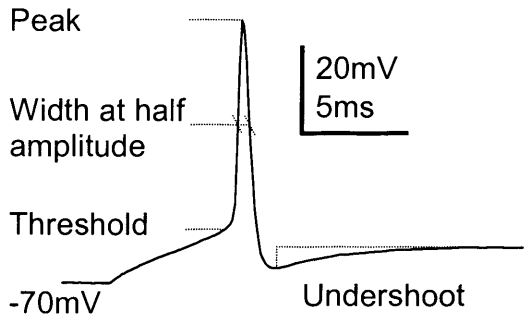

Figure 3.6. AP Parameters.
An example AP generated by a 200pA current injection showing points of measurement for quantification.

3.5 Synaptic currents in MNTB neurones

3.5.1 MNTB neurones generate a dual component EPSC

Glutamate release from the calyx evokes a large excitatory post synaptic current (EPSC) in MNTB neurones. To examine the role of K^+ channels in modulating synaptic transmission we electrically stimulated presynaptic axons using a bipolar stimulating electrode (see section 2.2.6.4) and recorded from voltage clamped MNTB neurones. In some cases, simultaneous recordings were made from both the presynaptic terminal (current clamp) and the postsynaptic MNTB neurone (voltage clamp) with the help of Dr Brian Billups (see Fig, 5.12). In these dual recordings, synaptic connections were detected using calcium imaging (for methods see Billups et al., 2002). When recording EPSCs alone, synaptic connections were found by chance. The probability of finding a connected pair was acceptable since visible calyces often had axons extending to the midline in slices that were cut with the brainstem mounted at approximately 20° (see methods section 2.2.1). In all EPSC recordings 5mM QX-314 was included in the intracellular solution to block voltage gated sodium channels.

Supra-threshold stimulation of the presynaptic axon resulted in a dual component EPSC in the MNTB neurone (n=7Fig, 3.7A). The two components arise because synaptic transmission in the MNTB is mediated by both AMPA (α-amino-3-hydroxy-5-methylisoxazole-propionate) and NMDA (non-methyl-D-aspartate) receptors. The fast component of the EPSC is mediated by AMPA receptors and can be blocked by 5μM CNQX (6-cyano-7-nitroquinoxaline, Forsythe and Barnes-Davies, 1993b). The AMPA receptor mediated EPSC component in the MNTB is much faster than those in non-auditory neurones (Trussell, 1999), matched only by those found in rod photoreceptors (Eliasof and Jahr, 1997). Examination of the AMPA receptor subunits in the MNTB revealed that high levels of the $GluR4_{flop}$ splice variant are expressed (Geiger et al., 1995). Receptors which contain high levels of $GluR4_{flop}$ but lack GluR2 have the most rapid kinetics (Mosbacher et al., 1994), which may account for the fact that auditory EPSCs are much faster than those in other neurones. Rapid EPSCs in conjunction with a short membrane time constant (facilitated by I_H and Kv1 channels) help to keep excitatory post synaptic potential (EPSPs) brief and therefore accommodate high frequency transmission.

The slow component of the EPSC is mediated by NMDA receptors and is sensitive to 30μM AP5 (2 -amino-5-phosphonovalerate, Forsythe and Barnes-Davies, 1993a). This slow component gradually decreases with development and is absent by P16 (Joshi and Wang, 2002). It is thought that calcium influx through NMDA receptors might be important for establishing the appropriate AMPA receptors at the synapse but are removed to prevent calcium overloading in mature MNTB neurones (Joshi and Wang, 2002).

The effect of these currents on AP firing can be investigated under current clamp. Presynaptic stimulation (whilst recording from an MNTB neurone under current clamp) resulted in an EPSP, which triggered a single AP (Fig, 3.7B). The long duration of the EPSP in this recording is attributable to the NMDA receptor mediated component (Forsythe and Barnes-Davies, 1993b).

Stimulation of presynaptic axons at high frequencies results in short-term synaptic depression (Otis et al., 1996; von Gersdorff et al., 1997; von Gersdorff and Borst, 2002). At 100Hz the amplitude of the 10^{th} EPSC is around a third of the control amplitude (Fig, 3.7C), although the amount of depression varies with the age of the animal (Taschenberger and von Gersdorff, 2000; Joshi and Wang, 2002). Synaptic depression at the calyx is probably caused by a combination of pre- and postsynaptic effects such as changes in release probability and postsynaptic receptor desensitisation (Scheuss et al., 2002). Although depression is observed during a train, some variability is observed in the amplitude of individual EPSCs (Fig, 3.7C asterisks). This variability is due to the probabilistic nature of neurotransmitter release.

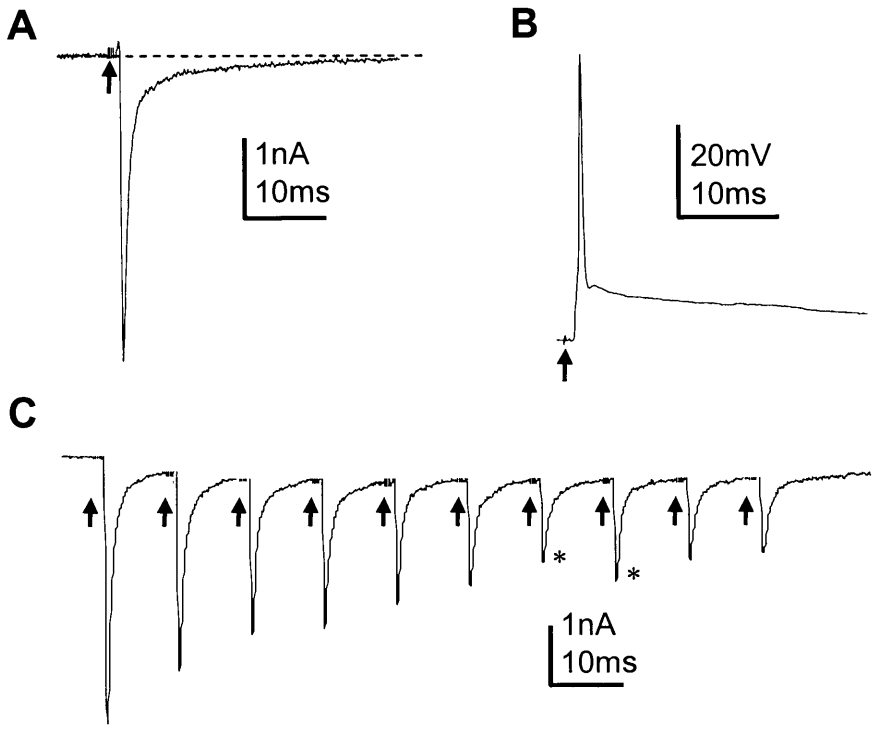

Figure 3.7. Synaptic currents in MNTB neurones.
A. EPSC recorded from an MNTB neurone (in voltage clamp) following electrical stimulation at the midline. **B.** Synaptic response recorded in a different MNTB neurone (under current clamp) in the absence of QX-314. Stimulation results in an AP followed by sustained depolarisation. **C.** EPSCs elicited by a 100Hz train of stimuli in a different neurone to A and B. Synaptic depression is observed during the train with some variability between individual EPSCs (*). A & C were recorded in the presence of 10μM bicuculline and 1μM strychnine and stimulation artefacts were removed. Arrows represent the time-point at which stimulation was applied.

3.6 Summary

In this chapter I have described inward and outward currents in MNTB neurones. Voltage-gated sodium channels generate inward currents upon depolarization, which are responsible for the upstroke of the AP. Hyperpolarisation-activated cation channels also generate an inward current (I_H) which helps to maintain a short membrane time-constant important in allowing MNTB neurones to respond rapidly and reset quickly during synaptic activity. These inward currents can be blocked to allow isolation of the outward potassium currents. K^+ currents consist of both high and low-voltage activated components and can be partially inactivated. Low-voltage activated K^+ currents act to oppose depolarisation and therefore ensure that MNTB neurones fire a single AP in response to sustained current injection. MNTB neurones generate a large, rapid EPSC in response to glutamate released from the calyx. The currents expressed in MNTB neurones act together to enable the neurone to faithfully follow AP firing in the presynaptic terminal and hence transmit information regarding sound location.

CHAPTER 4 – Results

Low-Voltage Activated K^+ Currents in MNTB Neurones

4.1 Introduction

Voltage-gated potassium channels are widely expressed in the nervous system and play important roles in regulating neuronal excitability. It has previously been shown that MNTB neurones possess low-voltage activated K^+ currents which limit repetitive AP generation (Forsythe and Barnes-Davies, 1993a; Brew and Forsythe, 1995). These low-voltage activated currents are sensitive to the snake-venom toxin dendrotoxin-I (DTX-I) and are therefore mediated by channels containing Kv1.1, Kv1.2 or Kv1.6 subunits (Harvey, 2001). Since the studies of MNTB neurone K^+ conductances were carried out, several other subunit-specific toxins have been characterised. These include dendrotoxin-K (DTX-K), a snake venom toxin specific for channels containing Kv1.1 subunits (Robertson et al., 1996) and Tityustoxin-Kα, which blocks channels containing Kv1.2 (Matteson and Blaustein, 1997; Hopkins, 1998). Since these toxins will block channels containing a single toxin-sensitive subunit (Hopkins, 1998), they allow more detailed investigation of the channels underlying the low-voltage activated conductance. We combined immunohistochemistry and the use of these subunit-specific toxins to further examine the K^+ conductances in the MNTB.

4.2 Kv1 expression in the MNTB

There are eight Kv1 family members identified to date (Kv1.1-1.7, Kalman et al., 1998; Catterall et al., 2002). Kv1.1-1.6 are expressed in the brain (Coetzee et al., 1999; Kashuba et al., 2001) and antibodies to these subunits are commercially available and are widely used. All appear to specifically label the appropriate Kv1 channels (Scott et al., 1994; Bekele-Arcuri et al., 1996; Chung et al., 2000) with the exception of those to Kv1.3. Kv1.3

immunoreactivity is observed in a Kv1.3 knockout mouse (L. Kaczmarek personal communication), which suggests that the antibody is binding to something other than Kv1.3.

4.2.1 Kv1.1, Kv1.2 and Kv1.6 are expressed in MNTB neurones

We applied Kv1.1, Kv1.2, Kv1.4, Kv1.5 and Kv1.6 antibodies to sections containing the MNTB. Immunoreactivity for Kv1.1, Kv1.2 and Kv1.6 was detected in MNTB neurones (Fig, 4.1). Immunofluorescence to these subunits is clearly above background and is significantly different from that when blocking peptide was applied with the primary antibody ($P<0.05$ paired t-test, n=3 animals). Immunofluorescence of Kv1.4 and Kv1.5 was only just above background and was not significantly different from that with blocking peptide ($P>0.5$; paired t test), suggesting that the fluorescence was due to non-specific binding of the primary antibody. Although the immunofluorescence detected will include cytoplasmic as well as membrane staining, it is clear that Kv1.1, Kv1.2 and Kv1.6 subunits are expressed whereas Kv1.4 and Kv1.5 expression is absent.

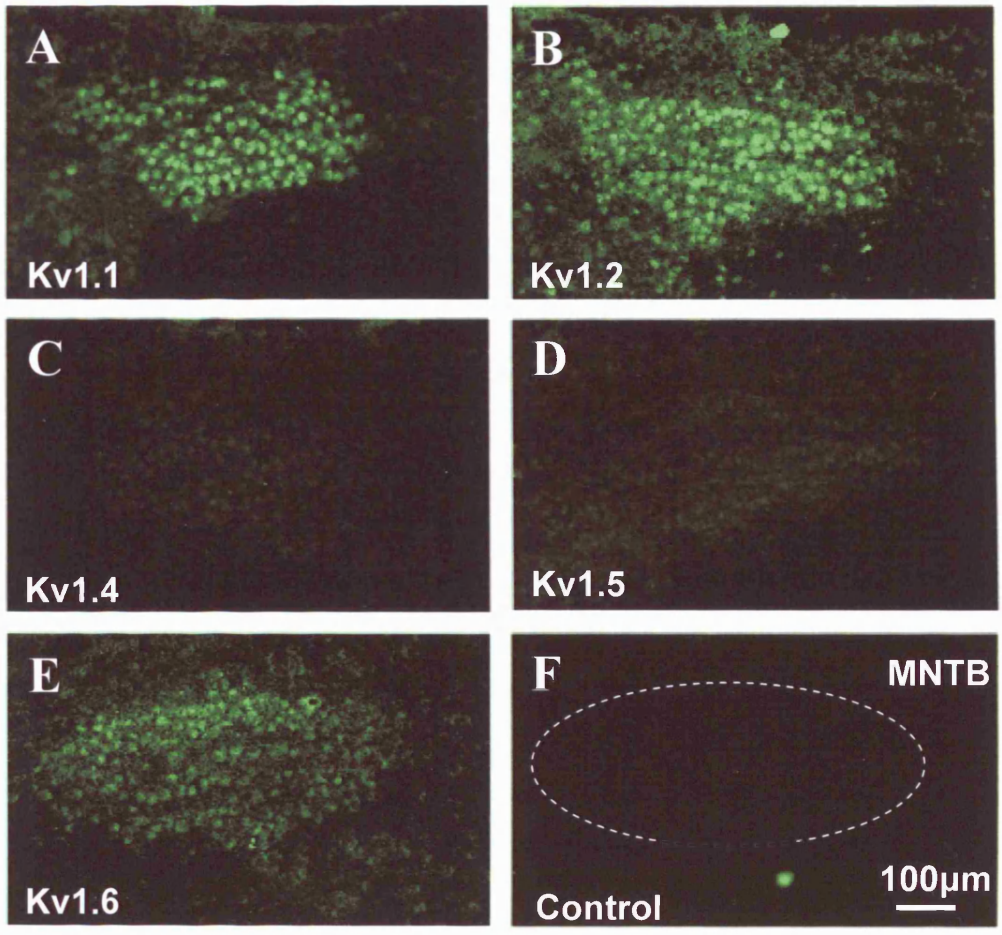

Figure 4.1. Kv1.1, Kv1.2 and Kv1.6 are expressed in MNTB neurones.

Immunoreactivity for Kv1.1 (**A**), Kv1.2 (**B**) and Kv1.6 (**E**) is significantly higher than when blocking peptide was incubated with the primary antibody ($P<0.05$ paired t-test, $n=3$ animals). Immunofluorescence for Kv1.4 (**C**) and Kv1.5 (**D**) was not significantly different from that in the presence of blocking peptide, suggesting the measured fluorescence was due to non-specific binding of these primary antibodies. In each panel an example low-power (10X Obj.) image of the MNTB is shown. The primary antibody used is indicated in the bottom left of each part. **F.** Control image denoting background fluorescence represents secondary antibody fluorescence with the primary antibody substituted for 10% goat serum. Immunolabelling was performed by M. Barker.

4.3 Pharmacology of the low-voltage activated K^+ current

4.3.1 DTX-I blocks the low-voltage activated current

Having established that Kv1.1, Kv1.2 and Kv1.6 are expressed in the MNTB we decided to investigate their contribution to the low-voltage activated K^+ current. We began by making whole cell recordings from MNTB principal neurones and applying 100nM DTX-I. The mean current at -45mV was 0.6±0.05nA (n=21) and should largely consist of the low-voltage activated current (Fig, 4.2C), we therefore measured the effects of toxin-block at this potential. DTX-I blocked 82±5% (range=67.6 to 91.7%, n=4) of the low-voltage activated current, leaving only the high-voltage activated current which activates around -50mV (Fig, 4.2D). Since the current traces are not leak subtracted (unlike the I/V curves, see methods), the trace in the presence of toxin will also contain a leak component; hence, block in figure 4.2C appears less than 82%. These data suggest that all of the low-voltage activated K^+ current is mediated by channels containing Kv1.1, Kv1.2 or Kv1.6, supporting the immunohistochemical evidence for the presence of these subunits. In addition, the partial inactivation observed during 200ms test pulses under control conditions (Fig, 4.2A) is abolished by DTX-I (Fig, 4.2B). This suggests that the partial inactivation is conferred by Kv1 channels.

In the presence of DTX-I the I/V curve often approaches or even crosses the control I/V at around 0mV (Fig, 4.2D). In the absence of series resistance changes, one would not expect to see an increase in one current resulting from block of another. We therefore attribute this to an improved clamp of the high-voltage activated current, which causes an apparent increase of the current measured at 0mV.

To be confident at which point maximum toxin block is achieved, we measured the time it took for DTX-I to get into the bath and block the low-voltage activated current (Fig, 4.2E). It is important that data is collected as soon as block is achieved to prevent problems associated with series resistance changes during the course of an experiment, or worse still, loss of the recording. After approximately 3.5 mins DTX-I had begun to take effect and by 6 mins the current measured at -40mV was maximally blocked (n=2, Fig, 4.2E). The time taken to block

the current is likely to represent the dead space of the perfusion lines, mixing of toxin and control solutions in the chamber, diffusion of toxin into the slice and binding to the appropriate channels. Time to block could be further reduced by priming the drug lines (as described in the methods section), but after 6 minutes of toxin application we could be confident that maximal block was achieved. In subsequent experiments toxin-block was measured at least 6 minutes after application.

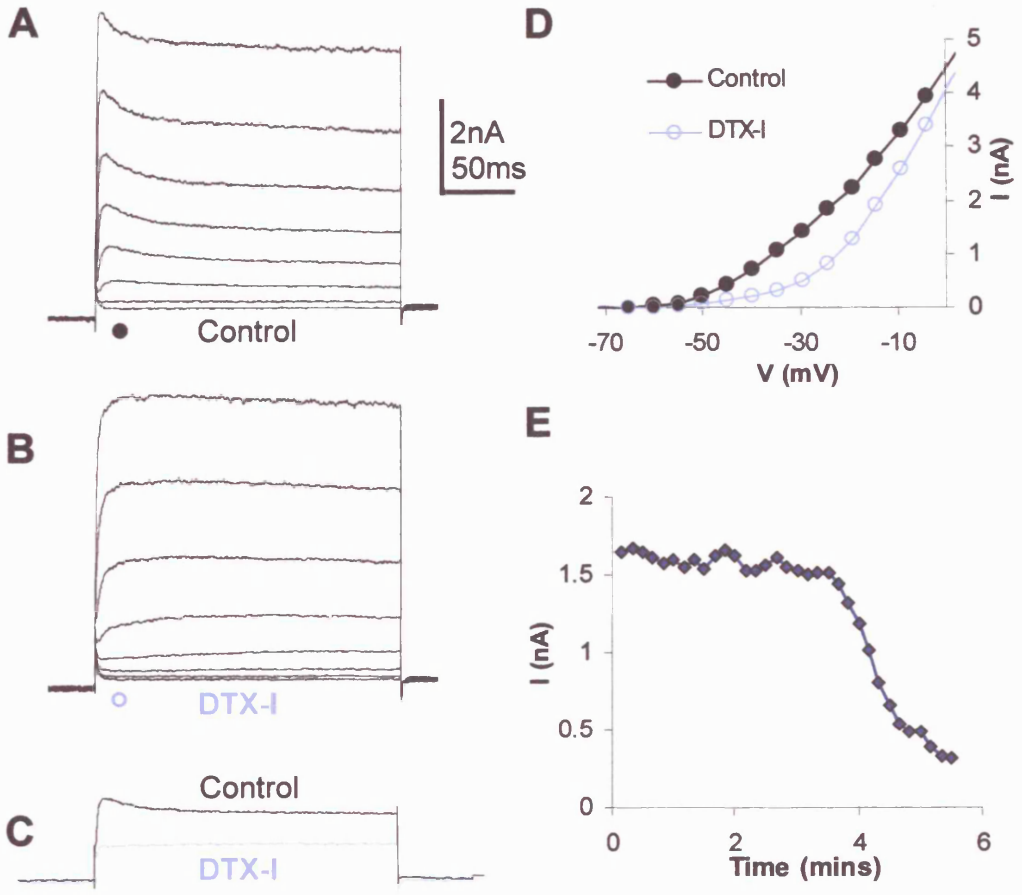

Figure 4.2. DTX-I blocks all of the low-voltage activated K+ current in MNTB neurones.

A. Currents activated following a pre-pulse to -100mV. **B.** DTX-I (100nM) blocks the low-voltage activated current, leaving only the high-voltage activated current. **C.** Enlarged traces from A and B showing block of currents measured at -45mV by DTX-I. **D.** I/V relationship of the data in A (●) and B (○). **E.** Time-course of DTX-I block. Current amplitude of a step to -40mV during DTX-I wash-on. The first time-point represents the time at which DTX-I perfusion began. The perfusion line was unprimed. Scale bar in A applies to parts A to C.

4.3.2 All Kv1 channels in MNTB neurones contain Kv1.1 subunits

To further investigate the subunit composition of Kv1 channels in MNTB neurones we applied dendrotoxin-K (DTX-K), which is specific for channels containing Kv1.1 subunits (IC_{50} 2.5nM for homomers, Robertson et al., 1996). Application of 100nM DTX-K blocked 90±4% of the low-voltage activated current in MNTB neurones (measured at -45mV, range=83 to 96%, n=4, Fig, 4.3A). Since the partial inactivation was also abolished by DTX-K (Fig, 4.3A), we produced a subtraction of the DTX-K sensitive current and measured the time-course of inactivation. The inactivation of the low-voltage activated current was fit with a single exponential with a τ of 63.7ms. Subtraction of currents can be misleading since slight changes in series resistance can appear as an effect of a drug. In this case however, the series resistance remained precisely constant throughout the experiment so the data were suitable for subtraction. Slight series resistance changes in the other three cells precluded further satisfactory subtractions.

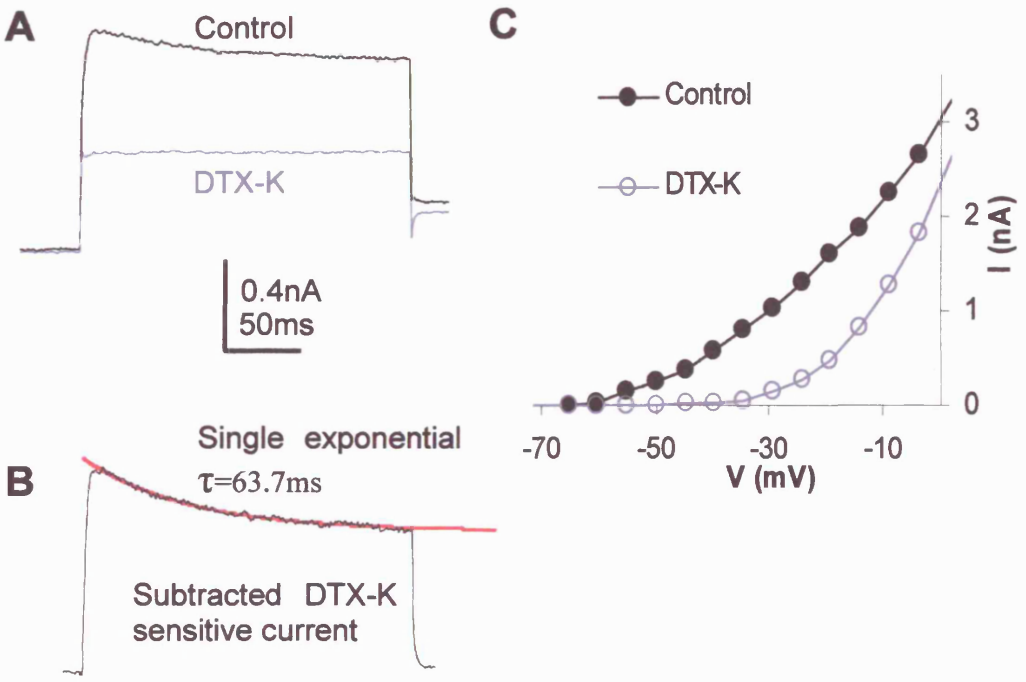

Figure 4.3. DTX K blocks the low voltage activated K+ current in MNTB neurones. **A.** Step to -45mV following a pre-pulse to -100mV in control (black trace) and 100nM DTX-K (blue trace), which blocks channels containing Kv1.1. **B.** DTX-K sensitive current produced by subtracting the traces in A. Inactivation of the DTX-K sensitive current could be fit with a single exponential with a time constant of 63.7ms. **C.** I/V relationship of control currents (●) and those in the presence of 100nM DTX-K (○).

4.3.3 Half of the Kv1 current is mediated by channels containing Kv1.2 subunits

Application of tityustoxin-Kα, a scorpion toxin selective for channels containing Kv1.2 or Kv1.3 (IC_{50}=0.55nM for homomers in oocytes, Hopkins, 1998; and 3.9nM for Kv1.3 homomers at pH 7.5, Rodrigues et al., 2003), permitted further dissection of the low-voltage activated current. TsTX-Kα (100nM) blocked around half (48±4% range=36.3 to 64.1%, measured at -45mV, n=7) of the low-voltage activated current (Fig, 4.4). Application of higher TsTX-Kα concentrations (up to 200nM) produced no additional block, suggesting that all channels containing Kv1.2 or Kv1.3 were selectively blocked by 100nM TsTX-Kα. Subsequent application of DTX-I resulted in complete block of the low-voltage activated current (Fig, 4.4B). This suggests that the low-voltage activated current consists of two components: both contain Kv1.1 subunits but only one contains Kv1.2 or Kv1.3 subunits. An

intriguing observation was made in the absence of TTX; during TsTX-Kα application (or indeed DTX-K or DTX-I) multiple action currents appeared (Fig, 4.4D). This suggests that the TsTX-Kα sensitive component of the low-voltage activated current normally suppressed these action currents.

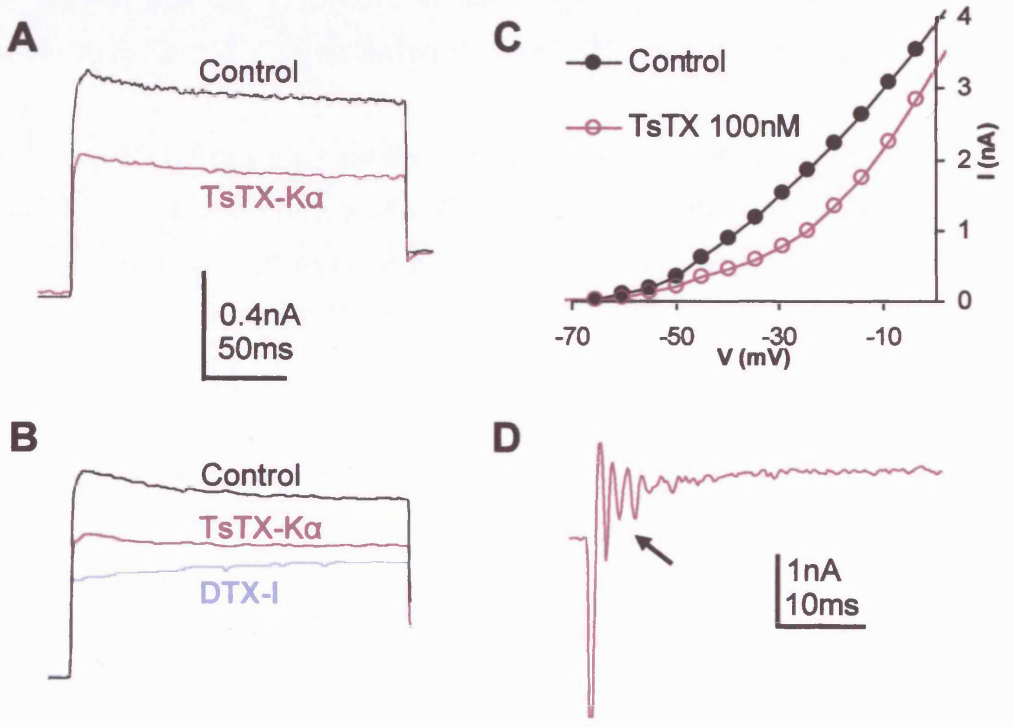

Figure 4.4. TsTX Kα only blocks part of the Kv1 current in MNTB neurones.
A. Step to -45mV following a pre-pulse to -100mV in control (black trace) and 100nM TsTX-Kα (purple trace), which blocks channels containing Kv1.2 or Kv1.3 subunits. **B.** Step to -45mV in a different neurone to that in A in control (black trace) and 100nM TsTX-Kα (purple trace) and 100nM DTX-I. **C.** I/V relationship of control currents (•), in the presence of 100nM TsTX-Kα (o). **D.** Application of TsTX-Kα in the absence of TTX results in multiple sodium spikes being fired (arrow). Parts A to C are from the same neurone and traces were leak subtracted.

4.3.4 Kv1.3 subunits do not contribute to the low-voltage activated current

Since no suitable antibody to Kv1.3 was available, we decided to use a pharmacological approach to investigate whether Kv1.3 contributes to the low-voltage activated current. We applied noxiustoxin (NTX; 100nM), a scorpion toxin selective for channels containing Kv1.2,

Kv1.3 or Kv1.7 subunits (Kd=2 nM for Kv1.2 homomers, Grissmer et al., 1994). NTX blocked 48±5% (range=42.1 to 56.9%, n=3) of the current at -45mV (Fig, 4.5A). Since NTX blocked a similar proportion of the current to TsTX-Kα and they both block Kv1.2 and Kv1.3 containing channels, this suggesting that NTX is blocking the same component as TsTX-Kα. These data do not exclude the involvement of Kv1.3 in the TsTX-Kα-sensitive component but they do suggest that the TsTX-Kα-resistant component does not contain Kv1.3 subunits (otherwise TsTX-Kα and NTX would have blocked all the low-voltage activated current).

To see whether Kv1.3 subunits contributed at all to the low-voltage activated current we used CP-339,818, a compound which blocks Kv1.3 and Kv1.4 containing channels (IC_{50}=0.23μM and 0.3 respectively for homomers, Nguyen et al., 1996; Jager et al., 1998). This compound is not entirely selective, since at higher concentrations (IC_{50}>14μM) it will block other Kv1 channels. Application of 1μM CP-339,818 had no effect on the low-voltage activated current (Fig, 4.5B), suggesting that Kv1.3 (or indeed Kv1.4) subunits do not contribute to the low-voltage activated current in MNTB neurones. On average CP-339,818 caused a 6±7% increase in the current (n=3, Fig, 4.5B1) which is probably a combination of slight changes in series resistance and the effects CP-339,818 has on C-type inactivation (Nguyen et al., 1996). We also tried higher concentrations of CP-339,818 on a few cells; concentrations greater than 10μM produced some block of the outward current but this was probably due to block of subunits other than Kv1.3 or Kv1.4.

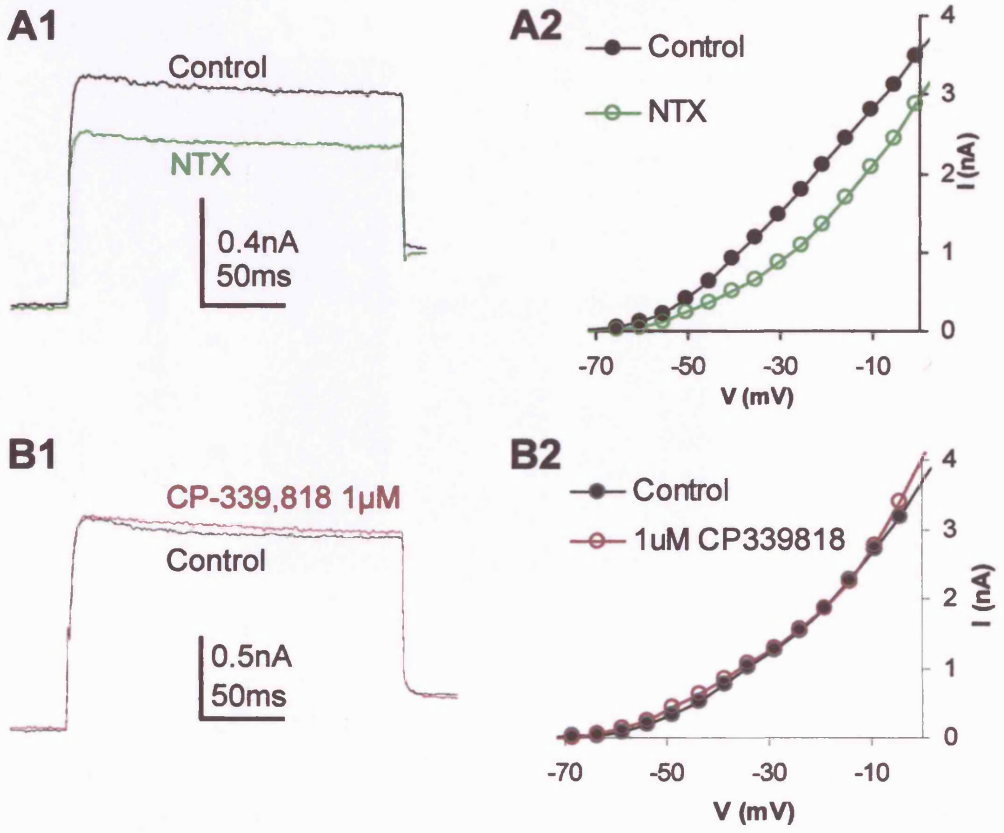

Figure 4.5. Kv1.3 subunits do not contribute to the Kv1 current in MNTB neurones. **A1.** Step to -45mV following a pre-pulse to -100mV in control (black trace) and 100nM NTX which blocks channels containing Kv1.2 Kv1.3 or Kv1.7 subunits (green trace). **A2.** I/V relationship of control currents (●) and in the presence of 100nM NTX (○). **B1.** Step to -45mV in a different neurone in control (black trace) and CP-339,818 which blocks channels containing Kv1.3 or Kv1.4 (brown trace). **B2.** I/V relationship of control currents (●) and in the presence of 1µM CP-339,818 (○). Traces were leak subtracted.

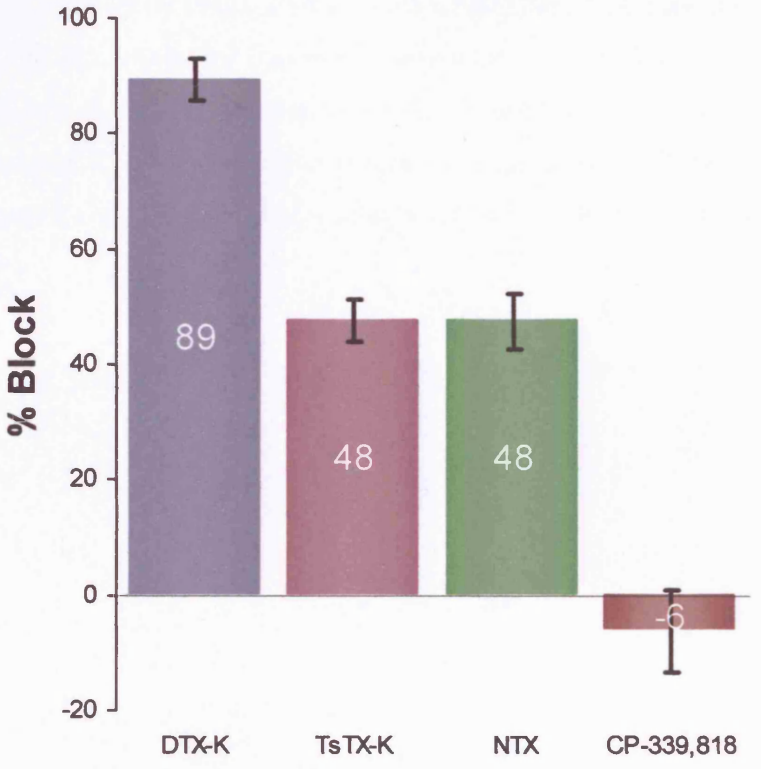

Figure 4.6. Percentage block of the low-voltage activated K^+ current by different toxins. Bar chart showing the percentage block of the current measured at -45mV by DTX-K (n=4), TsTX-Kα (n=7), NTX (n=3) and CP-339,818 (n=3).

4.4 Subcellular localisation of Kv1 subunits in MNTB neurones

4.4.1 Kv1.1 and Kv1.2 are localised to the initial segment of MNTB neurones

Our initial immunohistochemistry (Fig, 4.1) demonstrated which Kv1 subunits were present, but gave little information about their subcellular localisation. We therefore examine subcellular Kv1 localisation in more detail using a confocal microscope (Fig, 4.7). Although there was strong cytoplasmic labelling for all three antibodies in the soma, there was no obvious increase in fluorescence at the plasma membrane; suggesting that these subunits may not be localised to the soma. We were unable to visualise the dendrites of MNTB neurones (and therefore could not examine Kv1 localisation), probably due to their scarcity and small size (Banks and Smith, 1992). We then examined the axons of MNTB neurones; to be certain that we were examining MNTB axons and not those terminating in calyces round the MNTB neurones, we only examined those where we could see continuous fluorescence between the

soma and the axon (see Dodson et al., 2003). Both Kv1.1 (Fig, 4.7A) and Kv1.2 (Fig, 4.7B & D) showed the highest levels of immunofluorescence in the first 20μm of the axon. Co-localisation showed that there was overlap of Kv1.1 and Kv1.2 fluorescence in this region (Fig, 4.7C). In contrast, Kv1.6 immunofluorescence was not seen in MNTB axons (Fig, 4.7E), suggesting that channels containing Kv1.6 subunits might be localized to the soma or proximal dendrites.

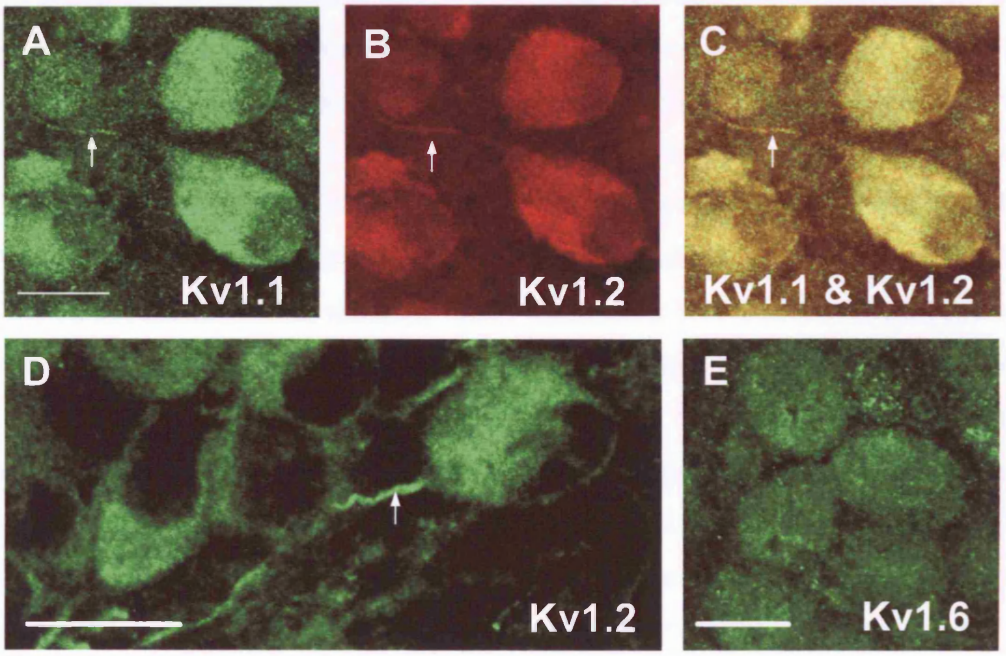

Figure 4.7. Kv1.1 and Kv1.2 are highly expressed in the axons of rat MNTB neurones. **A.** Kv1.1 immunofluorescence using a FITC conjugated secondary antibody. The initial 20μm of the axon has the highest level of immunoreactivity (arrows). Cytoplasmic staining was observed in the soma, with no obvious additional staining at the plasma membrane. The image is a Z-series projection of 5 images through an MNTB neurone with a step size of 0.675μm. **B.** Kv1.2 immunofluorescence using a Texas Red conjugated secondary antibody. A Z-series projection as in A. **C.** Co-localization of Kv1.1 (green) and Kv1.2 (red). **D.** Closer examination of Kv1.2 immunofluorescence (using a FITC conjugated secondary antibody). Image is a Z-series projection of 20 images with a step size of 0.175μm. **E.** Somatic but not axonal Kv1.6 immunofluorescence was observed (n=4 animals). Scale bars represent 20μm; the same scale was used for images A to C. Immunolabelling was performed by M. Barker.

4.5 Kv1 channel composition

4.5.1 Kv1.1/1.6 and Kv1.1/1.2 channels underlie the low-voltage activated current

Figure 4.6 shows that there are two components to the low-voltage activated current: one is blocked by either TsTX-Kα or NTX and both are blocked by DTX-K. Since we know from our immunohistochemistry and pharmacology that Kv1.1, Kv1.2 and Kv1.6 are the only Kv1 subunits expressed in MNTB neurones, we can draw some conclusions as to the probable subunit composition of the channels underlying the low-voltage activated current. The TsTX-Kα-sensitive current is also sensitive to DTX-K so this component must be a heteromer containing both Kv1.1 and Kv1.2 subunits (Fig, 4.8). We can exclude the involvement of Kv1.6 in these channels since Kv1.6 immunoreactivity does not overlap with Kv1.2 (Fig, 4.7). The TsTX-Kα-insensitive channels contain Kv1.1 subunits since they are DTX-K sensitive but obviously do not contain Kv1.2 subunits. Since homomeric Kv1.1 channels are TEA-sensitive (Hopkins, 1998), the absence of block of the Kv1 current by 1mM TEA (Brew and Forsythe, 1995) suggests that Kv1.1 homomers are not present. In addition, immunoprecipitation studies have been unable to isolate Kv1.1 homomers suggesting that these channels do not occur in the brain (Shamotienko et al., 1997; Koschak et al., 1998; Coleman et al., 1999). If the TsTX-Kα-insensitive channels are not Kv1.1 homomers, they must be Kv1.1/1.6 heteromers since Kv1.6 is the only other Kv1 subunit present in the MNTB (Fig, 4.8).

Whilst use of the toxins enables us to investigate which subunits are present, it provides little information about the proportions of subunits in each channel. For example Kv1.1/1.2 heteromers could either contain one, two or three Kv1 subunits out of the four Kvα-subunits in the channel (although the latter is unlikely since it would have a higher TEA sensitivity, Christie et al., 1990). It is also possible that rather than being a homogenous group of channels, the TsTX-Kα sensitive channels might be a mixture of those containing different Kv1.1 and Kv1.2 subunit proportions (for further discussion see section 7.2.2.2).

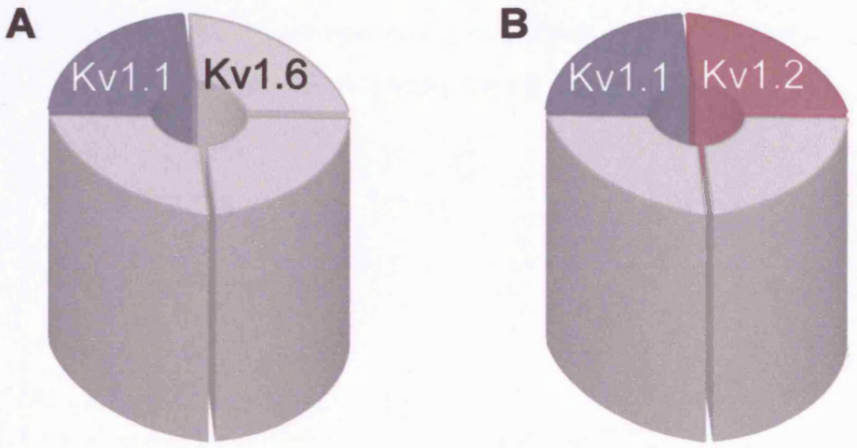

Figure 4.8. Channels comprising the low-voltage activated K^+ current.
A. Kv1.1/1.6 heteromers mediate the current that is TsTX-Kα resistant. **B.** Kv1.1/1.2 heteromers mediate the third of the current that is TsTX-Kα sensitive.

4.6 Low-voltage activated K^+ currents in mouse MNTB neurones

4.6.1 Different low-voltage activated K^+ currents are present in mice

To investigate the high-voltage activated current at the calyx (see chapter 6) we used mice for our experiments so we could take advantage of a Kv3.1 knockout mouse. During these studies we briefly examined the low-voltage activated current present in mouse MNTB neurones. On first examination, the currents seem similar to those in rat MNTB neurones; outward currents activate around -70mV and partially inactivate (Fig, 4.9). However, application of DTX-I revealed some differences: first, less current is blocked by DTX-I in mouse (only 41% of the current measured at the end of a step to -45mV; n=1), second, application of DTX-I revealed the presence of a transiently inactivating component (or A current, Fig, 4.9B). This current could clearly be seen in steps to -50mV (in 100nM DTX-I) by subtracting those with a -120mV pre-pulse from those with a -70mV pre-pulse (Fig, 4.9D). Brew *et al.* (2003) have since described this transient component which is blocked by 1mM 4-AP and present in mouse but not rat MNTB neurones (Fig, 4.9D). A-currents can be mediated by members of the Kv4 family, Kv3.4, Kv1.4 or other Kv1 channels with inactivating Kvβ subunits (Coetzee et al., 1999). Since this A-current activated at negative potentials, was blocked by 1mM 4-AP but resistant to 3mM TEA or 500nM DTX-I (Brew et al., 2003), Kv1.4 homomers seemed the

most likely candidates. We therefore investigated whether Kv1.4 subunits were expressed in mouse MNTB neurones; immunofluorescence for Kv1.4 was indeed detected in mouse MNTB neurones (Fig, 4.9E), suggesting that Kv1.4 homomers generate the A-current.

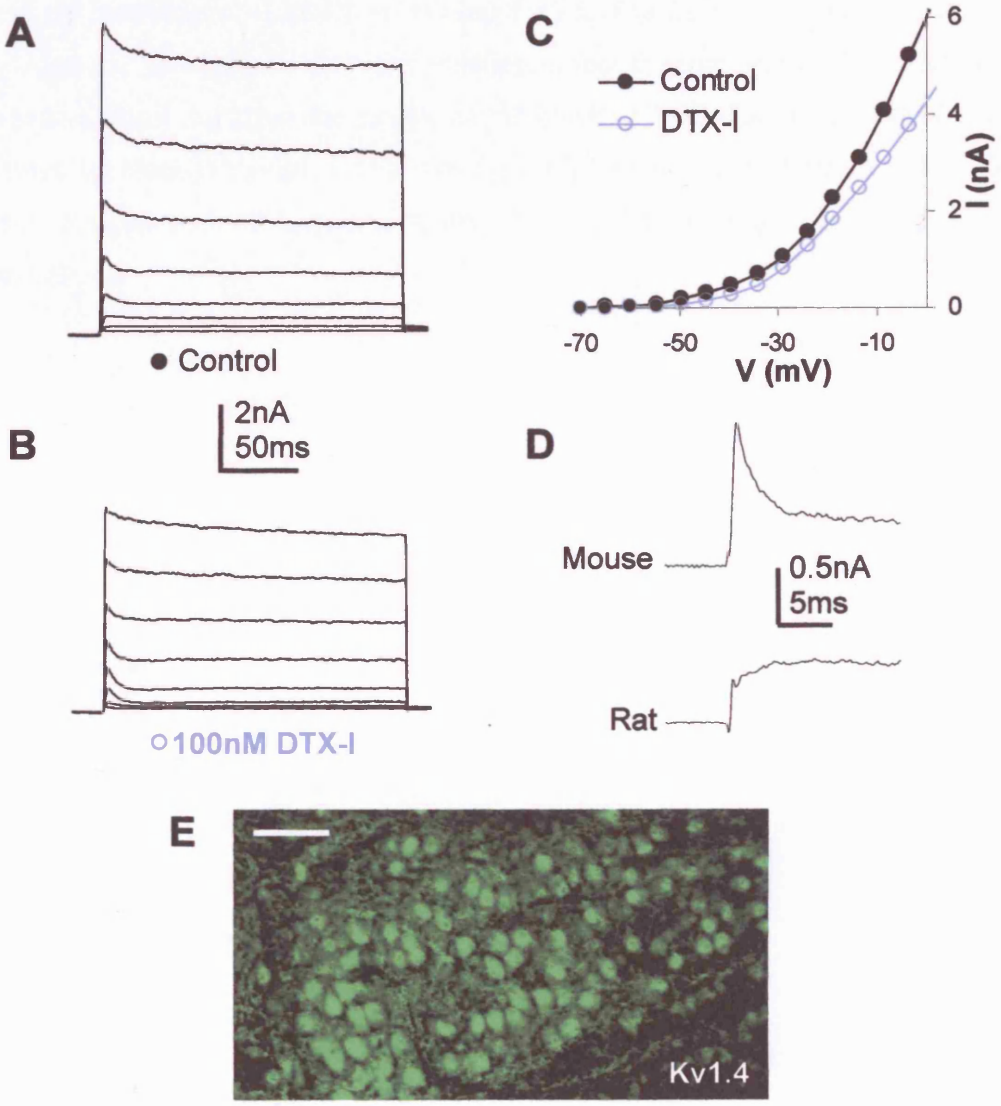

Figure 4.9. DTX I partially blocks the mouse MNTB low voltage activated K^+ current. **A.** Currents activation following a pre-pulse to -100mV. **B.** DTX-I (100nM) blocks the low-voltage activated current, leaving the high-voltage activated current and a transient current. **C.** I/V relationship of the currents in A (●) and B (○). **D.** The transient current (shown in a step to -50mV) is present in mouse but absent in rat MNTB neurones. Current records were obtained by subtracting the current elicited from a -70mV pre-pulse from those with a -120mV pre-pulse. **E.** Kv1.4 immunofluorescence in mouse MNTB neurones (P9; n=2 animals). Scale bar represents 100µm. Immunolabelling was performed by M. Barker.

In addition to applying DTX-I, we also applied other subunit specific toxins (Fig, 4.10). Application of these toxins only resulted in block of around half of the low-voltage activated current; this suggests that the low-voltage activated current may consist of a single component mediated by heteromeric channels containing Kv1.1, Kv1.2 (and perhaps Kv1.3, Kv1.4 or Kv1.6) subunits. A caveat to this interpretation is that the presence of Kv1.4 subunits in a heteromeric channel can affect the single-subunit block of TsTX-Kα, so higher concentrations are required for block (Hopkins, 1998). Owing to this potential complication and the desire to focus our attention upon other questions, we did not further investigate low-voltage activated currents in mice.

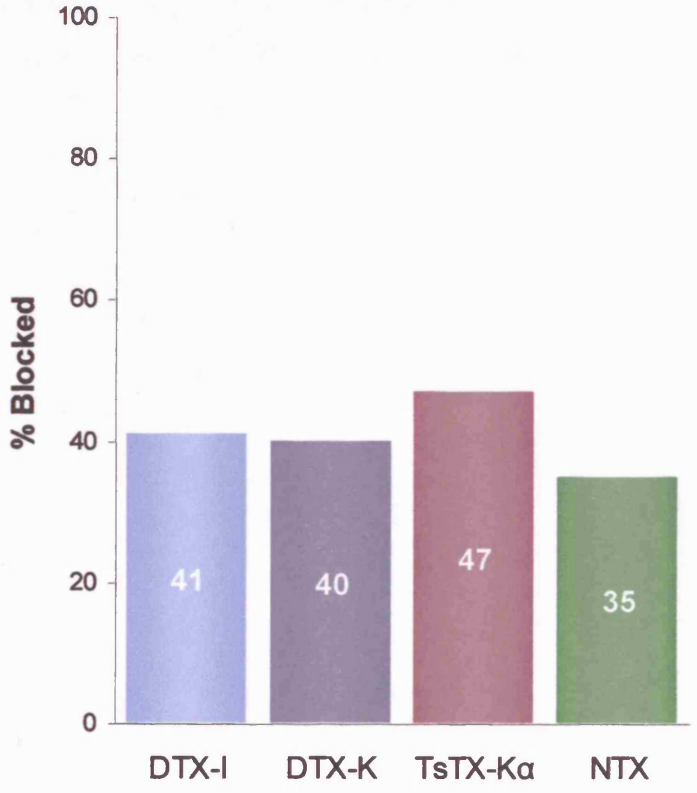

Figure 4.10. Block of the Kv1 current in mouse MNTB neurones by different toxins.
Bar chart showing the percentage block of the current measured at -45mV (n=1 for each toxin).

4.7 Role of low-voltage activated K^+ currents in rat MNTB neurones

MNTB neurones characteristically fire a single AP in response to the giant EPSP elicited during synaptic stimulation (Banks and Smith, 1992; Brew and Forsythe, 1995). This has been shown to be due to DTX-I sensitive potassium channels, block of which results in multiple AP firing (Brew and Forsythe, 1995).

4.7.1 Low-voltage activated currents ensure unitary firing in MNTB neurones

Application of DTX-K to block the low-voltage activated current resulted in multiple APs being generated (Fig, 4.11B). The mean number of APs fired during a 200ms step of 200pA was 18±4 (n=3). Surprisingly 100nM TsTX-Kα also caused multiple APs to be fired (18±4) at the same rate (n=3, Fig, 4.12B). DTX-K and TsTX-Kα had no effect of the AP waveform (Fig, 4.12C), confirming that low-voltage activated currents do not contribute to AP repolarisation. However, application of either toxin unsurprisingly lowered the threshold point for spiking (to 54mV, n=3 for each toxin, Fig, 4.12C), so AP firing occurred with less current injection (Fig, 4.11).

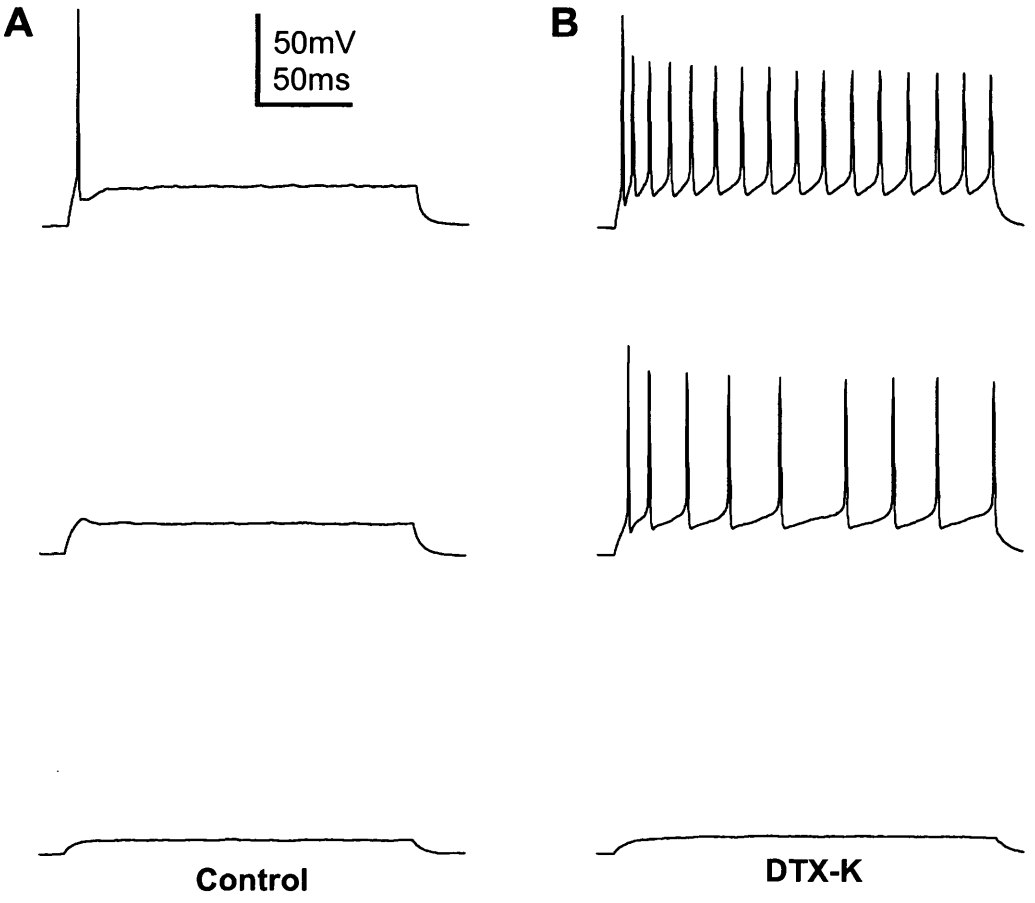

Figure 4.11. Blocking the Kv1 current in MNTB neurones causes multiple AP firing.
A. In control conditions a single AP is fired in response to suprathreshold sustained current injection. Traces represent 50, 150 and 250pA current injections. **B.** Application of 100nM DTX-K caused APs to be fired throughout the current injection (n=3).

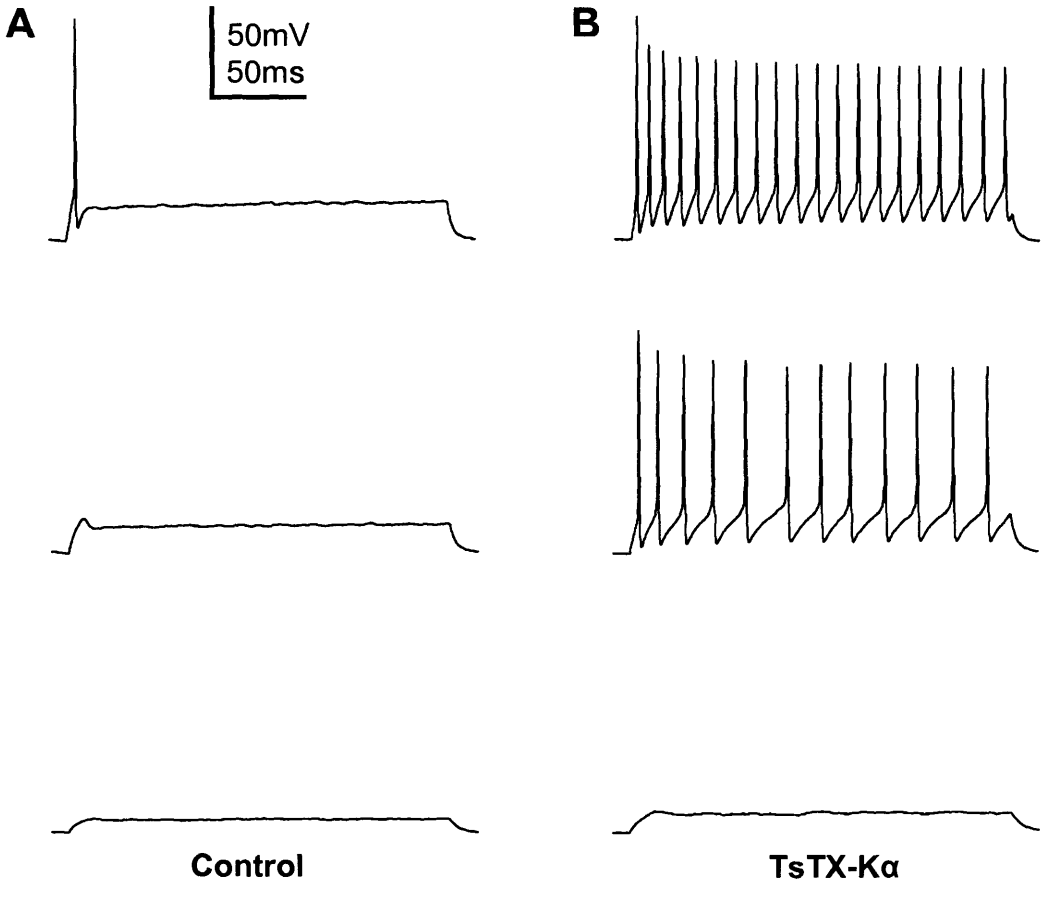

C

	n	Threshold (mV)	Peak (mV)	Width at ½ amplitude (μs)
Control	6	-50 ± 2	37 ± 2	575 ± 28
TsTX	3	-54 ± 2	37 ± 5	567 ± 33
DTX-K	3	-54 ± 1	39 ± 8	550 ± 29

Figure 4.12. Kv1.1/1.2 heteromers in MNTB neurones prevent multiple AP firing.
A. In control conditions a single AP is fired in response to sustained current injection. Traces represent 50, 150 and 250pA current injections. **B.** Application of 100nM TsTX-Kα caused APs to be fired throughout the current injection (n=3). **C.** Table of AP properties under different conditions.

These data suggest that it is the Kv1.1/1.2 heteromers (the channels blocked by TsTX-Kα) which regulate firing. However, an alternative explanation is that half-blocking the low-voltage activated current is sufficient to generate firing throughout the train.

4.7.2 Half-inactivating the low-voltage activated current does not generate multiple firing

We investigated whether we could half-block the low-voltage activated current by inducing voltage-dependent inactivation. We examined the current evoked by steps to -40mV following 750ms pre-pulses to between -100 and -40mV (Fig, 4.13A). The inactivation was well fit between -100 and -50mV with a fractional Boltzmann (Fig, 4.13B see methods). Following a pre-pulse to -50mV, 40% of the current (measured at -40mV) was inactivated. Since the current at -40mV includes some high-voltage activated current (Fig, 4.2), we can assume that at a holding potential of -50mV the low-voltage activated current will be half-inactivated. Since both the Kv1.1/1.6 and the Kv1.1/1.2 heteromers exhibit partial inactivation (Fig, 4.3, 4.4), at a membrane potential of -50mV both these channels will presumably be half-inactivated.

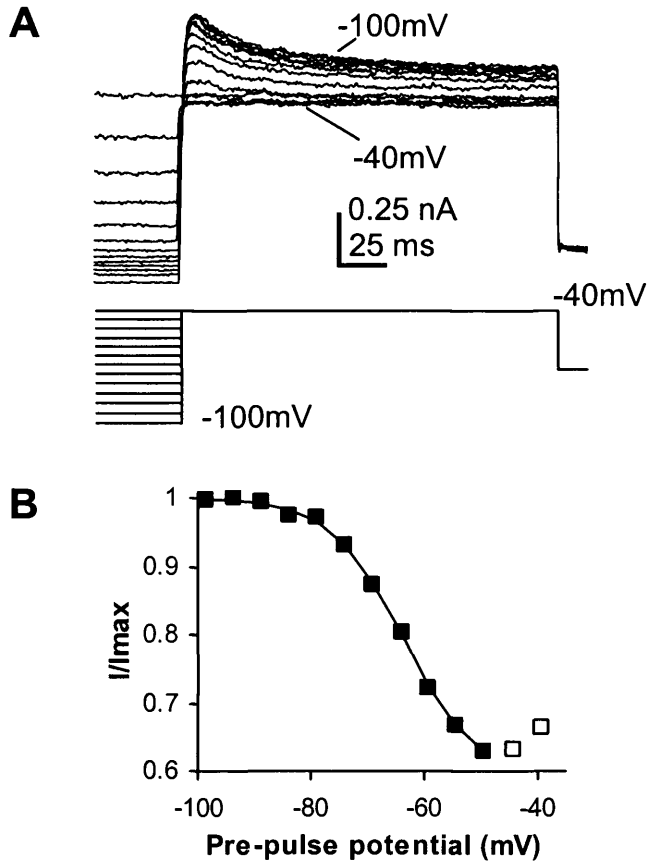

Figure 4.13. Half inactivation of the Kv1 current in rat MNTB neurones.
A. The current response to a test step at -40mV, following 750ms pre-pulses to potentials ranging from -100mV to -40mV. **B.** I/Imax is plotted against pre-pulse potential. The inactivation of the low threshold current was well fit by a fractional Boltzmann, with a $V_{½}$ of -63±3mV, a K value of 7.9±0.8mV and a fraction of 0.40±0.01 (n=4). The Boltzmann fit is to potentials from -100mV to -50mV (filled squares). At potentials more positive than -50mV the high threshold current begins to activate (open squares).

We then tested what effect half-blocking the low-voltage activated current by inactivation would have on firing. We compared AP firing from -70mV (control), -50mV (half-inactivated) and -70mV in TsTX-Kα (Kv1.1/1.2 heteromer block, Fig, 4.14). Blocking Kv1.1/1.2 heteromers with TsTX-Kα caused significantly more APs to be fired (26±5 APs in response to 350pA current injection; n=3) than by half-inactivating the low-voltage activated current at -50mV (6±2 APs, n=6; $P<0.05$, unpaired t test).

It could be argued that differences in the voltage-dependent inactivation of other membrane conductances (e.g. sodium conductances) at membrane potentials of -50mV and -70mV might

account for the differences observed in firing. To examine this we re-plotted the same data, as the number of APs against the potential reached in response to the current injection (measured at the end of the step, Fig, 4.14B). This enabled us to directly compare firing during Kv1.1/1.2 heteromer block and half-inactivation. At a given potential (e.g. -50mV) the membrane conductances will be the same, yet the number of APs fired is clearly different (Fig, 4.14B). Taken together, these data suggest that multiple firing in response to TsTX-Kα is not simply due to half-block of the low-voltage activated current but rather it implies that Kv1.1/1.2 heteromers regulate AP firing in MNTB neurones.

Why do Kv1.1/1.2 heteromers play a greater role than Kv1.1/1.6 heteromers in preserving AP firing? The properties of these two channels are similar (Fig, 4.3, 4.4), yet their subcellular location is different. Kv1.1/1.2 heteromers are concentrated at the axon initial segment whereas Kv1.1/1.6 heteromers have a somatodendritic localisation (Fig, 4.7). We suggest that it is localisation of Kv1.1/1.2 heteromers to the initial segment that allows them greater control over AP firing (see section 7.4.1.1 for further discussion).

In our investigation of AP firing, we noticed that in contrast to control (at -70mV), more than one AP could be generated from -50mV (Fig, 4.14A). Since at -50mV the Kv1.1/1.2 heteromers that prevent multiple firing will be half inactivated (and will therefore be less efficacious at preserving the single AP response than from -70mV), more than one AP is fired.

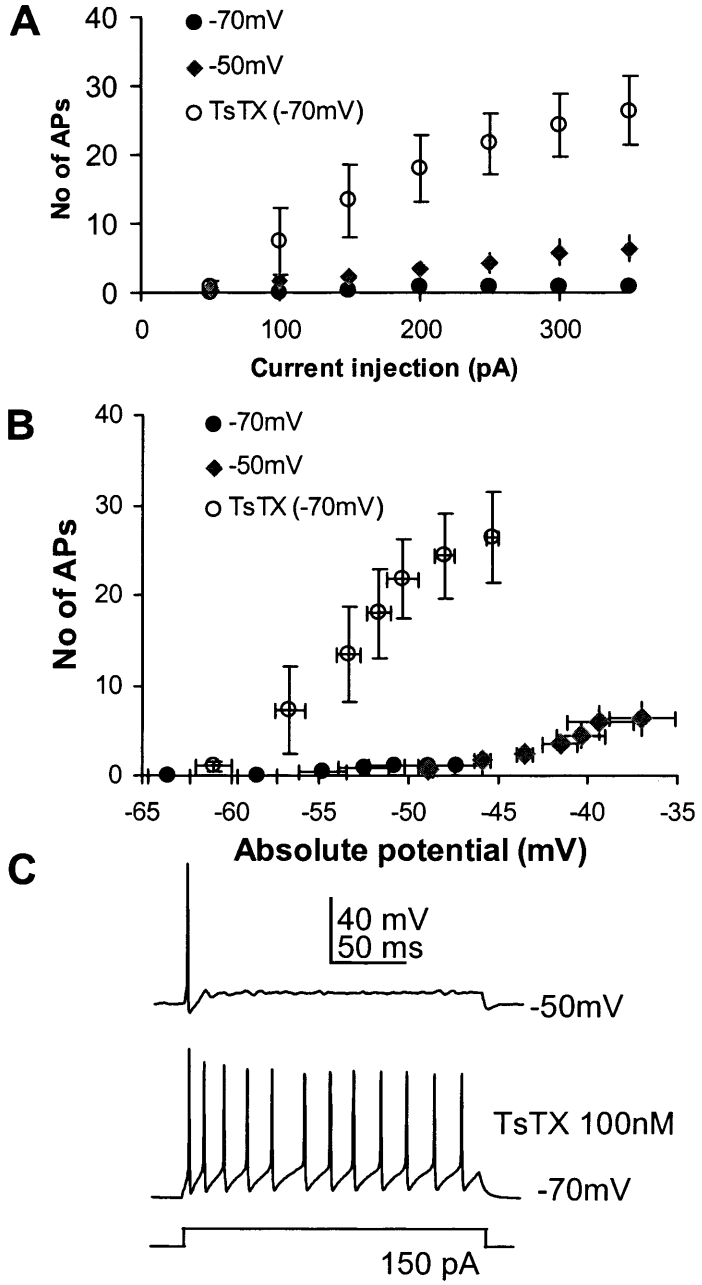

Figure 4.14. Multiple AP firing in TsTX-Kα is not due to half-block of the Kv1 current. **A.** The number of APs generated in response to 200ms current injections. More APs were fired when ILT was half-blocked with TsTX-Kα (open circles, n=3) than when half-inactivated at a membrane potential of -50mV (filled diamonds, n=6). In control conditions only 1 AP was fired throughout the range tested (filled circles, n=6). **B.** The same data are re-plotted as AP number against absolute potential. This was defined as the potential at the end of the current step and was equivalent to the threshold potential at high frequencies. **C.** Representative records from a current-clamped neurone depolarised from -50mV in control aCSF and from -70mV in 100nM TsTX-Kα.

4.8 Summary

We have combined immunohistochemistry with electrophysiology, using subunit-specific toxins to examine the low-voltage activated potassium currents present in MNTB neurones. Previously Brew and Forsythe (1995) demonstrated the presence of DTX-I sensitive currents which preserve the unitary firing of MNTB neurones. We have extended this work to examine the channels that underlie this current and their different roles in regulating neuronal excitability.

Our results show that Kv1.1, Kv1.2 and Kv1.6 subunits are expressed in rat MNTB neurones, with Kv1.1 and Kv1.2 highly concentrated in the axon initial segment. We have demonstrated that the low-voltage activated current is not mediated by homomeric channels as previously thought but by two distinct heteromeric channels. These two components both contribute around half of the low-voltage activated current and have similar properties, yet they differ in their subcellular localisation and function. The channels underlying one component are Kv1.1/1.2 heteromers whereas the other channels are Kv1.1/1.6 heteromers, providing one of the first characterisations of functional heteromeric Kv channels in native tissue. Our findings indicate that despite the similarities in the two components of the rat low-voltage activated current, it is the Kv1.1/1.2 heteromers that are functionally dominant in preserving the unitary firing of MNTB neurones important in the faithful transmission of information encoding sound localisation. We have also shown that channels underlying outward currents found in mouse MNTB neurones differ in their properties and subunit composition from those in the rat MNTB.

CHAPTER 5 - Results

Presynaptic Low-Voltage Activated K^+ Currents

5.1 Introduction

Although potassium currents have been extensively studied at neuronal cell bodies, little is known about the subunit composition of presynaptic voltage-gated K^+ channels or their function. Immunohistochemical labelling has been used to examine the localisation of K^+ channels in some of the larger terminals, indicating that members of the Kv1 family, particularly Kv1.1 and Kv1.2 are expressed presynaptically (Wang et al., 1994). In addition, subunit-specific toxins have been applied to indirectly examine the roles of K^+ channels in regulating transmitter release (Anderson and Harvey, 1988; Harvey et al., 1994; Southan and Robertson, 1998a; Cunningham and Jones, 2001; Lambe and Aghajanian, 2001). Direct examination of presynaptic K^+ channels has also been performed on some of the larger presynaptic terminals (Jackson et al., 1991; Forsythe, 1994; Southan and Robertson, 1998b; Geiger and Jonas, 2000; Southan and Robertson, 2000); both low and high-voltage activating K^+ conductances have been observed in several of these presynaptic terminals, including the calyx. Whilst the role of the high-voltage activating K^+ channels in regulating AP width has been well established (Fig, 5.1; Wang and Kaczmarek, 1998; Rudy and McBain, 2001), the role of presynaptic low-voltage activating K^+ currents is not clear. We investigated low-voltage activated K^+ currents at the calyx of Held by patch clamping terminals from 6-12 day Lister-hooded rats.

5.2 Examination of presynaptic currents

To examine the presynaptic low-voltage activated K^+ currents we made voltage clamp recordings from calyces. Calyces in brainstem slices were visualised using DIC optics (Fig, 5.1D) as a double membrane layer surrounding MNTB neurones. Currents were investigated by applying test steps between -70mV and 0mV following pre-pulses to either -100mV or -40mV (Fig, 5.1E).

Presynaptic currents were similar to those in MNTB neurones (see Fig, 3.3), consisting of both high and low-voltage activated components (Fig, 5.1; Forsythe, 1994; Dodson et al., 2003). Following a pre-pulse to -100mV, currents activated around -70mV and partially inactivated during the 200ms test pulse.(Fig, 5.1A) The mean current measured at -45mV was 0.42±0.05nA (n=13), whereas the mean current at 0mV was 2.8±0.31nA (with a mean current density of 189.1±17.6 pA pF^{-1}). K^+ currents were further inactivated during the pre-pulse to -40mV resulting in a decrease in current magnitude and abolition of the partial inactivation during test steps (Fig, 5.1B). However, the -40mV pre-pulse did not inactivate all of the low-voltage activated current since activation could be seen around -70mV (Fig, 5.1B).

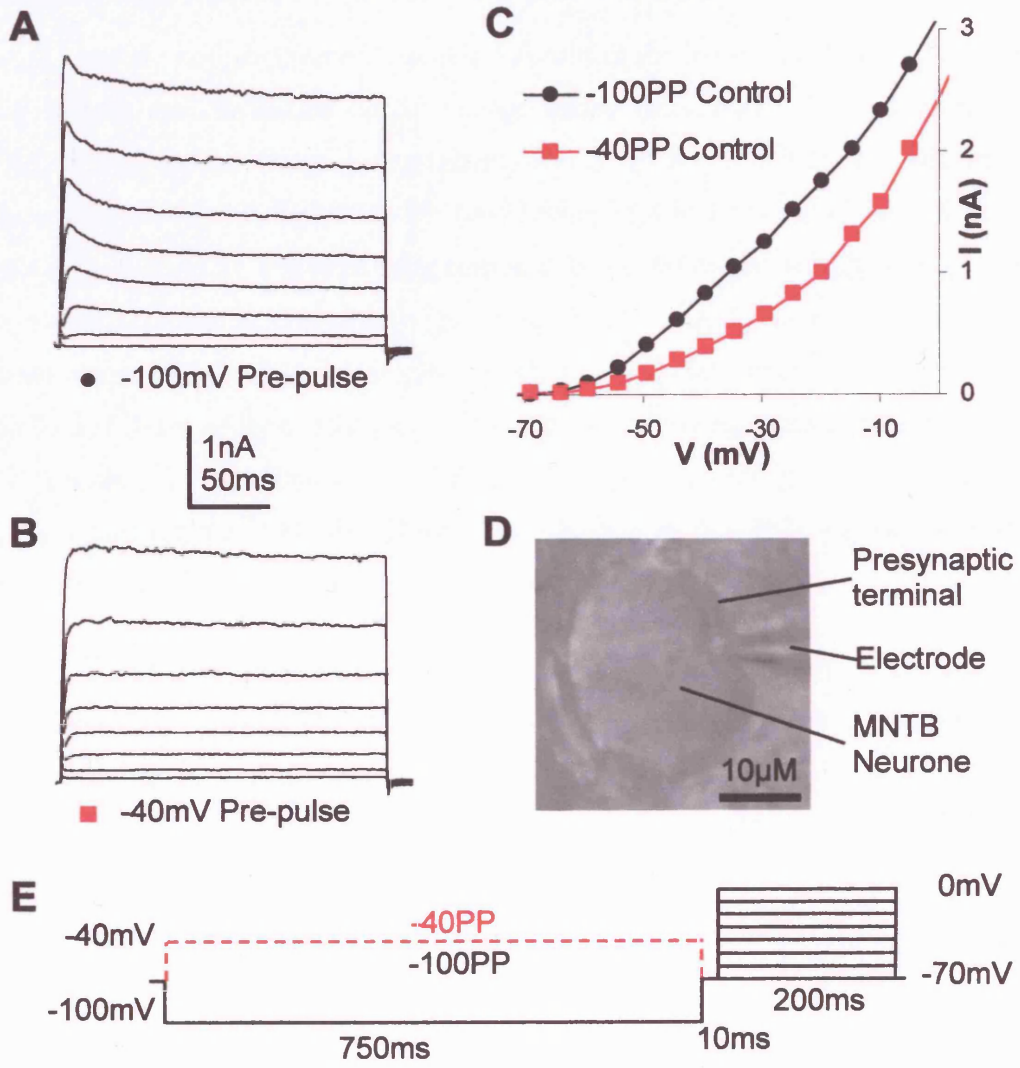

Figure 5.1. Presynaptic outward currents.
A. Representative currents evoked in presynaptic terminals in response to the activation protocol shown in part E (-70 to 0 mV in 10 mV increments following a 750ms pre-pulse to -100mV). **B.** Currents evoked following a 750ms pre-pulse to -40mV. **C.** I/V relationship of the data in A (●) and B (■). **D.** DIC image during recording from a calyx; the terminal can be seen surrounding the postsynaptic MNTB neurone. **E.** Protocols used for presynaptic voltage clamp experiments.

5.2.1 Low-voltage activated channels contain Kv1.2 subunits

We investigated the composition of channels comprising the low-voltage activated current by applying subunit specific toxins during voltage clamp recordings. Application of 100nM TsTX-Kα, which blocks channels containing Kv1.2 or Kv1.3 subunits (Hopkins, 1998; Rodrigues et al., 2003), blocked 87±4.8% (n=7; range 71.8 to 104.4%) of the current evoked at -45mV (Fig, 5.2B&C). The remaining current at this potential is the high-voltage activated current, which activates at potentials negative to -50mV (Fig, 5.2C) and inactivates with a slow time-course (Fig, 5.2B). Complete block of the presynaptic low-voltage activated currents by TsTX-Kα suggests that all of the channels underlying this current contain at least one Kv1.2 subunit. Application of TsTX-Kα also abolished the partial inactivation (Fig, 5.2B&D), suggesting that, like MNTB neurones (Dodson et al., 2002), partial inactivation of the presynaptic currents is conferred by Kv1 channels.

Following a -40mV pre-pulse in the presence of TsTX-Kα, the magnitude of the high-voltage activated current is reduced. The -40mV pre-pulse protocol has been used in other studies to isolate high-voltage activated currents by reportedly selectively inactivating the low-voltage activated currents (Brew and Forsythe, 1995; Wang et al., 1998b; Macica and Kaczmarek, 2001; Macica et al., 2003). Figure 5.2C demonstrates that the -40mV pre-pulse should not be used in this way since the pre-pulse also causes some inactivation of the high-voltage activated current.

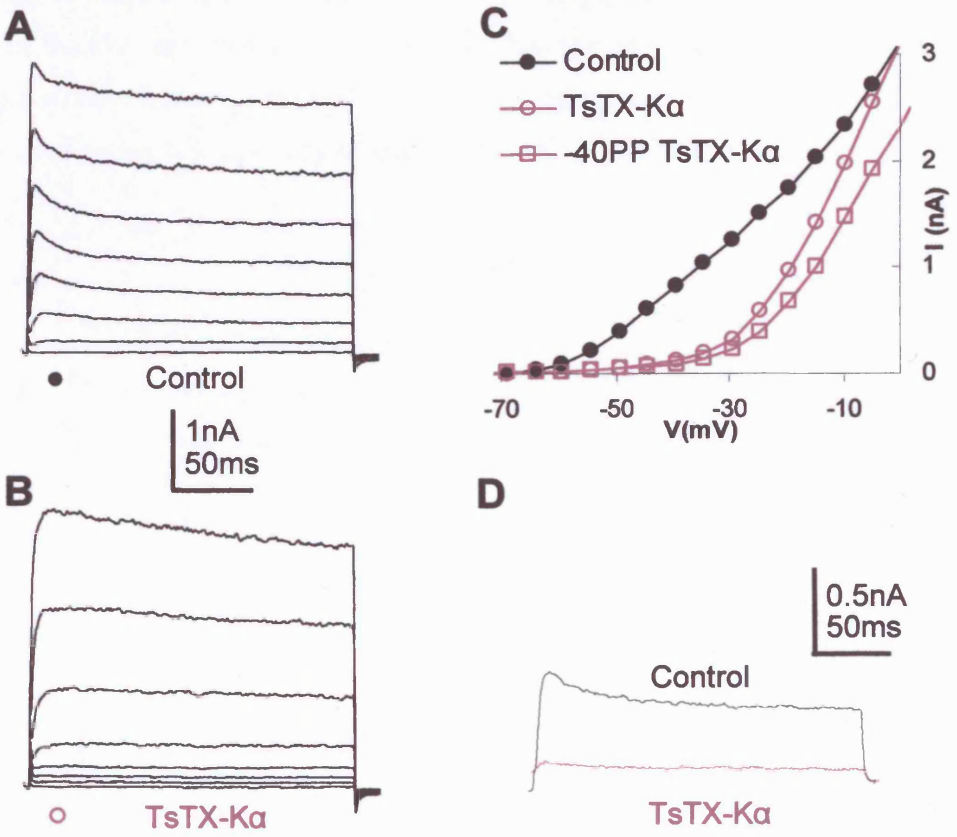

Figure 5.2. The presynaptic low-voltage activated K^+ current is blocked by TsTX-Kα. **A.** Outward K^+ currents evoked following a -100mV pre-pulse. **B.** TsTX-Kα (100nM, which blocks Kv1.2 and Kv1.3 containing channels blocks the low-voltage activated current, leaving only the high-voltage activated current. **C.** I/V relationship of the data in A (●) and B (○). □ represents currents activated following a 750ms pre-pulse to -40mV in the presence of TsTX-Kα. **D.** Enlarged traces from A and B showing block of currents measured at -45mV by TsTX-Kα.

5.2.2 Kv1.1 containing channels only contribute a third of the low-voltage activated K^+ current

Having established that all the low-voltage activated K^+ channels contain Kv1.2 subunits we wanted to investigate whether they also contained Kv1.1. We examined the effects of 100nM DTX-K, which blocks channels containing Kv1.1 subunits (Robertson et al., 1996), on the presynaptic low-voltage activated currents. DTX-K only blocked 32±4.1% (n=6; range 13.4 to 42.2%) of the current measured at -45mV (Fig, 5.3B D). This suggests that, like MNTB

neurones, the low-voltage activated currents in the calyx consist of more than one component. However, the pharmacological profile suggests that the pre- and postsynaptic channels differ. Some partial inactivation could also be seen in the presence of DTX-K (Fig, 5.3B), suggesting that the inactivation is at least in part conferred by Kv1.1 lacking channels.

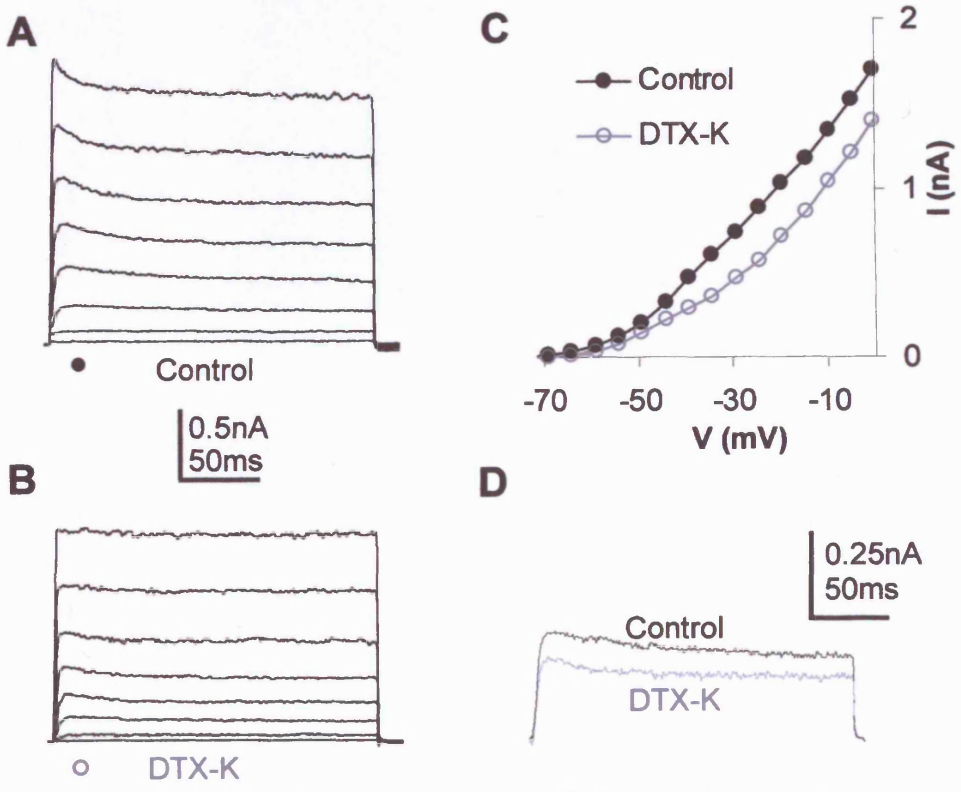

Figure 5.3. The presynaptic Kv1 current is partially blocked by DTX-K.
A. Currents activated following a -100mV pre-pulse. **B.** DTX-K (100nM, which blocks Kv1.1 containing channels) blocks part of the low-voltage activated current. **C.** I/V relationship of the data in A (●) and B (○). **D.** Enlarged traces from A and B showing DTX-K block of currents measured at -45mV.

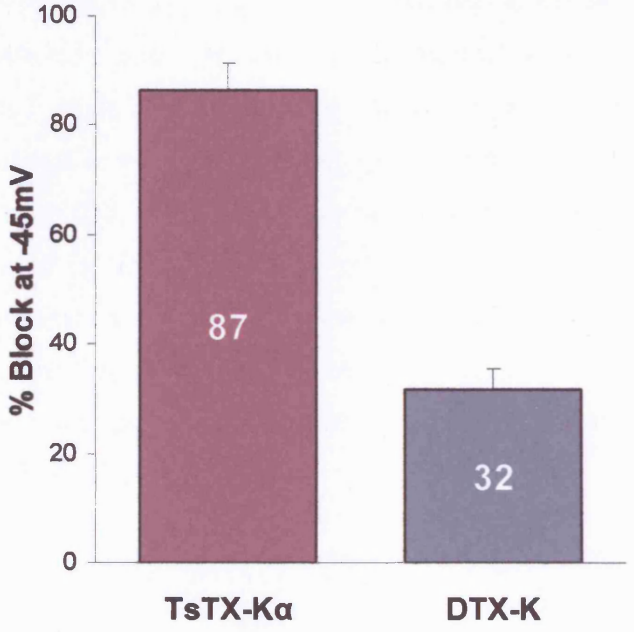

Figure 5.4. Histogram showing percentage block of the presynaptic Kv1 current. 100nM TsTX-Kα blocks 86.5±4.8% (n=7) of the current measured at -45mV whereas 100nM DTX-K only blocked 31.5±4.1% (n=6).

5.3 Subcellular localisation of presynaptic Kv1 channels

5.3.1 Presynaptic Kv1 channels are located in the transition zone between the axon and terminal

In order to gain further insight into presynaptic Kv1 channels, particularly their localisation, we used immunohistochemical labelling. To enable discrimination of pre- and postsynaptic labelling we labelled the terminals with an antibody directed towards Kv3.1b (since Kv3.1b is known to be expressed on the non release face of the calyx, Elezgarai et al., 2003); Kv3.1 is also expressed in MNTB neurones, but at lower levels (Perney et al., 1992; Gan and Kaczmarek, 1998; Grigg et al., 2000; Li et al., 2001; Elezgarai et al., 2003). Immunostaining for Kv3.1b confirmed that these subunits are expressed in the fingers of the calyx, the last 2μm of the presynaptic axon and at lower levels in MNTB neurones (Fig, 5.5A1).

Having established the ability to identify presynaptic terminals and their axons we examined the localisation of Kv1.1 and Kv1.2 subunits. We found that Kv1.2 is concentrated in the last

20μm of the presynaptic axon (Fig, 5.5A3) but not in the terminal membrane itself (Fig, 5.5A2&A3). Similarly, Kv1.1 is located at this transition zone between the presynaptic axon and terminal but is excluded from the calyceal fingers (Fig, 5.5B). In our sections Kv1.1 and Kv1.2 were confined to the final 20μm region of the presynaptic axon. It is conceivable that we did not see more that 20μm of immunostaining because the axons had been severed at this point; however, this is unlikely since this pattern was seen in all sections from 3 animals and in axons that were not at the surface of the section. In addition to the transition zone, Kv1.1 and Kv1.2 are also localised to juxtaparanodal regions of nodes of Ranvier in trapezoid axons (data not shown) and the initial segment of the postsynaptic cell (observed in the axons unlabeled by Kv3.1b, Fig, 5.5A3 *).

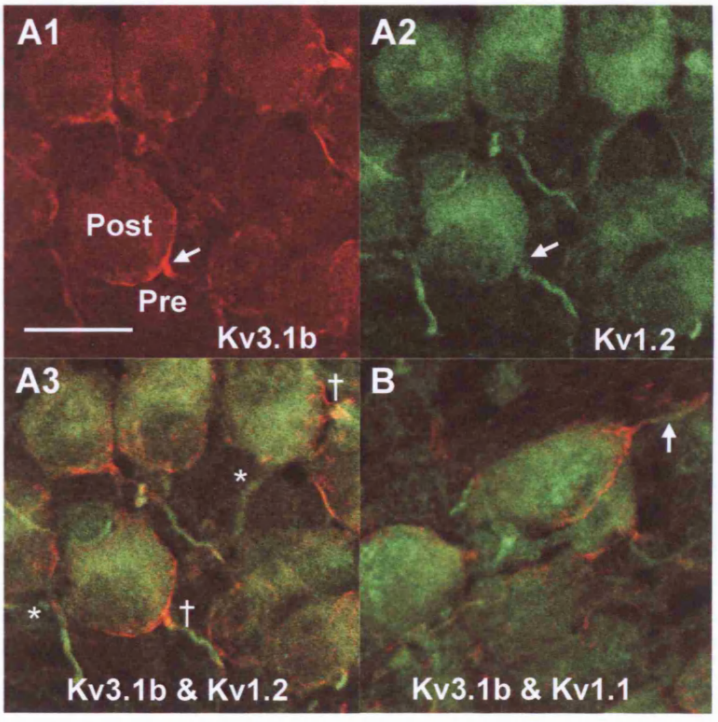

Figure 5.5. Kv1.1 and Kv1.2 are localised to the final 20μm of the presynaptic axon. **A1.** Kv3.1b is concentrated in the calyceal fingers of the terminal and the proximal region of the presynaptic axon (arrow) and is also expressed at lower levels in MNTB neurones. **A2.** Kv1.2 is located in a 20μm region of presynaptic axons in the same section as A1 but is absent from the calyceal fingers (arrow). **A3.** Co-localisation of Kv3.1b (red) and Kv1.2 (green), confirming that Kv1.2 is localised to presynaptic (†) as well as postsynaptic (*) axons. **B.** Co-localisation of Kv3.1b and Kv1.1 shows that Kv1.1 is located in an axonal region similar to Kv1.2 (arrow). Images in A and B are single confocal optical sections, n=3 animals. Scale bar in A1 is 20μm and applies to all parts. Immunolabelling was performed by M. Barker.

5.4 Subunit composition of Kv1 channels

5.4.1 Kv1.2 homomers mediate two-thirds of presynaptic Kv1 current and Kv1.1/1.2 heteromers the remaining third

By combining the immunohistochemistry with the electrophysiological data we can begin to draw conclusions regarding the subunit composition of the presynaptic Kv1 channels. Our previous immunohistochemistry demonstrated that Kv1.1 and Kv1.2 are the only Kv1 subunits in trapezoid axons (Fig, 4.7). Since all of the presynaptic low-voltage activated current was blocked by TsTX-Kα (Fig, 5.4), all channels must contain at least one Kv1.2 subunit. One third of the low-voltage activated K^+ current was blocked by DTX-K, suggesting that the channels underlying this third are heteromers containing Kv1.1/1.2 subunits (Fig, 5.6). The remaining two-thirds is sensitive to TsTX-Kα but resistant to DTX-K, suggesting that these channels are Kv1.2 homomers (Fig, 5.6).

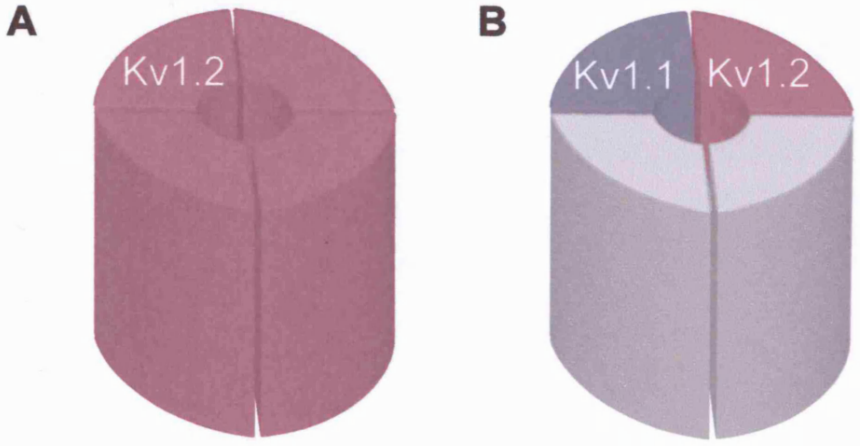

Figure 5.6. Channels comprising the presynaptic low-voltage activated K^+ current.
A. Kv1.2 homomers mediate the two-thirds of the current which is TsTX-Kα sensitive but DTX-K resistant. **B.** Kv1.1/1.2 heteromers mediate the third of the current that is DTX-K sensitive.

In the presence of DTX-K, all the Kv1 current is mediated by Kv1.2 homomers; this affords us the opportunity to compare native Kv1.2 homomers with those expressed in recombinant systems. Homomeric Kv1.2 channels are reported to have an activation threshold around 20mV more positive than Kv1.1 homomers (Coetzee et al., 1999); surprisingly the native presynaptic Kv1.2 homomers showed no such effect (Fig, 5.3D), activating at similar voltage

to the heteromeric channels. In some cases, the activation of Kv1.2 has been reported to be much slower than other Kv1 channels (Grissmer et al., 1994), although in other studies, activation occurs at a similar rate to other Kv1 channels (Hopkins, 1998). The native Kv1.2 homomers activate just as rapidly as Kv1.1/1.2 heteromers (Fig, 5.3D), similar to the findings of Hopkins (1998).

5.5 Presynaptic action potential firing

One of the roles of neuronal low-voltage activated conductances is to ensure unitary firing (Forsythe and Barnes-Davies, 1993a; Brew and Forsythe, 1995; Gamkrelidze et al., 1998; Rathouz and Trussell, 1998; Bal and Oertel, 2001; Dodson et al., 2002; Mo et al., 2002; Brew et al., 2003). We expected that presynaptic low-voltage activated conductances would perform a similar role. However, it had previously been reported that calyces fired trains of APs in response to sustained depolarisation (Forsythe, 1994), suggesting that Kv1 conductances may not maintain unitary firing. We hypothesised that there might be changes in the expression of Kv1 channels with development, so that in young animals, one would observe multiple firing in response to sustained depolarisation and in older animals unitary firing (much like that seen in vestibular neurones, Gamkrelidze et al., 1998).

5.5.1 Axon length affects presynaptic excitability

To test the hypothesis regarding a developmental change in AP firing properties we recorded from calyces of different aged rats. Surprisingly, AP firing did not change with development over the period we examined. We observed unitary and multiple firing over the entire range of P6 to P12 rats (mean age 9.54±0.18 days; n=38). The morphology of the sulphorhodamine filled terminal (see methods section) was always examined after recording to ensure that we had recorded from the presynaptic terminal and not the postsynaptic cell. We noticed that terminals with only short intact axons fired a few APs whereas those with long axons would typically fire multiple APs. Terminals could be divided into three categories: those with less than 20μm of intact axon fired a single AP (Fig, 5.7A), those with intermediate axons (20-150μm) fired several APs (Fig, 5.7B) and those with long axons (>150μm) fired APs

throughout the current injection (Fig, 5.7C). These data suggest that the number of APs fired during sustained depolarisation is not dependent upon the age of the animal but rather on axon length.

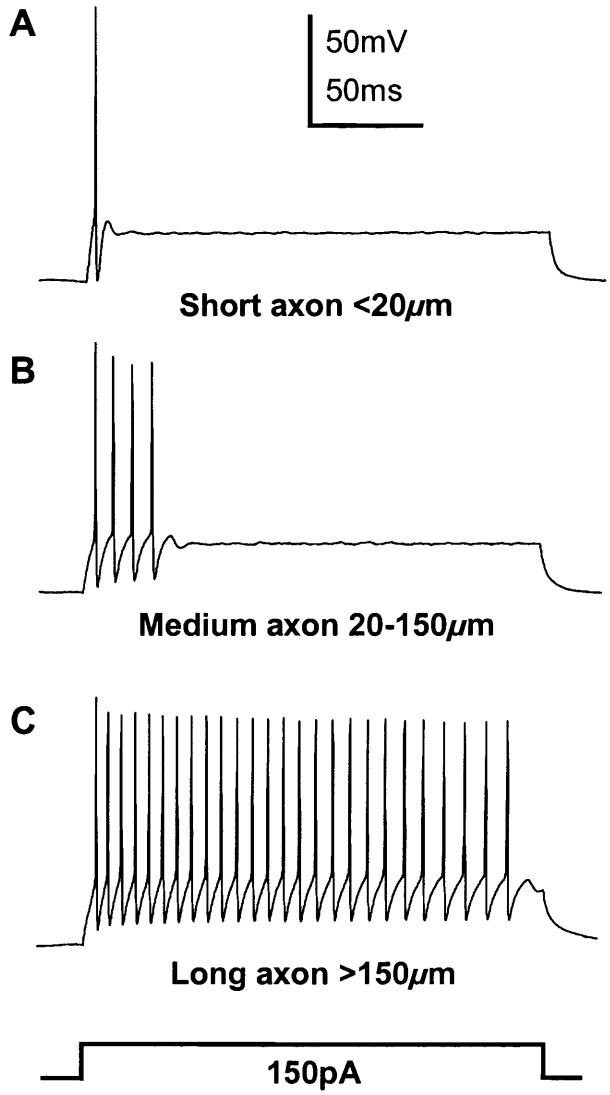

Figure 5.7. Presynaptic action potential firing is dependent upon axon length.
A. Presynaptic terminals that have axons cut within 20μm of the terminal fire a single AP in response to sustained 150pA current injection (n=10). **B.** Terminals with 20-150μm of uncut axon typically fire 4-6 APs during the current injection (n=11). **C.** Terminals with long axons (>150μm) fire APs throughout the current injection (n=17). Axon length was estimated from epifluorescent visualisation of sulforhodamine 101 filled terminals.

Obviously, trapezoid axons would be long *in vivo* (typically a few millimetres); so what does this tell us about AP firing in native calyces? First, it is important to remember that the recording conditions are somewhat artificial; the stimulus we are applying to generate APs is a 200ms square pulse of 150pA current injection. Under physiological conditions presynaptic axons would never experience such sustained depolarisation; a physiological stimulus would be an orthodromic propagating AP. The second artificiality is the site of the stimulus; in these experiments the stimulus is being applied (and the APs recorded from) the calyx whereas *in vivo* APs are generated far from the calyx, presumably at the bushy cell initial segment.

5.5.2 Kv1.1 containing channels do not affect presynaptic AP firing

Although the 200ms current injection is an unphysiological stimulus, we realised that it might provide a useful approach to investigate the roles of the Kv1 channels in regulating AP firing. We applied DTX-K to block the Kv1.1/1.2 heteromers (which contribute one-third of the presynaptic Kv1 current) in terminals that fired between 1 and 4 APs in response to 150pA injection (i.e. those with <150μm intact axon). Surprisingly, application of 100nM DTX-K had no effect on the number of APs fired during 200ms current injection (n=3, Fig, 5.8), suggesting that the Kv1.1/1.2 heteromers do not regulate AP firing at the terminal and therefore may have an alternative role.

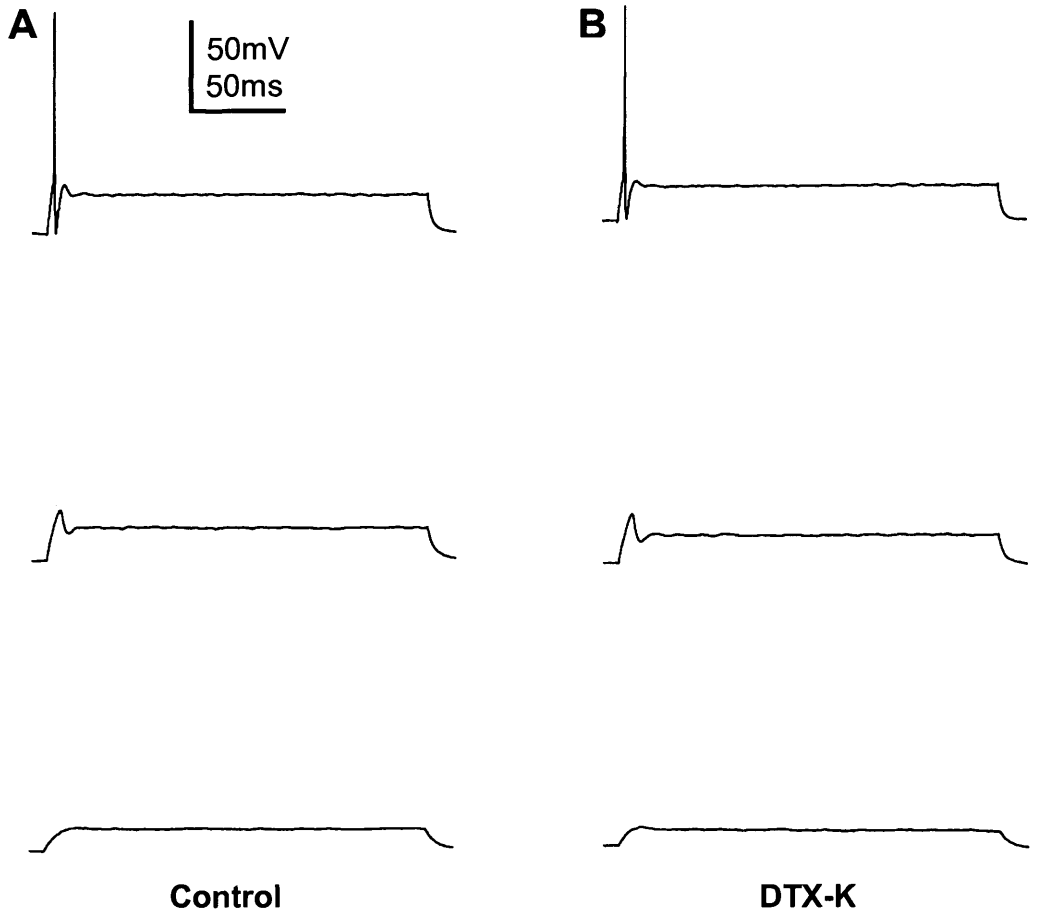

Figure 5.8. DTX-K has no effect on presynaptic AP firing.
A. In control conditions a single AP was fired by terminals with short axons. Each trace shows a 50pA increase in current injection. **B.** Application of 100nM DTX-K had no effect on AP firing (n=3).

5.5.3 Kv1.2 homomers regulate synaptic-terminal excitability

Since Kv1.1/1.2 heteromers did not affect AP firing at the terminal we applied TsTX-Kα to other short-axon terminals. In contrast to DTX-K, TsTX-Kα caused APs to be fired throughout the current injection (n=3, Fig, 5.9). These data suggest that Kv1.2 homomers located at the transition zone between the axon and the terminal do indeed have a role in regulating AP firing at the calyx.

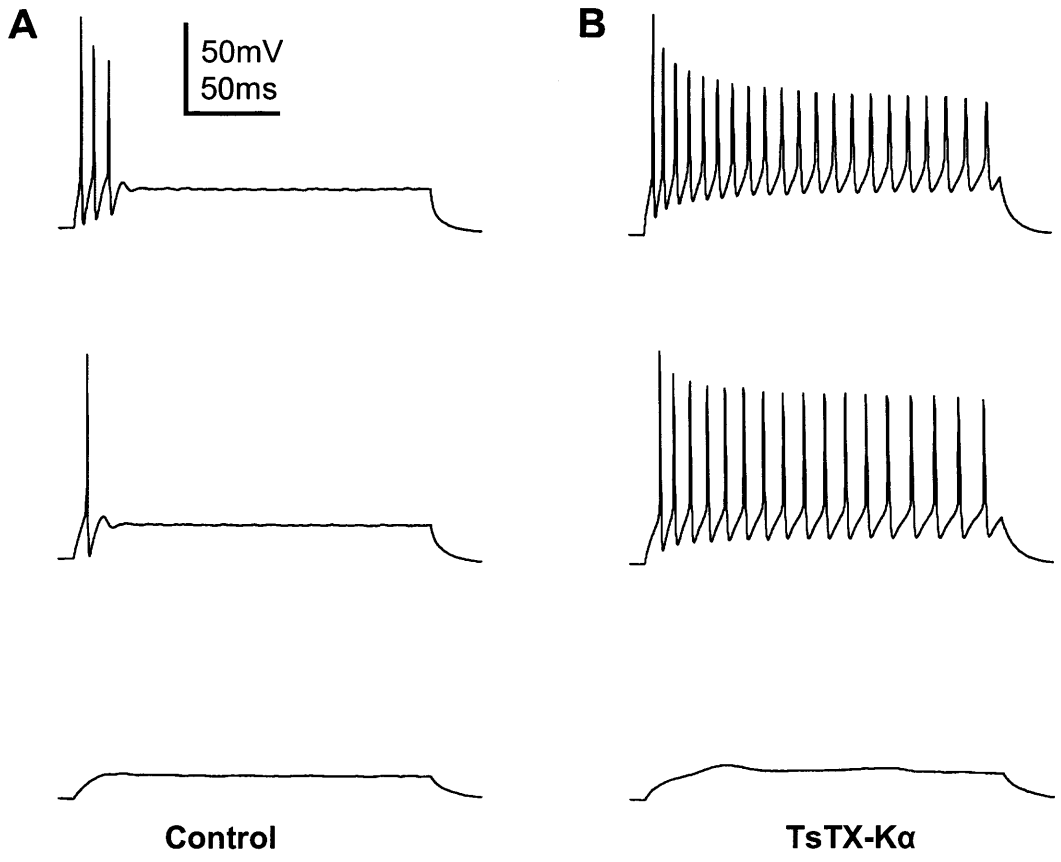

Figure 5.9. TsTX-Kα increases excitability of presynaptic terminals.
A. In control conditions fewer than four APs were observed in response to 150pA injection into terminals with less than 150μm of intact axon. Each trace shows a 50pA increase in current injection. **B.** Application of 100nM TsTX-Kα caused APs to be fired throughout the current injection (n=3).

5.5.4 Propagating APs are followed by a depolarising after-potential

Having established that Kv1.2 homomers can affect presynaptic firing, we examined their role in regulating firing in response to physiological stimuli. To achieve this we electrically triggered APs at the midline using a bipolar stimulating electrode (described in the methods section) and recorded from the calyx under current clamp. In some cases we simultaneously recorded the presynaptic AP and postsynaptic EPSC with assistance from Dr Brian Billups.

Orthodromic APs elicited from a membrane potential of -75mV peaked at 23±6.8mV, had a half-width of 414±30μs and an after-hyperpolarisation (AHP) which dipped to -71.2±2mV (n=10). APs were followed by a depolarizing after-potential (DAP), which peaked at -62.5±1.6mV and had a half width of 15.1±2.4ms (Fig, 5.10). Simultaneous dual-patch recordings demonstrated that each presynaptic AP results in a single postsynaptic EPSC (Fig, 5.10A). The DAP has been shown to be attributable to passive membrane properties in recordings from lizard motor axons (Barrett and Barrett, 1982) and the calyx (Borst et al., 1995). As the AP propagates down the myelinated axon, some of the charge is transferred into the myelin sheath. Once the AP has passed, the charge passively re-distributes, causing the membrane to be depolarised. The amplitude of the DAP is not changed by varying the membrane potential (Fig, 5.10B): at more negative potentials re-distribution of the charge depolarises the membrane to around -60mV, whereas at more positive potentials there is little charge flow to depolarise the membrane.

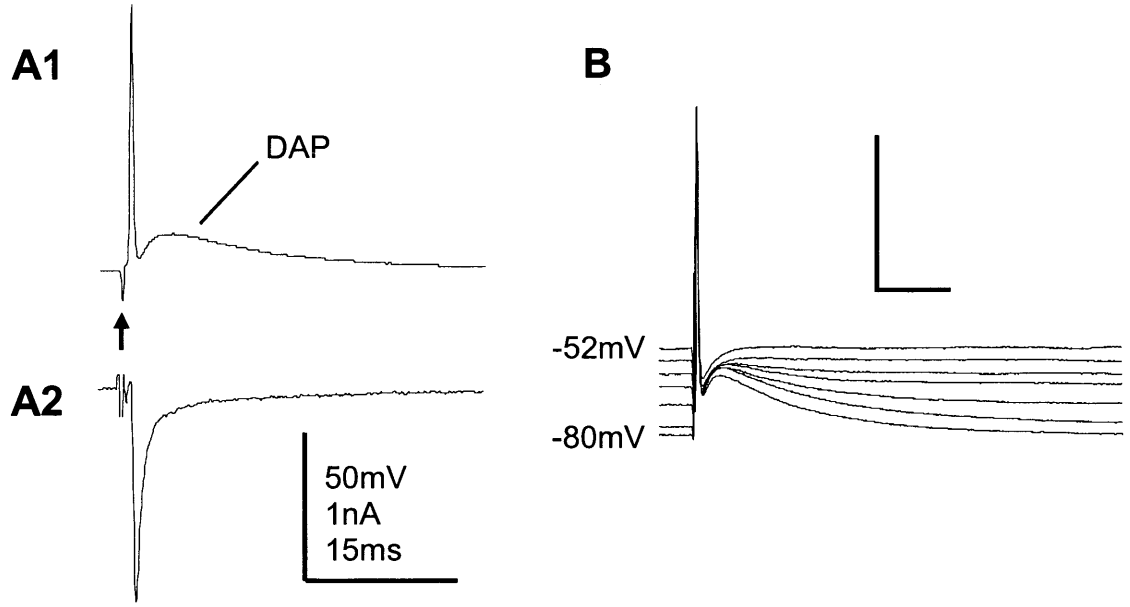

Figure 5.10. Stimulated presynaptic action potentials.
A1. Presynaptic current clamp recording. Stimulation of presynaptic axons generated a fast AP followed by a depolarizing after-potential (DAP); arrow represents time stimulation was applied. All APs are elicited from -75mV unless otherwise stated. **A2.** Simultaneous voltage clamp recording made from the postsynaptic MNTB neurone. The presynaptic AP evoked an EPSC in the MNTB neurone. Recording was made in the presence of 10μM bicuculline 1μM strychnine to block IPSCs and with 5mM QX-314 in the intracellular solution to block postsynaptic sodium channels; the stimulus artefact was removed for clarity. **B.** DAPs recorded from different membrane potentials in a different terminal to that in A. Dual recordings carried out with assistance from Dr B. Billups.

5.5.5 Kv1.2 homomers prevent aberrant AP firing

Since Kv1.2 homomers play a role in regulating presynaptic excitability (Fig, 5.9), we decided to examine their role during electrically evoked APs. As expected, application of 100nM TsTX-Kα had no effect on the AP half-width (P=0.59 2 tailed, paired t-test; n=7). However, the DAP was significantly larger (P=0.005), peaking at -55.4±1.5mV (Fig, 5.12B). The increase in the DAP amplitude brings the terminal closer to threshold for AP generation so that an aberrant AP is often observed on the DAP (Fig, 5.11). This suggests that the presynaptic Kv1.2 conductance normally serves to shunt and reduce the DAP; hence, when Kv1 currents are blocked, threshold is exceeded and a second AP is generated during the DAP. Aberrant firing has never been observed in control conditions but was observed in all terminals (n=7) in the presence of TsTX-Kα. Changing the membrane potential over the range

of -90 to -25mV had no effect on the generation of aberrant APs (Fig, 5.11B) although latency to the aberrant AP was often shorter when generated from more negative potentials. Raising the membrane potential above around -40mV resulted in spontaneous firing at the terminal without the need for stimulation (Fig, 5.11C).

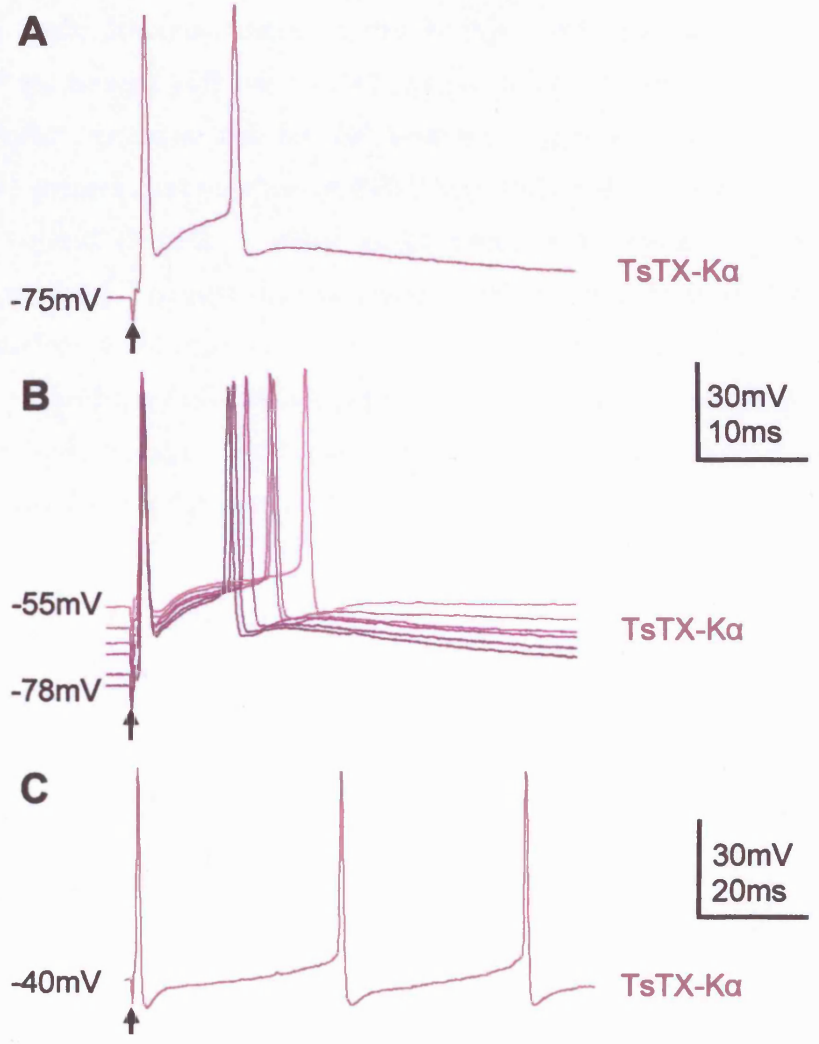

Figure 5.11. Blocking Kv1.2 channels causes aberrant AP firing.
A. Stimulated presynaptic AP. In the presence of 100nM TsTX-Kα the DAP amplitude increased bringing the terminal closer to threshold so that a single stimuli often resulted in an aberrant AP during the DAP. Aberrant firing was observed in 7 of 7 neurons. **B.** Aberrant APs recorded from different membrane potentials; aberrant firing was observed from all potentials tested (-90 to -25mV). APs from more positive membrane potentials are represented by a lighter shade of purple. **C.** Spontaneous firing was often observed in the presence of TsTX-Kα at potentials more positive than -40mV. Spontaneous firing was maintained until the calyx was returned to more negative potentials. Arrows represent time stimulation was applied.

Aberrant firing in the terminal generated an additional EPSC in the postsynaptic neurone (Fig, 5.12A2), so a single stimulus results in two EPSCs. An extracellular recording of the presynaptic AP can be seen in figure 5.12 A2 just preceding the aberrant AP; the absence of a stimulation artefact confirms that the AP was not triggered by stimulation. Blocking presynaptic Kv1 channels had no effect on EPSC amplitude since the first EPSC was the same magnitude as control (P=0.93, 2 tailed paired t-test; n=5), confirming that presynaptic low-voltage activated K^+ currents do not influence release probability (Brew and Forsythe, 1995). On occasion (≈30%) the aberrant EPSC was facilitated with respect to the first (Fig, 5.12A2). This paired-pulse facilitation is probably due to residual calcium in the terminal (due to the proximity of the stimuli) resulting in an increase of transmitter release during the second AP (Katz and Miledi, 1968; Charlton et al., 1982; Cuttle et al., 1998).

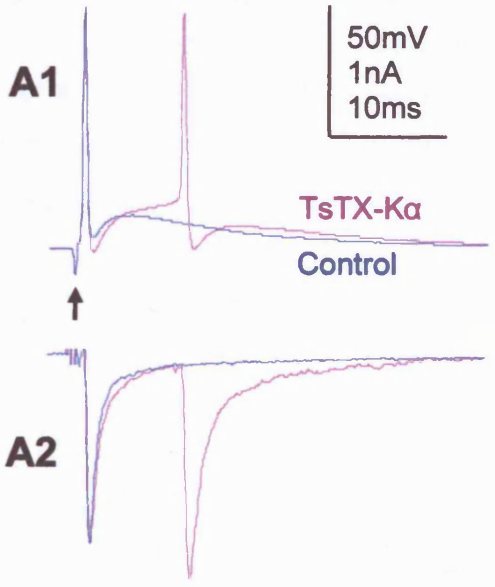

B

	Control	TsTX-Kα
DAP (mV)	-61.8±1.4	-55.4±1.5
AHP (mV)	-70.8±2	-68.4±1.6
Halfwidth (ms)	0.41±0.03	0.43±0.04
DAP Halfwidth (ms)	15.1±2.4	

Figure 5.12. Aberrant AP firing causes an extra EPSC in the postsynaptic neurone.
A1. In control conditions each stimulus elicited a single AP (blue trace). In the presence of 100nM TsTX-Kα (mauve trace) a single stimulus resulted in an aberrant AP during the DAP. **A2.** Simultaneous voltage clamp recording made from the postsynaptic MNTB neurone in control conditions (blue trace) and 100nM TsTX-Kα (mauve trace). In TsTX-Kα the aberrant AP also evoked an EPSC in the MNTB neurone so that two EPSCs are fired for a single stimulus. Recording was made in the presence of 10μM bicuculline 1μM strychnine to block IPSCs and with 5mM QX-314 in the intracellular patch solution to block postsynaptic sodium channels. The stimulus artefacts were removed for clarity. **B.** Table showing AP properties in control and 100nM TsTX-Kα (n=7). Dual recordings carried out with assistance from Dr B. Billups.

5.5.6 Aberrant firing also occurs during repetitive activation

The generation of aberrant firing after block of Kv1.2 homomers led us to examine the effect during trains of stimuli. In the presence of 100nM TsTX-Kα, a train of stimuli applied at 100Hz only results in aberrant firing following the first AP (Fig, 5.13A2). Although this aberrant response would clearly affect the fidelity of information transmission, particularly at this auditory synapse, we considered why aberrant firing was restricted to the first DAP. Examination of AP firing under control conditions revealed that at 100Hz the DAP does not have time to decay to baseline before the next stimuli arrives (Fig, 5.13A1). The amplitude of the subsequent DAPs is therefore smaller (Fig, 5.13A1) so they do not reach threshold. When stimulation is applied at a frequency where the DAP has enough time to return to baseline (e.g. 20Hz) DAP amplitudes are not reduced (Fig, 5.13B1). Therefore in the presence of TsTX-Kα all the DAPs are larger and threshold is often exceeded, resulting in aberrant firing (Fig, 5.13B2). The latency to the aberrant AP can be very variable (Fig, 5.13C) and sometimes the DAP fails to reach threshold for AP generation (Fig, 5.13C *). These data suggest that Kv1.2 homomers are important in preserving information fidelity by preventing hyperexcitability following AP invasion of the terminal.

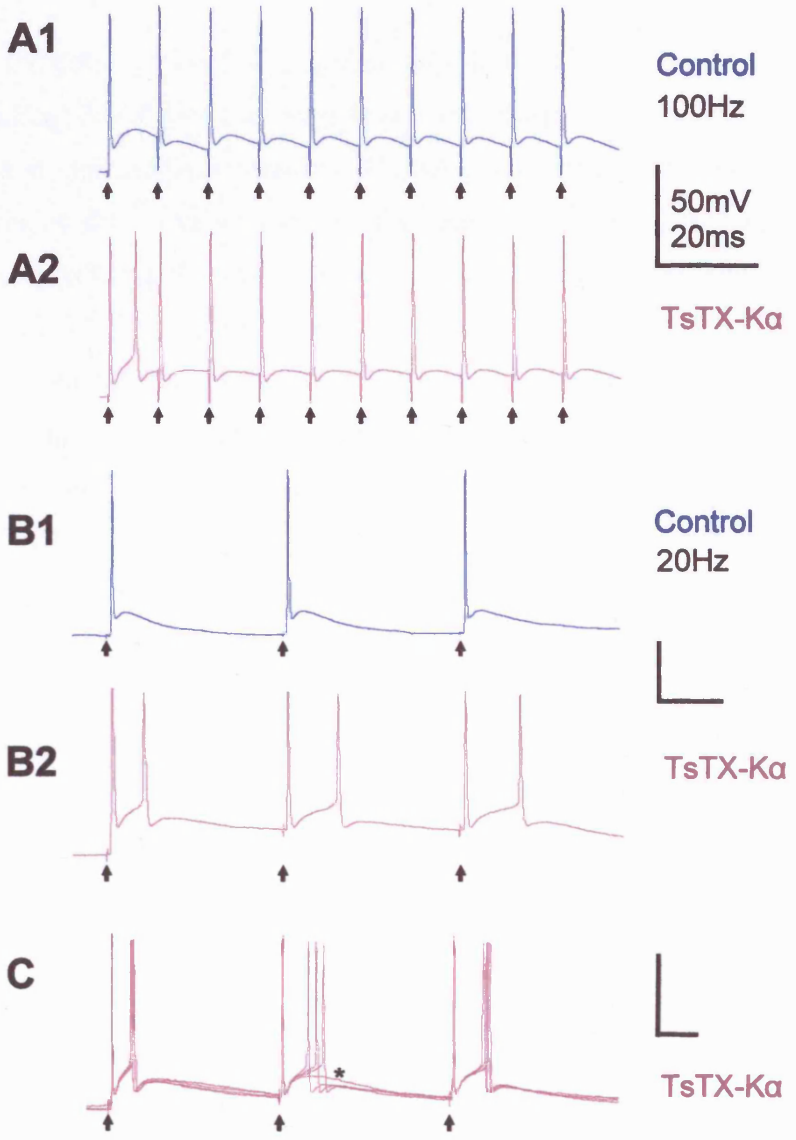

Figure 5.13. Aberrant AP firing also occurs during trains of stimuli.
A1. Presynaptic APs elicited by 100Hz trains of stimuli. **A2.** In the presence of 100nM TsTX-Kα an aberrant AP is fired following the first AP (n=3). **B1.** APs generated by 20Hz trains of stimuli. **B2.** At this frequency, aberrant firing in TsTX-Kα was more prevalent, occurring on almost all DAPs (n=3) **C.** Overlaid traces from 4 trains of stimuli; the timing of aberrant firing is less precise than for the evoked APs and sometimes (≈10% of the time) an aberrant AP would not be fired within a train (*). Arrows represent time stimulation was applied; parts A to C are recorded from 3 different terminals.

5.6 Summary

We have used the calyx of Held to examine the role of Kv1 channels at central excitatory synapses by making direct pre- and postsynaptic recordings, combined with subunit specific pharmacology and immunohistochemistry. We have demonstrated the presence and function of Kv1 channels at the calyx and shown that the low-voltage activated K^+ currents are mediated by two distinct groups of channels: Kv1.2 homomers contribute two-thirds of the current and Kv1.1/1.2 heteromers generate the remaining third. These channels are not located in the nerve terminal itself but in the transition zone between the axon and the presynaptic terminal. Kv1.2 homomers are important in regulating the excitability of the synaptic terminal whereas Kv1.1/1.2 heteromers have no effect on presynaptic firing. Blockade of Kv1 channels during electrical stimulation of presynaptic axons resulted in aberrant firing following the first AP; aberrant firing also occurred during trains of stimulation, and was particularly prevalent at lower frequencies. Our data suggest that Kv1.2 homomers located at the transition zone between the axon and terminal serve to shunt and reduce the DAP, preventing aberrant firing. Presynaptic Kv1 channels do not contribute to AP repolarisation but instead prevent nerve-terminal hyperexcitability and thus preserve fidelity during synaptic transmission.

CHAPTER 6 - Results

Presynaptic High-Voltage Activated K^+ Currents

6.1 Introduction

MNTB neurones and their presynaptic terminals (the calyx of Held) possess both high and low-voltage activated currents (Forsythe, 1994; Brew and Forsythe, 1995). It has previously been demonstrated that Kv3.1 subunits which comprise the high-voltage activated current in MNTB neurones are also expressed at the calyx (Wang et al., 1998b; Dodson et al., 2003; Elezgarai et al., 2003). Kv3 channels generally activate at potentials more positive than other K^+ channels and deactivate rapidly, making them particularly suited for a role in repolarising APs (Rudy and McBain, 2001). The fact that Kv3.1 can be phosphorylated by PKC (resulting in a decrease in current amplitude Critz et al., 1993; Macica et al., 2003), makes it an interesting candidate as a mechanism for the regulation of transmitter release. Although several presynaptic terminals have been shown to possess high-voltage activated currents (Augustine, 1990; Forsythe, 1994; Southan and Robertson, 2000), little is known about the channels which underlie them. To examine presynaptic high-voltage activated currents, we investigated the subunit composition, roles and modulation of those present at the calyx of Held.

6.2 Characterisation of presynaptic Kv3 currents at the mouse calyx

6.2.1 Mice express a slowly inactivating high-voltage activated current

To investigate the presynaptic high-voltage activated K^+ current we made whole cell recordings from mouse calyces. We chose to use mice rather than rats to take advantage of a Kv3.1 knockout mouse that we had access to (Ho et al., 1997). We elicited currents with a -100PP protocol (Fig, 6.1) stepping to potentials between -90 and +40mV. In all voltage clamp recordings we applied 100nM DTX-I to block the low-voltage activated current.

Voltage steps elicited currents which activated around -60mV (Fig, 6.1) had a mean amplitude of 4.12±0.82nA, a mean current density of 271±33.3 pA pF^{-1} (measured at 0mV, n=7) and were similar to those recorded in the rat calyx (see, Fig, 5.2B). However, unlike mouse MNTB neurones (Fig, 4.9B), the calyx did not possess a transient A-current (Fig, 6.1A). To investigate the inactivating properties of the high-voltage activated current we applied a three second test step to 20mV; the current inactivated by around 30%, demonstrating that the high-voltage activated current slowly inactivates (Fig, 6.1C).

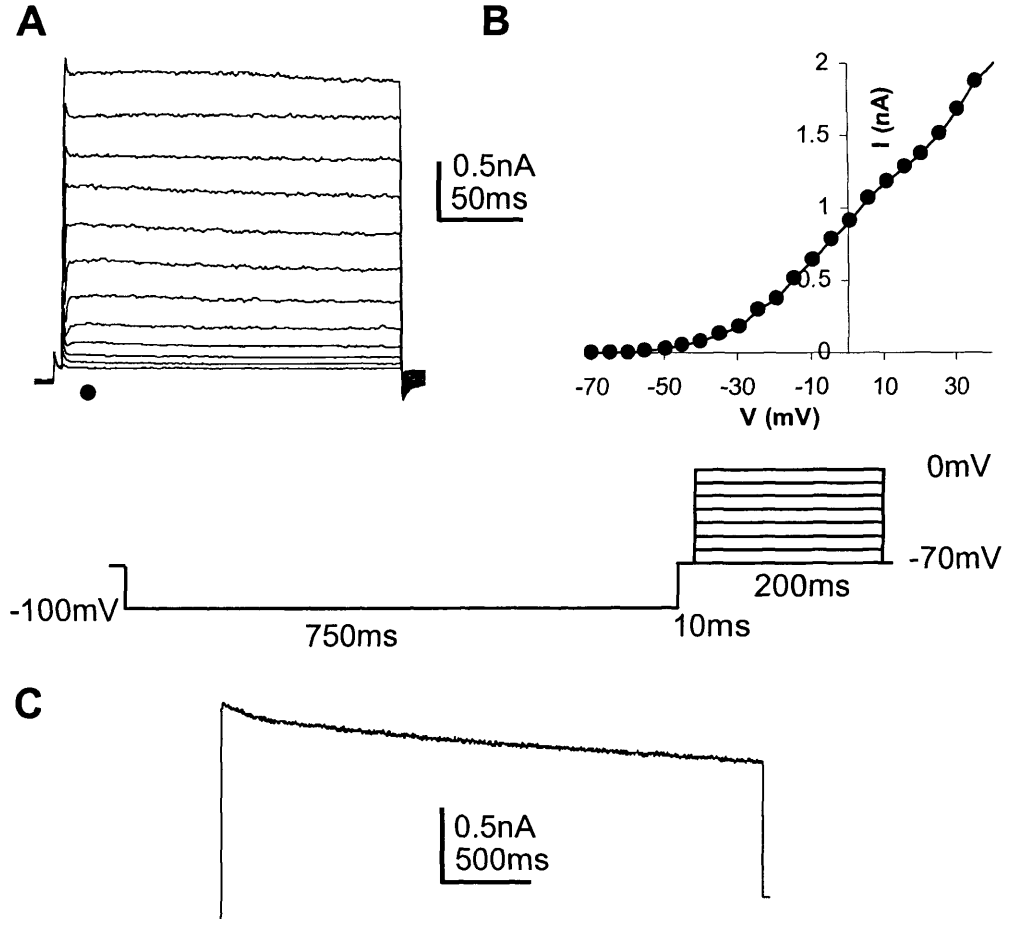

Figure 6.1. Outward currents in presynaptic terminals of WT mice.
A. Currents activated by a -100 pre-pulse protocol (middle panel) in the presence of 100nM DTX-I to block the low voltage-activated current. **B.** I/V relationship of the data in A. **C.** representative trace showing slow inactivation of the high voltage activated current during a 3 second step to 20mV from a holding potential of -100mV (n=4).

6.2.2 TEA-sensitive high-voltage activated channels are expressed on the non-release face of the calyx

Immunogold labelling indicates that Kv3.1 is expressed on the non-release face of the calyx in rats (Elezgarai et al., 2003). We excised patches from the mouse calyx to further characterise the high-voltage activated current. Currents recorded in outside-out patches were similar to those recorded in the whole cell configuration (Fig, 6.2A). Application of 3mM TEA completely abolished the current (n=2, Fig, 6.2B), suggesting that it was mediated by Kv3 channels.

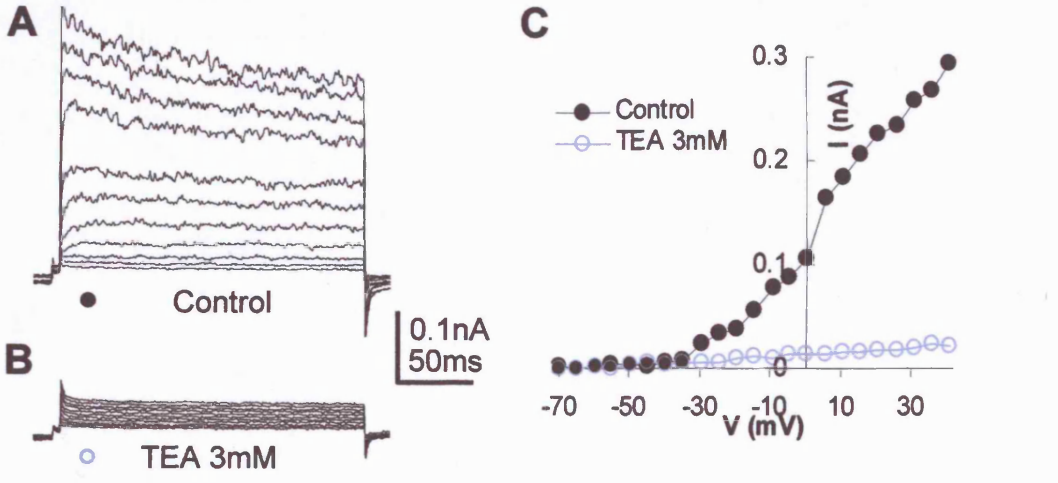

Figure 6.2. Currents in an outside out patch excised from a a WT mouse calyx.
A. Currents activated by a -100mV pre-pulse protocol in the presence of 100nM DTX-I. **B.** Currents in the presence of 3mM TEA. **C.** I/V relationship of the data in A (●) and B (○).

6.2.3 High-voltage activated currents are still present in mice lacking Kv3.1

Since Kv3.1 was highly expressed at the calyx (Dodson et al., 2003; Elezgarai et al., 2003) we thought that these channels might account for the presynaptic high-voltage activated current. We were also fortunate enough to have access to the Kv3.1 knockout mice generated by Ho *et al.* (1997). We examined the presynaptic current in the absence Kv3.1 subunits by making recordings from calyces in these KO mice. We bred Hz mice together (or an Hz female with a KO male) and genotyped the offspring (see methods and Fig, 6.3D) to select a KO.

We were surprised to find that high-voltage activated currents were still present in calyces from Kv3.1 KO animals (n=4, Fig, 6.3A). These currents resembled those from WT mice, activating at similar potentials and exhibiting little inactivation (Fig, 6.3A). Application of 3mM TEA blocked a large proportion of the current in Kv3.1 null calyces (n=2, Fig, 6.3B), suggesting that it was mediated by other members of the Kv3 family.

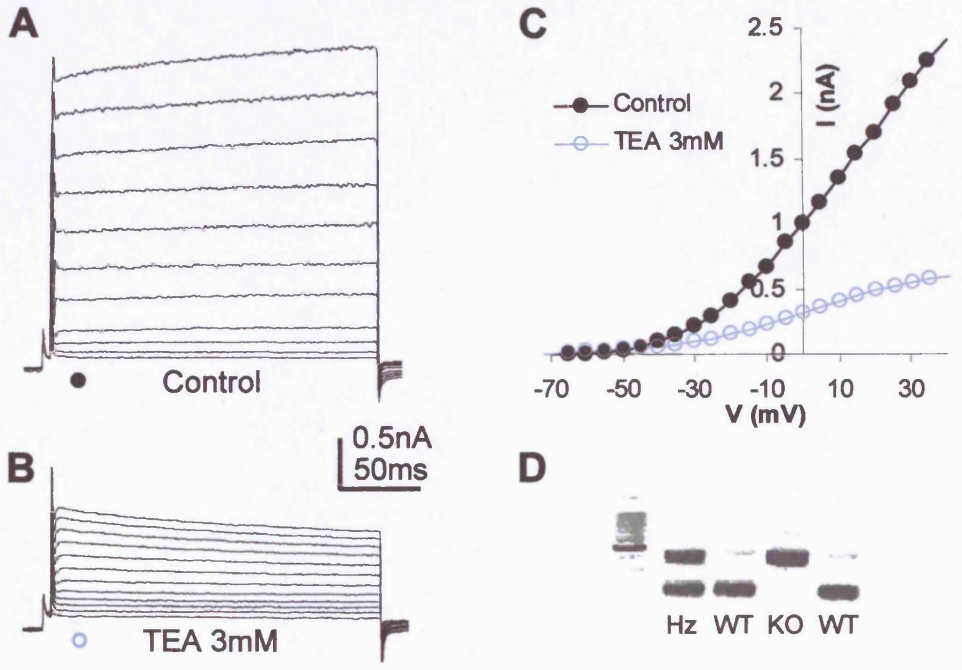

Figure 6.3. Outward currents in presynaptic terminals of Kv3.1 KO mice.
A. Currents activated by a -100mV pre-pulse protocol. **B.** Outward currents in the presence of 3mM TEA. **C.** I/V relationship of the data in A (●) and B (○). **D.** Genotyping results to confirm that the mouse was a Kv3.1 KO (see section 2.5.1). Left lane is 100base DNA ladder, dark band is 500base pairs. A single band at 400 base pairs denotes a knockout (KO), bands at both 400 and 200 base pairs a heterozygote (Hz), and a single band at 200 base pairs a wild type (WT).

6.3 Subcellular localisation of Kv3 subunits

6.3.1 Kv3.1, Kv3.3 and Kv3.4 are expressed in the MNTB

To investigate the contribution of other Kv3 subunits to the presynaptic high-voltage activated current we examined immunoreactivity for Kv3.1-3.4 in the MNTB. Kv3.1, Kv3.3 and Kv3.4 immunofluorescence was clearly visible (Fig, 6.4). Kv3.2 immunofluorescence was slightly above background (Fig, 6.4B), but at a very low level consistent with non-specific binding of the primary antibody (similar to that observed for Kv1.4 and Kv1.5, Fig, 4.1). Unlike Kv3.1 and Kv3.3, Kv3.4 did not appear to be expressed in the MNTB neurones themselves but was localised to the surrounding region; consistent with localisation at the calyx.

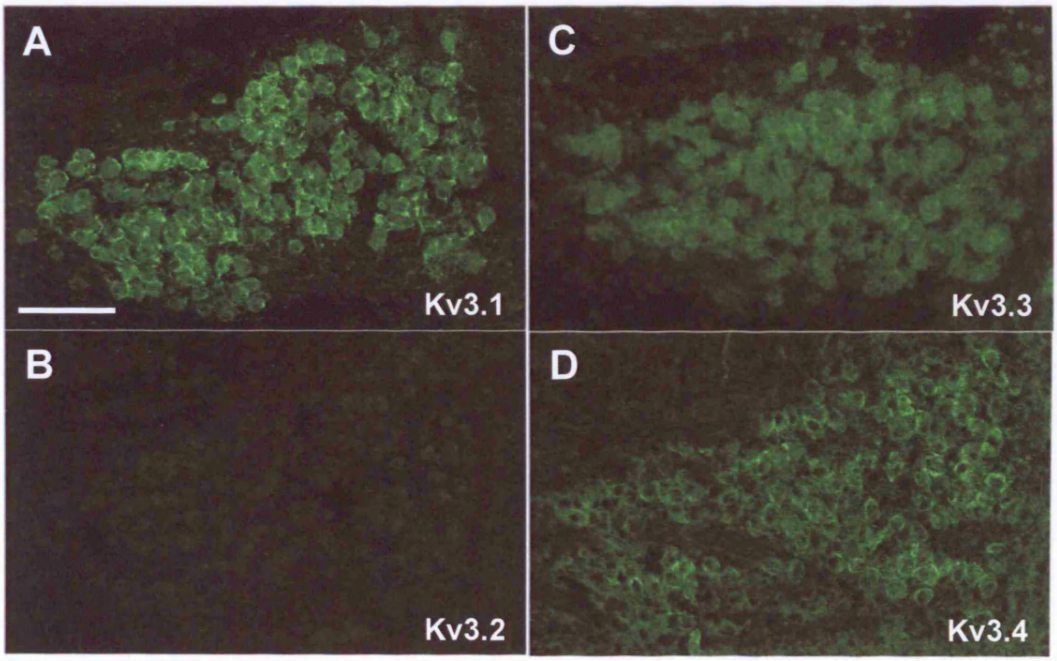

Figure 6.4. Kv3.1, Kv3.3 and Kv3.4 are expressed in the MNTB.
Immunoreactivity for Kv3.1 (**A**) and Kv3.3 (**C**) was detected in MNTB neurones and their calyces, whereas Kv3.4 immunofluorescence (**D**) was only seen presynaptically. Kv3.2 immunofluorescence (**B**) was not above background. Primary antibodies were from Alomone except Kv3.3 which was a gift from Dr T. Perney (Rutgers University, NJ) FITC-secondary (goat anti-rabbit) was from Jackson ImmunoResearch Laboratories (West Grove, PA). Scale bar represents 100μm, n=3 animals. Immunolabelling was performed by M. Barker.

6.3.2 Kv3.1, Kv3.3 and Kv3.4 are expressed in presynaptic terminals

To examine the expression of Kv3 subunits at the calyx we examined Kv3 immunoreactivity on the confocal microscope. Kv3.1 and Kv3.3 immunoreactivity was detected in MNTB neurones (*, Fig, 6.5), whereas Kv3.1, Kv3.3 and Kv3.4 were detected in calyceal terminals (arrows, Fig, 6.5). Interestingly only Kv3.1 immunofluorescence was observed in the final portion of the presynaptic axon (†, Fig, 6.5), suggesting that whilst channels in the terminal membrane may be heteromers, Kv3.1 homomers are present in the axon. This is consistent with localisation of Kv3.1 but not other Kv3 subunits to nodal regions of CNS axons (M. Barker unpublished observations, Devaux et al., 2003).

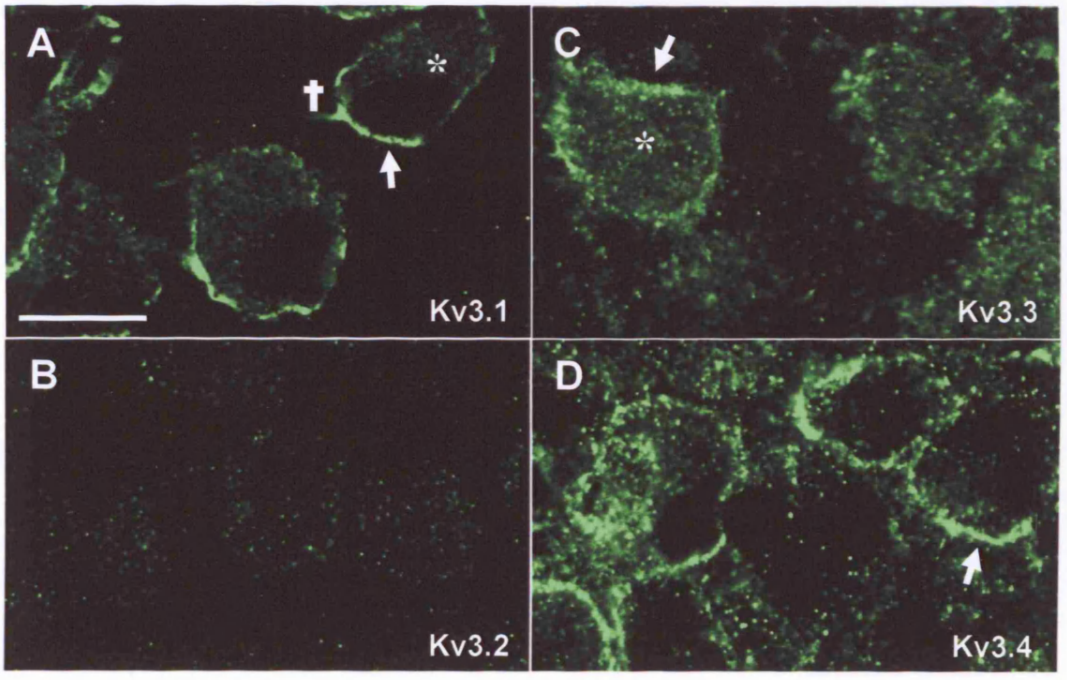

Figure 6.5. Kv3.1, Kv3.3 and Kv3.4 are localised to calyceal terminals.
A. Kv3.1 is localised to the postsynaptic cell (*), the presynaptic terminal (arrow) and the last portion of the presynaptic axon (†). **B.** Only non-specific immunofluorescence was observed for Kv3.2. **C.** Both presynaptic (arrow) and postsynaptic labelling (*) was observed for Kv3.3. **D.** Kv3.4 immunoreactivity was only observed in presynaptic terminals (arrow). Images are single optical sections, scale bar represents 20μm, n=3 animals. Immunolabelling was performed by M. Barker.

6.4 Roles of Kv3.3 and Kv3.4 subunits at the calyx

6.4.1 High-voltage activated currents in the calyx activate at more negative potentials than those in MNTB neurones

Given that Kv3.4 subunits were expressed in the calyx but not in MNTB neurones, we wondered what role they might be performing. Since the presynaptic current activated at quite negative potentials, even in the presence of DTX-I (Fig, 6.1), we compared the activation of the presynaptic high-voltage activated current with that of the postsynaptic current (Fig, 6.6).

We fit the normalised whole cell conductance, modified to account for a non-linear single channel current I/V (see section 2.3.1), with a Boltzmann distribution (Fig, 6.6). The presynaptic high-voltage activated K^+ current activated with a $V_{½}$ of -27.5±1mV and a k value of 11.9±0.5mV (n=6), significantly more negative compared to that in MNTB neurones (which had a $V_{½}$ of -17.8±1.7 and a k value of 10.3±0.4mV; n=4, $P<0.005$, unpaired t test). These data are compatible with the hypothesis that Kv3.3 and Kv3.4 subunits shift activation of presynaptic channels to more negative potentials.

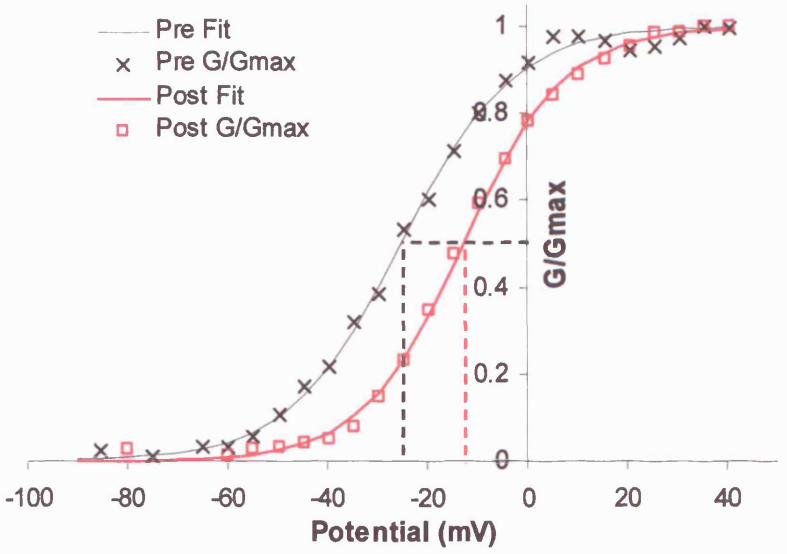

Figure 6.6. Activation of pre- and postsynaptic Kv3 currents in WT mice.
Presynaptic high-voltage activated currents had a $V_{½}$ of -27.5±1mV and a k value of 11.9±0.5mV (black dashed line, n=7), whereas postsynaptic high-voltage activated currents had a $V_{½}$ of -17.8±1.7mV and a k value of 10.3±0.4mV (red dashed line, n=4). The I/V data were transformed using a derivative of the GHK equation (see section 2.3.1) and fit using the least squares method with $V_{½}$ and k as variables. Example Boltzmann distributions are shown.

An alternative hypothesis is that there is a DTX-I resistant low-voltage activated current at the calyx (but not MNTB neurones), which contaminates the curves, making the total whole cell conductance activate at more negative potentials. This is unlikely for two reasons: first, the current was well fit with the GHK equation; if two currents with different $V_{½}$'s are present (e.g. if we do not apply DTX-I) we do not get a good fit (data not shown). Second, co-expression of Kv3.3 or Kv3.4 with Kv3.1 has been shown to shift activation to more negative potentials (Baranauskas et al., 2003; Desai et al., 2003), supporting our initial hypothesis.

6.4.2 Presynaptic APs are narrower and have a larger AHP than postsynaptic APs

The functional consequences of negative activation of Kv3 conductances were investigated by comparing pre-and postsynaptic APs. APs were elicited by 200ms current injection of 100pA (instead of by stimulation) to allow fair comparison (Fig, 6.7A). Presynaptic APs were significantly narrower than those in MNTB neurones ($P<0.05$, unpaired t test, Fig, 6.7B), with a width at half amplitude of 252±1.8μs (n=3) compared to 485±28.8μs (n=4) in MNTB neurones (even though the peak-current magnitude at 0mV was not significantly different; $P>0.1$, presynaptic n=7 and postsynaptic n=4). In addition, presynaptic APs repolarised to significantly more negative potentials, -78±0.6mV compared to -60.5±1.9mV ($P<0.02$, unpaired t test n=7 and 4 respectively). Since blocking the low-voltage activated current has no effect on AP waveform (Fig, 5.12), it is likely that the differences in pre- and postsynaptic currents are brought about by an increase in current at voltages between -40 and 0mV (i.e those more positive than the Kv1 current, Fig, 6.6). This seems particularly likely since these potentials would be reached during the rising phase of the AP. If more current was activated at these potentials (due to a negative shift in activation) repolarising efficiency would be enhanced and therefore the AP would be narrower.

A

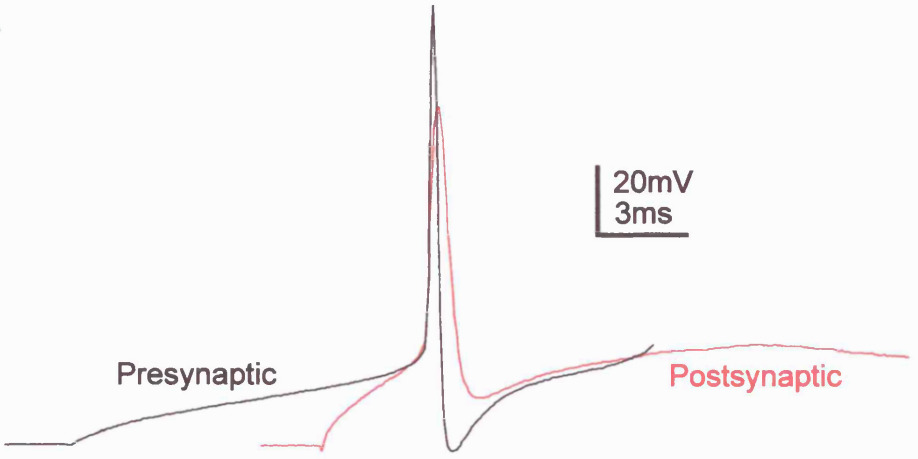

B

	AHP	½ Width (µs)
Presynaptic (n=3)	-78±0.6	252 ±1.8
Postsynaptic (n=4)	-60.5±1.9	485 ±28.8
T-Test (P)	0.0016	0.0037

Figure 6.7. Comparison of pre- and postsynaptic action potentials in WT mice.
A. Overlaid traces of a presynaptic (black trace) and postsynaptic (red trace) action potentials elicited by a 200ms current injection of 100pA. Traces were aligned at the AP threshold. **B.** Table showing mean AP parameters.

6.4.3 Blocking Kv3 currents broadens APs and reduces repolarisation

To further investigate our hypothesis that differences in the Kv3 current are responsible for differences in pre- and postsynaptic APs we decided to examine the effect on the AP waveform of blocking the Kv3 current. Application of 3mM TEA dramatically broadened the AP and decreased the AHP of stimulated APs (n=2 Fig, 6.8A2). However application of TEA had no effect on the amplitude of the DAP (Fig, 6.8).

On one occasion we also recorded electrically evoked APs in a calyx from a Kv3.1 KO mouse (Fig, 6.8B1). Although one must be wary of drawing conclusions from a single case, the AHP in the KO was considerably smaller than in the WT, suggesting a role for Kv3.1 subunits in repolarisation. Application of 3mM TEA to this terminal also resulted in broadening of the

AP (Fig, 6.8 B2). Taken together, these data suggest that heteromeric Kv3 channels at the calyx ensure a short duration AP thereby limiting calcium influx and transmitter release.

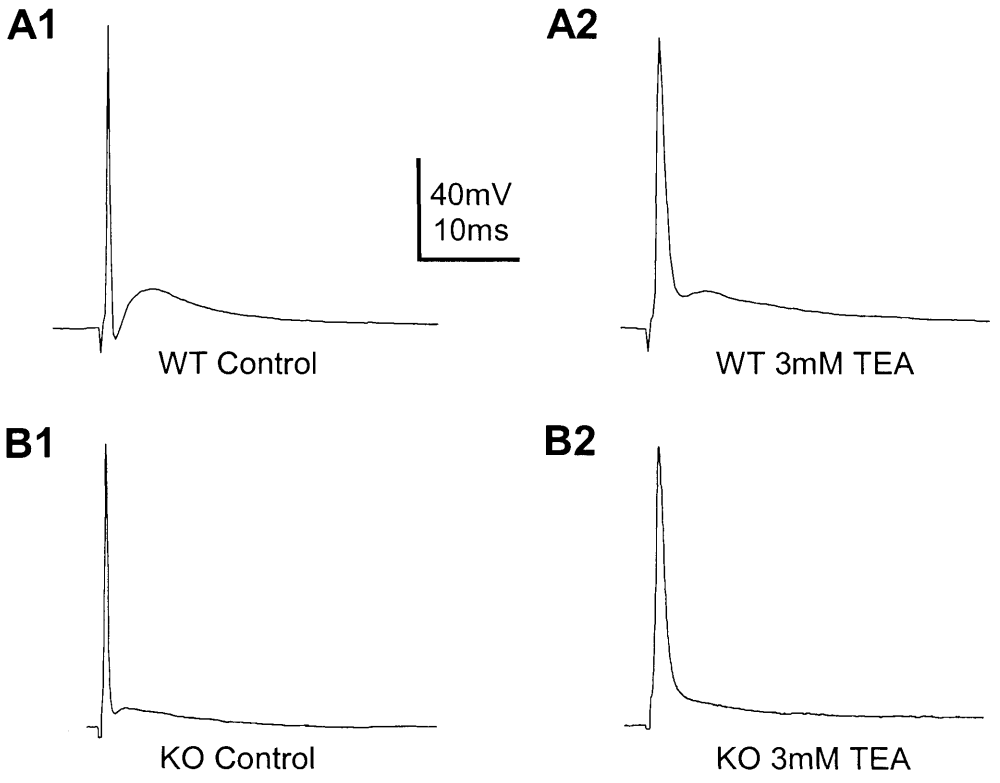

Figure 6.8. Blocking the high-voltage activated current broadens the presynaptic AP. **A1.** Control APs elicited by stimulation at the midline in a WT mouse. **A2.** AP after application of 3mM TEA. **B1.** Electrically evoked AP in a Kv3.1 KO mouse. **B2.** AP after application of 3mM TEA (n=1).

6.5 Effect of modulation on the high-voltage activated current

Modulation of Kv3.1 by PKC and casein kinase 2 is important in enabling MNTB neurones to fire at high frequencies (Macica and Kaczmarek, 2001; Macica et al., 2003). Given that the duration of the presynaptic AP is governed by Kv3 channels, we decided to investigate whether modulation of presynaptic Kv3 currents can influence transmitter release.

6.5.1 PKC activation does not affect the Kv3 current

Kv3.1 channels can be phosphorylated at a single site on their C-termini by PKC (Fig, 6.7). Since Kv3 subunits are present at the calyx, we decided to see what effect PKC activation would have on the high-voltage activated currents. We bath applied PMA (Phorbol 12-myristate 13-acetate;100nM, n=1 and 1μM n=3) to activate PKC; 2mM ATP and 0.5mM GTP were included in the intracellular solution to replace that which may be dialysed out during recording. Application of 100nM or 1μM PMA had no effect on the high-voltage activated current (Fig, 6.9; see also Hori et al., 1999). The current measured at 0mV only decreased by 0.8±3.9% in the presence of 1μM PMA (n=3).

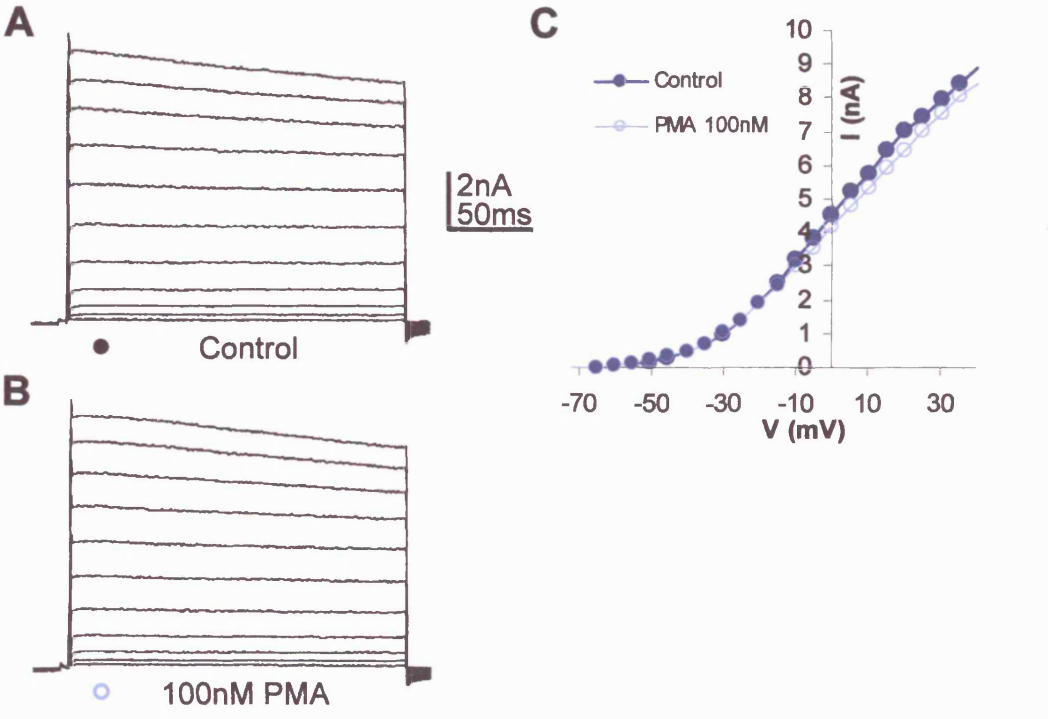

Figure 6.9. Effect of PKC activation on the high-voltage activated current.
A. Control current records following a pre-pulse to -100mV in the presence of DTX-I. 2mM ATP and 0.5mM GTP were included in the intracellular solution. **B.** 100nM PMA had no effect on the outward currents (n=3). **C.** I/V of the currents in A (●) and B (○).

6.5.2 Dephosphorylation has no effect on Kv3 current amplitude at the calyx.

The lack of effect of PKC activation led us to consider whether Kv3 channels were already maximally phosphorylated by PKC or another kinase. To test this hypothesis we added calf intestinal alkaline phosphatase (AP, 5 units in 1ml internal; Roche, UK) to our intracellular solution to dephosphorylate the high-voltage activated currents. There was no effect of alkaline phosphatase on the high-voltage activated current following a pre-pulse to -100mV (Fig, 6.10A). The current measured at 0mV only increased by 1±8.3% (n=4) after 15 minutes wash-in of alkaline phosphatase and no additional effects were seen after 30 minutes wash-in (n=2).

In MNTB neurones, the effect of alkaline phosphatase was most dramatic following a 2 minute pre-pulse to -40mV (Macica and Kaczmarek, 2001). We investigated the effect of alkaline phosphatase following this long inactivation protocol. In control conditions the two minute -40PP protocol resulted in a significant decrease in the current magnitude at 0mV (2.96±0.49nA, n=4, Fig, 6.10A1 & B1) compared to the -100PP (4.97±0.8nA, n=4, $P<0.05$, paired t test). Following the -40PP, the I/V is almost sigmoidal, approaching a maximum at more positive voltages (Fig, 6.10B3). This is because inactivation develops during the test steps to positive voltages and does not recover before the next test step. This does not occur in the -100PP protocol because each test step is preceded by a 750ms pre-pulse back to -100mV. Following 21 minutes of alkaline phosphatase wash-in, the current measured at 0mV (after -40PP) decreased by 33.7±9% (n=4). This suggests that dephosphorylation either enhances inactivation (similar to that observed in MNTB neurones, Macica and Kaczmarek, 2001) or slows recovery from inactivation.

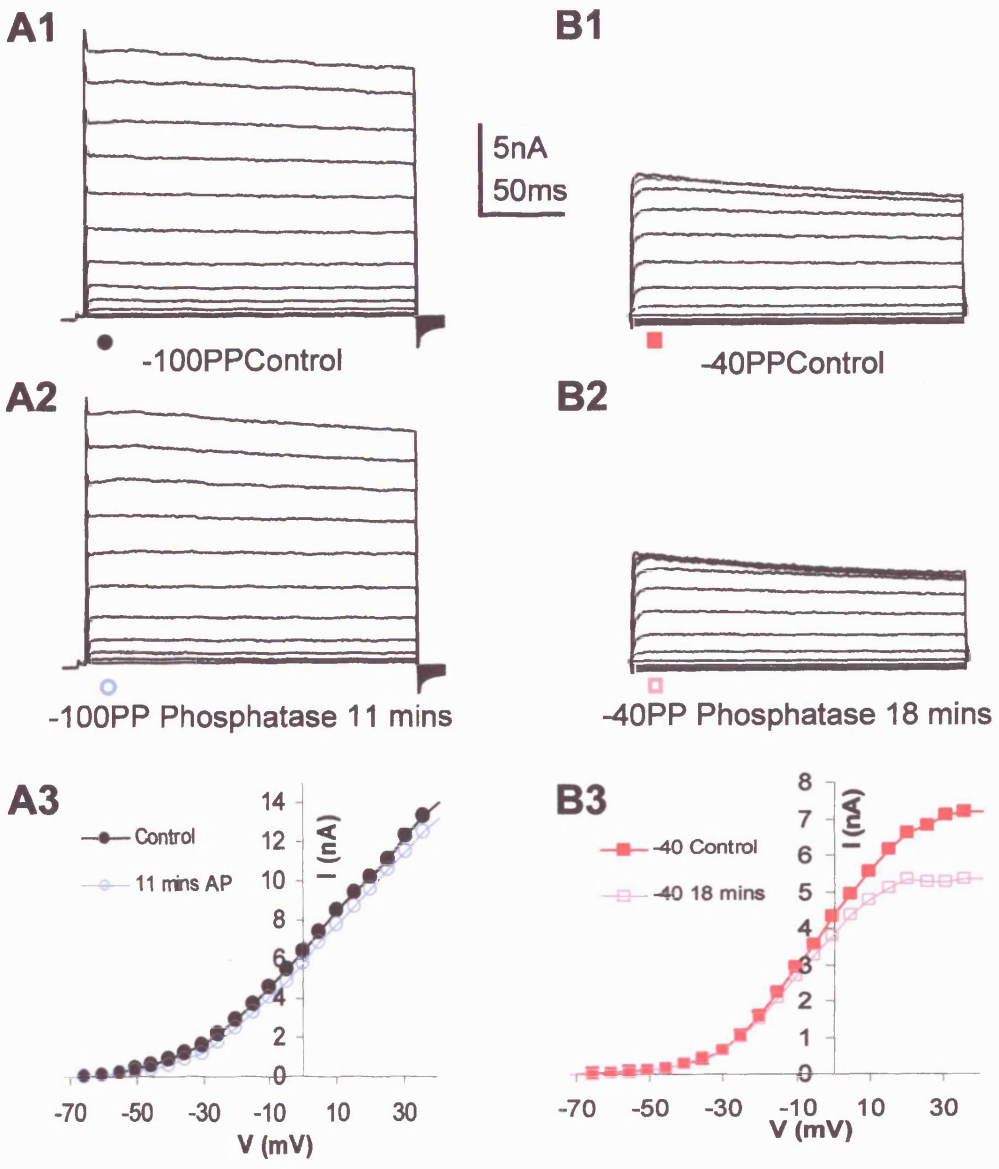

Figure 6.10. Effect of alkaline phosphatase on the high-voltage activated current.
A1. Control current records following a pre-pulse to -100mV in the presence of DTX-I. **A2.** Currents after 11 minutes with alkaline phosphatase in the internal solution. **A3.** I/V of the currents in A1 (●) and A2 (○). **B1.** Current records following a 2 minute pre-pulse to -40mV **B2.** Currents after 18 minutes phosphatase dialysis. **B3.** I/V of the currents in B1 (■) and B2 (▫).

6.5.3 Dephosphorylation has no effect on AP waveform

Since dephosphorylation results in an increase in inactivation, we considered whether inactivation might develop during long trains of stimuli and result in broadening of APs throughout the train. To test this idea, presynaptic axons were stimulated at 100Hz for 2 minutes and the 1st and last APs were compared in control and after 15 minutes alkaline phosphatase wash-in. Dephosphorylation had no effect on AP wave-form since the last AP in the train was identical to the first (n=3, Fig, 6.11A).

It is important to consider the possibility that the observed effect of changes in inactivation might not be a result of dephosphorylation but one of run-down during the recording. However, since the observed change seemed to have no physiological effect we did not investigate it further.

During long, high frequency trains failures in presynaptic AP generation are sometimes observed (<1% of the time, Fig, 6.11B). During these AP failures it is common to see a sub-threshold potential. This potential is presumably a recording of the AP from a distant node of Ranvier. The variability in the amplitude of these potentials (Fig, 6.11B) is likely to reflect the distance to the point of AP failure, with the smaller potentials resulting from failures at distant nodes.

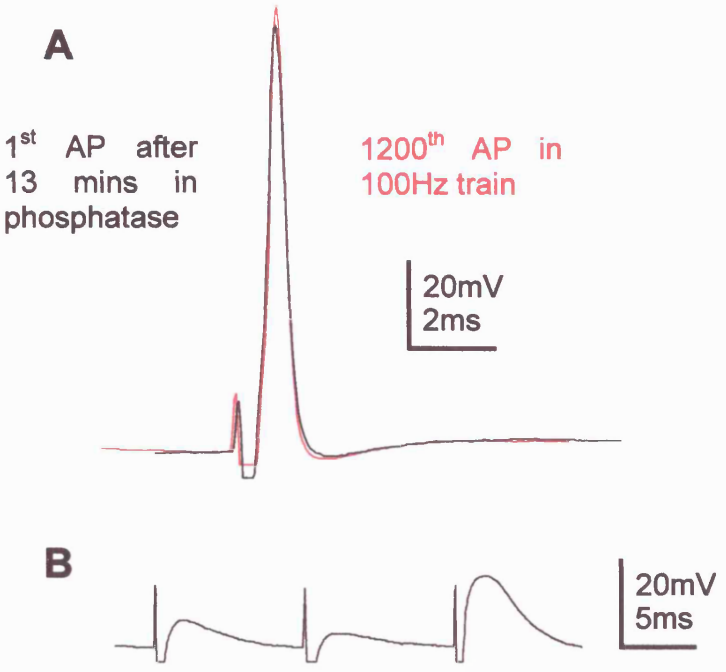

Figure 6.11. Effect of dephosphorylation during repetitive firing.
A. Presynaptic APs recorded from a membrane potential of -75mV after 13 minute dialysis of 5U alkaline phosphatase to dephosphorylate Kv3 channels. There were no activity-dependent changes in AP waveform since the 1st AP (black trace) and last AP (red trace) in a 2 minute train at 100Hz are the same (n=3). **B.** AP failures. During long trains of stimuli, AP failures can occur. In this example trace three stimuli failed to elicit an AP.

6.6 Summary

We used the calyx of Held to examine the role and subunit composition of presynaptic high-voltage activated K^+ channels and have shown that they are mediated by TEA-sensitive Kv3 channels which are present on the non-release face of the calyx. We have also demonstrated that, in addition to Kv3.1 subunits, Kv3.3 and Kv3.4 are present in calyceal terminals and that Kv3.1 and Kv3.3 are expressed in MNTB neurones. In the absence of Kv3.1 subunits it is likely that Kv3.3 and Kv3.4 form heteromeric channels at the calyx, accounting for the presynaptic high-voltage activated current present in Kv3.1 knockout mice. Kv3 currents at the calyx activate at much more negative potentials than those present in MNTB neurones, suggesting that the presence of Kv3.4 might shift the activation of the heteromeric channels. Activation of the presynaptic Kv3 channels at more negative potentials results in a shorter duration action potential than that of postsynaptic MNTB neurones. This

acts to reduce transmitter release, enabling the synapse to follow high frequency synaptic activity. In addition, presynaptic Kv3 currents were resistant to both phosphorylation by PKC and dephosphorylation, suggesting that transmitter release is not modulated via Kv3 phosphorylation.

CHAPTER 7 – Discussion

7.1 Summary

The aim of this study was to investigate voltage-gated K^+ conductances in MNTB neurones and their presynaptic terminals. Our investigation of the low-voltage activated K^+ current in MNTB neurones revealed that the current was mediated by two groups of heteromeric channels. These two channels had different subcellular localizations; Kv1.1/1.6 were localised to somatodendritic regions whereas Kv1.1/1.2 heteromers were concentrated at the axon initial segment, allowing them effective control of AP generation. This localisation enabled them to ensure that only one AP is generated during a sustained stimulus, thus preserving the AP firing fidelity important for conveying auditory information used to determine a sounds source.

Examination of presynaptic K^+ currents revealed that Kv1 channels were also important in preventing hyperexcitability in the presynaptic terminal. We found that at the calyx of Held, Kv1.2 homomers, located at the transition zone between the axon and presynaptic terminal, mediate two-thirds of the presynaptic low-voltage activated current and Kv1.1/1.2 heteromers contribute the remaining third. Whilst Kv1.1/1.2 heteromers seem to have no role in regulating presynaptic AP firing, Kv1.2 homomers prevent aberrant firing during AP invasion and are therefore important in ensuring the fidelity of presynaptic firing.

To complete our investigation of the K^+ currents at the calyx of Held, we also examined the high-voltage activated current. In addition to Kv3.1, Kv3.3 and Kv3.4 subunits contribute to the presynaptic channels, not only protecting them from modulation but also enabling them to activate at particularly negative potentials. This property tunes the Kv3 channels to ensure the extremely rapid repolarisation of the presynaptic AP (nearly twice as fast as in MNTB neurones) necessary to support high frequency firing.

We conclude that both low and high-voltage activated K^+ channels in MNTB neurones and their presynaptic terminals ensure that high frequency trains of APs are reliably transmitted across the synapse, thus facilitating sound source localisation.

7.2 Voltage-gated K^+ channels in the MNTB

7.2.1 K^+ channel expression in the MNTB

7.2.1.1 Kv1 subunit expression

Our immunohistochemistry indicates that Kv1.1 Kv1.2, and Kv1.6 subunits are expressed in the rat MNTB. Although this is the first published study in the rat brainstem, previous studies investigating Kv1.1 and Kv1.2 expression in the mouse have demonstrated that Kv1.1 and Kv1.2 mRNA and protein is produced in MNTB neurones (Wang et al., 1994; Grigg et al., 2000; Brew et al., 2003). These studies support our findings in the rat, although surprisingly, Wang *et al.* (1994) found less Kv1.2 immunoreactivity in mouse MNTB neurones. We also demonstrated Kv1.4 expression in mouse (Fig, 4.9E) but not rat (Fig, 4.1). This novel finding may explain the presence of an A-current in mouse MNTB neurones (Fig, 4.9; Brew et al., 2003). In spiral ganglion cells of the cochlear, the presence of brain derived neurotrophic factor (BDNF) triggers expression of Kv1.1 and Kv3.1 subunits (Adamson et al., 2002); it is possible that neurotrophins are involved in regulating ion channel expression in other auditory nuclei such as the MNTB.

7.2.1.2 Kv3 subunit expression

Immunoreactivity for Kv3.1 and Kv3.3 was detected in mouse MNTB neurones and Kv3.1, Kv3.3 and Kv3.4 at the calyx. Several other studies have shown Kv3.1 and Kv3.3 expression in MNTB neurones (Perney et al., 1992; Weiser et al., 1994; Grigg et al., 2000; Li et al., 2001) and Kv3.1 at the calyx (Dodson et al., 2003; Elezgarai et al., 2003); however, this is the first report of Kv3.3 or Kv3.4 localisation in the terminal, probably due to lack of availability of Kv3.3 antibodies and the report that Kv3.4 mRNA was not expressed in the MNTB (Weiser et al., 1994).

7.2.2 Channel composition

7.2.2.1 Diversity of combinations

We have demonstrated that the low-voltage activated current in MNTB neurones is mediated by Kv1.1/1.2 and Kv1.1/1.6 heteromers. In contrast, the majority of the presynaptic low-voltage activated current is mediated by Kv1.2 homomers, with a secondary contribution from Kv1.1/1.2 heteromers. A number of studies have examined the subunit composition of native neuronal K^+ channels using immunoprecipitation (Koch et al., 1997; Shamotienko et al., 1997; Koschak et al., 1998; Coleman et al., 1999; Wang et al., 1999a). Differences in species, region of the brain and which antibodies or toxins were used, make comparisons between these studies difficult; although it is possible to draw-out some conclusions relevant to our investigation. All studies identified Kv1.1/1.2 heteromers indicating that this channel combination may be found throughout the brain. Kv1.4 and Kv1.2 homomers were isolated in most studies (Shamotienko et al., 1997; Coleman et al., 1999; Wang et al., 1999a) but Kv1.1 homomers were not found. Kv1.1/1.6 heteromers were not identified; this is probably because the method used by those that examined Kv1.6 contribution precluded examination of this combination (Koch et al., 1997; Shamotienko et al., 1997; Wang et al., 1999a). Another pertinent finding is that Kv1.3 was not found associated with Kv1.1 (Shamotienko et al., 1997; Koschak et al., 1998; Coleman et al., 1999; Wang et al., 1999a), supporting our conclusion that Kv1.3 does not contribute to Kv1 channels in the MNTB. In addition, examination of Kvβ2.1 was found associated with Kv1.1/1.2 heteromers and Kv1.2 homomers. It would be interesting to examine immunoprecipitation of Kv1 subunits in the MNTB, perhaps as an extension of this project, although the large amount of tissue required would make it difficult, if not impossible.

7.2.2.2 Stoichiometry of Kv1 channels

Subunit-specific toxins provide information about the subunits contained in a channel, but since they only require one toxin-sensitive subunit to block the channel, they provide little information about the stoichiometry of the subunits (Akhtar et al., 2002). Therefore, it is

conceivable that Kv1.1/1.2 current in MNTB neurones might consist of channels with the following stoichiometry: $\begin{matrix}1.1 & 1.2\\ 1.2 & 1.1\end{matrix}$ $\begin{matrix}1.1 & 1.1\\ 1.2 & 1.2\end{matrix}$ $\begin{matrix}1.1 & 1.2\\ 1.2 & 1.2\end{matrix}$ $\begin{matrix}1.1 & 1.1\\ 1.1 & 1.2\end{matrix}$

Examination of subunit assembly in homomeric Kv1.3 channels has shown that subunits first form as dimers, then two dimers come together to form tetramers (Tu and Deutsch, 1999; Deutsch, 2002). Studies of GluR1/2 heteromers have shown that a similar mechanism occurs in AMPA receptors (Mansour et al., 2001); GluR subunits have a higher affinity for unlike subunits (GluR1 will bind to GluR2 and then bind to another GluR1/2 dimer), which means that identical subunits are positioned on opposite sides of the pore. If these were to be general principles in channel assembly, then Kv1.1/1.2 channels would have a $\begin{matrix}1.1 & 1.2\\ 1.2 & 1.1\end{matrix}$ stoichiometry.

7.2.2.3 Subunit composition can affect expression

Given that MNTB neurones express Kv1.1, Kv1.2 and Kv1.6 subunits, it is surprising that more channel combinations are not found, particularly since Kv1 channels are promiscuous with other Kv1 channels in expression systems (Coetzee et al., 1999). One explanation for this might be that of ER retention, which would also explain the strong cytoplasmic Kv1 immunostaining observed in MNTB neurones (Fig, 4.1). K_{ATP}, CFTR and $GABA_B$ receptor subunits contain cytoplasmic ER retention sequences which must be masked before the channels can be exported (Gilbert et al., 1998; Zerangue et al., 1999; Margeta-Mitrovic et al., 2000). Association of Kv channels with SAP97, a membrane-associated guanylate kinase (MAGUK) results in ER retention (Tiffany et al., 2000); phosphorylation of Kir 2.2 inhibits its association with SAP97 (Leonoudakis et al., 2001), providing an interesting mechanism for regulation of channel trafficking. Another way to regulate expression of certain channel combinations is via regulation of their release from the ER. Kir 1.1 contains ER export signals which promote export from the ER and surface expression (Ma et al., 2001); insertion of these sequences into Kv1.2 increased surface expression. It is conceivable that certain Kv1 subunits containing export sequences are readily expressed, aiding expression of other subunits in the heteromer (Manganas and Trimmer, 2000), whereas others require the formation in particular heteromeric channels to mask retention sequences.

7.2.3 Subcellular channel localisation

7.2.3.1 Channel segregation in the MNTB

In both MNTB neurones and the calyx, channels with different subunit composition seem to produce currents with almost identical properties (Figs 4.3; 4.4; 5.3); however, despite their similarities, the channels perform different functions (Dodson et al., 2002). One way this segregation of function might be achieved is by differential localisation. In MNTB neurones Kv1.1/1.2 heteromers are localised to the initial segment of the axon (Fig, 4.7), whereas Kv1.1/1.6 heteromers seem to be localised to the soma or proximal dendrites. In the calyx Kv1.2 homomers and Kv1.1/1.2 heteromers are localised to the transition zone between the axon and the terminal but both channels are excluded from the synaptic terminal itself (Fig, 5.5). In contrast, Kv1 channels in bushy cells of the aVCN (the cell bodies of the calyces, where the channels are made), consist of heteromers containing Kv1.1, Kv1.2 and Kv1.6 subunits (Dodson et al., 2003). This distinction between somatic/axonal and axonal/terminal channels has also been observed for calcium channels at the calyx (Doughty et al., 1998) and potassium channels in cerebellar basket cell terminals (Southan and Robertson, 1998b). Another intriguing finding is the segregation between Kv1 and Kv3 localisation. Kv3.1 and Kv3.3 are located on the MNTB neurone soma (Fig, 5.5) whereas we found no evidence for Kv1 immunofluorescence in somatic membrane (neither did we see evidence of Kv1 channels in somatic outside-out patches). Calyx Kv3 channels are localised to synaptic terminal membrane, whereas Kv1 immunostaining is axonal. The same differential distribution has been observed at basket cell terminals (Laube et al., 1996) and in the nodal region of CNS axons (Devaux et al., 2003), suggesting that specific mechanisms may exist to segregate Kv1 and Kv3 channels.

A general hypothesis consistent with our observations is that Kv1.4, Kv1.6 (and Kv4.2) subunits are restricted to somatic/dendritic regions, Kv1.2 to axonal regions and Kv3.3 and Kv3.4 to the terminal membrane. There are a number of mechanisms involved in trafficking which may contribute to the differential channel localisation observed in the MNTB.

7.2.3.2 Chaperoning by accessory subunits

It has long been proposed that potassium channel accessory proteins have a role in trafficking Kv channels to the cell surface (McCormack et al., 1995; Fink et al., 1996; Shi et al., 1996; Wang et al., 1996b; Nagaya and Papazian, 1997). One such chaperone protein is KChAP, it transiently interacts with Kv1.3, Kv2.1 and Kv4.3 subunits trafficking them to the cell surface and increasing protein expression (Abriel et al., 2000; Kuryshev et al., 2001). Kvβ subunits however can be considered as pseudo-chaperones since they stably bind to Kv1, Kv4 and Kv2.2 channels and may be involved in trafficking, regulating channel kinetics and have an oxidoreductase function (Xu et al., 1998; Coetzee et al., 1999; Kuryshev et al., 2001). Coexpression of Kvβ subunits increases surface expression of homo- and heteromeric Kv1.1 and Kv1.2 channels in COS cells and targets Kv1.2 to axons in cultured hippocampal neurones (Manganas and Trimmer, 2000; Campomanes et al., 2002; Gu et al., 2003). In addition, Kvβ2 was found to coimmunoprecipitate with Kv1.2 homomers and Kv1.1/1.2 heteromers, suggesting that Kvβ-subunits may also play a role *in vivo* (Shamotienko et al., 1997; Coleman et al., 1999). Since Kvβ2 is expressed in MNTB neurones (M. Barker unpublished observations), it is tempting to suggest a role for this accessory protein in selectively trafficking Kv1.1/1.2 or Kv1.1/1.6 heteromers. However, it has been suggested that Kvβ subunits may not be involved in trafficking at all but rather primarily concerned with inactivation (Rettig et al., 1994; Heinemann et al., 1996), modifying gating (Accili et al., 1997; McIntosh et al., 1997) or an oxidoreductase function (Gulbis et al., 1999; Campomanes et al., 2002). The later suggestion arises because of similarities of the Kvβ subunit with aldo-ketoreductase (AKR) enzymes (Gulbis et al., 1999). It has also been suggested that the oxidoreductase activity might be linked to other roles of the β-subunit; however, whilst mutations of the catalytic site removed inactivation effects (Bahring et al., 2001), it had no effect on trafficking (Campomanes et al., 2002) and no phenotype in knock-in animals (McCormack et al., 2002). Kvβ2 knockout studies also cast doubts over the role of Kvβ as a trafficking molecule since normal Kv1.1 and Kv1.2 expression was observed in Kvβ2-null mice (McCormack et al., 2002). All of these raise issues the possibility that Kvβ subunits have an alternate role, but because they contain an ER export sequence they are able to enhance trafficking of Kv channels in expression systems (Deutsch, 2002).

7.2.3.3 Membrane insertion

Another way to regulate subcellular localisation is by targeting proteins to particular sites in the membrane. For Kv channels the best studied example of such targeting is at nodes of Ranvier in myelinated axons. In CNS nodes Kv1.1, Kv1.2, Kv1.6 and Kvβ2 colocalise to juxtaparanodal regions (Wang et al., 1993; Rhodes et al., 1997; Rasband et al., 1998; Rasband et al., 1999), distinctly segregated from the paranodal and nodal regions (Fig, 7.1). A contactin-associated protein (Caspr) is present at the paranodal regions and the related Caspr2 at the juxtaparanodal regions (Fig, 7.1); these neurexins are thought to tether the axon to the myelin via interactions with proteins such as TAG-1 (Traka et al., 2002). Although Kv1.2, Kvβ2 and Caspr2 colocalise at juxtaparanodes, their immunoprecipitation is dependent upon C-terminal PDZ binding motifs, suggesting that interaction requires a scaffolding protein (Rasband and Shrager, 2000). In *Drosophila* the MAGUK protein DLG colocalises with *Shaker* potassium channels at synapses (Ruiz-Canada et al., 2002); mutation of the C-terminal of *Shaker* channels or DLG results in aberrant localisation. It has therefore been proposed that Kv1.2 containing channels are targeted to Caspr2, where they bind with a scaffolding protein, resulting in specific localisation. A possible candidate protein is PSD-95, which not only causes clustering of NMDA receptors and Kv1 channels *in vitro*, but has also been found at juxtaparanodes and cerebellar basket terminals (Kim et al., 1995; Kim and Sheng, 1996; Laube et al., 1996; Baba et al., 1999). However, normal juxtaparanodal Kv1 and Caspr2 localisation has recently been demonstrated in PSD-95-null mice (Rasband et al., 2002), suggesting that PSD-95 might perform an alternative signalling role. Sequences within the channel can also play important roles in trafficking. The cytoplasmic loop between domains II and III of the sodium channel $Na_v1.2$ are important for localisation at the axon initial segment by binding to ankyrin-G complexes (Garrido et al., 2003). Certain Kv subunits (e.g. Kv1.2) might contain analogous sequences directing the channels which contain those subunits to different locations. Indeed, several regions in the pore and C-terminus have been implicated in trafficking (Manganas et al., 2001; Zhu et al., 2003a, b). Kv1.1 and Kv1.2 are generally reported to be poorly expressed in cell lines, often being confined to the ER (Manganas and Trimmer, 2000). If these subunits do contain sequences important for axonal trafficking (Gu et al., 2003), it is possible that expression levels are low because the cell lines do not contain axons.

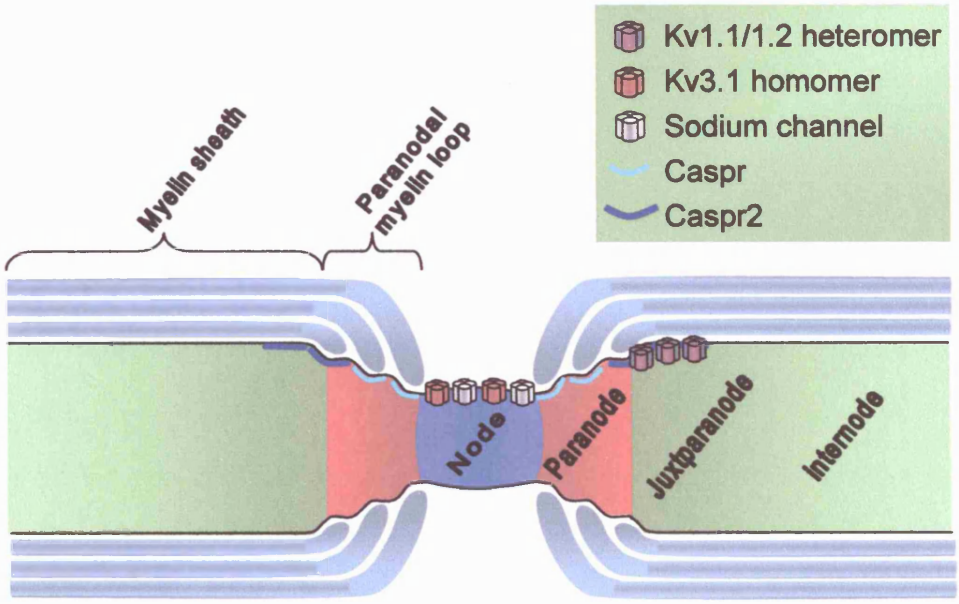

Figure 7.1. CNS node of Ranvier.
Heteromers containing Kv1.1, Kv1.2 and maybe other Kv1 subunits are localised to juxtaparanodal regions with Caspr2.

In MNTB neurones, Kv1.1/1.2 heteromers localise to the initial segment (Fig, 4.7) and at the calyx Kv1.2 homomers and Kv1.1/1.2 heteromers to the transition zone between the axon and the terminal (Fig, 5.5), both of which are thought to be unmyelinated regions of axon (Zhou et al., 1999). Kv1 immunostaining has also been observed in other unmyelinated regions, at the neuromuscular junction (Zhou et al., 1998b), the optic nerve (Baba et al., 1999) and spoon terminals of primary vestibular axons (Kv1.2 but not Kv1.1, Popratiloff et al., 2003). Examination of Kv1 localisation during hypomyelination showed diffuse Kv1 staining throughout the axon (Rasband et al., 1999), suggesting that it might be the lack of myelin that signals Kv1 localisation in these regions. It could be argued that the expression patterns we see in MNTB neurones and their presynaptic terminals reflect an immature stage of development and that localisation of Kv channels might continue during development. Whilst it is true that we are studying terminals in immature animals, there are a number of arguments which support the idea that Kv localisation in the MNTB is complete by P9. We have found no discernable difference in Kv1 immunostaining in the MNTB of P9 animals compared with a relatively small number of P20 to P35 animals investigated (M. Barker unpublished

observations). In addition, unlike axons in the PNS where Kv1 channels redistribute during development, in CNS axons Kv1 channels are inserted at their final location (Rasband et al., 1999); this suggests that initial segment and transition zone channels in the MNTB are unlikely to redistribute.

7.3 Voltage-gated K+ currents in the MNTB

7.3.1 Low-voltage activated currents in the MNTB

7.3.1.1 Kv1.1/1.2 heteromers

We have shown that low-voltage activated currents in MNTB neurones are comprised by Kv1.1/1.2 and Kv1.1/1.6 heteromers. These Kv1 currents activate at around -70mV, partially inactivate (Fig, 4.3) and slowly deactivate (Fig, 3.4), similar to Kv1.1/1.2 heteromers expressed in oocytes (Hopkins, 1998; D'Adamo et al., 1999; Akhtar et al., 2002). One difference in the native and heterologously expressed currents is that activation occurs at potentials ≈10mV more negative in MNTB neurones. It is possible that this negative activation is conferred by Kvβ2 subunits (Uebele et al., 1996), which are expressed in MNTB neurones (M.Barker unpublished observations).

7.3.1.2 Kv1.2 homomers

Examination of the presynaptic current in the presence of DTX-K revealed a current mediated by Kv1.2 homomers (Fig, 5.3). To our knowledge this is the first recording of native Kv1.2 homomers and therefore affords us the opportunity to examine the properties of native channels. Like the heteromeric channels in MNTB neurones, presynaptic Kv1.2 homomers activate at around -70mV, and partially inactivate. Kv1.2 homomers in expression systems tend to activate at more positive potentials, particularly in mammalian cell lines (with $V_{½}$'s of: -34mV, Stuhmer et al., 1989; 0mV, Werkman et al., 1992; 27mV, Grissmer et al., 1994; 27mV, Hopkins, 1998; 20mV, Kerr et al., 2001; 15mV, Akhtar et al., 2002). The differences in $V_{½}$'s in these studies suggest that, in some cases, modulation or the presence of accessory subunits such as Kvβ2 might be altering activation.

7.3.1.3 Differences in rat and mouse low-voltage activated currents

In our study of low-voltage activated K^+ currents in MNTB neurones, most of our experiments were done using Lister hooded rats. However, since we were using mice for our study of the presynaptic high-voltage activated currents, we also did a few experiments to examine Kv1 currents in mouse MNTB neurones. We were surprised to find that low-voltage activated currents in mice differ from those in the rat, the most prominent difference being the presence of a DTX-I insensitive A-current (Fig, 4.9). The expression of Kv1.4 subunits in mice, combined with the fact that Kv1.4 homomers are readily expressed at the surface (Manganas and Trimmer, 2000), suggest that the A-current current may be mediated by Kv1.4 homomers. The other surprising observation was that, in the absence of DTX-I, outward currents are almost indistinguishable from those in the rat (Fig, 4.9A). This suggests that mouse DTX-I sensitive conductances may activate slower or inactivate less than those in rat; hence, when superimposed upon the A-current, the resulting current appears the same as that in rat. Although it is likely to be largely inactivated at rest, the A-current in mouse MNTB neurones might act to boost the low-voltage activated conductances during initial depolarisation and thus help to prevent multiple AP firing (Rothman and Manis, 2003).

In addition to the presence of I_A, DTX-I blocked less of the current at -45mV in mouse than in rat (Fig, 4.9 and ; Brew et al., 2003). Application of 100nM DTX-I, DTX-K, TsTX-Kα or NTX only blocked around half of the low-voltage activated current in the mouse (Fig, 4.10). Although each of these experiments was only performed once, the data suggest that the mouse Kv1 current is mediated by just one type of channel, a heteromer containing Kv1.1, Kv1.2 and perhaps Kv1.6 subunits. Given that in the rat Kv1.1/1.2 heteromers were dominant in suppressing repetitive firing and that Kv1.1/1.6 heteromers may act to boost the current (Dodson et al., 2002), it is possible that in the mouse Kv1.1/1.2 heteromers and Kv1.4 homomers (I_A) perform a similar role. However, since the current was measured later in the step to avoid contribution of I_A this still doesn't explain why only 50% of the current at -45mV was DTX-I sensitive. It has been demonstrated that Slack, which has sequence like a Ca^{2+}-activated potassium channel (although does not form Ca^{2+} activated channels unless coexpressed with Slo1, Joiner et al., 1998), is expressed in the mouse MNTB (Bhattacharjee et al., 2002). It is possible that these channels may contribute the DTX-I insensitive portion of

the current at -45mV. Alternatively the DTX-I insensitive current at this potential could be mediated by the high-voltage activated current. If Kv3 channels activated at more negative potentials in mouse than rat, owing to phosphorylation or a different subunit composition, they may contribute a larger proportion of the current at -45mV (more than the 13% seen in rat, Fig, 4.6). One question that remains unanswered is whether the differences in low-voltage activated currents in the rat and mouse arise because of different requirements for computing ITD and ILDs or whether they simply reflect different ways of producing the same overall current.

7.3.1.4 Inactivation

In studies of Kv1.1/1.2 heteromers expressed in oocytes, the amount of inactivation varies somewhat between studies (Hopkins, 1998; D'Adamo et al., 1999; Akhtar et al., 2002), but appears to be less than that observed in the MNTB. In MNTB neurones, the low-voltage activated current only partially inactivates (by about 40%, Fig, 4.13), with a time-course of 63.7ms (Fig, 4.3). Interestingly, the amount and time-course of inactivation observed in Kv1.1/1.2 and Kv1.1/1.6 heteromers in MNTB neurones (Fig, 4.4) and Kv1.2 homomers at the presynaptic terminal (Fig, 5.3) were similar. This relatively slow inactivation could be C-type (Choi et al., 1991; Liu et al., 1996; Yi and Jan, 2000), or Kvβ subunit mediated N-type inactivation (Rettig et al., 1994; Pongs et al., 1999).

Kvβ1.1-1.3 and Kvβ3.1 all induce inactivation of Kv1α channels (Heinemann et al., 1996; Martens et al., 1999; Pongs et al., 1999); some Kvβ subunits (e.g. Kvβ1.1) induce rapid N-terminal inactivation by the pore-blocking effects of the inactivation ball (Rettig et al., 1994; Wissmann et al., 1999), whereas others (e.g. Kvβ1.2) enhance the slower C-type inactivation (Morales et al., 1996; Accili et al., 1998). The amount of Kvβ inactivation can also be varied by phosphorylation of the Kvα subunit (Kupper et al., 1995; Levy et al., 1998; Jing et al., 1999) and the scope for varying inactivation is further increased by the possibility of different numbers of Kvβ-subunits (between zero and four Kvβ1) being bound to the Kv1 channel (Xu et al., 1998). It should be pointed out however, that Kvβ2 subunits prevent the inactivation conferred by Kvβ1.1 (Xu and Li, 1997) because Kvβ2 forms homotetramers which then preferentially bind to the channel (Xu et al., 1998), preventing Kvβ1.1 binding.

Things are further complicated if Kv1.6 subunits are present because they have an N-type inactivation-prevention domain (NIP, Roeper et al., 1998), which causes less inactivation in Kv1.6 containing heteromers. In MNTB neurones it seems unlikely that N-type inactivation plays a role for three reasons: first, inactivation is much slower than would be expected for N-type; second, Kvβ2 subunits are present which would presumably prevent Kvβ-mediated inactivation; and third, the amount of inactivation is comparable for Kv1.1/1.6 (in which some of the subunits contain NIPs) and Kv1.1/1.2 heteromers. This leaves the possibility that C-type inactivation may be occurring in the absence of Kvβ-subunits. If this were the case however, one might expect to observe different amounts of inactivation in the three channel types (Kv1.2 homomers and Kv1.1/1.6 & Kv1.1/1.2 heteromers). Therefore, the most likely possibilities are either increase of C-type inactivation by Kvβ subunits or phosphorylation of Kvβ containing channels.

7.3.1.5 Modulation of Kv1 containing channels

Since the activation and inactivation properties of Kv1 channels in MNTB neurones and their terminals do not exactly match those of cloned channels, it is possible that modulation is responsible for some of the observed differences. Modulation of Kv1 channels is known to affect both inactivation and current magnitude (Jonas and Kaczmarek, 1996). Phosphorylation of serine/threonine residues in Kv1.2 by PKA results in increased current amplitude by increasing the time the channels spends in higher conductance states (Huang et al., 1994). The current magnitude of Kv1.1 channels can also be increased by PKA phosphorylation, but by a different mechanism (Jonas and Kaczmarek, 1996); long-term application of PKA increases both the rate of synthesis and accumulation of Kv1.1 at the plasma membrane (Levin et al., 1995). In contrast to PKA, PKC can suppress Kv1.1 and Kv1.2 currents (Huang et al., 1993; Boland and Jackson, 1999). For Kv1.2 this occurs via activation of the tyrosine kinase PYK2 which is able to directly phosphorylate the channel (Lev et al., 1995).

In addition to modulation of current amplitude, phosphorylation can affect channel inactivation. The extent of inactivation is decreased by PKC phosphorylation of Kv1.1/Kvβ1.1 channels (Levy et al., 1998), but increased by activation of Gβγ subunits (Jing et al., 1999). Modulation can also affect the rate of C-type inactivation (Kupper et al., 1995),

which accounts for the changes in inactivation observed upon excision of Kv1.3 containing patches.

It is clear that Kv1 currents can be modulated *in vitro*, but does modulation of Kv1 currents occur *in vivo*? DTX-sensitive currents in pyramidal neurones of the medial prefrontal cortex have been shown to be inhibited by dopamine receptor activation via a cAMP/PKA pathway (Dong and White, 2003). Similarly DTX-sensitive currents in hippocampal neurones (I_D) can be modulated by metabotropic glutamate receptor (mGluR) activation, resulting in increased excitability and AP width (Wu and Barish, 1999). In MNTB neurones however, similar changes would be disadvantageous as they might reduce the ability to discriminate sound source, hence one might expect the absence of dynamic regulation of low voltage-activated currents in the MNTB. Consistent with this idea, Macica *et al.* (2001; 2003) not only demonstrate that PKC activation has no effect on AP firing in MNTB neurones, but also that dephosphorylation does not seem to affect low-voltage activated current magnitude. Although these results point to the fact that phosphorylation may not play a role in shaping MNTB Kv1 currents, more detailed analysis would be necessary to completely rule out the involvement of pre- or postsynaptic Kv1 modulation.

Differential modulation of different Kv1 subunits might provide an explanation as to why the low-voltage activated current in the MNTB consists of two components. For example, phosphorylation of Kv1.6 would affect Kv1.1/1.6 heteromers without modulating Kv1.1/1.2 channels. An alternative hypothesis is that rather than modulating Kv1 channels themselves, low-voltage activated currents might be enhanced by modulating I_H (Rothman and Manis, 2003). Activation of I_H can be shifted to more positive potentials by cAMP (DiFrancesco and Tortora, 1991); this will result in depolarisation and therefore the activation of Kv1 channels. The net affect would be to reduce the membrane time constant, thereby reducing EPSP duration and facilitating high frequency firing (Rothman and Manis, 2003).

7.3.1.6 Similar Kv1 currents in other neurones

Several DTX-sensitive low-voltage activated currents, similar to those in the MNTB, have been found in other neurones in rat, mouse and avian brain. Such currents are particularly

common in auditory neurones, aiding them in faithfully following AP trains. Bushy cells of the cochlear nucleus (and the avian homologue, the nucleus magnocellularis) express low-voltage activated currents which are comprised by heteromers containing Kv1.1, Kv1.2 and Kv1.6 subunits (Manis and Marx, 1991; Rathouz and Trussell, 1998; Rusznak et al., 2000; Dodson et al., 2003). Other neurones in the binaural pathway also express similar currents: MSO (and the avian, nucleus laminaris, Kuba et al., 2002; Svirskis et al., 2002); LSO (Barnes-Davies et al., 2003); and spiral ganglion (Mo et al., 2002). In addition, the octopus cells of the cochlear nucleus express Kv1 subunits but these form as heteromers with Kv1.4 and therefore have inactivating phenotypes (Bal and Oertel, 2001).

Similar DTX-sensitive currents are also expressed in several non-auditory nuclei including: neocortical pyramidal neurones (Bekkers and Delaney, 2001), vestibular neurones (Gamkrelidze et al., 1998; Chabbert et al., 2001), in the nodose ganglia (Stansfeld et al., 1986; Glazebrook et al., 2002), superior cervical ganglia (SCG, Wang and McKinnon, 1995), some cells of the dorsal root ganglia (Everill et al., 1998) and hippocampal pyramidal neurones (Wu and Barish, 1992).

In addition to somatic/axonal channels, DTX-sensitive currents have been identified in several nerve terminals. Direct studies of cerebellar basket terminals have demonstrated the presence of DTX-sensitive currents similar to those recorded from the calyx (Southan and Robertson, 1998b, 2000). Indirect study of several terminals has also been performed by investigating the effects of toxins on transmitter release; these studies have identified: putative homomeric Kv1.2 channels in thalamocortical terminals (Lambe and Aghajanian, 2001), DTX-sensitive channels which lack Kv1.1 in the entorhinal cortex (Cunningham and Jones, 2001) and Kv1.1 containing channels at the neuromuscular junction (Vatanpour and Harvey, 1995) (Zhou et al., 1999).

The prevalence of DTX-sensitive currents similar to those in the MNTB neurones, particularly in neurones which display unitary spiking, suggest that many neurones may use heteromeric Kv1 channels to control AP firing. The slight differences in the current observed in different

neurones probably reflect the use of different subunit combinations to fine-tune the channels to their role.

7.3.1.7 The use of subunit-specific toxins

To dissect out the different components of the low-voltage activated current we used subunit specific toxins. This approach has several advantages over the use of transgenic animals when the appropriate selective toxins are available. The major advantage is the ability to study native channels in the absence of compensation or changes in the expression of other genes. Data from transgenic studies can be difficult to interpret where heteromeric channels or several channels with different subunit compositions underlie a current. For example, in Kv1.1 KO mice DTX-I sensitive currents were still observed (Brew et al., 2003), suggesting that Kv1.2 homomers or Kv1.2/1.6 heteromers generate the low-voltage activated current in the knockout, with only a slight increase in neuronal excitability (Brew et al., 2003).

We applied toxins at 100nM to block components of the low-voltage activated current. This concentration was chosen to ensure rapid, selective block of Kv1 channels (Fig, 4.2E). These toxins have IC_{50}'s in the picomolar and low nanomolar ranges when applied to cloned channels in expression systems (Table, 1); however, higher concentrations are generally required in slice preparations since toxin-block can be hampered by non-specific binding to debris in the slice. Some of the toxins, e.g. δ-DTX, have been shown to be less specific at 100nM (blocking around 20% of Kv1.2 current in oocytes, Hopkins, 1998). We tried TsTX-Kα at 70, 100 and 200nM and observed ≈50% block of the MNTB neurone low-voltage activated current in each case (data not shown), suggesting that the toxin was specifically blocking the same component at all concentrations. The fact that NTX (which also blocks Kv1.2) blocked the same percentage (Fig, 4.6), further supports the selectivity of TsTX-Kα. In addition, in the presynaptic terminal the effect of the toxins was reversed; DTX-K only blocked ≈30% of the presynaptic Kv1 current whereas TsTX-Kα blocked it all (Fig, 5.4). This suggests that complete block of Kv1 currents in MNTB neurones was not due to non-specific block of DTX-K. It is conceivable that the ≈30% block of the presynaptic Kv1 current by DTX-K was due to non-specific block of Kv1.2 homomers; however, given that our

immunohistochemistry shows Kv1.1 located with Kv1.2 (Fig, 5.5), it seems more likely that DTX-K is specifically blocking Kv1.1/1.2 heteromers.

The major disadvantage of using subunit-specific toxins to dissect out different components of a current is that the method is relatively insensitive to currents that comprise a small percentage of the total. It is conceivable that channels with different subunit compositions do occur in the MNTB, but at such low concentrations that we cannot detect them using subunit-specific toxins. Another problem with the toxin method is that it does not provide information about channel number. When a toxin blocks half of a current, it is tempting to think that half of the channels were blocked; however, since the conductance of the channels is unknown, one cannot draw this conclusion. It is possible that 90% of MNTB Kv1 channels might be Kv1.1/1.2 heteromers but if Kv1.1/1.6 heteromers have a higher conductance, block of Kv1.2 channels will only block half the current. Another disadvantage of the method is that toxins may not block channels located under the myelin sheath (Chiu and Ritchie, 1980; Vabnick et al., 1999; Devaux et al., 2002). An alternative approach to using toxins, which may be particularly useful where good subunit-specific toxins are unavailable (e.g. for Kv3 channels), is the use of antibodies as blockers. Micromolar concentrations of Kv1.2 and Kv3.1 antibodies directed against the external vestibule have been used to block their respective channels with only around 20% block of other channels (Zhou et al., 1998a); antibodies such as these might prove useful tools for the identification of Kv3 heteromers.

7.3.2 High-voltage activated currents in the MNTB

In addition to the low-voltage activated current, we examined the high-voltage activated current at the calyx and compared them to those in MNTB neurones. We found that although the Kv3 currents in MNTB neurones and their presynaptic terminals are similar they differ in their activation.

7.3.2.1 Kv3 currents in MNTB neurones

In mouse MNTB neurones, high-voltage activated currents began to activate around -60mV and have a $V_{½}$ of -18mV (Fig, 6.6). Activation of these channels occurs at potentials around 40mV more negative than that of Kv3.1 homomers in expression systems (Coetzee et al., 1999), suggesting that there may be some modifying factor present. However, Macica *et al.* (2001) demonstrated the opposite, that casein kinase 2 (CK2) basally phosphorylates MNTB neurones, shifting activation by ≈+20mV. One possible explanation for the observed differences in native channels and expressed homomers is the presence of several subunits in native channels. Akhtar *et al.* (2002) established that the higher the ratio of Kv1.1 to Kv1.2 subunits in Kv1.1/1.2 channels, the more negative the $V_{½}$, which seems to make sense since Kv1.1 is reported to have a more negative $V_{½}$ than Kv1.2 (Coetzee et al., 1999). However, unlike the Kv1's, none of the other Kv3 homomers are reported to have significantly different $V_{½}$'s to Kv3.1, (Coetzee et al., 1999). So could the addition of other subunits shift the $V_{½}$ of Kv3.1 containing channels? In expression systems, co-expression of Kv3.3 or Kv3.4 with Kv3.1 has been shown to shift activation to more negative potentials (Desai et al., 2003), although the mechanism is unknown. Examination of Kv3 subunits expressed in the MNTB revealed that Kv3.3 is localised to MNTB neurone somata (Fig, 6.4). If Kv3 channels in MNTB neurones are indeed Kv3.1/3.3 heteromers, this might explain why their activation is more negative than that reported for Kv3.1 homomers.

7.3.2.2 Kv3 currents at the calyx

In terminals the high-voltage activated currents activate at even more negative potentials than in the postsynaptic neurones (around 75mV with a V½ of 27mV, Fig, 6.6). Perhaps the term high-voltage activated no longer applies! In addition to Kv3.1 and Kv3.3, Kv3.4 is also expressed at the calyx (Fig, 6.5), suggesting that this additional subunit might shift the $V_{½}$ to even more negative potentials. In fast-spiking globus pallidus neurones the inclusion of Kv3.4 with Kv3.1 and Kv3.2 shifts the $V_{½}$ to negative potentials and enhances repolarisation (Baranauskas et al., 2003), suggesting that the use of subunit composition to modify activation may be of general importance.

7.3.2.3 High-voltage activated currents in Kv3.1 null mice

To examine the contribution of Kv3.1 to the presynaptic high-voltage activated current we recorded from calyces in Kv3.1 null mice (Fig, 6.3). We were surprised to find calyces in Kv3.1 KO's exhibit a high-voltage activated current the properties of which closely resemble those of WT currents. We subsequently examined immunoreactivity of Kv3 subunits in terminals from these mice (data not shown) and detected both Kv3.3 and Kv3.4; this suggests that the current in Kv3.1 null mice is mediated by Kv3.3/3.4 heteromers. Interestingly, deleting Kv3.1 did not result in compensation by other genes but instead the existing subunits filled the vacant positions in the channel.

The fact that functional Kv3.3/3.4 heteromers seem almost indistinguishable from Kv3.1/3.3/3.4 heteromers raises the question of why Kv3.1 is expressed at all. One clue to the answer to this question might come from our investigation of AP firing in Kv3.1 null mice. APs in KO terminals seemed to be of a similar duration to WT but have smaller AHPs (Fig, 6.8), suggesting that Kv3.1 might be important in generating a large AHP. However, since this result was only from one recording further work would be required to determine whether the AHP is reduced in all Kv3.1 null terminals.

7.3.2.4 Modulation of Kv3 channels

Given that Kv3 channels play important roles in AP repolarisation (Rudy et al., 1999), it seems likely that these channels might be dynamically regulated *in vivo*. Kv3 containing channels can be modulated by a number of kinases and phosphatases (Critz et al., 1993; Covarrubias et al., 1994; Kanemasa et al., 1995; Moreno et al., 1995; Macica and Kaczmarek, 2001; Moreno et al., 2001; Rudy and McBain, 2001; Macica et al., 2003). Activation of PKC produces a decrease in Kv3.1b currents in expression systems (Critz et al., 1993; Kanemasa et al., 1995). In MNTB neurones PKC activation is reported to decrease the high-voltage activated current (Macica et al., 2003). However, there seems to be no effect on AP half-width; in contrast, application of 1mM TEA to produce a similar decrease in the Kv3 current, results in significant broadening of the AP (Brew and Forsythe, 1995). An alternative interpretation of the data of Macica *et al.* (2003) is that phosphorylation by PKC increases

inactivation similar to our observations in the presynaptic terminal (Fig, 6.9). Since Macica *et al.* (2003) used An inactivating pre-pulse to -40mV to investigate the effect of PKC activation on the current, changes in inactivation may result in an apparent decrease in current amplitude which is not observed from resting potentials (and hence does not change the AP half width). The authors went on to demonstrate that PKC activation increases firing fidelity by reducing time to AP firing following stimulus onset and hence reducing AP failures. If PKC activation was enhancing cumulative inactivation, one might expect to observe a similar effect during high frequency stimulation. Although PKC activation reduces Kv3.1b currents in CHO cells, it does not affect the current magnitude of Kv3.1/3.3 heteromers (R. Desai, personal communication). Since both Kv3.1 and Kv3.3 are expressed in MNTB, it seems likely that the observed effects of PKC activation may have been due to changes in inactivation rather than a direct reduction in current magnitude.

Activation of PKC has a different effect on Kv3.4 homomers, resulting in elimination of rapid inactivation (Covarrubias et al., 1994). Phosphorylation of residues on the N-terminus of this channel prevents inactivation, converting this A-current to a delayed rectifier. Given that Kv3.4 is a component of high-voltage activated K^+ channels at the calyx (Fig, 6.5), it is surprising that we see no effect of PKC activation on presynaptic Kv3 currents (Fig, 6.9). However, this might be explained by the fact that the presence of Kv3.3 subunits seems to prevent N-type inactivation of the heteromer (observed in Kv3.1 KO animals, Fig, 6.3).

In addition to PKC phosphorylation, Kv3.1 can also be phosphorylated by casein kinase 2 (CK2, Macica and Kaczmarek, 2001). These authors also demonstrate that Kv3.1 currents are constitutively phosphorylated in CHO cells, causing them to activate at potentials around 20mV more positive. This is an interesting observation which might explain why the reported $V_{½}$'s for Kv3 channels in expression systems are more positive than those observed in native neurones. In the same paper, Macica *et al.* (2001) claim that the Kv3 current in MNTB neurones is constitutively phosphorylated by CK2, shifting activation to more positive potentials. However, caution should be exercised with these data since they were obtained using a pre-pulse to -40mV which, in addition to inactivating the Kv1 current, also inactivates part of the high-voltage activated current (Fig, 5.2). Like presynaptic Kv3 currents (Fig, 6.10),

dephosphorylating MNTB Kv3 channels with alkaline phosphatase shifts inactivation in the negative direction; this means that during the -40mV pre-pulse, even more of the Kv3 current is inactivated. An alternative explanation for the effect of dephosphorylation on MNTB Kv3 currents is an increase in the rate of recovery from inactivation; if this were the case, the current increase observed at negative potentials (Macica and Kaczmarek, 2001) may represent recovery of Kv3 channels from pre-pulse induced inactivation. A simple experiment to investigate this would be to use DTX-I to block the Kv1 currents and then apply a -100mV pre-pulse protocol in control and alkaline phosphatase. This would overcome the known problems with the -40mV pre-pulse protocol and demonstrate whether the effect of dephosphorylation was due to a change in inactivation.

7.3.2.5 Modulation of the presynaptic high-voltage activated current

Since Kv3.1 and Kv3.4 homomers can be modulated *in vitro* (Covarrubias et al., 1994; Macica and Kaczmarek, 2001; Macica et al., 2003), we investigated whether phosphorylation of Kv3 channels occurs at the calyx. Neither activating PKC nor dephosphorylation had any effect on activation of presynaptic Kv3 currents (Fig, 6.9, 6.10). Despite the fact that dephosphorylation with alkaline phosphatase shifted inactivation to more negative potentials (Fig, 6.9, 6.10), there was no effect on AP firing (Fig, 6.11).

Since PKC modulation affects neurotransmitter release at the calyx by a mechanism not involving Kv3 channels (Saitoh et al., 2001), the channels may be resistant to phosphorylation. Interestingly, whilst some heteromeric Kv3 channels can be phosphorylated, others cannot (R. Desai, personal communication), raising the possibility that Kv3.1/3.3/3.4 heteromers may be resistant to modulation. So why would resistance to phosphorylation be advantageous? PKC induced potentiation of transmitter release occurs via phosphorylation of release machinery at the calyx, independent of K^+ channels (Hori et al., 1999). If PKC also reduced presynaptic Kv3 currents (and therefore broadened presynaptic APs), the combined effects would lead to rapid vesicle depletion. By having phosphorylation resistant Kv3 channels it makes it easier to fine-tune levels of transmitter release.

7.4 Role of Kv1 currents

7.4.1 Function of Kv1 currents in MNTB neurones

7.4.1.1 Unitary action potential firing

Low-voltage activated K^+ currents in MNTB neurones play important roles in regulating AP firing. In response to small current injections, Kv1 conductances open resulting in hyperpolarisation of the membrane, which prevents the generation of an AP (Fig, 3.5); this effect is observed as a "hump" during sub-threshold current injections (Fig, 3.5). Kv1 conductances therefore ensure that MNTB neurones only fire APs in response to large EPSPs.

In response to supra-threshold current injections, MNTB neurones typically fire a single AP (Fig, 3.5; Wu and Kelly, 1991; Banks and Smith, 1992; Forsythe and Barnes-Davies, 1993a; Brew and Forsythe, 1995). *In vivo* the sustained depolarisation arises from the slow, NMDA receptor mediated component of the EPSP (Forsythe and Barnes-Davies, 1993b). Depolarisation opens the Kv1 channels, which then act to oppose the depolarisation, keeping the membrane potential below threshold and thus preventing subsequent APs. Blockade of the low-voltage activated conductance by DTX-I or 4-AP, results in multiple APs in response to sustained depolarisation (Fig, 4.11; Banks and Smith, 1992; Forsythe and Barnes-Davies, 1993a) or synaptic stimulation (Brew and Forsythe, 1995). Since MNTB neurones are involved in the transmission of information necessary for sound localisation (Carr and Soares, 2002), it is critical that they preserve the fidelity of this information. Changes in the timing or frequency of APs will affect the determination of sound location by the LSO and MSO. MNTB low-voltage activated conductances therefore serve to ensure that each AP in the bushy cell generates a single precisely timed AP in the corresponding MNTB neurone. This one-to-one firing in the calyx and MNTB neurone has been observed in extracellular *in vivo* recordings in response to axon stimulation and sound (Guinan and Li, 1990).

Many auditory and non-auditory neurones which contain low-voltage activated K^+ conductances also fire single APs (Dubois, 1981; Stansfeld et al., 1986; Poulter et al., 1989; Manis and Marx, 1991; Banks and Smith, 1992; Wang and McKinnon, 1995; Gamkrelidze et al., 1998; Rathouz and Trussell, 1998; Bal and Oertel, 2001; Mo et al., 2002; Svirskis et al.,

2002). In these neurones the low-voltage activated currents do not contribute to AP repolarisation (except in octopus cells, Bal and Oertel, 2001), but instead prevent multiple firing. The prevalence of unitary firing suggests that low-voltage activated K^+ conductances play important roles in the reliable transmission of information throughout the brain.

It is amazing that even though the low-voltage activated K^+ currents in MNTB neurones are so small they are able to prevent multiple firing in response to large current injections. We have demonstrated that Kv1.1/1.2 heteromers, which account for only half of the low-voltage activated current, are able to prevent multiple AP firing (Fig, 4.12). We also demonstrated that this was not simply an effect of blocking half of the current, but rather a specific effect of Kv1.1/1.2 heteromers (Fig, 4.14). How are such small conductances able to prevent repetitive firing? We suggest that the location of Kv1.1/1.2 heteromers at the axon initial segment is critical to their function in preventing multiple AP firing. The axon initial segment is thought to be the site of AP generation in many neurones (Stuart and Sakmann, 1994; Hausser et al., 1995); although APs can also be generated at other sites, particularly in neurones with large dendritic trees (Luscher and Larkum, 1998; Martina et al., 2000). Localisation of Kv1.1/1.2 heteromers to this site will afford them greatest control over the membrane potential at this spike initiation region.

7.4.1.2 Multiple firing in mouse MNTB neurones

Whilst only single APs are fired in response to sustained depolarisation in rat MNTB neurones (Fig, 3.5; Banks and Smith, 1992), in the mouse two or more APs are occasionally observed (Wu and Kelly, 1991; Brew et al., 2003). In our limited study of mouse MNTB neurones we found that the low threshold currents differed from those in rat, consisting of a heteromer containing Kv1.1, Kv1.2 and maybe Kv1.6 subunits (Fig, 4.10) and an A-current (Fig, 4.9D). It is possible that the reduced ability to prevent repetitive firing is a result of these differences; however, since the heteromeric channel is located at the axon initial segment (Brew et al., 2003), this explanation seems unlikely. An alternative explanation is that the apparent ability to fire more than one AP is an artefact generated by the patch clamp amplifier. The current-clamp mode of many patch clamp amplifiers can result in errors and in some cases current being injected back into the cell (discussed in methods section 2.2.6.1). It is possible

that subsequent APs were fired in response to current injected as the amplifier attempted to follow the voltage. This hypothesis is supported by the fact that we never observed more that one AP in recordings from mouse MNTB neurones using the true current-clamp mode of an Optopatch amplifier (n=4 Fig, 6.7).

7.4.1.3 Reducing membrane time-constant

Low-voltage activated currents act in concert with I_H to reduce the membrane time constant and input resistance (Trussell, 1999). In MNTB neurones a short membrane time constant, in conjunction with rapidly desensitising AMPA receptors, aids high frequency synaptic fidelity by causing rapid decay of the EPSP (Brew and Forsythe, 1995); rapid EPSPs produced by a short membrane time constant will also prevent delayed summation of inputs, instead acting more like a coincidence detector, so only coincident inputs summate (Rothman and Manis, 2003). Whilst this is unlikely to be important for calyceal EPSPs, it maybe important in relation to the non-calyceal inputs, which are smaller and have a greater jitter; MNTB neurones receive both excitatory and inhibitory non-calyceal inputs (Banks and Smith, 1992; Forsythe and Barnes-Davies, 1993b; Hamann et al., 2003), suggesting that in addition to one-to-one transmission, other signal processing occurs in MNTB neurones (Guinan and Li, 1990; Kopp-Scheinpflug et al., 2003). Non-calyceal inputs are presumed to occur on the soma and proximal dendrites (Smith et al., 1991), the same location as Kv1.1/1.6 heteromers. It is conceivable that these heteromeric channels serve to regulate the impact of these inputs so that only large or coincident inputs result in an AP. It has also been proposed that rapid EPSPs are important in discriminating sound evoked responses from spontaneous activity of the auditory nerve (Svirskis et al., 2002).

Another consequence of a short membrane time constant is that the AHP is brief (Fig, 6.7). Rothman and Manis (2003) have used their bushy cell model to demonstrate that decreasing the membrane time-constant by the addition of I_H and Kv1 currents reduces the refractory period. Having a short refractory period also helped the model neurone to follow high frequency inputs (Rothman and Manis, 2003), which might be important both in the terminal and the MNTB neurone in ensuring faithful AP firing during high frequency trains.

7.4.2 Function of Kv1 currents in presynaptic terminals

We have demonstrated that, like postsynaptic Kv1.1/1.2 channels, presynaptic Kv1.2 homomers are important in ensuring unitary firing at the calyx (Fig, 5.11). Unlike the postsynaptic cell, which experiences sustained depolarisation during an EPSP (Forsythe and Barnes-Davies, 1993b), the calyx only experiences brief depolarisation from propagating APs. However, as APs propagate down the axon, charge builds up and then discharges following the AP (Barrett and Barrett, 1982), generating a depolarising after-potential (DAP, Fig, 5.10). Kv1.2 homomers prevent aberrant APs being fired during the DAP (Fig, 5.11).

7.4.2.1 Prevention of aberrant firing during the depolarising after-potential

DAPs were first described during intracellular recordings from lizard motor axons (Barrett and Barrett, 1982). In this paper, Barrett and Barrett showed that the DAP was not due to active conductances but instead due to passive membrane properties. Like the calyceal DAP, the motor axon DAP disappears at potentials more positive than -60mV and does not reverse (Fig, 5.10; Barrett and Barrett, 1982). The DAP was not influenced by changes in external Ca^{2+}, Cl^-, K^+ or Na^+; suggesting that it is not mediated by conductances specific for these ions. In addition, cooling did not affect the DAP, suggesting that the Na^+ pump is not involved. However, the similarity of the DAP to the passive response of the axon to current injection led the authors to conclude that the DAP is due to capacitive discharge of internodal capacitance beneath or through the myelin sheath (Barrett and Barrett, 1982). Borst *et al.* (1995) first described the DAP at the calyx, demonstrating that it was not dependent on intracellular Ca^{2+} or transmitter release. DAPs recorded at the calyx had similar duration (and amplitude) to those in rat motor axons (15ms and 11ms respectively, David et al., 1995; Dodson et al., 2003); although DAPs in lizard motor axons have a longer duration (35ms, Barrett and Barrett, 1982). In addition, the decay of calyceal DAPs is also very similar to the passive membrane properties of the calyx (Borst et al., 1995). These data suggest that DAPs at the calyx are generated by passive current discharge during AP propagation.

The depolarisation generated by the DAP increases axonal excitability, causing a hyperexcitable period in myelinated and unmyelinated axons following AP firing (Grundfest

and Gasser, 1938; Gardner-Medwin, 1972; Dudel, 1973; Zucker, 1974; Waxman and Swadlow, 1976; Raymond, 1979). This hyperexcitability may be important for conduction through axonal branch points or unmyelinated terminals during high frequency firing (Raymond, 1979). Application of 4-AP or TsTX-Kα results in an increase in DAP amplitude (Fig, 5.12; David et al., 1995), suggesting that Kv1 channels serve to reduce the amplitude of the DAP below threshold for AP generation. Kv1 channels may therefore act to preserve AP fidelity in axons throughout the nervous system.

Hyperexcitability during the DAP resulted in aberrant firing at the calyx during trains of stimuli (Fig, 5.13). At high frequencies, only a single aberrant AP was observed in a train (Fig, 5.13A2); nevertheless, in the auditory pathway such aberrant firing would clearly disrupt spike timing which is important for ITD and ILD sensitivity (Trussell, 1999). In most neurones, firing frequency is relatively modest compared to the calyx (Llinas et al., 1998; Stevens and Zador, 1998; Magee, 2003). At these lower frequencies aberrant firing was observed following the majority of APs (Fig, 5.13B2 & C), suggesting that Kv1 channels may play important roles in many neurones in preserving the integrity of information encoded as AP trains.

7.4.2.2 Other roles of presynaptic Kv1 channels

We have shown that Kv1 channels located at the transition zone between the bushy cell axon and the calyx (Fig, 5.5) prevent hyperexcitability (Fig, 5.11); Kv1 channels localised at transition zones at the neuromuscular junction play a similar role (Zhou et al., 1998b). Deletion of Kv1.1 or application of 4-AP results in repetitive activity near the neuromuscular junction following nerves stimulation (Kocsis et al., 1982; Vabnick et al., 1999; Zhou et al., 1999). This suggests that Kv1 channels raise the firing threshold to minimize the risk of back-firing following an AP. It has also been proposed that Kv1 channels prevent aberrant firing in response to depolarization from presynaptic ACh receptors (Zhou et al., 1998b). It is possible that Kv1 channels may play a similar role in response to depolarisation from presynaptic glycine receptors at the calyx (Turecek and Trussell, 2001) and in suppressing the dorsal root reflex following primary afferent depolarisation in 1a primary afferents in the spinal cord (Willis, 1999).

In the cerebellum, Kv1.1 and Kv1.2 are highly concentrated in basket cell terminals, localised to septate-like junctions preceding the terminal (Wang et al., 1994; Rhodes et al., 1997). Block of the presynaptic Kv1 channels or deletion of Kv1.1 increases both the frequency and amplitude of spontaneous IPSCs recorded from Purkinje cells (Southan and Robertson, 1998b; Zhang et al., 1999). It is thought that Kv1 channels located at branch points or axonal swellings result in conduction failure of a proportion of spontaneous APs; hence, removal of Kv1 conductances increases the number of APs that reach the terminal (Zhang et al., 1999). An alternative hypothesis is that Kv1 channels are playing a similar role to that at the calyx and neuromuscular junction; preventing aberrant firing during DAPs in these unmyelinated axons. Blockade of Kv1 channels would result in aberrant firing during the DAP, accounting for the doubling in IPSCs recorded from in Purkinje cells (Southan and Robertson, 1998b; Zhang et al., 1999). In either case it is clear that Kv1 channels are involved in AP conduction in myelinated and unmyelinated axons in the central and peripheral nervous system.

7.4.2.3 Role of Kv1 currents at nodes

The localisation of Kv1 channels to the juxtaparanodal regions has long been established (Fig, 7.1). Chui and Ritchie (1981) first described K^+ channels located under the myelin adjacent to nodes of Ranvier and since then the properties (Kocsis et al., 1982; Jonas et al., 1989; Roper and Schwarz, 1989; Brau et al., 1990; Corrette et al., 1991; Reid et al., 1999; Devaux et al., 2002) and subunit composition (Wang et al., 1993; Rhodes et al., 1997; Rasband et al., 1998; Rasband et al., 1999; Rasband and Trimmer, 2001; Scherer and Arroyo, 2002) of these channels have been extensively studied. Until recently it was thought that juxtaparanodal channels were Kv1.1/1.2 heteromers that also contain Kvβ2 (Rasband and Shrager, 2000). However identification of Kv1.6 in some nodes (Rasband et al., 1999) and the presence of channels sensitive to DTX-I but insensitive to kaliotoxin (which blocks Kv1.1, Kv1.3 and BK channels, Devaux et al., 2002), imply that other Kv1 channels may also be present in CNS axons.

Although juxtaparanodal channels have been extensively investigated, little is known about their role. The most widely accepted hypothesis is that juxtaparanodal channels both serve to

set the internodal resting potential (Chiu and Ritchie, 1984) and to prevent repetitive activation of nodal sodium channels (Chiu and Ritchie, 1981). Consistent with this idea, application of 4-AP to CNS axons (which is thought to be able to penetrate under the myelin) generated repetitive firing (Gordon et al., 1988). In the PNS, 4-AP can also induce repetitive firing (Kocsis et al., 1983), particularly at low temperatures, although this effect disappeared at around P60 (Vabnick et al., 1999). This effect led Vabnick *et al.* (1999) to conclude that K^+ channels only play a role in preventing repetitive firing during development, before they are sequestered to the juxtaparanodes. However, in the CNS there is no redistribution of Kv1 channels during development, they are immediately expressed at the juxtaparanodes (Rasband et al., 1999). If juxtaparanodal Kv1 channels do not play a role in development, what is their function in the CNS?

In our experiments, application of DTX-K had no effect on AP firing in medium length axons which are presumed to contain several nodes (Fig, 5.8), suggesting that nodal Kv1.1 containing channels may not have a role in preventing repetitive firing; however, it is possible that DTX is unable to reach channels below the myelin (Vabnick et al., 1999; Devaux et al., 2002). Inaccessibility to the channels may explain why 4-AP-induced repetitive firing disappeared in mature axons as axoglial junctions tighten (Vabnick et al., 1999). Therefore, the idea that juxtaparanodal channels improve conduction by setting the internodal resting potential and preventing re-excitation of sodium channels still seems the most plausible. It is likely that Kv1.1/1.2 double knockout mice might provide further clues to the role that juxtaparanodal channels play in AP propagation.

7.4.2.4 Action potential firing and axon length

It had previously been demonstrated that multiple APs were fired at the calyx in response to sustained depolarization, which was surprising given that low-voltage activated K^+ conductances were present (Forsythe, 1994). During our investigation of presynaptic K^+ channels we found that firing was dependent upon the length of uncut axon; short-axon terminals fired a single AP whereas long-axon terminals fired multiple APs (Fig, 5.7). It is important to remember that the long depolarisations applied at the terminal membrane are unphysiological; the normal stimulus is a brief propagating AP (Fig, 5.10). However, despite

its unphysiological nature, the mechanism behind the multiple firing in long-axon terminals is intriguing.

Figure 7.2 explains our hypothesis of the mechanism underlying the observed differences in AP firing. In short-axon terminals a single AP is generated at the transition zone in response to sustained depolarisation (Fig, 7.2A); the transition zone Kv1.2 homomers prevent subsequent APs being generated during the sustained current injection. In terminals with medium length axons a single AP is still generated at the transition zone, but at the node a few APs are fired (Fig, 7.2B); therefore, several APs are recorded at the calyx. Multiple firing at the node occurs because the juxtaparanodal Kv1 channels are unable to prevent re-excitation of the sodium channels during such a long depolarisation. The reason APs are not fired throughout the train is probably because the transition zone Kv1.2 homomers still exert some influence due to the short internodal distance as the axon approaches the terminal (Chiu et al., 1999). In long-axon terminals the penultimate node is too far away from the influence of the transition zone Kv1.2 homomers, so multiple firing occurs (Fig, 7.2C).

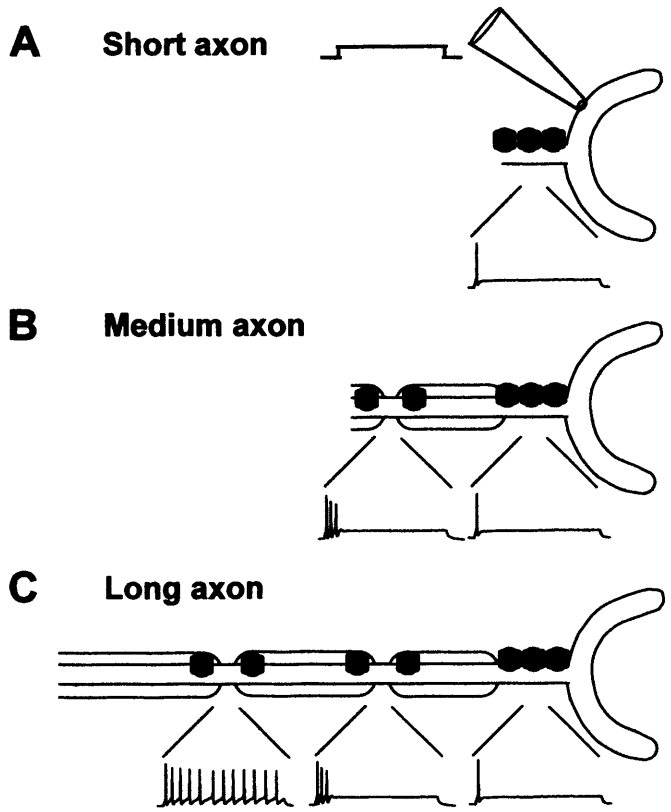

Figure 7.2. Proposed mechanism for AP firing in different length axons.
A. In a short-axon terminal a single AP is recorded in response to a sustained current pulse injected at the calyx. Kv1.2 homomers (●) which preserve the single AP are located at the transition zone along with Kv1.1/1.2 heteromers (●). **B.** In medium axons, a single AP is triggered at the transition zone but several APs are also triggered at the first node, since the influence of the Kv1.2 homomers is not as strong here. At the calyx, several APs will be recorded. **C.** In long axons multiple APs will be triggered at distant nodes outside the influence of the Kv1.2 homomers, resulting in multiple APs recorded at the calyx. The traces below each diagram represent our proposal for AP firing at each node in response to current injected at the calyx.

7.5 Role of Kv3 currents

7.5.1 Role of Kv3 subunits in presynaptic action potential repolarisation

We have demonstrated that Kv3.1, Kv3.3 and Kv3.4 are localised to presynaptic terminals in the MNTB (Fig, 6.5). Application of 3mM TEA results in AP broadening (Fig, 6.8), suggesting that Kv3 channels are important in repolarising the presynaptic AP.

7.5.1.1 Kv3.1 subunits

Consistent with a role in AP repolarisation, Kv3.1 channels only activate on the falling phase of the AP (Rudy et al., 1999). If Kv3.1 homomers are capable of repolarising the AP, what are the other subunits doing? Although Kv3.1 has been assumed to be responsible for repolarising the AP in many neurones (Wang et al., 1998b; Rudy et al., 1999), repolarisation was unaffected by Kv3.1 deletion at the calyx (Fig, 6.8B1) and in neurones of the reticular thalamic nucleus (RTN) (Porcello et al., 2002). Since both RTN neurones and the calyx also contain Kv3.3 subunits (Fig, 6.5C; Porcello et al., 2002), it is likely that Kv3.3 homomers are able to repolarise the AP on their own. Why then is Kv3.1 associated with Kv3.3 in both locations; what is the role of Kv3.1? One clue might come from the reduction in the AHP observed in both cases (Fig, 6.8B1; Porcello et al., 2002). Fast AHPs are found in many fast-spiking neurones and are thought to be important in aiding both recovery of sodium channels from inactivation and Kv3 deactivation (Wang et al., 1998b; Baranauskas et al., 1999; Erisir et al., 1999; Rudy and McBain, 2001). This has the effect of rapidly resetting the resting condition without increasing the refractory period (Rudy and McBain, 2001; Lien and Jonas, 2003). It is possible that inclusion of Kv3.1 subunits in the channels is necessary to increase the AHP and thus facilitate high frequency firing.

7.5.1.2 Kv3.3 subunits

Aside from aiding repolarisation, the role of Kv3.3 subunits in presynaptic high-voltage activated channels is less clear. Since Kv3.1/3.4 heteromers exhibit pronounced inactivation (Baranauskas et al., 2003; Desai et al., 2003), inclusion of Kv3.3 might convert the channels to the delayed rectifier phenotype (Fig, 6.1) and hence prevent frequency dependent AP broadening.

7.5.1.3 Kv3.4 subunits

Kv3 channels in MNTB neurones are identical to those at the calyx except in their lack of Kv3.4 subunits (Fig, 6.5). By comparing pre- and postsynaptic APs we can therefore examine the role of Kv3.4 in regulating firing. Presynaptic APs are much narrower than those in the MNTB neurone and have a significantly larger AHP (Fig, 6.7). This suggests that Kv3.4 may

not only further increase the AHP; aiding high frequency firing, but also reduce the duration of the AP and thus limit transmitter release. Why does inclusion of Kv3.4 have this effect? It is likely that the presence of Kv3.4 results in activation of presynaptic channels at more negative potentials (discussed in section 7.3.2.2). A similar effect of Kv3.4 is thought to be responsible for decreasing the AP duration in globus pallidus neurones (Baranauskas et al., 2003). The role of Kv3.4 in generating a fast spiking phenotype might explain the limited expression of this subunit in the brain (Rudy and McBain, 2001).

7.5.2 Brevity of presynaptic action potentials

Presynaptic APs elicited by current injection were only half the width of MNTB neurone APs (Fig, 6.7), which are themselves considered to be rapid (Wang et al., 1998b). Why is the presynaptic AP so brief and why does it need to be faster than its postsynaptic counterpart? A short duration AP will result in less calcium entry and less transmitter release (Wang and Kaczmarek, 1998); it is likely that the AP is brief in order to minimise vesicle depletion and therefore synaptic depression (Scheuss et al., 2002). The brevity of the presynaptic AP is therefore, not to enable the calyx to fire at higher frequencies than MNTB neurones, but rather to preserve transmission fidelity.

7.5.3 Prevention of aberrant firing

Since presynaptic Kv3 currents activate at much more negative potentials than those in MNTB neurones (at around -70mV, Fig, 6.6), some Kv3 channels are likely to be activated during the DAP (or during sustained current injections). Consequently these channels may act with the Kv1 conductances to help prevent aberrant firing. Obviously Kv3 channels cannot prevent aberrant firing in isolation, otherwise it would not be observed in TsTX-Kα (Fig, 5.11). However, their influence might explain why Kv1.1/1.2 heteromer block by DTX-K did not generate multiple firing (Fig, 5.8). Although this seems a nice hypothesis, application of 3mM TEA had no effect on DAP amplitude, suggesting that whilst Kv3 channels might still reduce excitability during current injections (and therefore contribute to a lack of effect of DTX-K), they are unlikely to contribute to the prevention of aberrant firing during the DAP.

7.6 Further experiments

We have investigated the subunit composition and function of channels underlying the Kv1 currents in MNTB neurones and Kv1 and Kv3 currents at the calyx. However, time-constraints have meant that we have tended to follow the questions that interested us most; consequently there are many questions that remain unresolved and areas that could be explored in continuation of this project.

7.6.1 Further examination of low-voltage activated currents in the MNTB

7.6.1.1 Properties of Kv1 currents

Whilst we have been able to investigate the properties of native homo- and heteromeric channels, there are a number of questions that remain unanswered such as: What is the stiochiometry of heteromeric channels and what is the role of Kvβ subunits? It may be possible to resolve some of these questions by examining Kv1 channels expressed in heterologous systems. By injecting the appropriate Kvα subunits or by constructing concatamers one could examine the properties of channels with different stoichiometries. By comparing their properties with native channels it may be possible to determine the likely stoichiometry of Kv1.1/1.2 and Kv1.1/1.6 heteromers in MNTB neurones (see section 7.2.2.2). It would also be interesting to investigate the effects of co-expressing different Kvβ subunits with these channels to examine effects on kinetics and expression.

7.6.1.2 Role of different heteromeric channels

We have established the importance of Kv1.1/1.2 heteromers in preserving unitary firing in MNTB neurones but we still know little about the role of Kv1.1/1.6 heteromers. One experiment that might provide further clues is to use a recorded EPSP waveform as the voltage command when recording from voltage clamped MNTB neurones. One could then investigate activation of the low-voltage activated currents as a whole, or specifically Kv1.1/1.6 heteromers (by applying TsTX-Kα). A similar approach would be the use of dynamic clamp (e.g. Lien and Jonas, 2003); Kv1 currents could be blocked by DTX-I, then previously recorded currents from the different heteromers could be 'added in' with the dynamic clamp.

This might also be a way of removing Kv1.1/1.6 heteromers (which cannot be blocked separately from Kv1.1/1.2 by available toxins). A third way to further investigate the roles of heteromeric Kv1 channels in the MNTB would be to create a cable model of an MNTB neurone using the properties of the different channels. If this model were particularly sophisticated, one might also be able to investigate the effects of differential localisation of channels. The model could also be extended to examine the role of Kv1.1/1.2 heteromers in presynaptic transition zones and nodes of Ranvier.

7.6.1.3 Role of Kv1 channels in axonal propagation

Our investigation into presynaptic Kv1 channels demonstrated that they are involved in preventing aberrant AP firing; however, the role of Kv1.1/1.2 heteromers, juxtaparanodal channels and nodal Kv3.1 channels still remains unresolved. One way to investigate this might be through the use of transgenic animals. First, it would be interesting to investigate presynaptic Kv1 channels in a Kv1.2 null mouse. Aside from the expectation that these animals would have hyperexcitable calyces, one could examine whether Kv1.1 homomers would be expressed presynaptically or whether another subunit would be up-regulated. Similarly, examination of channels in Kv1.1/1.2 double knockout mice (or even Kv1.1/1.2/1.6 triple knockouts) might enable examination of the roles of Kv1 channels at juxtaparanodal regions. It may be possible to investigate the latter without using transgenic animals by focally applying toxins (or TEA to block nodal Kv3 channels) to the trapezoid fibres. Whilst there may be problems with this technique such as length of uncut axon, blocking channels below the myelin sheath and ensuring block of nodal channels without affecting those at the transition zone, it might provide a novel way to examine the role of Kv channels in axonal propagation.

7.6.1.4 The role of Kv1 channels in transmitter release from MNTB neurones

Since Kv1 channels are highly expressed in MNTB neurones, it might be interesting to examine their effect on neurotransmitter release. MNTB neurones send glycinergic projections to the LSO and MSO (Banks and Smith, 1992); examination of the effects of blocking Kv1 channels on IPSCs in MSO and LSO neurones could provide information about

channels in the MNTB neurone terminals. A potential problem would be separating the effects of blocking initial segment versus terminal channels, although focal application of toxins to the terminals might overcome this.

7.6.1.5 The effect on sound source localisation of increasing excitability in the MNTB

In this study we demonstrated a role of Kv1 channels in regulating both the excitability of the presynaptic terminal and postsynaptic cell; but what effect would this increased excitability have on sound source localisation? One way to investigate this would be to perform *in vivo* experiments on animals trained to perform sound localisation tasks (e.g. Parsons et al., 1999). The effect of increasing excitability could be investigated by injection of DTX-I into the MNTB of anaesthetised animals before they performed the task. It might also be possible to dissect out pre and postsynaptic effects by using DTX-K which would not affect presynaptic excitability.

7.6.1.6 Subcellular channel localisation

In this study we employed immunohistochemical techniques to examine the subcellular localisation of Kv1 channels. Whilst this method provided useful information about Kv1 expression and localization, it was limited because the Kv1 antibodies are raised to intracellular regions of the channel. As a result the antibody does not just label channels at the membrane, but also those in the process of being trafficked and those restricted to the ER. The limited number of extracellular residues in potassium channels means that external Kv1 antibodies (Tiffany et al., 2000) are not very good for use in slices (M. Barker unpublished data) because they have a high level of non specific binding. An alternative approach is to either fluorescently label toxins or to raise antibodies against the toxin. Since the toxins bind from outside the channel, one could use this method to examine the localisation of functional channels. Labelling of an area by DTX-K but not TsTX-Kα would demonstrate Kv1.1/1.6 heteromer localisation in MNTB neurones. It might also be interesting to use this approach to investigate changes in membrane inserted Kv1 channels during development.

7.6.2 Further examination of the high-voltage activated current

7.6.2.1 Properties of Kv3 channels

In this study we examined Kv3 channels present at the calyx. Although we found that several Kv3 subunits are localised to the terminal, we were unable to examine their subunit composition owing to the lack of subunit-specific pharmacological agents. One approach which could be used to examine the subunit composition would be to use antibodies to block the channels. Antibodies raised to pore regions of Kv3 channels have been used to block currents in expression systems (Zhou et al., 1998a), although it remains to be seen whether this approach could be used in a slice preparation. However, even if these antibodies could be used in slices, there might still be concerns over selectivity and ability to completely block the channel. One toxin which does exhibit some specificity for Kv3.4 subunits is blood depressing substance (BDS-I and BDS-II, Diochot et al., 1998). We did not try this toxin because it partly blocks Kv3.1 currents (Diochot et al., 1998) and seems to change the kinetics of Kv3.1/3.2/3.4 channels (Baranauskas et al., 2003). However, despite these problems it might be worth trying this toxin, since complete block would indicate that all channels contain Kv3.4.

7.6.2.2 Roles of different Kv3 subunits

We examined Kv3 currents in Kv3.1 null mice to explore the effect removing this subunit would have on the presynaptic high-voltage activated current. We found that the presence of other subunits in the channel compensated for the absence of Kv3.1 and therefore we did not investigate the Kv3.1 KO currents in great detail. Further examination of the presynaptic Kv3 currents in Kv3.1 null mice might cast more light on the effects removing Kv3.1 have on the AHP and allow comparison with Kv3.3/3.4 heteromers in expression systems. To extend this study one may also want to examine EPSCs in a Kv3.1 KO mouse to see if removing Kv3.1 has any effect on transmitter release.

To further probe the effect of removing subunits one could examine the currents in Kv3.1/3.3 double knockouts or Kv3.1/3.3/3.4 triple knockouts. A similar approach would be to use siRNA (Shi, 2003) to knockdown Kv3 channels; however, difficulties in maintaining slices in

culture, the time required for localisation along the bushy cell axon to the calyx and incomplete knock-down of the channels may make this approach unfavourable.

7.6.3 The effect of Kv channel modulation

7.6.3.1 Modulation of Kv3 current

While phosphorylation reportedly affects the postsynaptic Kv3 currents (Macica and Kaczmarek, 2001; Macica et al., 2003), we found no effect of phosphorylation or dephosphorylation on presynaptic Kv3 currents; it might be worthwhile considering these differences in more detail. Initially one would want to repeat the experiments of Macica *et al.* using a pre-pulse to -100mV in the presence of DTX-I to ascertain whether the effects they observed in MNTB neurones were due to changes in channel inactivation. It would also be interesting to see whether the Kv3 currents can be modulated by other second messengers. For instance, Moreno *et al.* (2001) recently showed that Kv3.1 and Kv3.2 currents were suppressed by nitric oxide or cyclic-GMP via activation of a phosphatase. Another question that has not been answered is whether activity dependent phosphorylation of Kv channels occurs in the MNTB. This could be addressed by applying phosphospecific antibodies to control and stimulated slices.

7.6.3.2 Modulation of Kv1 currents

Although dynamic regulation of Kv1 currents in the MNTB seems counter intuitive given their role in preventing hyperexcitability, the properties of the channels may be set by basal phosphorylation. In addition, the potential for differential modulation may explain why MNTB neurones express Kv1.1/1.2 and Kv1.1/1.6 heteromers. It would be relatively easy to examine the effects of Kv1 modulation by inducing phosphorylation or dephosphorylation of the channel.

7.7 Conclusion

We conclude that Kv1.1/1.2 heteromers in MNTB neurones and Kv1.2 homomers in the presynaptic terminal maintain AP firing fidelity by ensuring that only a single AP is generated for each bushy cell AP. This role is important in preserving the integrity of precisely-timed auditory information used by the MSO and LSO to determine the origin of a sound. Presynaptic Kv3 channels have an alternative role in repolarising the presynaptic AP. Inclusion of Kv3.1, Kv3.3 and Kv3.4 subunits confers negative activation to these channels enabling them to rapidly repolarise the presynaptic AP, minimizing the depletion of synaptic vesicles. This property facilitates sustained high frequency firing important for sound source localisation. Voltage-gated K^+ channels therefore play important roles in preserving the accuracy of the information transmitted across this central synapse.

References

Abriel H, Motoike H, Kass RS (2000) KChAP: a novel chaperone for specific K+ channels key to repolarization of the cardiac action potential. Focus on "KChAP as a chaperone for specific K+ channels". Am J Physiol Cell Physiol 278:C863-864.

Accili EA, Kuryshev YA, Wible BA, Brown AM (1998) Separable effects of human Kvbeta1.2 N- and C-termini on inactivation and expression of human Kv1.4. J Physiol (Lond) 512:325-336.

Accili EA, Kiehn J, Yang Q, Wang Z, Brown AM, Wible BA (1997) Separable Kvbeta Subunit Domains Alter Expression and Gating of Potassium Channels. J Biol Chem 272:25824-25831.

Adam TJ, Schwarz DW, Finlayson PG (1999) Firing properties of chopper and delay neurons in the lateral superior olive of the rat. Exp Brain Res 124:489-502.

Adamson CL, Reid MA, Davis RL (2002) Opposite actions of brain-derived neurotrophic factor and neurotrophin-3 on firing features and ion channel composition of murine spiral ganglion neurons. J Neurosci 22:1385-1396.

Adelman JP, Bond CT, Pessia M, Maylie J (1995) Episodic ataxia results from voltage-dependent potassium channels with altered functions. Neuron 15:1449-1454.

Aidley DJ, Stanfield PR (1996) Ion Channels - Molecules in action. Cambridge: Cambridge University Press.

Akhtar S, Shamotienko O, Papakosta M, Ali F, Dolly JO (2002) Characteristics of brain Kv1 channels tailored to mimic native counterparts by tandem linkage of alpha subunits: implications for K+ channelopathies. J Biol Chem 277:16376-16382.

Anderson AJ, Harvey AL (1988) Effects of the potassium channel blocking dendrotoxins on acetylcholine release and motor nerve terminal activity. Br J Pharmacol 93:215-221.

Ashcroft FM (2000) Chapter 6 Voltage-Gated K+ channels. San Diego CA: Academic Press.

Augustine GJ (1990) Regulation of Transmitter Release at the Squid Giant Synapse by Presynaptic Delayed Rectifier Potassium Current. J Physiol 431:343-364.

Baba H, Akita H, Ishibashi T, Inoue Y, Nakahira K, Ikenaka K (1999) Completion of myelin compaction, but not the attachment of oligodendroglial processes triggers K(+) channel clustering. J Neurosci Res 58:752-764.

Babila T, Moscucci A, Wang H, Weaver FE, Koren G (1994) Assembly of mammalian voltage-gated potassium channels: evidence for an important role of the first transmembrane segment. Neuron 12:615-626.

Bahring R, Milligan CJ, Vardanyan V, Engeland B, Young BA, Dannenberg J, Waldschutz R, Edwards JP, Wray D, Pongs O (2001) Coupling of voltage-dependent potassium channel inactivation and oxidoreductase active site of Kvbeta subunits. J Biol Chem 276:22923-22929.

Bal R, Oertel D (2000) Hyperpolarization-activated, mixed-cation current (I(h)) in octopus cells of the mammalian cochlear nucleus. J Neurophysiol 84:806-817.

Bal R, Oertel D (2001) Potassium Currents in Octopus Cells of the Mammalian Cochlear Nucleus. J Neurophysiol 86:2299-2311.

Bal T, McCormick DA (1997) Synchronized oscillations in the inferior olive are controlled by the hyperpolarization-activated cation current I(h). J Neurophysiol 77:3145-3156.

Banks MI, Smith PH (1992) Intracellular recordings from neurobiotin-labeled cells in brain slices of the rat medial nucleus of the trapezoid body. J Neurosci 12:2819-2837.

Baranauskas G, Tkatch T, Surmeier DJ (1999) Delayed rectifier currents in rat globus pallidus neurons are attributable to Kv2.1 and Kv3.1/3.2 K(+) channels. J Neurosci 19:6394-6404.

Baranauskas G, Tkatch T, Nagata K, Yeh JZ, Surmeier DJ (2003) Kv3.4 subunits enhance the repolarizing efficiency of Kv3.1 channels in fast-spiking neurons. Nat Neurosci 6:258-266.

Barnes-Davies M, Forsythe ID (1995) Pre- and postsynaptic glutamate receptors at a giant excitatory synapse in rat auditory brainstem slices. J Physiol (Lond) 488:387-406.

Barnes-Davies M, Owens S, Forsythe ID (2001) Calcium channels triggering transmitter release in the rat medial superior olive. Hear Res 162:134-145.

Barnes-Davies M, Osmani F, Barker MC, Forsythe ID (2003) Kv1 conductances regulating principal neurone excitability

in the rat LSO follow the tonotopic axis. J Physiol 547.P.

Barrett EF, Barrett JN (1982) Intracellular recording from vertebrate myelinated axons: mechanism of the depolarizing afterpotential. J Physiol 323:117-144.

Bauer CK, Schwarz JR (2001) Physiology of EAG K+ channels. J Membr Biol 182:1-15.

Bekele-Arcuri Z, Matos MF, Manganas L, Strassle BW, Monaghan MM, Rhodes KJ, Trimmer JS (1996) Generation and Characterization of Subtype-specific Monoclonal

Antibodies to K+ Channel [alpha]- and [beta]-subunit Polypeptides. Neuropharmacology 35:851-865.

Bekkers JM, Delaney AJ (2001) Modulation of excitability by alpha-dendrotoxin-sensitive potassium channels in neocortical pyramidal neurons. J Neurosci 21:6553-6560.

Bhattacharjee A, Gan L, Kaczmarek LK (2002) Localization of the Slack potassium channel in the rat central nervous system. J Comp Neurol 454:241-254.

Biacabe B, Chevallier JM, Avan P, Bonfils P (2001) Functional anatomy of auditory brainstem nuclei: application to the anatomical basis of brainstem auditory evoked potentials. Auris Nasus Larynx 28:85-94.

Billups B, Wong AY, Forsythe ID (2002) Detecting synaptic connections in the medial nucleus of the trapezoid body using calcium imaging. Pflugers Arch 444:663-669.

Boland LM, Jackson KA (1999) Protein kinase C inhibits Kv1.1 potassium channel function. Am J Physiol Cell Physiol 46:C100-C110.

Borst JG, Helmchen F, Sakmann B (1995) Pre- and postsynaptic whole-cell recordings in the medial nucleus of the trapezoid body of the rat. J Physiol 489:825-840.

Brand A, Behrend O, Marquardt T, McAlpine D, Grothe B (2002) Precise inhibition is essential for microsecond interaural time difference coding. Nature 417:543-547.

Brau ME, Dreyer F, Jonas P, Repp H, Vogel W (1990) A K+ Channel in Xenopus Nerve-Fibers Selectively Blocked by Bee and Snake Toxins - Binding and Voltage-Clamp Experiments. Journal of Physiology-London 420:365-385.

Brawer JR, Morest DK, Kane EC (1974) The neuronal architecture of the cochlear nucleus of the cat. J Comp Neurol 155:251-300.

Brew HM, Forsythe ID (1995) Two voltage-dependent K+ conductances with complementary functions in postsynaptic integration at a central auditory synapse. J Neurosci 15:8011-8022.

Brew HM, Hallows JL, Tempel BL (2003) Hyperexcitability and reduced low threshold potassium currents in auditory neurons of mice lacking the channel subunit Kv1.1. J Physiol 548:1-20.

Brown DA (2000) Neurobiology: the acid test for resting potassium channels. Curr Biol 10:R456-459.

Brown HF, DiFrancesco D, Noble SJ (1979) How does adrenaline accelerate the heart? Nature 280:235-236.

Browne DL, Gancher ST, Nutt JG, Brunt ER, Smith EA, Kramer P, Litt M (1994) Episodic ataxia/myokymia syndrome is associated with point mutations in the human potassium channel gene, KCNA1. Nat Genet 8:136-140.

Campomanes CR, Carroll KI, Manganas LN, Hershberger ME, Gong B, Antonucci DE, Rhodes KJ, Trimmer JS (2002) Kvbeta subunit oxidoreductase activity and kv1 potassium channel trafficking. J Biol Chem 277:8298-8305.

Cant NB, Morest DK (1979a) The bushy cells in the anteroventral cochlear nucleus of the cat. A study with the electron microscope. Neuroscience 4:1925-1945.

Cant NB, Morest DK (1979b) Organization of the neurons in the anterior division of the anteroventral cochlear nucleus of the cat. Light-microscopic observations. Neuroscience 4:1909-1923.

Cant NB, Casseday JH (1986) Projections from the anteroventral cochlear nucleus to the lateral and medial superior olivary nuclei. J Comp Neurol 247:457-476.

Carr CE, Konishi M (1990) A circuit for detection of interaural time differences in the brain stem of the barn owl. J Neurosci 10:3227-3246.

Carr CE, Soares D (2002) Evolutionary convergence and shared computational principles in the auditory system. Brain Behav Evol 59:294-311.

Castellano A, Chiara MD, Mellstrom B, Molina A, Monje F, Naranjo JR, Lopez-Barneo J (1997) Identification and Functional Characterization of a K+ Channel alpha -Subunit with Regulatory Properties Specific to Brain. J Neurosci 17:4652-4661.

Castle NA, Fadous SR, Logothetis DE, Wang GK (1994a) 4-Aminopyridine binding and slow inactivation are mutually exclusive in rat Kv1.1 and Shaker potassium channels. Mol Pharmacol 46:1175-1181.

Castle NA, Fadous S, Logothetis DE, Wang GK (1994b) Aminopyridine block of Kv1.1 potassium channels expressed in mammalian cells and Xenopus oocytes. Mol Pharmacol 45:1242-1252.

Catterall WA, Gutman GA, Chandy KG, eds (2002) The IUPHAR Compendium of Voltage-gated Ion Channels: IUPHAR Media, Leeds, UK.

Chabbert C, Chambard JM, Sans A, Desmadryl G (2001) Three types of depolarization-activated potassium currents in acutely isolated mouse vestibular neurons. J Neurophysiol 85:1017-1026.

Charlton M, Smith S, Zucker R (1982) Role of presynaptic calcium ions and channels in synaptic facilitation and depression at the squid giant synapse. J Physiol (Lond) 323:173-193.

Chemin J, Girard C, Duprat F, Lesage F, Romey G, Lazdunski M (2003) Mechanisms underlying excitatory effects of group I metabotropic glutamate receptors via inhibition of 2P domain K+ channels. EMBO J 22:5403-5411.

Chiu SY, Ritchie JM (1980) Potassium channels in nodal and internodal axonal membrane of mammalian myelinated fibres. Nature 284:170-171.

Chiu SY, Ritchie JM (1981) Evidence for the presence of potassium channels in the paranodal region of acutely demyelinated mammalian single nerve fibres. J Physiol 313:415-437.

Chiu SY, Ritchie JM (1984) On the physiological role of internodal potassium channels and the security of conduction in myelinated nerve fibres. Proc R Soc Lond B Biol Sci 220:415-422.

Chiu SY, Zhou L, Zhang CL, Messing A (1999) Analysis of potassium channel functions in mammalian axons by gene knockouts. Journal of Neurocytology 28:349-364.

Choi K, Aldrich R, Yellen G (1991) Tetraethylammonium Blockade Distinguishes Two Inactivation Mechanisms in Voltage-Activated K+ Channels. PNAS 88:5092-5095.

Christie MJ, North RA, Osborne PB, Douglass J, Adelman JP (1990) Heteropolymeric potassium channels expressed in Xenopus oocytes from cloned subunits. Neuron 4:405-411.

Chung YH, Shin C-m, Kim MJ, Cha CI (2000) Immunohistochemical study on the distribution of six members of the Kv1 channel subunits in the rat basal ganglia. Brain Research 875:164-170.

Clay JR (2000) Determining K+ channel activation curves from K+ channel currents. Eur Biophys J 29:555-557.

Clopton BM, Winfield JA (1973) Tonotopic organization in the inferior colliculus of the rat. Brain Res 56:355-358.

Coetzee WA, Amarillo Y, Chiu J, Chow A, Lau D, McCormack T, Moreno H, Nadal MS, Ozaita A, Pountney D, Saganich M, Vega-Saenz de Miera E, Rudy B (1999) Molecular diversity of K+ channels. Ann N Y Acad Sci 868:233-285.

Cohen BE, Grabe M, Jan LY (2003) Answers and Questions from the KvAP Structures. Neuron 39:395-400.

Cohen YE, Knudsen EI (1999) Maps versus clusters: different representations of auditory space in the midbrain and forebrain. Trends Neurosci 22:128-135.

Cole KS (1949) Dynamic electrical Characteristics of the squid axon membrane. Archives Sci Physiol 3:253-258.

Coleman SK, Newcombe J, Pryke J, Dolly JO (1999) Subunit composition of Kv1 channels in human CNS. J Neurochem 73:849-858.

Connor JA, Stevens CF (1971) Prediction of repetitive firing behaviour from voltage clamp data on an isolated neurone soma. J Physiol 213:31-53.

Corrette BJ, Repp H, Dreyer F, Schwarz JR (1991) Two types of fast K+ channels in rat myelinated nerve fibres and their sensitivity to dendrotoxin. Pflugers Arch 418:408-416.

Covarrubias M, Wei A, Salkoff L, Vyas TB (1994) Elimination of rapid potassium channel inactivation by phosphorylation of the inactivation gate. Neuron 13:1403-1412.

Critz S, Wible B, Lopez H, Brown A (1993) Stable expression and regulation of a rat brain K+ channel. J Neurochem 60:1175-1178.

Cunningham MO, Jones RS (2001) Dendrotoxin sensitive potassium channels modulate GABA but not glutamate release in the rat entorhinal cortex in vitro. Neuroscience 107:395-404.

Cuttle MF, Tsujimoto T, Forsythe ID, Takahashi T (1998) Facilitation of the presynaptic calcium current at an auditory synapse in rat brainstem. J Physiol 512 (Pt 3):723-729.

Cuttle MF, Rusznak Z, Wong AY, Owens S, Forsythe ID (2001) Modulation of a presynaptic hyperpolarization-activated cationic current (I(h)) at an excitatory synaptic terminal in the rat auditory brainstem. J Physiol 534:733-744.

D'Adamo MC, Imbrici P, Sponcichetti F, Pessia M (1999) Mutations in the KCNA1 gene associated with episodic ataxia type-1 syndrome impair heteromeric voltage-gated K+ channel function. FASEB J 13:1335-1345.

David G, Modney B, Scappaticci KA, Barrett JN, Barrett EF (1995) Electrical and morphological factors influencing the depolarizing after-potential in rat and lizard myelinated axons. J Physiol 489 (Pt 1):141-157.

Deal KK, Lovinger DM, Tamkun MM (1994) The brain Kv1.1 potassium channel: in vitro and in vivo studies on subunit assembly and posttranslational processing. J Neurosci 14:1666-1676.

Desai R, Dodson PD, Barker MC, Forsythe ID, Kaczmarek LK (2003) Contribution of Kv3 channels to potassium current in the calyx of Held. Soc Neurosci Abstr.

Deutsch C (2002) Potassium channel ontogeny. Annu Rev Physiol 64:19-46.

Devaux J, Gola M, Jacquet G, Crest M (2002) Effects of K+ channel blockers on developing rat myelinated CNS axons: identification of four types of K+ channels. J Neurophysiol 87:1376-1385.

Devaux J, Alcaraz G, Grinspan J, Bennett V, Joho R, Crest M, Scherer SS (2003) Kv3.1b Is a Novel Component of CNS Nodes. J Neurosci 23:4509-4518.

DiFrancesco D (1993) Pacemaker mechanisms in cardiac tissue. Annu Rev Physiol 55:455-472.

DiFrancesco D, Tortora P (1991) Direct activation of cardiac pacemaker channels by intracellular cyclic AMP. Nature 351:145-147.

Diochot S, Schweitz H, Beress L, Lazdunski M (1998) Sea Anemone Peptides with a Specific Blocking Activity against the Fast Inactivating Potassium Channel Kv3.4. J Biol Chem 273:6744-6749.

Dodson PD, Barker MC, Forsythe ID (2002) Two Heteromeric Kv1 Potassium Channels Differentially Regulate Action Potential Firing. J Neurosci 22:6953-6961.

Dodson PD, Billups B, Rusznak Z, Szucs G, Barker MC, Forsythe ID (2003) Presynaptic Kv1.2 channels suppress synaptic terminal hyperexcitability following action potential invasion. J Physiol 550:27-33.

Dong Y, White FJ (2003) Dopamine D1-Class Receptors Selectively Modulate a Slowly Inactivating Potassium Current in Rat Medial Prefrontal Cortex Pyramidal Neurons. J Neurosci 23:2686-2695.

Doughty JM, Barnes-Davies M, Rusznak Z, Harasztosi C, Forsythe ID (1998) Contrasting Ca2+ channel subtypes at cell bodies and synaptic terminals of rat anterioventral cochlear bushy neurones. J Physiol 512 (Pt 2):365-376.

Doyle DA, Cabral JM, Pfuetzner RA, Kuo AL, Gulbis JM, Cohen SL, Chait BT, MacKinnon R (1998) The structure of the potassium channel: Molecular basis of K+ conduction and selectivity. Science 280:69-77.

Dryer SE, Fujii JT, Martin AR (1989) A Na+-activated K+ current in cultured brain stem neurones from chicks. J Physiol 410:283-296.

Dubois JM (1981) Evidence for the existence of three types of potassium channels in the frog Ranvier node membrane. J Physiol 318:297-316.

Dudel J (1973) Recording of action potentials and polarization of a single crayfish motor axon through a sucrose-gap capillary suction electrode. Pflugers Arch 338:187-199.

Elezgarai I, Diez J, Puente N, Azkue JJ, Benitez R, Bilbao A, Knopfel T, Donate-Oliver F, Grandes P (2003) Subcellular localization of the voltage-dependent potassium channel Kv3.1b in postnatal and adult rat medial nucleus of the trapezoid body. Neuroscience 118:889-898.

Eliasof S, Jahr CE (1997) Rapid AMPA receptor desensitization in catfish cone horizontal cells. Vis Neurosci 14:13-18.

Ellis KC, Tenenholz TC, Jerng H, Hayhurst M, Dudlak CS, Gilly WF, Blaustein MP, Weber DJ (2001) Interaction of a toxin from the scorpion Tityus serrulatus with a cloned K+ channel from squid (sqKv1A). Biochemistry 40:5942-5953.

Erisir A, Lau D, Rudy B, Leonard CS (1999) Function of specific K(+) channels in sustained high-frequency firing of fast-spiking neocortical interneurons [published erratum appears in J Neurophysiol 2000 Jul;84(1):following table of contents]. J Neurophysiol 82:2476-2489.

Eunson LH, Rea R, Zuberi SM, Youroukos S, Panayiotopoulos CP, Liguori R, Avoni P, McWilliam RC, Stephenson JB, Hanna MG, Kullmann DM, Spauschus A (2000) Clinical, genetic, and expression studies of mutations in the potassium channel gene KCNA1 reveal new phenotypic variability. Ann Neurol 48:647-656.

Everill B, Rizzo MA, Kocsis JD (1998) Morphologically identified cutaneous afferent DRG neurons express three different potassium currents in varying proportions. J Neurophysiol 79:1814-1824.

Fink M, Duprat F, Lesage F, Heurteaux C, Romey G, Barhanin J, Lazdunski M (1996) A new K+ channel beta subunit to specifically enhance Kv2.2 (CDRK) expression. J Biol Chem 271:26341-26348.

Finlayson PG, Caspary DM (1989) Synaptic potentials of chinchilla lateral superior olivary neurons. Hear Res 38:221-228.

Forsythe ID (1994) Direct Patch Recording from Identified Presynaptic Terminals Mediating Glutamatergic EPSCs in the Rat CNS, in vitro. J Physiol 479:381-387.

Forsythe ID, Barnes-Davies M (1993a) Outward Currents Limiting Repetitive Action-Potential Generation in Principal Neurons of the Rat Mntb in-Vitro Are Blocked by Micromolar 4-Aminopyridine (4-Ap) Concentrations. J Physiol (Lond) 467:P172-P172.

Forsythe ID, Barnes-Davies M (1993b) The binaural auditory pathway: excitatory amino acid receptors mediate dual timecourse excitatory postsynaptic currents in the rat medial nucleus of the trapezoid body. Proc R Soc Lond B Biol Sci 251:151-157.

Gale JE, Ashmore JF (1997) An intrinsic frequency limit to the cochlear amplifier. Nature 389:63-66.

Gamkrelidze G, Giaume C, Peusner KD (1998) The differential expression of low-threshold sustained potassium current contributes to the distinct firing patterns in embryonic central vestibular neurons. J Neurosci 18:1449-1464.

Gan L, Kaczmarek LK (1998) When, where, and how much? Expression of the Kv3.1 potassium channel in high-frequency firing neurons. Journal of Neurobiology 37:69-79.

Gardner-Medwin AR (1972) An extreme supernormal period in cerebellar parallel fibres. J Physiol 222:357-371.

Garrido JJ, Giraud P, Carlier E, Fernandes F, Moussif A, Fache MP, Debanne D, Dargent B (2003) A targeting motif involved in sodium channel clustering at the axonal initial segment. Science 300:2091-2094.

Gasparini S, Danse JM, Lecoq A, Pinkasfeld S, Zinn-Justin S, Young LC, de Medeiros CC, Rowan EG, Harvey AL, Menez A (1998) Delineation of the functional site of alpha-dendrotoxin. The functional topographies of dendrotoxins are different but share a conserved core with those of other Kv1 potassium channel-blocking toxins. J Biol Chem 273:25393-25403.

Geiger JR, Jonas P (2000) Dynamic control of presynaptic Ca(2+) inflow by fast-inactivating K(+) channels in hippocampal mossy fiber boutons. Neuron 28:927-939.

Geiger JR, Melcher T, Koh DS, Sakmann B, Seeburg PH, Jonas P, Monyer H (1995) Relative abundance of subunit mRNAs determines gating and Ca2+ permeability of AMPA receptors in principal neurons and interneurons in rat CNS. Neuron 15:193-204.

Gentschev T, Sotelo C (1973) Degenerative patterns in the ventral cochlear nucleus of the rat after primary deafferentation. An ultra-structural study. Brain Res 62:37-60.

Gilbert A, Jadot M, Leontieva E, Wattiaux-De Coninck S, Wattiaux R (1998) Delta F508 CFTR localizes in the endoplasmic reticulum-Golgi intermediate compartment in cystic fibrosis cells. Exp Cell Res 242:144-152.

Gittelman JX, Brew HM, Tempel BL (2002) KCNA channels curtail subthreshold Na channel activity, thus limiting variability of action potential timing. Biophys J (Annual Meeting Abstracts) 2002::578b.

Glazebrook PA, Ramirez AN, Schild JH, Shieh CC, Doan T, Wible BA, Kunze DL (2002) Potassium channels Kv1.1, Kv1.2 and Kv1.6 influence excitability of rat visceral sensory neurons. J Physiol 541:467-482.

Glendenning KK, Brunso-Bechtold JK, Thompson GC, Masterton RB (1981) Ascending auditory afferents to the nuclei of the lateral lemniscus. J Comp Neurol 197:673-703.

Glendenning KK, Hutson KA, Nudo RJ, Masterton RB (1985) Acoustic chiasm II: Anatomical basis of binaurality in lateral superior olive of cat. J Comp Neurol 232:261-285.

Glendenning KK, Baker BN, Hutson KA, Masterton RB (1992) Acoustic chiasm V: inhibition and excitation in the ipsilateral and contralateral projections of LSO. J Comp Neurol 319:100-122.

Golding NL, Ferragamo MJ, Oertel D (1999) Role of Intrinsic Conductances Underlying Responses to Transients in Octopus Cells of the Cochlear Nucleus. J Neurosci 19:2897-2905.

Goldstein SA, Bockenhauer D, O'Kelly I, Zilberberg N (2001) Potassium leak channels and the KCNK family of two-P-domain subunits. Nat Rev Neurosci 2:175-184.

Gordon TR, Kocsis JD, Waxman SG (1988) Evidence for the presence of two types of potassium channels in the rat optic nerve. Brain Res 447:1-9.

Grigg JJ, Brew HM, Tempel BL (2000) Differential expression of voltage-gated potassium channel genes in auditory nuclei of the mouse brainstem. Hear Res 140:77-90.

Grissmer S, Nguyen AN, Aiyar J, Hanson DC, Mather RJ, Gutman GA, Karmilowicz MJ, Auperin DD, Chandy KG (1994) Pharmacological characterization of five cloned voltage-gated K+ channels, types Kv1.1, 1.2, 1.3, 1.5, and 3.1, stably expressed in mammalian cell lines. Mol Pharmacol 45:1227-1234.

Grothe B (2003) New roles for synaptic inhibition in sound localization. Nat Rev Neurosci 4:540-550.

Grothe B, Sanes DH (1994) Synaptic inhibition influences the temporal coding properties of medial superior olivary neurons: an in vitro study. J Neurosci 14:1701-1709.

Grundfest H, Gasser HS (1938) Properties of mammalian nerve fibres of slowest conduction. Am J Physiol 123:307-318.

Gu C, Jan YN, Jan LY (2003) A conserved domain in axonal targeting of Kv1 (Shaker) voltage-gated potassium channels. Science 301:646-649.

Guinan JJ, Jr., Li RY (1990) Signal processing in brainstem auditory neurons which receive giant endings (calyces of Held) in the medial nucleus of the trapezoid body of the cat. Hear Res 49:321-334.

Guinan JJ, Jr., Norris BE, Guinan SS (1972) Single auditory units in the superior olivary complex II: Locations of unit catagories and tonotopic organization. Int J Neurosci 4:147-166.

Gulbis JM, Mann S, MacKinnon R (1999) Structure of a voltage-dependent K+ channel beta subunit. Cell 97:943-952.

Halliwell JV, Plant TD, Robbins J, Standen NB (1994) Voltage clamp techniques. In: Microelectrode techniques, Second Edition (Ogden D, ed), pp 17-35: The Company of Biologists Limited, Cambridge.

Hamann M, Billups B, Forsythe ID (2003) Non-calyceal excitatory inputs mediate low fidelity synaptic transmission in rat auditory brainstem slices. Eur J Neurosci In press.

Hamill OP, Marty A, Neher E, Sakmann B, Sigworth FJ (1981) Improved patch-clamp techniques for high-resolution current recording from cells and cell-free membrane patches. Pflugers Arch 391:85-100.

Harvey AL (2001) Twenty years of dendrotoxins. Toxicon 39:15-26.

Harvey AL, Rowan EG, Vatanpour H, Fatehi M, Castaneda O, Karlsson E (1994) Potassium channel toxins and transmitter release. Ann N Y Acad Sci 710:1-10.

Hausser M, Stuart G, Racca C, Sakmann B (1995) Axonal initiation and active dendritic propagation of action potentials in substantia nigra neurons. Neuron 15:637-647.

Heginbotham L, MacKinnon R (1992) The aromatic binding site for tetraethylammonium ion on potassium channels. Neuron 8:483-491.

Heginbotham L, Abramson T, MacKinnon R (1992) A functional connection between the pores of distantly related ion channels as revealed by mutant K+ channels. Science 258:1152-1155.

Heginbotham L, Lu Z, Abramson T, MacKinnon R (1994) Mutations in the K+ channel signature sequence. Biophys J 66:1061-1067.

Heinemann SH, Rettig J, Graack HR, Pongs O (1996) Functional characterization of Kv channel beta-subunits from rat brain. J Physiol 493 (Pt 3):625-633.

Held H (1893) Die centraleGehörleitung. Arch Anat Physiol, Anat Abt:201-248.

Helfert RH, Schwartz IR (1986) Morphological evidence for the existence of multiple neuronal classes in the cat lateral superior olivary nucleus. J Comp Neurol 244:533-549.

Helfert RH, Schwartz IR (1987) Morphological features of five neuronal classes in the gerbil lateral superior olive. Am J Anat 179:55-69.

Hille B (2001) Ion channels of Excitable Membranes. In, 3rd Edition. Sunderland, MA: Sinauer.

Ho CS, Grange RW, Joho RH (1997) Pleiotropic effects of a disrupted K+ channel gene: Reduced body weight, impaired motor skill and muscle contraction, but no seizures. Proceedings of the National Academy of Sciences of the United States of America 94:1533-1538.

Hodgkin AL, Huxley AF (1952) A quantitative description of membrane current and its application to conduction and excitation in nerve. J Physiol (Lond) 117:500-544.

Hodgkin AL, Huxley AF, Katz B (1949) Ionic currents underlying activity in the giant axon of the squid. Archives Sci Physiol 3:129-130.

Hopkins WF (1998) Toxin and Subunit Specificity of Blocking Affinity of Three Peptide Toxins for Heteromultimeric, Voltage-Gated Potassium Channels Expressed in Xenopus Oocytes. J Pharmacol Exp Ther 285:1051-1060.

Hopkins WF, Allen ML, Houamed KM, Tempel BL (1994) Properties of voltage-gated K+ currents expressed in Xenopus oocytes by mKv1.1, mKv1.2 and their heteromultimers as revealed by mutagenesis of the dendrotoxin-binding site in mKv1.1. Pflugers Arch 428:382-390.

Hori T, Takai Y, Takahashi T (1999) Presynaptic Mechanism for Phorbol Ester-Induced Synaptic Potentiation. J Neurosci 19:7262-7267.

Hoshi T, Zagotta WN, Aldrich RW (1990) Biophysical and molecular mechanisms of Shaker potassium channel inactivation. Science 250:533-538.

Huang X, Morielli A, Peralta E (1994) Molecular Basis of Cardiac Potassium Channel Stimulation by Protein Kinase A. Proc Natl Acad Sci U S A 91:624-628.

Huang XY, Morielli AD, Peralta EG (1993) Tyrosine kinase-dependent suppression of a potassium channel by the G protein-coupled m1 muscarinic acetylcholine receptor. Cell 75:1145-1156.

Irvine DR, Park VN, McCormick L (2001) Mechanisms underlying the sensitivity of neurons in the lateral superior olive to interaural intensity differences. J Neurophysiol 86:2647-2666.

Isaacson JS, Walmsley B (1995) Receptors underlying excitatory synaptic transmission in slices of the rat anteroventral cochlear nucleus. J Neurophysiol 73:964-973.

Jackson M, Konnerth A, Augustine G (1991) Action Potential Broadening and Frequency-Dependent Facilitation of Calcium Signals in Pituitary Nerve Terminals. Proc Natl Acad Sci U S A 88:380-384.

Jager H, Rauer H, Nguyen AN, Aiyar J, Chandy KG, Grissmer S (1998) Regulation of mammalian Shaker-related K+ channels: evidence for non-conducting closed and non-conducting inactivated states. J Physiol (Lond) 506:291-301.

Jan LY, Jan YN (1997) Annual Review Prize Lecture - Voltage-gated and inwardly rectifying potassium channels. Journal of Physiology-London 505:267-282.

Jeffress LA (1948) A place theory of sound localisation. J Comp Physiol & Psychol 41:35-39.

Jentsch TJ (2000) Neuronal KCNQ potassium channels: physiology and role in disease. Nat Rev Neurosci 1:21-30.

Jiang Y, Ruta V, Chen J, Lee A, MacKinnon R (2003a) The principle of gating charge movement in a voltage-dependent K+ channel. Nature 423:42-48.

Jiang Y, Lee A, Chen J, Ruta V, Cadene M, Chait BT, MacKinnon R (2003b) X-ray structure of a voltage-dependent K+ channel. Nature 423:33-41.

Jing J, Chikvashvili D, Singer-Lahat D, Thornhill WB, Reuveny E, Lotan I (1999) Fast inactivation of a brain K+ channel composed of Kv1.1 and Kvbeta 1.1 subunits modulated by G protein beta gamma subunits. EMBO J 18:1245-1256.

Joiner WJ, Tang MD, Wang LY, Dworetzky SI, Boissard CG, Gan L, Gribkoff VK, Kaczmarek LK (1998) Formation of intermediate-conductance calcium-activated potassium channels by interaction of Slack and Slo subunits. Nat Neurosci 1:462-469.

Jonas EA, Kaczmarek LK (1996) Regulation of potassium channels by protein kinases. Curr Opin Neurobiol 6:318-323.

Jonas P, Brau ME, Hermsteiner M, Vogel W (1989) Single-channel recording in myelinated nerve fibers reveals one type of Na channel but different K channels. Proc Natl Acad Sci U S A 86:7238-7242.

Joris PX, Smith PH, Yin TC (1998) Coincidence detection in the auditory system: 50 years after Jeffress. Neuron 21:1235-1238.

Joris PX, Carney LH, Smith PH, Yin TC (1994) Enhancement of neural synchronization in the anteroventral cochlear nucleus. I. Responses to tones at the characteristic frequency. J Neurophysiol 71:1022-1036.

Joseph AW, Hyson RL (1993) Coincidence detection by binaural neurons in the chick brain stem. J Neurophysiol 69:1197-1211.

Joshi I, Wang L-Y (2002) Developmental profiles of glutamate receptors and synaptic transmission at a single synapse in the mouse auditory brainstem. J Physiol (Lond) 540:861-873.

Kalman K, Nguyen A, Tseng-Crank J, Dukes ID, Chandy G, Hustad CM, Copeland NG, Jenkins NA, Mohrenweiser H, Brandriff B, Cahalan M, Gutman GA, Chandy KG (1998) Genomic Organization, Chromosomal Localization, Tissue Distribution, and Biophysical Characterization of a Novel Mammalian Shaker-related Voltage-gated Potassium Channel, Kv1.7. J Biol Chem 273:5851-5857.

Kandler K, Friauf E (1995) Development of electrical membrane properties and discharge characteristics of superior olivary complex neurons in fetal and postnatal rats. Eur J Neurosci 7:1773-1790.

Kanemasa T, Gan L, Perney TM, Wang LY, Kaczmarek LK (1995) Electrophysiological and pharmacological characterization of a mammalian Shaw channel expressed in NIH 3T3 fibroblasts. J Neurophysiol 74:207-217.

Kapfer C, Seidl AH, Schweizer H, Grothe B (2002) Experience-dependent refinement of inhibitory inputs to auditory coincidence-detector neurons. Nat Neurosci 5:247-253.

Kashuba VI, Kvasha SM, Protopopov AI, Gizatullin RZ, Rynditch AV, Wahlestedt C, Wasserman WW, Zabarovsky ER (2001) Initial isolation and analysis of the human Kv1.7 (KCNA7) gene, a member of the voltage-gated potassium channel gene family. Gene 268:115-122.

Katz B, Miledi R (1968) The role of calcium in neuromuscular facilitation. J Physiol 195:481-492.

Kaupp UB, Seifert R (2002) Cyclic Nucleotide-Gated Ion Channels. Physiol Rev 82:769-824.

Kelly JB, Liscum A, van Adel B, Ito M (1998) Projections from the superior olive and lateral lemniscus to tonotopic regions of the rat's inferior colliculus. Hear Res 116:43-54.

Kerr PM, Clement-Chomienne O, Thorneloe KS, Chen TT, Ishii K, Sontag DP, Walsh MP, Cole WC (2001) Heteromultimeric Kv1.2-Kv1.5 channels underlie 4-aminopyridine-sensitive delayed rectifier K(+) current of rabbit vascular myocytes. Circ Res 89:1038-1044.

Kerschensteiner D, Stocker M (1999) Heteromeric Assembly of Kv2.1 with Kv9.3: Effect on the State Dependence of Inactivation. Biophys J 77:248-257.

Kharkovets T, Hardelin JP, Safieddine S, Schweizer M, El-Amraoui A, Petit C, Jentsch TJ (2000) KCNQ4, a K+ channel mutated in a form of dominant deafness, is expressed in the inner ear and the central auditory pathway. Proc Natl Acad Sci U S A 97:4333-4338.

Kil J, Kageyama GH, Semple MN, Kitzes LM (1995) Development of ventral cochlear nucleus projections to the superior olivary complex in gerbil. J Comp Neurol 353:317-340.

Kim E, Sheng M (1996) Differential K+ channel clustering activity of PSD-95 and SAP97, two related membrane-associated putative guanylate kinases. Neuropharmacology 35:993-1000.

Kim E, Niethammer M, Rothschild A, Jan YN, Sheng M (1995) Clustering of Shaker-type K+ channels by interaction with a family of membrane-associated guanylate kinases. Nature 378:85-88.

Kim G, Kandler K (2003) Elimination and strengthening of glycinergic/GABAergic connections during tonotopic map formation. Nat Neurosci 6:282-290.

Kiss L, LoTurco J, Korn SJ (1999) Contribution of the selectivity filter to inactivation in potassium channels. Biophys J 76:253-263.

Koch RO, Wanner SG, Koschak A, Hanner M, Schwarzer C, Kaczorowski GJ, Slaughter RS, Garcia ML, Knaus H-G (1997) Complex Subunit Assembly of Neuronal Voltage-gated K+ Channels. J Biol Chem 272:27577-27581.

Kocsis JD, Ruiz JA, Waxman SG (1983) Maturation of mammalian myelinated fibers: changes in action-potential characteristics following 4-aminopyridine application. J Neurophysiol 50:449-463.

Kocsis JD, Waxman SG, Hildebrand C, Ruiz JA (1982) Regenerating mammalian nerve fibres: changes in action potential waveform and firing characteristics following blockage of potassium conductance. Proc R Soc Lond B Biol Sci 217:77-87.

Kopp-Scheinpflug C, Lippe WR, Dorrscheidt GJ, Rubsamen R (2003) The medial nucleus of the trapezoid body in the gerbil is more than a relay: comparison of pre- and postsynaptic activity. J Assoc Res Otolaryngol 4:1-23.

Koschak A, Bugianesi RM, Mitterdorfer J, Kaczorowski GJ, Garcia ML, Knaus HG (1998) Subunit composition of brain voltage-gated potassium channels determined by hongotoxin-1, a novel peptide derived from Centruroides limbatus venom. J Biol Chem 273:2639-2644.

Kramer JW, Post MA, Brown AM, Kirsch GE (1998) Modulation of potassium channel gating by coexpression of Kv2.1 with regulatory Kv5.1 or Kv6.1 alpha -subunits. Am J Physiol Cell Physiol 274:C1501-1510.

Kuba H, Koyano K, Ohmori H (2002) Development of membrane conductance improves coincidence detection in the nucleus laminaris of the chicken. J Physiol (Lond) 540:529-542.

Kubisch C, Schroeder BC, Friedrich T, Lutjohann B, El-Amraoui A, Marlin S, Petit C, Jentsch TJ (1999) KCNQ4, a novel potassium channel expressed in sensory outer hair cells, is mutated in dominant deafness. Cell 96:437-446.

Kullmann DM (2002) The neuronal channelopathies. Brain 125:1177-1195.

Kupper J, Bowlby MR, Marom S, Levitan IB (1995) Intracellular and extracellular amino acids that influence C-type inactivation and its modulation in a voltage-dependent potassium channel. Pflugers Arch 430:1-11.

Kuryshev YA, Wible BA, Gudz TI, Ramirez AN, Brown AM (2001) KChAP/Kv{beta}1.2 interactions and their effects on cardiac Kv channel expression. Am J Physiol Cell Physiol 281:C290-299.

Kuwabara N, Zook JM (1991) Classification of the principal cells of the medial nucleus of the trapezoid body. J Comp Neurol 314:707-720.

Kuwabara N, Zook JM (1992) Projections to the medial superior olive from the medial and lateral nuclei of the trapezoid body in rodents and bats. J Comp Neurol 324:522-538.

Laine M, Lin MA, Bannister JP, Silverman WR, Mock AF, Roux B, Papazian DM (2003) Atomic Proximity between S4 Segment and Pore Domain in Shaker Potassium Channels. Neuron 39:467-481.

Lambe EK, Aghajanian GK (2001) The Role of Kv1.2-Containing Potassium Channels in Serotonin-Induced Glutamate Release from Thalamocortical Terminals in Rat Frontal Cortex. J Neurosci 21:9955-9963.

Laube G, Roper J, Pitt JC, Sewing S, Kistner U, Garner CC, Pongs O, Veh RW (1996) Ultrastructural localization of Shaker-related potassium channel subunits and synapse-associated protein 90 to septate-like junctions in rat cerebellar Pinceaux. Brain Res Mol Brain Res 42:51-61.

Lenn NJ, Reese TS (1966) The fine structure of nerve endings in the nucleus of the trapezoid body and the ventral cochlear nucleus. Am J Anat 118:375-389.

Leonoudakis D, Mailliard W, Wingerd K, Clegg D, Vandenberg C (2001) Inward rectifier potassium channel Kir2.2 is associated with synapse-associated protein SAP97. J Cell Sci 114:987-998.

Lesage F, Lazdunski M (2000) Molecular and functional properties of two-pore-domain potassium channels. Am J Physiol Renal Physiol 279:F793-801.

Lev S, Moreno H, Martinez R, Canoll P, Peles E, Musacchio JM, Plowman GD, Rudy B, Schlessinger J (1995) Protein tyrosine kinase PYK2 involved in Ca(2+)-induced regulation of ion channel and MAP kinase functions [see comments]. Nature 376:737-745.

Levin G, Keren T, Peretz T, Chikvashvili D, Thornhill WB, Lotan I (1995) Regulation of RCK1 Currents with a cAMP Analog via Enhanced Protein Synthesis and Direct Channel Phosphorylation. J Biol Chem 270:14611-14618.

Levy M, Jing J, Chikvashvili D, Thornhill WB, Lotan I (1998) Activation of a metabotropic glutamate receptor and protein kinase C reduce the extent of inactivation of the K+ channel Kv1.1/Kv beta 1.1 via dephosphorylation of Kv1.1. Journal of Biological Chemistry 273:6495-6502.

Li W, Kaczmarek LK, Perney TM (2001) Localization of two high-threshold potassium channel subunits in the rat central auditory system. J Comp Neurol 437:196-218.

Lien CC, Jonas P (2003) Kv3 potassium conductance is necessary and kinetically optimized for high-frequency action potential generation in hippocampal interneurons. J Neurosci 23:2058-2068.

Lipkind GM, Fozzard HA (1997) A model of scorpion toxin binding to voltage-gated K+ channels. J Membr Biol 158:187-196.

Liu Y, Jurman ME, Yellen G (1996) Dynamic rearrangement of the outer mouth of a K+ channel during gating. Neuron 16:859-867.

Llinas R, Ribary U, Contreras D, Pedroarena C (1998) The neuronal basis for consciousness. Philos Trans R Soc Lond B Biol Sci 353:1841-1849.

Lu J, Robinson JM, Edwards D, Deutsch C (2001) T1-T1 interactions occur in ER membranes while nascent Kv peptides are still attached to ribosomes. Biochemistry 40:10934-10946.

Luo M, Perkel DJ (1999) A GABAergic, strongly inhibitory projection to a thalamic nucleus in the zebra finch song system. J Neurosci 19:6700-6711.

Luscher HR, Larkum ME (1998) Modeling action potential initiation and back-propagation in dendrites of cultured rat motoneurons. J Neurophysiol 80:715-729.

Ma D, Zerangue N, Lin YF, Collins A, Yu M, Jan YN, Jan LY (2001) Role of ER export signals in controlling surface potassium channel numbers. Science 291:316-319.

Macica CM, Kaczmarek LK (2001) Casein kinase 2 determines the voltage dependence of the Kv3.1 channel in auditory neurons and transfected cells. J Neurosci 21:1160-1168.

Macica CM, von Hehn CA, Wang LY, Ho CS, Yokoyama S, Joho RH, Kaczmarek LK (2003) Modulation of the kv3.1b potassium channel isoform adjusts the fidelity of the firing pattern of auditory neurons. J Neurosci 23:1133-1141.

Magee JC (1999) Dendritic Ih normalizes temporal summation in hippocampal CA1 neurons. Nat Neurosci 2:848.

Magee JC (2003) A prominent role for intrinsic neuronal properties in temporal coding. Trends Neurosci 26:14-16.

Magistretti J, Mantegazza M, Guatteo E, Wanke E (1996) Action potentials recorded with patch-clamp amplifiers: are they genuine? Trends Neurosci 19:530-534.

Magistretti J, Mantegazza M, de Curtis M, Wanke E (1998) Modalities of Distortion of Physiological Voltage Signals by Patch-Clamp Amplifiers: A Modeling Study. Biophys J 74:831-842.

Manganas LN, Trimmer JS (2000) Subunit composition determines Kv1 potassium channel surface expression. J Biol Chem 275:29685-29693.

Manganas LN, Wang Q, Scannevin RH, Antonucci DE, Rhodes KJ, Trimmer JS (2001) Identification of a trafficking determinant localized to the Kv1 potassium channel pore. PNAS 98:14055-14059.

Manis PB, Marx SO (1991) Outward currents in isolated ventral cochlear nucleus neurons. J Neurosci 11:2865-2880.

Mansour M, Nagarajan N, Nehring RB, Clements JD, Rosenmund C (2001) Heteromeric AMPA Receptors Assemble with a Preferred Subunit Stoichiometry and Spatial Arrangement. Neuron 32:841-853.

Margeta-Mitrovic M, Jan YN, Jan LY (2000) A trafficking checkpoint controls GABA(B) receptor heterodimerization. Neuron 27:97-106.

Marmont G (1949) Studies on the axon membrane I. A new method. Journal of Cellular and Comparative Physiology 34:351-382.

Martens JR, Kwak Y-G, Tamkun MM (1999) Modulation of Kv Channel [alpha]/[beta] Subunit Interactions. Trends in Cardiovascular Medicine 9:253-258.

Martin AR, Dryer SE (1989) Potassium channels activated by sodium. Q J Exp Physiol 74:1033-1041.

Martina M, Vida I, Jonas P (2000) Distal initiation and active propagation of action potentials in interneuron dendrites. Science 287:295-300.

Mathie A, Clarke CE (2002) Background potassium channels move into focus. J Physiol 542:334.

Matteson DR, Blaustein MP (1997) Scorpion toxin block of the early K+ current (IKf) in rat dorsal root ganglion neurones. J Physiol 503 (Pt 2):285-301.

McAlpine D, Grothe B (2003) Sound localization and delay lines--do mammals fit the model? Trends Neurosci 26:347-350.

McAlpine D, Jiang D, Palmer AR (2001) A neural code for low-frequency sound localization in mammals. Nat Neurosci 4:396-401.

McCormack K, McCormack T, Tanouye M, Rudy B, Stuhmer W (1995) Alternative splicing of the human Shaker K+ channel beta 1 gene and functional expression of the beta 2 gene product. FEBS Lett 370:32-36.

McCormack K, Connor JX, Zhou L, Ho LL, Ganetzky B, Chiu SY, Messing A (2002) Genetic analysis of the mammalian K+ channel beta subunit Kvbeta 2 (Kcnab2). J Biol Chem 277:13219-13228.

McCormick DA, Pape HC (1990) Properties of a hyperpolarization-activated cation current and its role in rhythmic oscillation in thalamic relay neurones. J Physiol 431:291-318.

McIntosh P, Southan AP, Akhtar S, Sidera C, Ushkaryov Y, Dolly JO, Robertson B (1997) Modification of rat brain Kv1.4 channel gating by association with accessory Kvbeta1.1 and beta2.1 subunits. Pflugers Arch 435:43-54.

McIntyre CC, Richardson AG, Grill WM (2002) Modeling the Excitability of Mammalian Nerve Fibers: Influence of Afterpotentials on the Recovery Cycle. J Neurophysiol 87:995-1006.

Meuth SG, Budde T, Kanyshkova T, Broicher T, Munsch T, Pape H-C (2003) Contribution of TWIK-Related Acid-Sensitive K+ Channel 1 (TASK1) and TASK3 Channels to the Control of Activity Modes in Thalamocortical Neurons. J Neurosci 23:6460-6469.

Millar JA, Barratt L, Southan AP, Page KM, Fyffe RE, Robertson B, Mathie A (2000) A functional role for the two-pore domain potassium channel TASK-1 in cerebellar granule neurons. Proc Natl Acad Sci U S A 97:3614-3618.

Mo ZL, Adamson CL, Davis RL (2002) Dendrotoxin-sensitive K(+) currents contribute to accommodation in murine spiral ganglion neurons. J Physiol 542:763-778.

Morais-Cabral JH, Zhou Y, MacKinnon R (2001) Energetic optimization of ion conduction rate by the K+ selectivity filter. Nature 414:37-42.

Morales MJ, Wee JO, Wang S, Strauss HC, Rasmusson RL (1996) The N-terminal domain of a K+ channel beta subunit increases the rate of C-type inactivation from the cytoplasmic side of the channel. PNAS 93:15119-15123.

Moreno H, Vega-Saenz de Miera E, Nadal MS, Amarillo Y, Rudy B (2001) Modulation of Kv3 potassium channels expressed in CHO cells by a nitric oxide-activated phosphatase. J Physiol 530:345-358.

Moreno H, Kentros C, Bueno E, Weiser M, Hernandez A, Vega-Saenz de Miera E, Ponce A, Thornhill W, Rudy B (1995) Thalamocortical projections have a K+ channel that is phosphorylated and modulated by cAMP-dependent protein kinase. J Neurosci 15:5486-5501.

Morest DK (1968) The collateral system of the medial nucleus of the trapezoid body of the cat, its neuronal architecture and relation to the olivo-cochlear bundle. Brain Res 9:288-311.

Mosbacher J, Schoepfer R, Monyer H, Burnashev N, Seeburg PH, Ruppersberg JP (1994) A molecular determinant for submillisecond desensitization in glutamate receptors. Science 266:1059-1062.

Nagaya N, Papazian DM (1997) Potassium channel alpha and beta subunits assemble in the endoplasmic reticulum. J Biol Chem 272:3022-3027.

Neher E, Sakmann B (1976) Single-channel currents recorded from membrane of denervated frog muscle fibres. Nature 260:799-802.

Neises GR, Mattox DE, Gulley RL (1982) The maturation of the end bulb of Held in the rat anteroventral cochlear nucleus. Anat Rec 204:271-279.

Nguyen A, Kath JC, Hanson DC, Biggers MS, Canniff PC, Donovan CB, Mather RJ, Bruns MJ, Rauer H, Aiyar J, Lepple-Wienhues A, Gutman GA, Grissmer S, Cahalan MD, Chandy KG (1996) Novel non-peptide agents potently block the C-type inactivated conformation of Kv1.3 and suppress T cell activation. Mol Pharmacol 50:1672-1679.

Nicol MJ, Walmsley B (2002) Ultrastructural basis of synaptic transmission between endbulbs of Held and bushy cells in the rat cochlear nucleus. J Physiol (Lond) 539:713-723.

Noma A, Irisawa H (1976) Membrane currents in the rabbit sinoatrial node cell as studied by the double microelectrode method. Pflugers Arch 364:45-52.

Oertel D (1983) Synaptic responses and electrical properties of cells in brain slices of the mouse anteroventral cochlear nucleus. J Neurosci 3:2043-2053.

Oertel D (1997) Encoding of timing in the brain stem auditory nuclei of vertebrates. Neuron 19:959-962.

Ogden D, Stanfield PR (1994) Patch clamp techniques for single channel and whole-cell recording. In: Microelectrode techniques, Second Edition (Ogden D, ed), pp 53-78: The Company of Biologists Limited, Cambridge.

Otis T, Zhang S, Trussell LO (1996) Direct Measurement of AMPA Receptor Desensitization Induced by Glutamatergic Synaptic Transmission. J Neurosci 16:7496-7504.

Ottschytsch N, Raes A, Van Hoorick D, Snyders DJ (2002) Obligatory heterotetramerization of three previously uncharacterized Kv channel alpha -subunits identified in the human genome. PNAS 99:7986-7991.

Overholt EM, Rubel EW, Hyson RL (1992) A circuit for coding interaural time differences in the chick brainstem. J Neurosci 12:1698-1708.

Owen D, Hall A, Stephens G, Stow J, Robertson B (1997) The relative potencies of dendrotoxins as blockers of the cloned voltage-gated K+ channel, mKv1.1 (MK-1), when stably expressed in Chinese hamster ovary cells. Br J Pharmacol 120:1029-1034.

Palay SL, Chan-Palay V (1974) Cerebellar cortex. Cytology and organisation. Berlin: Springer.

Papazian DM, Schwarz TL, Tempel BL, Jan YN, Jan LY (1987) Cloning of genomic and complementary DNA from Shaker, a putative potassium channel gene from Drosophila. Science 237:749-753.

Pape HC (1996) Queer current and pacemaker: the hyperpolarization-activated cation current in neurons. Annu Rev Physiol 58:299-327.

Pape HC, McCormick DA (1990) Ionic mechanisms of modulatory brain stem influences in the thalamus. J Basic Clin Physiol Pharmacol 1:107-117.

Park TJ, Monsivais P, Pollak GD (1997) Processing of interaural intensity differences in the LSO: role of interaural threshold differences. J Neurophysiol 77:2863-2878.

Park TJ, Grothe B, Pollak GD, Schuller G, Koch U (1996) Neural delays shape selectivity to interaural intensity differences in the lateral superior olive. J Neurosci 16:6554-6566.

Parsons CH, Lanyon RG, Schnupp JWH, King AJ (1999) Effects of Altering Spectral Cues in Infancy on Horizontal and Vertical Sound Localization by Adult Ferrets. J Neurophysiol 82:2294-2309.

Patel AJ, Honore E (2001) Properties and modulation of mammalian 2P domain K+ channels. Trends Neurosci 24:339-346.

Perney TM, Marshall J, Martin KA, Hockfield S, Kaczmarek LK (1992) Expression of the mRNAs for the Kv3.1 potassium channel gene in the adult and developing rat brain. J Neurophysiol 68:756-766.

Pollak GD (2002) Neurobiology: model hearing. Nature 417:502-503.

Pongs O (1999) Voltage-gated potassium channels: from hyperexcitability to excitement. Febs Letters 452:31-35.

Pongs O, Leicher T, Berger M, Roeper J, Bahring R, Wray D, Giese KP, Silva AJ, Storm JF (1999) Functional and molecular aspects of voltage-gated K+ channel beta subunits. Ann N Y Acad Sci 868:344-355.

Popratiloff A, Giaume C, Peusner KD (2003) Developmental change in expression and subcellular localization of two Shaker-related potassium channel proteins (Kv1.1 and Kv1.2) in the chick tangential vestibular nucleus. J Comp Neurol 461:466-482.

Porcello DM, Ho CS, Joho RH, Huguenard JR (2002) Resilient RTN Fast Spiking in Kv3.1 Null Mice Suggests Redundancy in the Action Potential Repolarization Mechanism. J Neurophysiol 87:1303-1310.

Post MA, Kirsch GE, Brown AM (1996) Kv2.1 and electrically silent Kv6.1 potassium channel subunits combine and express a novel current. FEBS Lett 399:177-182.

Poulter MO, Hashiguchi T, Padjen AL (1989) Dendrotoxin blocks accommodation in frog myelinated axons. J Neurophysiol 62:174-184.

Rasband MN, Shrager P (2000) Ion channel sequestration in central nervous system axons. J Physiol (Lond) 525:63-73.

Rasband MN, Trimmer JS (2001) Developmental Clustering of Ion Channels at and near the Node of Ranvier. Developmental Biology 236:5-16.

Rasband MN, Trimmer JS, Peles E, Levinson SR, Shrager P (1999) K+ channel distribution and clustering in developing and hypomyelinated axons of the optic nerve. J Neurocytol 28:319-331.

Rasband MN, Trimmer JS, Schwarz TL, Levinson SR, Ellisman MH, Schachner M, Shrager P (1998) Potassium channel distribution, clustering, and function in remyelinating rat axons. J Neurosci 18:36-47.

Rasband MN, Park EW, Zhen D, Arbuckle MI, Poliak S, Peles E, Grant SGN, Trimmer JS (2002) Clustering of neuronal potassium channels is independent of their interaction with PSD-95. J Cell Biol 159:663-672.

Rathouz M, Trussell L (1998) Characterization of outward currents in neurons of the avian nucleus magnocellularis. J Neurophysiol 80:2824-2835.

Rayleigh L, O. M. (1907) On our perception of sound direction. Phil Mag 13:214-232.

Raymond SA (1979) Effects of nerve impulses on threshold of frog sciatic nerve fibres. J Physiol 290:273-303.

Rea R, Spauschus A, Eunson LH, Hanna MG, Kullmann DM (2002) Variable K+ channel subunit dysfunction in inherited mutations of KCNA1. J Physiol (Lond) 538:5-23.

Reid G, Scholz A, Bostock H, Vogel W (1999) Human axons contain at least five types of voltage-dependent potassium channel. J Physiol (Lond) 518:681-696.

Rettig J, Heinemann SH, Wunder F, Lorra C, Parcej DN, Dolly JO, Pongs O (1994) Inactivation Properties of Voltage-Gated K+ Channels Altered by Presence of Beta-Subunit. Nature 369:289-294.

Reyes AD, Rubel EW, Spain WJ (1994) Membrane properties underlying the firing of neurons in the avian cochlear nucleus. J Neurosci 14:5352-5364.

Rhodes KJ, Strassle BW, Monaghan MM, Bekele-Arcuri Z, Matos MF, Trimmer JS (1997) Association and colocalization of the Kvbeta1 and Kvbeta2 beta-subunits with Kv1 alpha-subunits in mammalian brain K+ channel complexes. J Neurosci 17:8246-8258.

Rietzel HJ, Friauf E (1998) Neuron types in the rat lateral superior olive and developmental changes in the complexity of their dendritic arbors. J Comp Neurol 390:20-40.

Robbins J (2001) KCNQ potassium channels: physiology, pathophysiology, and pharmacology. Pharmacol Ther 90:1-19.

Robertson B, Owen D, Stow J, Butler C, Newland C (1996) Novel effects of dendrotoxin homologues on subtypes of mammalian Kv1 potassium channels expressed in Xenopus oocytes. FEBS Lett 383:26-30.

Robinson RB, Siegelbaum SA (2003) Hyperpolarization-Activated Cation Currents: From Molecules To Physiological Function. Annual Review of Physiology 65:453-480.

Rodrigues ARA, Arantes EC, Monje F, Stuhmer W, Varanda WA (2003) Tityustoxin-K(alpha) blockade of the voltage-gated potassium channel Kv1.3. Br J Pharmacol 139:1180-1186.

Roeper J, Sewing S, Zhang Y, Sommer T, Wanner SG, Pongs O (1998) NIP domain prevents N-type inactivation in voltage-gated potassium channels. Nature 391:390-393.

Roper J, Schwarz JR (1989) Heterogeneous distribution of fast and slow potassium channels in myelinated rat nerve fibres. J Physiol 416:93-110.

Rosenberg RL, East JE (1992) Cell-free expression of functional Shaker potassium channels. Nature 360:166-169.

Rothman JS, Manis PB (2003) The roles potassium currents play in regulating the electrical activity of ventral cochlear nucleus neurons. J Neurophysiol 89:3097-3113.

Roux B, MacKinnon R (1999) The cavity and pore helices in the KcsA K+ channel: electrostatic stabilization of monovalent cations. Science 285:100-102.

Rudy B, McBain CJ (2001) Kv3 channels: voltage-gated K+ channels designed for high-frequency repetitive firing. Trends in Neurosciences 24:517-526.

Rudy B, Chow A, Lau D, Amarillo Y, Ozaita A, Saganich M, Moreno H, Nadal MS, Hernandez-Pineda R, Hernandez-Cruz A, Erisir A, Leonard C, Vega-Saenz de Miera E (1999) Contributions of Kv3 channels to neuronal excitability. Ann N Y Acad Sci 868:304-343.

Ruiz-Canada C, Koh YH, Budnik V, Tejedor FJ (2002) DLG differentially localizes Shaker K+-channels in the central nervous system and retina of Drosophila. J Neurochem 82:1490-1501.

Russell SN, Overturf KE, Horowitz B (1994) Heterotetramer formation and charybdotoxin sensitivity of two K+ channels cloned from smooth muscle. Am J Physiol 267:C1729-1733.

Rusznak Z, Forsythe ID, Stanfield PR (1996) Characterization of the hyperpolarization activated nonspecific cation current (Ih) of bushy neurones from the rat anteroventral cochlear nucleus studied in a thin brain slice preparation. Neurobiology (Bp) 4:275-276.

Rusznak Z, Harasztosi C, Stanfield PR, Forsythe ID, Szucs G (2000) Depolarization-activated K+ currents determining the firing pattern of bushy neurones in the ventral cochlear nucleus of the rat. Journal of Physiology-London 526:55P-56P.

Ruta V, Jiang Y, Lee A, Chen J, MacKinnon R (2003) Functional analysis of an archaebacterial voltage-dependent K+ channel. Nature 422:180-185.

Ryugo DK, Sento S (1991) Synaptic connections of the auditory nerve in cats: relationship between endbulbs of held and spherical bushy cells. J Comp Neurol 305:35-48.

Ryugo DK, Wu MM, Pongstaporn T (1996) Activity-related features of synapse morphology: a study of endbulbs of held. J Comp Neurol 365:141-158.

Ryugo DK, Pongstaporn T, Huchton DM, Niparko JK (1997) Ultrastructural analysis of primary endings in deaf white cats: morphologic alterations in endbulbs of Held. J Comp Neurol 385:230-244.

Saganich MJ, Machado E, Rudy B (2001) Differential Expression of Genes Encoding Subthreshold-Operating Voltage-Gated K+ Channels in Brain. J Neurosci 21:4609-4624.

Saitoh N, Hori T, Takahashi T (2001) Activation of the epsilon isoform of protein kinase C in the mammalian nerve terminal. Proc Natl Acad Sci U S A 98:14017-14021.

Salinas M, Duprat F, Heurteaux C, Hugnot J-P, Lazdunski M (1997) New Modulatory alpha Subunits for Mammalian Shab K+ Channels. J Biol Chem 272:24371-24379.

Salkoff L, Baker K, Butler A, Covarrubias M, Pak MD, Wei A (1992) An essential 'set' of K+ channels conserved in flies, mice and humans. Trends Neurosci 15:161-166.

Sanes DH (1990) An in vitro analysis of sound localization mechanisms in the gerbil lateral superior olive. J Neurosci 10:3494-3506.

Sanes DH, Friauf E (2000) Development and influence of inhibition in the lateral superior olivary nucleus. Hear Res 147:46-58.

Santoro B, Tibbs GR (1999) The HCN gene family: molecular basis of the hyperpolarization-activated pacemaker channels. Ann N Y Acad Sci 868:741-764.

Santoro B, Baram TZ (2003) The multiple personalities of h-channels. Trends Neurosci 26:550-554.

Santoro B, Chen S, Luthi A, Pavlidis P, Shumyatsky GP, Tibbs GR, Siegelbaum SA (2000) Molecular and functional heterogeneity of hyperpolarization-activated pacemaker channels in the mouse CNS. J Neurosci 20:5264-5275.

Satzler K, Sohl LF, Bollmann JH, Borst JG, Frotscher M, Sakmann B, Lubke JH (2002) Three-dimensional reconstruction of a calyx of Held and its postsynaptic principal neuron in the medial nucleus of the trapezoid body. J Neurosci 22:10567-10579.

Scheibel ME, Scheibel AB (1974) Neuropil organization in the superior olive of the cat. Exp Neurol 43:339-348.

Scherer SS, Arroyo EJ (2002) Recent progress on the molecular organization of myelinated axons. J Peripher Nerv Syst 7:1-12.

Scheuss V, Schneggenburger R, Neher E (2002) Separation of Presynaptic and Postsynaptic Contributions to Depression by Covariance Analysis of Successive EPSCs at the Calyx of Held Synapse. J Neurosci 22:728-739.

Schreiber M, Wei A, Yuan A, Gaut J, Saito M, Salkoff L (1998) Slo3, a novel pH-sensitive K+ channel from mammalian spermatocytes. J Biol Chem 273:3509-3516.

Schulteis CT, Nagaya N, Papazian DM (1998) Subunit folding and assembly steps are interspersed during Shaker potassium channel biogenesis. J Biol Chem 273:26210-26217.

Schwarz DW, Puil E (1997) Firing properties of spherical bushy cells in the anteroventral cochlear nucleus of the gerbil. Hear Res 114:127-138.

Scott VE, Muniz ZM, Sewing S, Lichtinghagen R, Parcej DN, Pongs O, Dolly JO (1994) Antibodies specific for distinct Kv subunits unveil a heterooligomeric basis for subtypes of alpha-dendrotoxin-sensitive K+ channels in bovine brain. Biochemistry 33:1617-1623.

Shamotienko OG, Parcej DN, Dolly JO (1997) Subunit combinations defined for K+ channel Kv1 subtypes in synaptic membranes from bovine brain. Biochemistry 36:8195-8201.

Shen NV, Chen X, Boyer MM, Pfaffinger PJ (1993) Deletion analysis of K+ channel assembly. Neuron 11:67-76.

Shi G, Nakahira K, Hammond S, Rhodes KJ, Schechter LE, Trimmer JS (1996) Beta subunits promote K+ channel surface expression through effects early in biosynthesis. Neuron 16:843-852.

Shi Y (2003) Mammalian RNAi for the masses. Trends Genet 19:9-12.

Shieh CC, Coghlan M, Sullivan JP, Gopalakrishnan M (2000) Potassium channels: molecular defects, diseases, and therapeutic opportunities. Pharmacol Rev 52:557-594.

Shneiderman A, Henkel CK (1987) Banding of lateral superior olivary nucleus afferents in the inferior colliculus: a possible substrate for sensory integration. J Comp Neurol 266:519-534.

Smart SL, Lopantsev V, Zhang CL, Robbins CA, Wang H, Chiu SY, Schwartzkroin PA, Messing A, Tempel BL (1998) Deletion of the K(V)1.1 potassium channel causes epilepsy in mice. Neuron 20:809-819.

Smith PH (1995) Structural and functional differences distinguish principal from nonprincipal cells in the guinea pig MSO slice. J Neurophysiol 73:1653-1667.

Smith PH, Joris PX, Yin TC (1993) Projections of physiologically characterized spherical bushy cell axons from the cochlear nucleus of the cat: evidence for delay lines to the medial superior olive. J Comp Neurol 331:245-260.

Smith PH, Joris PX, Carney LH, Yin TC (1991) Projections of physiologically characterized globular bushy cell axons from the cochlear nucleus of the cat. J Comp Neurol 304:387-407.

Sommer I, Lingenhohl K, Friauf E (1993) Principal cells of the rat medial nucleus of the trapezoid body: an intracellular in vivo study of their physiology and morphology. Exp Brain Res 95:223-239.

Southan AP, Robertson B (1998a) Modulation of inhibitory post-synaptic currents (IPSCs) in mouse cerebellar Purkinje and basket cells by snake and scorpion toxin K+ channel blockers. British Journal of Pharmacology 125:1375-1381.

Southan AP, Robertson B (1998b) Patch-clamp recordings from cerebellar basket cell bodies and their presynaptic terminals reveal an asymmetric distribution of voltage-gated potassium channels. J Neurosci 18:948-955.

Southan AP, Robertson B (2000) Electrophysiological characterization of voltage-gated K(+) currents in cerebellar basket and Purkinje cells: Kv1 and Kv3 channel subfamilies are present in basket cell nerve terminals. J Neurosci 20:114-122.

Spauschus A, Eunson L, Hanna MG, Kullmann DM (1999) Functional Characterization of a Novel Mutation in KCNA1 in Episodic Ataxia Type 1 Associated with Epilepsy. Ann NY Acad Sci 868:442-446.

Stansfeld CE, Marsh SJ, Halliwell JV, Brown DA (1986) 4-Aminopyridine and dendrotoxin induce repetitive firing in rat visceral sensory neurones by blocking a slowly inactivating outward current. Neurosci Lett 64:299-304.

Stevens CF, Zador AM (1998) Input synchrony and the irregular firing of cortical neurons. Nat Neurosci 1:210-217.

Strydom DJ (1977) Snake venom toxins. The amino-acid sequence of a short-neurotoxin homologue from Dendroaspis polylepis polylepis (black mamba) venom. Eur J Biochem 76:99-106.

Stuart GJ, Sakmann B (1994) Active propagation of somatic action potentials into neocortical pyramidal cell dendrites. Nature 367:69-72.

Stuhmer W, Ruppersberg JP, Schroter KH, Sakmann B, Stocker M, Giese KP, Perschke A, Baumann A, Pongs O (1989) Molecular basis of functional diversity of voltage-gated potassium channels in mammalian brain. Embo J 8:3235-3244.

Svirskis G, Kotak V, Sanes DH, Rinzel J (2002) Enhancement of Signal-to-Noise Ratio and Phase Locking for Small Inputs by a Low-Threshold Outward Current in Auditory Neurons. J Neurosci 22:11019-11025.

Talley EM, Solorzano G, Lei Q, Kim D, Bayliss DA (2001) CNS Distribution of Members of the Two-Pore-Domain (KCNK) Potassium Channel Family. J Neurosci 21:7491-7505.

Tan YP, Llano I (1999) Modulation by K+ channels of action potential-evoked intracellular Ca2+ concentration rises in rat cerebellar basket cell axons. J Physiol 520:65-78.

Taschenberger H, von Gersdorff H (2000) Fine-tuning an auditory synapse for speed and fidelity: developmental changes in presynaptic waveform, EPSC kinetics, and synaptic plasticity. J Neurosci 20:9162-9173.

Thomas MV (2000) Optopatch manual: Cairn Research Limited.

Thorn PJ, Wang XM, Lemos JR (1991) A fast, transient K+ current in neurohypophysial nerve terminals of the rat. J Physiol 432:313-326.

Tiffany AM, Manganas LN, Kim E, Hsueh Y-P, Sheng M, Trimmer JS (2000) PSD-95 and SAP97 Exhibit Distinct Mechanisms for Regulating K+ Channel Surface Expression and Clustering. J Cell Biol 148:147-158.

Tollin DJ (2003) The lateral superior olive: a functional role in sound source localization. Neuroscientist 9:127-143.

Traka M, Dupree JL, Popko B, Karagogeos D (2002) The Neuronal Adhesion Protein TAG-1 Is Expressed by Schwann Cells and Oligodendrocytes and Is Localized to the Juxtaparanodal Region of Myelinated Fibers. J Neurosci 22:3016-3024.

Trussell LO (1999) Synaptic mechanisms for coding timing in auditory neurons. Annu Rev Physiol 61:477-496.

Tu L, Deutsch C (1999) Evidence for Dimerization of Dimers in K+ Channel Assembly. Biophys J 76:2004-2017.

Tu L, Santarelli V, Sheng Z, Skach W, Pain D, Deutsch C (1996) Voltage-gated K+ channels contain multiple intersubunit association sites. J Biol Chem 271:18904-18911.

Turecek R, Trussell LO (2001) Presynaptic glycine receptors enhance transmitter release at a mammalian central synapse. Nature 411:587-590.

Tytgat J, Debont T, Carmeliet E, Daenens P (1995) The alpha-Dendrotoxin Footprint on a Mammalian Potassium Channel. J Biol Chem 270:24776-24781.

Uebele VN, England SK, Chaudhary A, Tamkun MM, Snyders DJ (1996) Functional Differences in Kv1.5 Currents Expressed in Mammalian Cell Lines Are Due to the Presence of Endogenous Kvbeta2.1 Subunits. J Biol Chem 271:2406-2412.

Ulens C, Tytgat J (2001) Functional heteromerization of HCN1 and HCN2 pacemaker channels. J Biol Chem 276:6069-6072.

Vabnick I, Trimmer JS, Schwarz TL, Levinson SR, Risal D, Shrager P (1999) Dynamic Potassium Channel Distributions during Axonal Development Prevent Aberrant Firing Patterns. J Neurosci 19:747-758.

Vatanpour H, Harvey AL (1995) Modulation of acetylcholine release at mouse neuromuscular junctions by interaction of three homologous scorpion toxins with K+ channels. Br J Pharmacol 114:1502-1506.

Veh RW, Lichtinghagen R, Sewing S, Wunder F, Grumbach IM, Pongs O (1995) Immunohistochemical localization of five members of the Kv1 channel subunits: contrasting subcellular locations and neuron-specific co-localizations in rat brain. Eur J Neurosci 7:2189-2205.

Vergara C, Latorre R, Marrion NV, Adelman JP (1998) Calcium-activated potassium channels. Curr Opin Neurobiol 8:321-329.

Vetter DE, Mann JR, Wangemann P, Liu J, McLaughlin KJ, Lesage F, Marcus DC, Lazdunski M, Heinemann SF, Barhanin J (1996) Inner ear defects induced by null mutation of the isk gene. Neuron 17:1251-1264.

von Gersdorff H, Borst JG (2002) Short-term plasticity at the calyx of held. Nat Rev Neurosci 3:53-64.

von Gersdorff H, Schneggenburger R, Weis S, Neher E (1997) Presynaptic Depression at a Calyx Synapse: The Small Contribution of Metabotropic Glutamate Receptors. J Neurosci 17:8137-8146.

Wang FC, Parcej DN, Dolly JO (1999a) alpha subunit compositions of Kv1.1-containing K+ channel subtypes fractionated from rat brain using dendrotoxins. Eur J Biochem 263:230-237.

Wang FC, Bell N, Reid P, Smith LA, McIntosh P, Robertson B, Dolly JO (1999b) Identification of residues in dendrotoxin K responsible for its discrimination between neuronal K+ channels containing Kv1.1 and 1.2 alpha subunits. Eur J Biochem 263:222-229.

Wang H, Kunkel DD, Schwartzkroin PA, Tempel BL (1994) Localization of Kv1.1 and Kv1.2, 2 K-Channel Proteins, to Synaptic Terminals, Somata, and Dendrites in the Mouse-Brain. J Neurosci 14:4588-4599.

Wang H, Kunkel DD, Martin TM, Schwartzkroin PA, Tempel BL (1993) Heteromultimeric K+ channels in terminal and juxtaparanodal regions of neurons. Nature 365:75-79.

Wang HS, McKinnon D (1995) Potassium currents in rat prevertebral and paravertebral sympathetic neurones: control of firing properties. J Physiol 485 (Pt 2):319-335.

Wang HS, Pan Z, Shi W, Brown BS, Wymore RS, Cohen IS, Dixon JE, McKinnon D (1998a) KCNQ2 and KCNQ3 potassium channel subunits: molecular correlates of the M-channel. Science 282:1890-1893.

Wang LY, Kaczmarek LK (1998) High-frequency firing helps replenish the readily releasable pool of synaptic vesicles. Nature 394:384-388.

Wang LY, Gan L, Forsythe ID, Kaczmarek LK (1998b) Contribution of the Kv3.1 potassium channel to high-frequency firing in mouse auditory neurones. J Physiol (Lond) 509:183-194.

Wang Q, Curran ME, Splawski I, Burn TC, Millholland JM, VanRaay TJ, Shen J, Timothy KW, Vincent GM, de Jager T, Schwartz PJ, Toubin JA, Moss AJ, Atkinson DL, Landes GM, Connors TD, Keating MT (1996a) Positional cloning of a novel potassium channel gene: KVLQT1 mutations cause cardiac arrhythmias. Nat Genet 12:17-23.

Wang Z, Kiehn J, Yang Q, Brown AM, Wible BA (1996b) Comparison of binding and block produced by alternatively spliced Kvbeta1 subunits. J Biol Chem 271:28311-28317.

Warmke J, Drysdale R, Ganetzky B (1991) A distinct potassium channel polypeptide encoded by the Drosophila eag locus. Science 252:1560-1562.

Warr WB (1966) Fiber degeneration following lesions in the anterior ventral cochlear nucleus of the cat. Exp Neurol 14:453-474.

Waxman SG, Swadlow HA (1976) Morphology and physiology of visual callosal axons: evidence for a supernormal period in central myelinated axons. Brain Res 113:179-187.

Weiser M, Demiera EVS, Kentros C, Moreno H, Franzen L, Hillman D, Baker H, Rudy B (1994) Differential Expression of Shaw-Related K+ Channels in the Rat Central-Nervous-System. Journal of Neuroscience 14:949-972.

Werkman TR, Kawamura T, Yokoyama S, Higashida H, Rogawski MA (1992) Charybdotoxin, dendrotoxin and mast cell degranulating peptide block the voltage-activated K+ current of fibroblast cells stably transfected with NGK1 (Kv1.2) K+ channel complementary DNA. Neuroscience 50:935-946.

Willis WD, Jr. (1999) Dorsal root potentials and dorsal root reflexes: a double-edged sword. Exp Brain Res 124:395-421.

Wissmann R, Baukrowitz T, Kalbacher H, Kalbitzer HR, Ruppersberg JP, Pongs O, Antz C, Fakler B (1999) NMR Structure and Functional Characteristics of the Hydrophilic N Terminus of the Potassium Channel beta -Subunit Kvbeta 1.1. J Biol Chem 274:35521-35525.

Wu RL, Barish ME (1992) Two pharmacologically and kinetically distinct transient potassium currents in cultured embryonic mouse hippocampal neurons. J Neurosci 12:2235-2246.

Wu RL, Barish ME (1999) Modulation of a slowly inactivating potassium current, I-D, by metabotropic glutamate receptor activation in cultured hippocampal pyramidal neurons. Journal of Neuroscience 19:6825-6837.

Wu SH, Oertel D (1984) Intracellular injection with horseradish peroxidase of physiologically characterized stellate and bushy cells in slices of mouse anteroventral cochlear nucleus. J Neurosci 4:1577-1588.

Wu SH, Kelly JB (1991) Physiological properties of neurons in the mouse superior olive: membrane characteristics and postsynaptic responses studied in vitro. J Neurophysiol 65:230-246.

Wu SH, Kelly JB (1992) Binaural interaction in the lateral superior olive: time difference sensitivity studied in mouse brain slice. J Neurophysiol 68:1151-1159.

Xu J, Li M (1997) Kvbeta 2 Inhibits the Kvbeta 1-mediated Inactivation of K+ Channels in Transfected Mammalian Cells. J Biol Chem 272:11728-11735.

Xu J, Yu W, Wright JM, Raab RW, Li M (1998) Distinct functional stoichiometry of potassium channel beta subunits. Proc Natl Acad Sci U S A 95:1846-1851.

Yellen G (2002) The voltage-gated potassium channels and their relatives. Nature 419:35-42.

Yi BA, Jan LY (2000) Taking apart the gating of voltage-gated K+ channels. Neuron 27:423-425.

Young SR, Rubel EW (1983) Frequency-specific projections of individual neurons in chick brainstem auditory nuclei. J Neurosci 3:1373-1378.

Young SR, Rubel EW (1986) Embryogenesis of arborization pattern and topography of individual axons in N. laminaris of the chicken brain stem. J Comp Neurol 254:425-459.

Yuan A, Santi CM, Wei A, Wang ZW, Pollak K, Nonet M, Kaczmarek L, Crowder CM, Salkoff L (2003) The sodium-activated potassium channel is encoded by a member of the Slo gene family. Neuron 37:765-773.

Zerangue N, Schwappach B, Jan YN, Jan LY (1999) A new ER trafficking signal regulates the subunit stoichiometry of plasma membrane K(ATP) channels. Neuron 22:537-548.

Zerr P, Adelman JP, Maylie J (1998) Characterization of three episodic ataxia mutations in the human Kv1.1 potassium channel. Febs Letters 431:461-464.

Zhang C-L, Messing A, Chiu SY (1999) Specific Alteration of Spontaneous GABAergic Inhibition in Cerebellar Purkinje Cells in Mice Lacking the Potassium Channel Kv1.1. J Neurosci 19:2852-2864.

Zhou B-Y, Ma W, Huang X-Y (1998a) Specific Antibodies to the External Vestibule of Voltage-gated Potassium Channels Block Current. J Gen Physiol 111:555-563.

Zhou L, Messing A, Chiu SY (1999) Determinants of excitability at transition zones in Kv1.1- deficient myelinated nerves. Journal of Neuroscience 19:5768-5781.

Zhou L, Zhang CL, Messing A, Chiu SY (1998b) Temperature-sensitive neuromuscular transmission in Kv1.1 null mice: Role of potassium channels under the myelin sheath in young nerves. J Neurosci 18:7200-7215.

Zhou M, Morais-Cabral JH, Mann S, MacKinnon R (2001a) Potassium channel receptor site for the inactivation gate and quaternary amine inhibitors. Nature 411:657-661.

Zhou Y, Morais-Cabral JH, Kaufman A, MacKinnon R (2001b) Chemistry of ion coordination and hydration revealed by a K+ channel-Fab complex at 2.0 A resolution. Nature 414:43-48.

Zhu J, Watanabe I, Gomez B, Thornhill WB (2003a) Trafficking of Kv1.4 potassium channels: interdependence of a pore region determinant and a cytoplasmic C-terminal VXXSL determinant in regulating cell surface trafficking. Biochem J Pt.

Zhu J, Watanabe I, Gomez B, Thornhill WB (2003b) Heteromeric Kv1 potassium channel expression: amino acid determinants involved in processing and trafficking to the cell surface. J Biol Chem 278:25558-25567.

Zuberi SM, Eunson LH, Spauschus A, De Silva R, Tolmie J, Wood NW, McWilliam RC, Stephenson JPB, Kullmann DM, Hanna MG (1999) A novel mutation in the human voltage-gated potassium channel gene (Kv1.1) associates with episodic ataxia type 1 and sometimes with partial epilepsy. Brain 122:817-825.

Zucker RS (1974) Excitability changes in crayfish motor neurone terminals. J Physiol 241:111-126.

Solutions

Artificial Cerebro-Spinal Fluid (aCSF, composition in mM)

	Normal aCSF	Low Na^+ aCSF
NaCl	125	0
Sucrose	0	250
KCl	2.5	2.5
Glucose	10	10
NaH_2PO_4	26	1.25
$NaHCO_3$	26	26
$CaCl_2$	2	0.1
$MgCl_2$	1	4
Myo-inositol	3	3
Ascorbic acid	0.5	0.5
Sodium pyruvate	2	2

Patch Solution (composition in mM)

K Gluconate	97.5
KCL	32.5
HEPES	10
EGTA	5
$MgCl_2$	1
pH	7.2 (adjusted with KOH)
Osmolarity	291 mOsm

Sources

All compounds were obtained from Sigma (Poole, UK) unless otherwise stated. DTX-I, NTX, Kv1.1, Kv1.2, Kv1.4, Kv1.6 and Kv3.1b antibodies were from Alomone Labs (Jerusalem, Israel); Texas Red and FITC (goat anti-rabbit) were from Jackson ImmunoResearch Laboratories (West Grove, PA); Kv1.1, Kv1.2 and Kv1.6 antibodies from Upstate Biotechnology (NY) were used for co-localisation; Kv3.3 antibodies were a gift from Teresa Perney, Rutgers University, NJ; TsTX-Kα was from the Peptide Institute (Osaka, Japan) and DTX-K was a kind gift from Brian Robertson, University of Strathclyde, Glasgow.

Abbreviations

4-AP	4-aminopyridine
aCSF	artificial cerebrospinal fluid
AHP	afterhyperpolarisation
AMPA	α-amino-3-hydroxy-5-methylisoxazole-propionate
AP	action potential
AP5	2-amino-5-phosphonovalerate
ATP	adenosine triphosphate
aVCN	anterior ventral cochlear nucleus
cAMP	cyclic adenosine monophosphate
cGMP	cyclic guanosine monophosphate
CK2	casein kinase 2
CN	cochlear nucleus
CNG	cyclic nucleotide-gated
CNQX	6-cyano-7-nitroquinoxaline
DAP	depolarising after-potential
DCN	dorsal cochlear nucleus
DIC	differential interference contrast
dNTP	deoxynucleotide triphosphate
DTX	dendrotoxin
EAG	*Ether-à-go-go* K^+ channels
EPSC	excitatory post synaptic current
EPSP	excitatory postsynaptic potential
FITC	fluorescein isothiocyanate
GABA	gamma-aminobutyric acid
GBC	globular bushy cell
GTP	Guanosine triphosphate
Hz	heterozygote
I/V	current-voltage relationships
IC	inferior colliculus
ILD	interaural level difference
IPSC	inhibitory postsynaptic current
IPSP	inhibitory postsynaptic potential
ITD	interaural timing differences
K^+	potassium
Kir	inwardly rectifying K^+ channel
KO	knockout
LNTB	lateral nucleus of the trapezoid body
LSO	lateral superior olive
MAGUK	membrane associated guanylate kinase
MFB	mossy fibre bouton
MNTB	medial nucleus of the trapezoid body
MSO	medial superior olive
NMDA	non-methyl-D-aspartate
NTX	noxiustoxin
PBS	phosphate buffered saline
PCR	polymerase chain reaction
PKA	protein kinase A
PKC	protein kinase C
PMA	Phorbol 12-myristate 13-acetate
PMT	photomultiplier tube
PSP	postsynaptic potential
R_s	series resistance
RTN	reticular thalamic nucleus
SBC	spherical bushy cell
sEPSC	spontaneous excitatory postsynaptic current
sIPSC	spontaneous inhibitory postsynaptic current
SOC	superior olivary complex
TAE	Tris-acetate-ethylene-diamine-tetra-acetic acid
TEA	tetraethylammonium
TMD	transmembrane domains
TsTX-Kα	tityustoxin-Kα
TTX	tetrodotoxin
VCN	ventral cochlear nucleus
WT	wild type